

2014

# Investigation of bio-derived material and chemical technologies as sustainable warm mix asphalt additives

Joseph Herbert Podolsky  
*Iowa State University*

Follow this and additional works at: <https://lib.dr.iastate.edu/etd>

 Part of the [Civil Engineering Commons](#)

## Recommended Citation

Podolsky, Joseph Herbert, "Investigation of bio-derived material and chemical technologies as sustainable warm mix asphalt additives" (2014). *Graduate Theses and Dissertations*. 14275.  
<https://lib.dr.iastate.edu/etd/14275>

This Dissertation is brought to you for free and open access by the Iowa State University Capstones, Theses and Dissertations at Iowa State University Digital Repository. It has been accepted for inclusion in Graduate Theses and Dissertations by an authorized administrator of Iowa State University Digital Repository. For more information, please contact [digirep@iastate.edu](mailto:digirep@iastate.edu).

# **Investigation of bio-derived material and chemical technologies as sustainable warm mix asphalt additives**

by

**Joseph Herbert Podolsky**

A dissertation submitted to the graduate faculty  
in partial fulfillment of the requirements for the degree of

**DOCTOR OF PHILOSOPHY**

Major: Civil Engineering (Civil Engineering Materials)

Program of Study Committee:  
Ronald Christopher Williams, Major Professor  
Vernon R. Schaefer  
Kejin Wang  
Jeramy Curtis Ashlock  
W. Robert Stephenson

Iowa State University

Ames, Iowa

2014

Copyright © Joseph Herbert Podolsky, 2014. All rights reserved.

## **DEDICATION**

I would like to dedicate this work to my family -- my children Aryeh and Yochana and my wife Lisa who believed in me every step of the way.

## TABLE OF CONTENTS

|   | Page |
|---|------|
| LIST OF FIGURES .....   | vii  |
| LIST OF TABLES .....  | xi   |
| ACKNOWLEDGEMENTS .....  | xiii |
| ABSTRACT .....  | xiv  |
| CHAPTER 1. INTRODUCTION .....   | 1    |
| 1.1. Background .....   | 1    |
| 1.2. Problem Statement & Objectives .....   | 3    |
| 1.3. Research Methodology .....   | 4    |
| 1.4. Dissertation Organization .....  | 7    |
| 1.5. References .....   | 9    |
| CHAPTER 2. LITERATURE REVIEW .....  | 11   |
| 2.1. Warm Mix Asphalt Background .....  | 12   |
| 2.2. Warm Mix Asphalt Technologies .....  | 14   |
| 2.2.1. Foaming – water based .....  | 15   |
| 2.2.2. Foaming – water bearing additive .....   | 17   |
| 2.2.3. Chemical additive .....  | 18   |
| 2.2.4. Organic/bio-derived additive .....   | 20   |
| 2.3. Binder and Mixture Testing Methods Used throughout Research Work .....                           | 23   |
| 2.3.1. Binder rheology .....  | 23   |
| 2.3.2. Moisture susceptibility and compaction .....   | 28   |
| 2.3.3. $E^*_{mix}$ and $G^*_{binder}$ master curve construction .....                                 | 33   |
| 2.3.3.1. Sigmoidal $E^*_{mix}$ master curves using measured data .....                                | 33   |
| 2.3.3.2. Predicted $G^*$ binder master curve methods from measured data .....                         | 37   |
| 2.3.4. Semi-circular bend test at low temperatures .....  | 41   |
| 2.3.5. AASHTOWare Pavement ME Design .....  | 43   |
| 2.4. Warm Mix Asphalt Emissions & Benefits .....  | 45   |
| 2.5. Present Use of Warm Mix Asphalt in the United States .....                                       | 46   |
| 2.6. Literature Review Summary .....  | 48   |
| 2.7. References .....   | 48   |
| CHAPTER 3. INVESTIGATION OF ISOSORBIDE DISTILLATION BOTTOMS<br>AS A BIO-BASED WARM-MIX ADDITIVE ..... | 57   |
| 3.1. Abstract .....   | 57   |
| 3.2. Introduction .....   | 58   |
| 3.3. Experimental Materials and Methods .....   | 59   |
| 3.3.1. Asphalt binder experimental testing plan .....   | 61   |
| 3.3.2. Asphalt mixture experimental testing plan .....  | 62   |

|  |     |
|--|-----|
| 3.4. Discussion of Binder and Mixture Test Results .....   | 64  |
| 3.4.1. Binder test results .....   | 64  |
| 3.4.1.1. High and intermediate temperature binder test results .....   | 66  |
| 3.4.1.2. Low temperature binder test results .....   | 69  |
| 3.4.2. Mixture data and analysis .....   | 71  |
| 3.4.2.1. Compaction study .....  | 71  |
| 3.4.2.2. Indirect tensile strength study .....   | 73  |
| 3.5. Conclusions.....  | 76  |
| 3.6. References.....   | 78  |
| <br>   |     |
| CHAPTER 4. ESTIMATION AND ASSESSMENT OF HIGH TEMPERATURE<br>MIX PERFORMANCE GRADE FOR SELECT BIO-BASED WMA<br>ADDITIVES .....  | 81  |
| 4.1. Abstract.....   | 81  |
| 4.2. Introduction.....   | 82  |
| 4.3. Experimental Materials.....   | 84  |
| 4.3.1. Materials .....   | 84  |
| 4.3.2. Mix design, sample preparation, and testing .....   | 86  |
| 4.3.2.1. Dynamic shear rheometer binder sample experimental testing plan .....   | 86  |
| 4.3.2.2. Dynamic modulus asphalt mixture experimental testing plan .....   | 86  |
| 4.4. Experimental Methods.....   | 87  |
| 4.4.1. Estimated G* binder master curve methods back-calculated from<br>measured E* data.....  | 87  |
| 4.4.1.1. Sigmoidal E* master curves using measured data.....   | 88  |
| 4.4.1.2. Hirsch model.....   | 92  |
| 4.4.1.3. Al-Khateeb model.....   | 95  |
| 4.4.2. Predicted G* binder master curve methods from measured data.....  | 97  |
| 4.5. Analysis of Results and Discussion.....   | 101 |
| 4.5.1. Comparison of G* sigmoidal models from binder data.....   | 101 |
| 4.5.2. Statistical analysis of measured E* results .....   | 105 |
| 4.5.3. Prediction of high temperature mix performance grade using Hirsch<br>model .....  | 111 |
| 4.5.4. Prediction of high temperature mix performance grade using<br>Al-Khateeb model.....   | 114 |
| 4.6. Conclusions and Recommendations .....   | 120 |
| 4.7. References.....   | 122 |
| <br>   |     |
| CHAPTER 5. INVESTIGATION OF WARM MIX ASPHALT PERFORMANCE<br>WITH AND WITHOUT SELECT BIO-DERIVED/CHEMICAL<br>ADDITIVES IN IOWA USING AASHTOWARE PAVEMENT ME<br>DESIGN ..... | 125 |
| 5.1. Abstract.....   | 125 |
| 5.2. Introduction.....   | 127 |
| 5.2.1. Objectives .....  | 130 |

|  |     |
|--|-----|
| 5.3. Laboratory Testing Program .....  | 131 |
| 5.3.1. Material description .....  | 131 |
| 5.3.2. Dynamic modulus test.....   | 132 |
| 5.3.3. Dynamic shear rheometer test.....   | 134 |
| 5.4. AASHTOWare Pavement ME Design SETUP .....   | 134 |
| 5.4.1. Normalcy of measured E* results using @RISK.....  | 134 |
| 5.4.2. RTFO aged DSR data as Level 1 inputs .....  | 138 |
| 5.4.3. Pavement structure, traffic level, and climatic locations .....   | 138 |
| 5.5. Discussion of Results and Analysis .....  | 140 |
| 5.5.1. Dynamic modulus test results .....  | 140 |
| 5.5.2. RTFO aged DSR test results .....  | 146 |
| 5.5.3. Performance evaluation using AASHTOWare Pavement ME Design .....  | 150 |
| 5.5.3.1. Asphalt concrete (AC) bottom up cracking .....  | 151 |
| 5.5.3.2. Rutting.....  | 153 |
| 5.5.3.3. Smoothness .....  | 154 |
| 5.6. Conclusions.....  | 156 |
| 5.7. Acknowledgements.....   | 158 |
| 5.8. References.....   | 159 |
| <br>   |     |
| CHAPTER 6. COMPARATIVE PERFORMANCE OF BIO-DERIVED/<br>CHEMICAL ADDITIVES IN WARM MIX ASPHALT AT LOW<br>TEMPERATURE .....           | 161 |
| 6.1. Abstract.....   | 161 |
| 6.2. Introduction.....   | 162 |
| 6.3. Objectives .....  | 165 |
| 6.4. Materials & Methods .....   | 165 |
| 6.4.1. Material description .....  | 165 |
| 6.4.2. Binder testing methods .....  | 166 |
| 6.4.3. Mixture testing methods .....   | 167 |
| 6.5. Results & Discussion .....  | 168 |
| 6.5.1. Binder results & discussion .....   | 168 |
| 6.5.1.1. Multiple stress creep recovery (MSCR) results .....   | 168 |
| 6.5.1.2. Bending beam rheometer (BBR) results .....  | 170 |
| 6.5.2. Mix test results & discussion .....   | 172 |
| 6.5.2.1. Low temperature semi-circular bend (SCB) test results .....   | 172 |
| 6.5.2.2. Statistical analysis of SCB test results .....  | 175 |
| 6.6. Conclusions.....  | 179 |
| 6.7. Future Research .....   | 181 |
| 6.8. Acknowledgements.....   | 181 |
| 6.9. References.....   | 181 |
| <br>   |     |
| CHAPTER 7. CORRELATION BETWEEN LOW TEMPERATURE WARM MIX<br>ASPHALT BINDER AND MIX TEST RESULTS – AN INVESTIGATIVE<br>ANALYSIS..... | 184 |
| 7.1. Abstract.....   | 184 |

|   |     |
|---|-----|
| 7.2. Introduction.....  | 185 |
| 7.3. Experimental Materials and Methods .....                           | 189 |
| 7.3.1. Materials .....  | 189 |
| 7.3.2. Sample preparation and testing procedure .....                   | 190 |
| 7.3.2.1. Binder testing.....  | 190 |
| 7.3.2.2. Asphalt mixture testing.....                                   | 190 |
| 7.4. Discussion of Results and Analysis.....                            | 192 |
| 7.4.1. Analysis of BBR results.....                                     | 192 |
| 7.4.2. Analysis of SCB results .....                                    | 194 |
| 7.4.3. BBR stiffness vs. SCB stiffness.....                             | 197 |
| 7.5. Conclusions & Recommendations.....                                 | 200 |
| 7.6. Future Research .....  | 201 |
| 7.7. References.....  | 201 |
| <br>CHAPTER 8. CONCLUSIONS AND RECOMMENDATIONS FOR FUTURE<br>WORK ..... |     |
| 8.1. Summary.....   | 203 |
| 8.2. Conclusions.....   | 203 |
| 8.3. Recommendations for Future Work .....                              | 207 |

## LIST OF FIGURES

|  | Page |
|--|------|
| Figure 1.1. Relationship between Research Methodology and Dissertation Layout .....  | 8    |
| Figure 2.1. Foamed Asphalt System (Csanyi 1959) .....  | 13   |
| Figure 2.2. Astec Double Barrel Green System (Astec Industries 2014; Middleton and Forfyflow 2009) .....                             | 17   |
| Figure 2.3. Advera Synthetic Zeolite WMA Additive for Foaming Asphalt .....  | 18   |
| Figure 2.4. Warm Mix Additive Evotherm® J-1 and M1 Manufactured by MeadWestvaco .....  | 19   |
| Figure 2.5. Temperature Viscosity Behavior of Asphalt Binder Modified with Organic Additive Sasobit (Hurley and Prowell 2005b) ..... | 21   |
| Figure 2.6. Warm Mix Asphalt Additive Sasobit .....  | 21   |
| Figure 2.7. AASHTO M320 Performance Grading of Blends (AASHTO M 320-10 2010) .....   | 24   |
| Figure 2.8. Log Shift Factors ( $\log(a(T))$ ) vs. Temperature for Method 1 and 2 .....  | 39   |
| Figure 2.9. Depiction of SCB Test Specimen with Knives Glued On, SCB Test Specimen Dimensions .....                                  | 42   |
| Figure 2.10. SCB Test Loading Setup .....  | 43   |
| Figure 2.11. Status of WMA Implementation in 2010 (NCAT 2012) .....  | 47   |
| Figure 2.12. WMA Production as a Percentage of Total Asphalt Mix Production (Hansen and Copeland 2013) .....                         | 47   |
| Figure 3.1. Molecular Changes from Corn to Isosorbide .....  | 59   |
| Figure 3.2. Separation Test Results for Montana Binder PG 64-22 for 2% and 5% IDB .....  | 65   |
| Figure 3.3. Separation Test Results for Polymer Modified Montana Binder PG 70-22 for 2% and 5% IDB .....                             | 65   |
| Figure 3.4. Separation Test Results for Texas Binder PG 67-22 for 2% and 5% IDB .....  | 66   |
| Figure 3.5. Bending Beam Rheometer Test Results .....  | 70   |
| Figure 3.6. Average Number of Gyration to 62.5mm with 95% Confidence Intervals ...   | 71   |



|  |     |
|--|-----|
| Figure 4.1. Mix Design Gradation Chart (12.5mm NMAS).....  | 85  |
| Figure 4.2. Final Alternate Version of the Modified Hirsch Model .....                                     | 93  |
| Figure 4.3. Log Shift Factors ( $\log(a(T))$ ) vs. Temperature for Method 1 and 2 .....                    | 100 |
| Figure 4.4. Binder G* Master Curve for Sample 2 of PG 70-22 using Method 2 .....                           | 101 |
| Figure 4.5. Short-Term-Aged High Temperature Grade of PG 64-22 using<br>Method 1 and Method 2 .....        | 104 |
| Figure 4.6. Short-Term-Aged High Temperature Grade of PG 70-22 using<br>Method 1 and Method 2 .....        | 105 |
| Figure 4.7. Comparison of all Measured E* Results across Additive and Binder<br>Type .....                 | 105 |
| Figure 4.8. Distribution of E* Results not Transformed .....   | 106 |
| Figure 4.9. Distribution of E* Results after Logarithmic Transformation .....                              | 107 |
| Figure 4.10. Distribution of E* Results after Square Root Transformation .....                             | 107 |
| Figure 4.11. Interaction Plot for A*B (Binder Type*Additive) .....   | 109 |
| Figure 4.12. Interaction Plot for A*B*C (Binder Type*Additive*Temperature (°C))...                         | 110 |
| Figure 4.13. Interaction Plot for A*B*D (Binder Type*Additive*Frequency (Hz)) .....                        | 111 |
| Figure 4.14. Back-Calculated Hirsch Binder G* vs. Measured Binder G* at 1.59<br>Hz for PG 64-22 .....      | 112 |
| Figure 4.15. Back-Calculated Hirsch Binder G* vs. Measured Binder G* at 1.59<br>Hz for PG 70-22 .....      | 112 |
| Figure 4.16. Back-Calculated Al-Khateeb Binder G* vs. Measured Binder G* at<br>1.59 Hz for PG 64-22 .....  | 115 |
| Figure 4.17. Back-Calculated Al- Khateeb Binder G* vs. Measured Binder G* at<br>1.59 Hz for PG 70-22 ..... | 115 |
| Figure 4.18. Predicted vs. High Temperature Grades for PG 64-22.....                                       | 117 |
| Figure 4.19. Predicted vs High Temperature Grades for PG 70-22.....  | 117 |
| Figure 5.1. Visual Description of Process in @RISK.....  | 135 |
| Figure 5.2. Pavement: Structure Designs for Various Traffic Levels.....                                    | 139 |

|   |     |
|---|-----|
| Figure 5.3. Locations of Climatic Files Used in AASHTOWare .....  | 140 |
| Figure 5.4. Comparison of all Measured E* Results across Additive and Binder Type.....  | 141 |
| Figure 5.5. Distribution of E* Results not Transformed .....  | 141 |
| Figure 5.6. Distribution of E* Results after Logarithmic Transformation .....   | 142 |
| Figure 5.7. Distribution of E* Results after Square Root Transformation .....   | 142 |
| Figure 5.8. Plot for B (Additive) using Least Squares (LS) Means.....   | 144 |
| Figure 5.9. 50% and 95% Reliability Measured E* Results Shifted with Reduced Frequency .....  | 145 |
| Figure 5.10. Comparison of Average G* Results Used in AASHTOWare.....   | 146 |
| Figure 5.11. Comparison of Average Phase Angle Results Used in AASHTOWare.....  | 146 |
| Figure 5.12. Comparison of AC Bottom Up Cracking Results .....  | 152 |
| Figure 5.13. Comparison of Asphalt Concrete Rutting Results.....  | 154 |
| Figure 5.14. Comparison of Total Pavement System Rutting Results .....  | 154 |
| Figure 5.15. Comparison of Smoothness/International Roughness Index (IRI) Results .....   | 155 |
| Figure 6.1. Mix Design Gradation Chart (12.5mm NMAS).....   | 166 |
| Figure 6.2. Recovery vs. $J_{nr3.2}$ for MSCR Results.....  | 169 |
| Figure 6.3. Fracture Energy Results .....   | 173 |
| Figure 6.4. Fracture Energy Results .....   | 173 |
| Figure 6.5. Stiffness Results .....   | 174 |
| Figure 6.6. Least Square Means Plots and Student's t test for Additive Choice, 1 <sup>st</sup> Fracture Energy, 2 <sup>nd</sup> Fracture Toughness, and 3 <sup>rd</sup> Stiffness from Top to Bottom..... | 178 |
| Figure 7.1. Average SCB Stiffness Results at 4% Air Voids .....   | 195 |
| Figure 7.2. Average SCB Stiffness Results at 7% Air Voids .....   | 196 |

|  |     |
|--|-----|
| Figure 7.3. Average BBR Stiffness Compared to Average SCB Stiffness at Low Temperature PG+10 .....               | 198 |
| Figure 7.4. Average BBR Stiffness Compared to Average SCB Stiffness by Binder Type at Low Temperature PG+10..... | 199 |

## LIST OF TABLES

|   | Page |
|---|------|
| Table 2.1. List of Standards Used in Binder Rheology Testing .....  | 24   |
| Table 3.1. Binder Testing Experimental Plan Repeated for Each Binder .....  | 62   |
| Table 3.2. Mixture Testing Experimental Plan.....   | 63   |
| Table 3.3. DSR Results for Original, RTFO Aged and PAV Aged Binders .....   | 67   |
| Table 3.4. IDB Mass Loss.....   | 67   |
| Table 3.5. Bending Beam Rheometer Test Results .....  | 70   |
| Table 3.6. Tukey HSD Multiple Comparison for Compactability.....  | 72   |
| Table 3.7. Tensile Strength Ratios.....   | 73   |
| Table 3.8. Average IDT Strength Values.....   | 74   |
| Table 4.1. Mix Design Gradation and Supplier Information .....  | 85   |
| Table 4.2. Results from Comparing Methods Used in Constructing Binder G*<br>Master Curves.....                    | 102  |
| Table 4.3. ANOVA of ROOT(E*, MPa) Results Using Split Plot Repeated Measure<br>Design .....                       | 108  |
| Table 5.1. Mix Design Gradation and Supplier Information .....  | 131  |
| Table 5.2. Compiled Output for PG 64-22 with No Additive Using @RISK .....  | 136  |
| Table 5.3. Example of Data used for E* <sub>mix</sub> in AASHTOWare Pavement ME Design...                         | 137  |
| Table 5.4. Example of RTFO Aged DSR Results Used in AASHTOWare .....  | 138  |
| Table 5.5. General Traffic Information.....   | 139  |
| Table 5.6. ANOVA of ROOT(E*, MPa) Using Split Plot Repeated Measure Design ..                                     | 143  |
| Table 5.7. Tukey Honestly Significant Differences Comparison for Additive (B) .....                               | 145  |
| Table 5.8. ANOVA of G* and Phase Angle Using Split Plot Repeated Measure<br>Design .....                          | 147  |
| Table 5.9. Tukey Honestly Significant Differences Comparison of G* (Pa) for<br>Additive (B) within PG 64-22 ..... | 148  |

|   |     |
|---|-----|
| Table 5.10. Tukey Honestly Significant Differences Comparison of Phase Angle (*) for Additive (B) within PG 64-22 ..... | 148 |
| Table 5.11. Tukey Honestly Significant Differences Comparison of G* (Pa) for Additive (B) within PG 70-22 .....         | 149 |
| Table 5.12. Tukey Honestly Significant Differences Comparison of Phase Angle (°) for Additive (B) within PG 70-22 ..... | 149 |
| Table 6.1. MSCR Results.....  | 169 |
| Table 6.2. Average BBR Results for PG 64-22 .....   | 171 |
| Table 6.3. Average BBR Results for PG 70-22 .....   | 171 |
| Table 6.4. ANOVA Results for Fracture Energy.....   | 176 |
| Table 6.5. ANOVA Results for Fracture Toughness.....  | 176 |
| Table 6.6. ANOVA Results for Stiffness.....   | 177 |
| Table 7.1. Mix Design Gradation and Source Information .....  | 190 |
| Table 7.2. Summary of BBR Results.....  | 193 |
| Table 7.3. ANOVA Results for BBR Stiffness at -12°C .....   | 194 |
| Table 7.4. SCB Stiffness Results at 4% Air Voids.....   | 195 |
| Table 7.5. SCB Stiffness Results at 7% Air Voids.....   | 196 |
| Table 7.6. ANOVA Results for SCB Stiffness at -12°C.....  | 197 |

## ACKNOWLEDGEMENTS

First, I would like to thank God for all the blessings and opportunities that have been bestowed upon me through this long road called graduate school. I would not have made it if not for the support, love, and encouragement from both my family and friends. My wife and children have especially sustained me through this long journey.

This research work was conducted under the supervision of Dr. R. Christopher Williams, from the Department of Civil, Construction and Environmental Engineering of Iowa State University, whom I would like to give many thanks for the guidance, patience, and assistance given to me throughout my doctoral studies. I would also like to express my thanks to my other committee members, Drs. Vernon Schaefer, Kejin Wang, Jeramy Ashlock, and W. Robert Stephenson, for their guidance and support throughout my studies, research, and dissertation.

Graduate school has been an experience that will forever enrich my life. I would like to thank the present and former graduate students from my research group (Dr. Ashley Buss, Dr. Sheng Tang, Andy Cascione, Jianhua Yu, Dr. Joana Peralta, Ka Lai Ng, M.D. Rahman, Dr. Can Chen, Dr. Mohamed Rashwan, Oscar Echavarria, Yu Kuang, Grace Mercado, Zahra Sotoodeh, Paul Ledtje, Carlie Mander, and Conglin Chen). I would also like to thank the support staff whom I have had the opportunity to work with every day throughout my doctoral studies. Thank you for all the help in the laboratory and in the field. I have enjoyed working together and building life-long friendships.

## ABSTRACT

Historically, growth of bio-based chemical products in the world market has typically been stunted due to their higher production costs as compared to crude petroleum derived products. However due to the rising cost of oil, increasing demand for environmentally friendly products from a growing population and limited amount of nonrenewable resources, growth for bio-based chemical products has increased. This market growth has propelled the number and size of bio-refineries to increase in the past 10 years.

However, the rise in the cost of oil has been accompanied by soaring prices for asphalt because of reductions in its supply. This reduction is primarily due to oil refiners maximizing on the production of transportation fuels through coking. As a result, a substantial amount of binder is produced that cannot be used for production of asphalt mixtures.

Warm mix asphalt occurs when mixing and compaction temperatures are lowered by 20°C to 55°C in the production and laydown of asphalt mix. This has also led to the development of bio-derived material additives for warm mix asphalt applications. Depending on the production process, bio-refineries can produce a sizable amount of material with surfactant characteristics. Due to surfactant characteristics, these materials can be used as a bio-based warm mix asphalt (WMA) additive technology.

Within this thesis, a bio-derived material - isosorbide distillation bottoms (IDB) - was studied as a warm mix asphalt additive technology, as opposed to other commercially available additive technologies, through a thorough examination of binder

rheology and mix performance with various asphalt binders. The first step of this study was to investigate binder rheology to determine the optimum dosage rate of the IDB to various asphalt binders for use in warm mix asphalt. This part of the work resulted in an estimated dosage rate of 0.5% by weight of the total binder. Then, the additive was blended at the recommended dosage rate of 0.5% to create binders for use in mix production. Warm mix asphalt mixtures were produced for testing at intermediate and low temperatures and compared to warm mix asphalt without an additive and with commercially available additives at the recommended dosage rate. The results showed that IDB performs statistically the same as the other commercial additives; as well as, the same as the control mix. IDB neither harms nor benefits the mixes.



## CHAPTER 1. INTRODUCTION

### 1.1. Background

The notion or idea of warm mix asphalt (WMA) came about when the European Union (EU) started creating more sustainable technologies after the ratification of the Kyoto Protocol in the mid-1990s. Several companies in Europe researched different ways of implementing the Kyoto Protocol, one of which was to lower emissions by reducing production temperatures in asphalt mix plants. This brought about the creation of WMA. WMA was first introduced in the United States by the National Asphalt Pavement Association (NAPA) in 2002. In 2003, a joint meeting was held between NAPA, the Federal Highway Administration (FHWA), and the National Center for Asphalt Technology to explore further opportunities for WMA use in the United States. The next year, the “World of Asphalt Show and Conference” had a live demonstration of WMA being made. In 2007, the Federal Highway Administration’s International Technology Scanning Program organized a team of U.S. experts to visit four European countries and evaluate whether WMA use in the United States was feasible. After the visit, the team of experts recommended WMA as an alternative to HMA for use in the United States (D'Angelo 2008; Newcomb 2007).

Warm mix asphalt technologies reduce binder viscosity as well as mixing and compaction temperatures by 20-55°C during asphalt mix production and laydown. Reducing mixing temperatures provides the asphalt industry the ability to both lower their carbon footprint and save money due to reduced energy use in mixing plants. Due to the reduced binder viscosity, compaction temperatures in the field can be reduced

which improves mix compactibility, extends the paving season, allows longer haul distances, and increases the potential for using more reclaimed asphalt pavement (RAP) in mixes. Reductions in both mixing and compacting temperatures also lessen the fumes workers are exposed to during the production and laydown process of an asphalt mix (Button et al. 2007; D'Angelo 2008; Gandhi 2008; Hassan 2009; Hurley and Prowell 2006; Jenkins et al. 1999; Kim et al. 2012; Kristjánsdóttir 2006; Kristjánsdóttir et al. 2007; Larsen et al. 2004; Perkins 2009; Prowell et al. 2007).

WMA technologies are generally split between four groups: foaming – water based, foaming – water bearing additive, chemical additive, and organic/bio-derived additive. The first of the two foaming technologies (water based) is physical in terms of the production process due to introduction of water to create the foaming effect. There are two main methods for foaming (water based) asphalt at lower temperatures – the WAM-foam method and the Astec Double Barrel Green method (Anderson et al. 2008; Koenders et al. 2002; Middleton and Forfylow 2009). The second foaming technology (water bearing additive) creates the foaming effect in asphalt through the release of water from additives during the mixing process. The two most commonly used water bearing additive technologies are Advera and Aspha-min (Anderson et al. 2008; Hossain et al. 2011; Hurley and Prowell 2005a). Both chemical and organic/bio-derived additives when blended to asphalt binder reduce the binder viscosity. Commonly used chemical and organic/bio-based additives in WMA are Evotherm® 3G, Sasobit®, and Asphaltan B (Button et al. 2007; Corrigan 2006; Hurley and Prowell 2005b; Hurley and Prowell 2006).

## 1.2. Problem Statement & Objectives

Historically, growth of bio-based chemical products in the world market has been stunted due to their higher production costs as compared to crude petroleum derived products. However due to the rising cost of oil, increasing demand for environmentally friendly products from a growing population and limited amount of nonrenewable resources, growth for bio-based chemical products has increased. This market growth has propelled the number and size of bio-refineries to increase in the past 10 years. Furthermore, with the rise in the cost of oil, asphalt prices have soared due to reductions in its supply. This reduction is primarily due to oil refiners maximizing on the production of transportation fuels through coking. As a result, a substantial amount of binder is produced that cannot be used for production of asphalt mixtures. Warm mix asphalt occurs when mixing and compaction temperatures are lowered by 20°C-55°C in the production and laydown of asphalt mix (D'Angelo 2008). This has also led to the development of bio-derived material additives for warm mix asphalt application. Depending on the production process, bio-refineries can produce a sizable amount of material with surfactant characteristics. Due to surfactant characteristics, these materials can be used as bio-based warm mix asphalt (WMA) additive technologies.

Isosorbide distillation bottoms (IDB) is a recently bio-derived co-product from corn that has surfactant properties. IDB is produced from the conversion of sorbitol to isosorbide by using sorbitan to perform a dehydration reaction twice. Sorbitol is produced by hydrogenating the glucose from the corn biomass (Werpy et al. 2004). In the past the cost for producing a bio-based WMA additive such as IDB would not have been viable due to the lower cost of petro-chemical based additives (Werpy et al. 2004).

With the increasing number and growth of emerging markets around the globe as well as increasing demand for bio-based renewable products, a bio-based WMA additive such as IDB becomes viable from an economic and environmental perspective. However, a bio-based material must also be viable in terms of performance as compared to the material it is intended to replace (Werpy et al. 2004). The main objective of this dissertation is to examine the performance of IDB as compared to alternative or commercially available WMA chemical and organic based additives through binder testing and mix testing, in order to see if IDB could be another viable WMA additive.

### **1.3. Research Methodology**

To achieve the main objective of this research work, a comprehensive study of several WMA chemical and organic additive technologies in binder and mix performance must be done. The first phase of this doctoral work includes a thorough literature review covering the main topic in question with discussion of methods used to achieve this goal. This research work was done through the review of relevant publications from international journals, conference papers and proceedings, and technical meetings, along with electronic scientific documents.

The next phase of this research work is the study of IDB as an additive with several asphalt binders. Within this phase, the main focus is the determination of the optimum dosage rate at which IDB can be used for each of the binders. Another section of this phase covers the rheology of commercially available WMA additives in asphalt binders. Therefore, Phase 2 is the study of the rheological properties of IDB when used as

an additive in warm mix asphalt binder and conversely, the study of rheological properties of WMA additives currently used in warm mix asphalt binders.

The investigation of moisture susceptibility and compaction in warm mix asphalt samples with and without IDB is covered in Phase 3. Within this phase, moisture susceptibility of hot and warm mix asphalt mixtures is measured using the modified Lottman test (AASHTO T 283-07 2007). Currently, AASHTO T 283 is being phased out and replaced by the Hamburg Wheel-Track test (AASHTO T 324-11 2011). The latter is used to measure rutting resistance and moisture susceptibility. Mix compactibility comparisons were evaluated between warm mix asphalt and hot mix asphalt using the average number of gyrations needed to compact each group's samples. Since bio-derived WMA additives such as IDB are new products, it is advantageous to collect and report data that shows no adverse impacts on mix compactability.

After determining that IDB did not negatively impact the compaction or moisture susceptibility of warm mix asphalt, IDB was used further in mix performance testing and binder characterization to examine the dynamic modulus of the mix and the binder shear complex modulus. Within Phase 4, performance of IDB was compared to that of select commercially available warm mix asphalt additives – all used with the same binders at the same dosage rate and with the same mix gradation. An end goal of Phase 4 was to see if it was possible to back calculate to the high temperature binder performance grade if the dynamic modulus mix test results were known.

The main objective of Phase 5 was to examine if IDB additive negatively impacted warm mix asphalt performance at low temperatures, as compared to control warm mix asphalt with no additive, by studying low temperature fracture mechanics

through the semi-circular bend (SCB) test. Within Phase 5 comparisons were made to low temperature performance of asphalt binders modified with commercially available WMA additives. Low temperature binder testing was done to binders with and without the additives using the bending beam rheometer to find creep stiffness and determine the low temperature grade. Another aspect of this study was to see if a correlation exists between the stiffness gained in mix testing and the creep stiffness gained in binder testing at low temperatures.

Phase 6 encompasses the use of the AASHTOWare Pavement ME Design program from the American Association of State Highway and Transportation Officials (AASHTO). This program is a mechanistic empirical pavement design software program that allows an engineer to estimate pavement performance using both engineering mechanics and historical data from the field. The program uses mechanistic models and historical calibrated data from the field to predict pavement responses due to traffic loads and pavement performance. Within this phase, the program will be used to compare and contrast pavement performance between control groups, groups with commercially available WMA additives, and groups with IDB.

Lastly, Phase 7 is the culmination of the previous phases that form this doctoral dissertation. This was done by writing about the work accomplished within this research, as well as proposing new topics for future research that are of critical importance for bio-based product development within warm mix asphalt. The research work presented in this dissertation was validated through the dissemination of publications and presentations at international conferences. The publications that make up this dissertation show that the

research was properly done and that there is a future for bio-based warm mix asphalt additives in the current market.

#### **1.4. Dissertation Organization**

This PhD dissertation presents a thorough review of the methodology, results, analysis and discussion gained from investigating bio-derived materials and chemical technologies as sustainable warm mix asphalt additives. The dissertation is divided into eight chapters, composed of an introduction, literature review, five research articles, and a summary. The eighth or summary chapter contains the final conclusions and gives recommendations on new topics for future investigations. Each of the five research chapters contain an article that was submitted to or published by an international journal or conference. The five articles/chapters (chapters three through seven) discuss different facets of the research done within this study and fulfill the main objective of this investigation by presenting findings for bio-based and chemical materials technologies used as warm mix asphalt additives. A flow chart of how this dissertation is organized is displayed in Figure 1.1.

After the introduction, Chapter Two presents the literature review. The literature review covers the history of warm mix asphalt, benefits of warm mix asphalt use, technologies used to produce warm mix asphalt, test methodologies used in this investigation, and the current use of warm mix asphalt in the United States. Chapter Three is the first article, which covers the rheology of three asphalt binders with IDB at varying dosage rates and studies mix compactibility and moisture susceptibility of warm mix asphalt with IDB against that of hot mix asphalt. Chapter three was a joint project

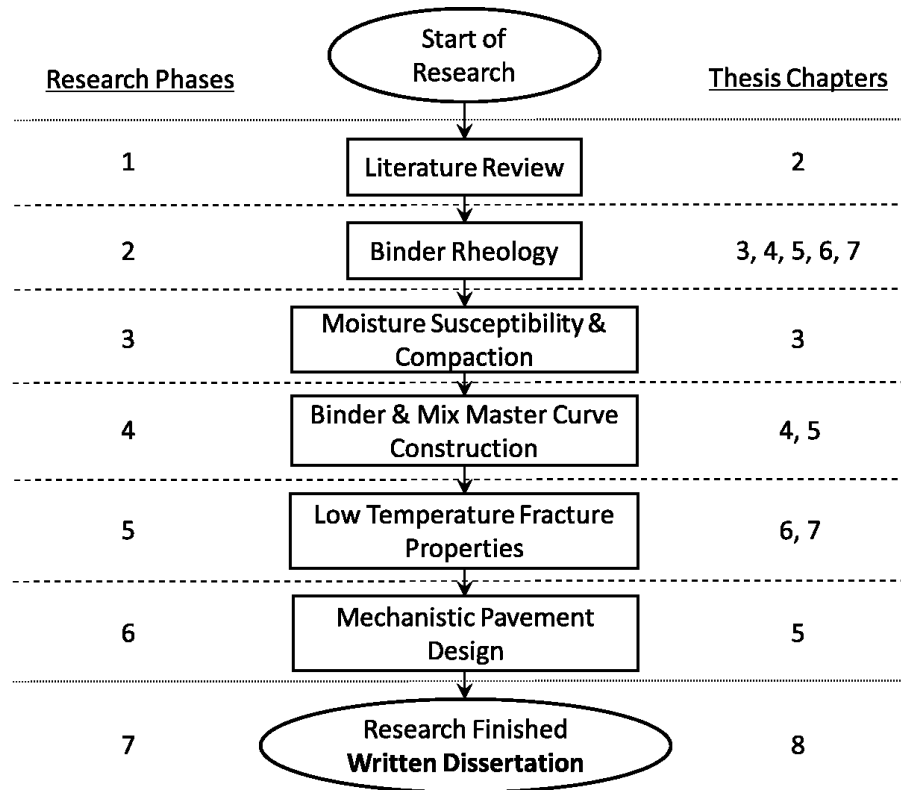


**Figure 1.1. Relationship between Research Methodology and Dissertation Layout**

between Dr. Ashley Buss, Joseph Podolsky, Dr. Williams, and Dr. Cochran in both research testing, analysis and writing of the journal paper. Each author put in an equal amount of work into the development and publication of the paper. Next, Chapter Four contains an article detailing whether mix performance results from the dynamic modulus test can be used to back calculate to the binder shear complex modulus at high temperature for warm mix asphalts containing various bio-based and chemical additives.

Chapter Five consists of an article where pavement performance is studied between WMA with and without bio-based and chemical additives using a mechanic based empirical pavement design program. Chapter Six has an article that contrasts fracture and binder performance of select bio-based and chemical additives against a



control at low temperatures. Chapter Seven contains a study that examines if a relationship exists between mix fracture stiffness and binder creep stiffness at low temperatures. Finally, Chapter Eight contains conclusions and recommendations for future research projects.

## 1.5. References

- Anderson, R., Baumgardner, G., May, R., & Reinke, G. (2008). Engineering properties, emissions, and field performance of warm mix asphalt technologies *NCHRP 9-47, Interim Report*. Washington D.C.: National Cooperation Highway Research Program.
- Button, J. W., Estakhri, C., & Wimsatt, A. (2007). A synthesis of warm mix asphalt *Rep. No. FHWA/TX-07/0-5597-1*. College Station, TX.: Texas Transportation Institute.
- Corrigan, M. (2006). Warm mix asphalt technologies and research. *Federal Highway Administration Office of Pavement Technology*, 3(10), 26-28.
- D'Angelo, J., et al. (2008). Warm-mix asphalt: European practice *Publication FHWA-PL-08-007*: FHWA, U.S. Dept. of Transportation, Washington, DC.
- Gandhi, T. (2008). *Effects of warm asphalt additives on asphalt binder and mixture properties*. Ph.D. dissertation, Clemson Univ., Clemson, SC.
- Hassan, M. (2009). *Life-cycle assessment of warm-mix asphalt: An environmental and economic perspective*. Paper presented at the Transportation Research Board 88th Annual Meeting.
- Hossain, Z., Zaman, M., O'Rear, E., & Chen, D. (2011, June 9-11). *Effectiveness of Advera in Warm Mix Asphalt*. Paper presented at the ASCE GeoHunan 2011.
- Hurley, G. C., & Prowell, B. D. (2005a). Evaluation of Aspha-Min zeolite for use in warm mix asphalt *NCAT Rep. No. 05-04*. Auburn, AL.: National Center for Asphalt Technology.
- Hurley, G. C., & Prowell, B. D. (2005b). Evaluation of Sasobit for use in warm mix asphalt *NCAT Rep. No. 05-06*. Auburn, AL.: National Center for Asphalt Technology.
- Hurley, G. C., & Prowell, B. D. (2006). Evaluation of Evotherm for use in warm mix asphalt *Rep. No. 06-02 (Vol. 6)*. Auburn, AL.: National Center for Asphalt Technology.
- Jenkins, K., De Groot, J., van de Ven, M., & Molenaar, A. (1999). *Half-warm foamed bitumen treatment, a new process*. Paper presented at the 7th Conference on asphalt pavements for Southern Africa (CAPSA 99).
- Kim, H., Lee, S., & Amirhanian, S. (2012). Influence of Warm Mix Additives on PMA Mixture Properties. *Journal of Transportation Engineering*, 138(8), 991-997. doi:10.1061/(ASCE)TE.1943-5436.0000406

- Koenders, B., Stoker, D., Robertus, C., Larsen, O., & Johansen, J. (2002). *WAM-Foam, asphalt production at lower operating temperatures*. Paper presented at the Ninth International Conference on Asphalt Pavements, Copenhagen, Denmark.
- Kristjánssdóttir, Ó. (2006). *Warm-mix asphalt for cold weather paving*. Master's thesis, Univ. of Washington, Seattle, WA.
- Kristjánssdóttir, Ó., Muench, S. T., Michael, L., & Burke, G. (2007). Assessing potential for warm-mix asphalt technology adoption. *Transp. Res. Rec.*, 2040, 91-99.
- Larsen, O., Moen, Ø., Robertus, C., & Koenders, B. (2004). *WAM Foam asphalt production at lower operating temperatures as an environmental friendly alternative to HMA*. Paper presented at the 3rd Eurasphalt & Eurobitume Congress.
- Middleton, B., & Forfylyow, R. W. (2009). Evaluation of warm-mix asphalt produced with the double barrel green process. *Transp. Res. Rec.*, 2126, 19-26.
- Newcomb, D. (2007). An introduction to warm-mix asphalt. Retrieved August, 2, 2013.
- Perkins, S. W. (2009). Synthesis of warm mix asphalt paving strategies for use in Montana highway construction *Rep. No. FHWA/MT-09-009/8117-38*. Helena, MT.: Western Transportation Institute.
- Prowell, B. D., Hurley, G. C., & Crews, E. (2007). *Field performance of warm-mix asphalt at the NCAT test track*. Paper presented at the Transportation Research Board 86th Annual Meeting.
- Werpy, T. A., Holladay, J. E., & White, J. F. (2004). Top Value Added Chemicals From Biomass: I. Results of Screening for Potential Candidates from Sugars and Synthesis Gas (pp. Medium: ED; Size: PDFN).

## CHAPTER 2. LITERATURE REVIEW

During asphalt mix and laydown, warm mix asphalt (WMA) enables reductions in viscosity and reductions in mixing and compaction temperatures by as much as 20°C-55°C. These reductions in temperatures are made possible through the use of additives and technologies to produce WMA. By lowering the temperatures at which asphalt mix is mixed and compacted, money is saved due to lower fuel use; less fuel consumption also reduces the carbon footprint. By reducing binder viscosity, lower compaction temperatures can be used in the field; which in turn improves mix compactibility. This also extends the time paving can be done and allows for longer haul distances. In addition, reductions in viscosity allow for increased use of reclaimed asphalt pavement (RAP) in a mix. An added benefit from lower mixing and compacting temperatures is that less fumes are produced so workers are exposed to fewer harmful gasses (Button et al. 2007; D'Angelo 2008; Gandhi 2008; Hassan 2009; Hurley and Prowell 2006; Jenkins et al. 1999; Kim, H. et al. 2012; Kristjánsdóttir 2006; Kristjánsdóttir et al. 2007; Larsen et al. 2004; Perkins 2009; Prowell et al. 2007).

The primary focus of this literature review is to assemble the latest WMA research and findings, while the secondary focus is to include a brief history of the development of WMA. Within the literature review, early studies in WMA research are summarized and an overview of WMA technologies is also presented. Since the inception of WMA in the United States, the main concern of the asphalt industry has been moisture susceptibility. Other research areas that are presented include binder rheology, compaction, dynamic modulus, low temperature fracture, MEPDG, and DARWIN-ME.

A brief overview of studies involved with monitoring of emissions and fuel benefit quantification as well as the present use of WMA and its technologies in the United States is also included in this literature review. Warm mix asphalt is a very important topic in Iowa as well as the rest of the world.

## **2.1. Warm Mix Asphalt Background**

The concept of warm mix asphalt was created in the 1950s with the development of foamed asphalt by Professor L. H. Csanyi from Iowa State University (Csanyi 1959). By using a specially developed foaming device as shown in Figure 2.1, saturated steam at a pressure of 40 psi could be introduced into asphalt binder. The equipment enabled controlled foaming of the asphalt binder. Foaming asphalt binder through this process made it possible to improve the coating of cold, wet aggregates and/or soils primarily due to reduced viscosity at lower temperatures. The patent rights for Csanyi's foaming process were obtained by Mobil of Australia in 1968. The process was modified by partially replacing steam with 1-2% cold water and using a more rigorous mixing process. Later studies showed that there were no differences between using steam or water in the process nor in the resulting foamed asphalt mix. However, using water required less energy so water replaced steam as the main component in this process (Lee 1980).

During the mid-1980s foamed asphalt was studied more extensively. It was observed in these studies that curing temperature, length of curing, and the surrounding moisture conditions impacted the strength of asphalt mixtures made with sand and recycled asphalt pavement (RAP) (Roberts et al. 1984). Over the next decade, very few

studies were undertaken in warm mix asphalt. This changed when the European Union (EU) developed more sustainable technologies after the ratification of the Kyoto Protocol in the mid-1990s. Several companies in Europe researched different ways to implement the Kyoto Protocol, one of which was to lower emissions by reducing production temperatures in asphalt mix plants (Jones 2004). This brought about the creation of the modern form of warm mix asphalt by means of additives and/or processes (Newcomb 2007). Shell filed a patent in 1995 for a two-component process for producing warm mix asphalt (Harrison and Christodoulaki 2000). This patented process became known as WAM-Foam® (Koenders et al. 2000).

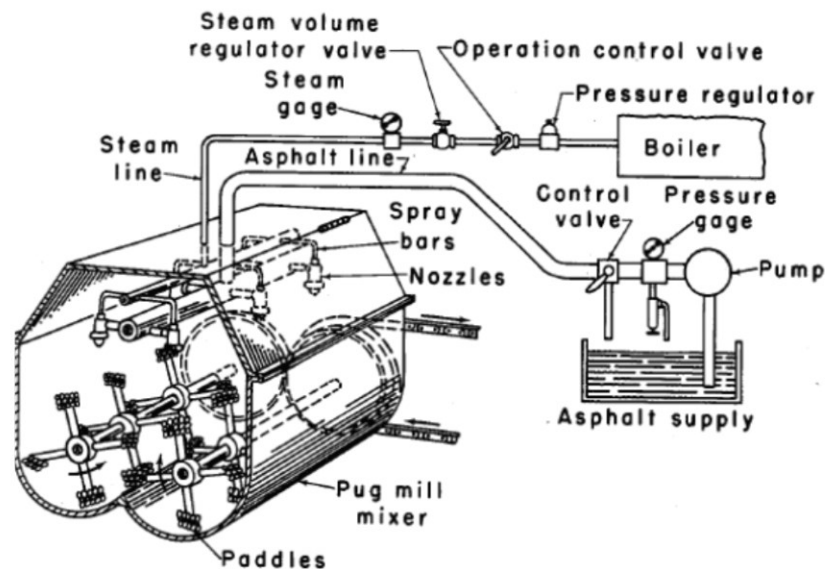


Figure 2.1. Foamed Asphalt System (Csanyi 1959)

In 1997, Sasobit®, a long chained hydrocarbon additive (organic derived) began to be marketed in Europe by the company Sasol Wax International; first, it was sold as a hot mix asphalt compaction aid and secondly, as an additive for use in the production of

warm mix asphalt (Damm et al. 2002; Hurley and Prowell 2005b). Later in 1999, a process called half-warm foamed bitumen was introduced through research from Jenkins et al.1999. Within this research work, the effects of heating aggregates at various temperatures (above ambient but below 100°C) before using them with the foamed bitumen were examined. This work showed that preheating allowed for better particle coating, mix cohesion, tensile strength as well as better compaction. This process is especially helpful when using RAP or densely graded crushed aggregates in a mix design (Button et al. 2007; Jenkins et al. 1999).

WMA was first introduced in the United States by the National Asphalt Pavement Association (NAPA) in 2002. In 2003, a joint meeting was held between NAPA, the Federal Highway Administration (FHWA), and the National Center for Asphalt Technology to explore further opportunities for WMA use in the United States. The next year, the “World of Asphalt Show and Conference” had a live demonstration of WMA being constructed. In 2007, the Federal Highway Administration’s International Technology Scanning Program organized a team of U.S. experts to visit four European countries and evaluate whether WMA use in the United States was feasible. After the visit, the team of experts recommended WMA as an alternative to HMA for use in the United States (D'Angelo 2008; Newcomb 2007).

## **2.2. Warm Mix Asphalt Technologies**

WMA technologies are generally split between four groups: foaming – water based, foaming – water bearing additive, chemical additive, and organic/bio-derived additive. The first of the two foaming technologies (water based) is physical in terms of

the production process due to introduction of water to create the foaming effect. There are two main methods for foaming (water based) asphalt at lower temperatures – the WAM-foam method and the Astec Double Barrel Green method (Anderson et al. 2008; Koenders et al. 2002; Middleton and Forfyflow 2009). The second foaming technology (water bearing additive) creates the foaming effect in asphalt through the release of water from additives during the mixing process. The two most commonly used water bearing additive technologies are Advera and Aspha-min (Anderson et al. 2008; Hossain et al. 2011; Hurley and Prowell 2005a). Both chemical and organic/bio-derived additives when blended to asphalt binder reduce the binder viscosity. Commonly used chemical and organic/bio-based additives in WMA are Evotherm® 3G, Sasobit®, and Asphaltan B (Button et al. 2007; Corrigan 2006; Hurley and Prowell 2005b; Hurley and Prowell 2006). Although chemical and organic derived additives are used throughout the studies detailed in this dissertation, it was felt that the most common methods of producing warm mix asphalt should be discussed in the literature review.

### **2.2.1. Foaming – water based**

WAM-Foam and the Astec Double Barrel Green methods are the most commonly used methods for foaming asphalt binder in Europe and the United States, respectively (Anderson et al. 2008; Koenders et al. 2002; Middleton and Forfyflow 2009). During the foaming process a given amount of water is added to hot asphalt binder. Upon combining with the hot asphalt binder, the water turns into steam and produces air bubbles throughout the binder resulting in an exponential increase in volume. This leads to a reduction in the viscosity (Middleton and Forfyflow 2009; Wielinski et al. 2009).

WAM-Foam was developed in a joint venture between Shell International Petroleum Company Ltd., London, UK, and Kolo-Veidekke, Oslo, Norway, in the mid-1990s (Larsen et al. 2004). In the United States, the patent for this process was filed in 2003 and accepted in 2005 (Larsen and Robertus 2005). Currently, BP has the patent rights for WAM-Foam in the United States, while Shell Bitumen controls the patent rights for all the other countries in the world (D'Angelo 2008). WAM-Foam is formed from two separate binder components (a soft and a hard binder) that are introduced during different stages of the mixing process. In the first stage, the soft binder component is mixed with the aggregates at a temperature between 210°F and 250°F so the binder can fully coat the aggregates. During the second stage, the hard binder in the form of foam is mixed with the soft binder coated aggregates. To achieve this, cold water is injected into the heated hard binder. This causes a rapid expansion in the mix and allows for the foamed hard binder to fully coat the already soft binder coated aggregates much more rapidly, thereby allowing a mixture to be laid out and compacted in the field at temperatures between 175°F and 195°F (Button et al. 2007). It has been reported that the production of WAM-Foam as compared to the production of typical hot mix asphalt (HMA) has led to fuel savings of 30% in plants. This in turn would lead to a 30% reduction in CO<sub>2</sub> emissions (Larsen et al. 2004).

The Astec Double Barrel Green system produced by Astec, Inc. is the most commonly used foaming warm mix asphalt method in the United States (Anderson et al. 2008; Astec Industries 2008). A schematic of the system is shown in Figure 2.2. It is installed as a modification at existing asphalt mix plants. This system uses only one stage to foam all the asphalt binder by injecting both asphalt binder and water simultaneously



into a chamber. With this process, it has been found that the temperature during laydown and compaction can be reduced by 50°F which amounts to a 14% reduction in fuel use (Astec Industries 2008). Further details about the effects of these foaming methods on mix performance will not be discussed as the research work in this dissertation focused on chemical and bio-derived additive modified warm mix asphalt.

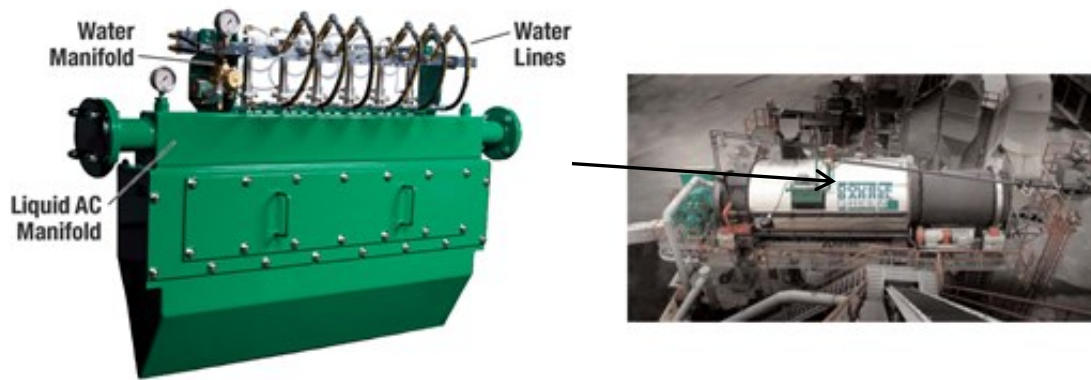


Figure 2.2. Astec Double Barrel Green System (Astec Industries 2014; Middleton and Forfylow 2009)

### 2.2.2. Foaming – water bearing additive

Water bearing additives are materials that induce foaming when added to asphalt binder. Advera® and Aspha-min® are the most commonly used water bearing additives; the former is manufactured in the United States and the later, in Europe (aspha-min GmbH 2009; PQ Corporation 2014). Both Advera® and Aspha-min® are synthetic zeolites formed from the combination of alumin-silicates and alkali metals. These additives contain by weight one fifth of crystalline water which is released when the additive is mixed with asphalt binder heated at or above 212°F. Thus, as the water is released a foaming effect is created which produces an expansion in volume. This

expansion causes a reduction in viscosity making it easier to coat aggregates more fully at a lower temperature (Anderson et al. 2008; Corrigan 2006). The zeolite based additives can both lose and absorb water, thereby having little impact on the asphalt binder rheology (Corrigan 2006; Hurley and Prowell 2005a; Yin 2009; Zaman et al. 2011). The recommended dosage rates for Advera® and Aspha-min® are 0.25% and 0.30% by weight of the total mix, respectively (Corrigan 2006; Hurley and Prowell 2005a; PQ Corporation 2009; Yin 2009; Zaman et al. 2011).



**Figure 2.3. Advera Synthetic Zeolite WMA Additive for Foaming Asphalt**

### **2.2.3. Chemical additive**

Evotherm® is a chemical additive developed in 2003 by MeadWestvaco. Over the past decade, there have been three generations of products developed from this series with the most recent generation being Evotherm® 3G/REVIX™. Evotherm® 3G/REVIX™ was co-developed by MeadWestvaco, Paragon Technical Services, Inc., and Mathy Technology and Engineering Services (Anderson et al. 2008). Evotherm® is used to produce warm mix asphalt through a dispersed asphalt technology (DAT) system of delivery. Figure 2.4 shows some of the currently used forms of Evotherm® 3G – the

Evotherm® J-1 and M1 additives. From current literature, it recommended that Evotherm® be added at a dosage rate of 0.5% by weight of the binder to asphalt bitumen (Hurley and Prowell 2006). According to MeadWestvaco, a 100°F reduction in mixing temperatures is possible with the use of Evotherm®. A reduction this large leads to substantial reductions in fuel consumption and emissions at the plant.

By using the DAT system, a unique chemistry customized for aggregate compatibility is produced and put into an emulsion (Corrigan 2006). Through the use of the DAT system with Evotherm®, aggregate coating, mixture workability and adhesion are enhanced. This is due to cationic emulsifiers present in Evotherm® additives (Takamura 2005). Currently, this chemistry is delivered with a relatively high asphalt residue (approximately 70 percent) which enables the mixture temperature to be lowered to around 203°F. Unlike traditional asphalt binders, Evotherm® is stored at 176°F (80°C). When Evotherm® is used in the field, it is pumped directly off a tanker truck (Hurley and Prowell 2006).



Figure 2.4. Warm Mix Additive Evotherm® J-1 and M1 Manufactured by MeadWestvaco

#### 2.2.4. Organic/bio-derived additive

There are three organic based additives that are currently used for the production of warm mix asphalt – Sasobit®, Sasoflex, and Asphaltan B. Sasobit® is a long chained aliphatic polymethylene hydrocarbon produced from coal gasification using the Fischer-Tropsch (FT) process; chain lengths contain between 45 – 100 carbon atoms (Corrigan 2006; Damm et al. 2002; U. S. Department of Transportation Federal Highway Administration ; Zhou et al. 2004). Sasobit® is produced by Sasol Wax of South Africa. Sasobit® has been marketed in both Europe and Asia since 1997 (D'Angelo 2008). Macrocrystalline bituminous paraffin waxes only have chain lengths that range from 25 – 50 carbon atoms (Damm et al. 2002). Having longer carbon chains leads to a higher melting point for an FT wax as compared to the melting point for a macrocrystalline bituminous paraffin wax. Thus, the FT wax can be preserved as a wax during the blending process with asphalt binder and has the ability to reduce binder viscosity at typical mixture and compaction temperatures. Sasobit® is an organic additive that can chemically alter the temperature-viscosity curve of an asphalt binder because it melts at approximately 210°F (100°C) and is fully dissolved in the asphalt binder at 240°F (116°C) as shown in Figure 2.5 (Anderson et al. 2008; Corrigan 2006; Hurley and Prowell 2005b).

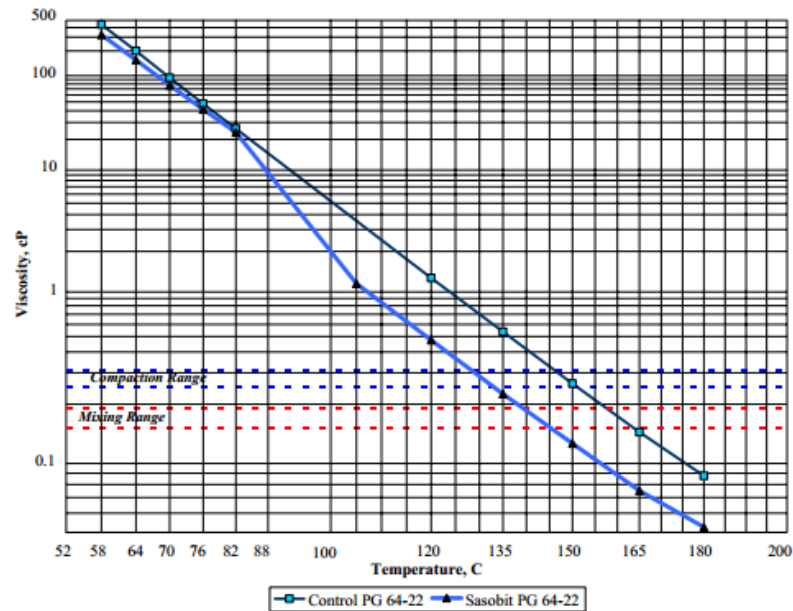


Figure 2.5. Temperature Viscosity Behavior of Asphalt Binder Modified with Organic Additive Sasobit (Hurley and Prowell 2005b)



Figure 2.6. Warm Mix Asphalt Additive Sasobit

Another benefit of longer carbon chains is that FT wax has a much smaller crystalline structure than that of a macrocrystalline bituminous paraffin wax. This means FT wax has less brittleness at low temperatures (Anderson et al. 2008; Butz et al. 2001; Damm et al. 2002; Gandhi 2008; Hurley and Prowell 2005b). A picture of Sasobit® is

shown in Figure 2.6. Sasobit® can be described as an “asphalt flow improver” and its usage allows mixture and compaction temperatures to be reduced by 32-97°F (18-54°C) (Damm et al. 2002).

It is recommended that Sasobit® be added in increments of 0.8% or more by weight of the binder and that the total amount added to binder not exceed 3 percent (Hurley and Prowell 2005b). Sasoflex is a technology developed by Sasol that modifies Sasobit® with SBS polymers using a proprietary cross-linking agent and a technology for creating transportable Super Concentrates. This process enables the high temperature performance grade (PG) to be enhanced and minimizes the impact to the low temperature performance grade (Glare Group ; Hurley and Prowell 2005b).

Asphaltan B is a combination of Montan (lignite) wax and higher molecular weight hydrocarbons. It is produced by Romonta GmbH, of Amsdorf, Germany through the extraction of lignite coal deposits using toluene solvents. Asphaltan B is specifically designed for hot rolled asphalt/fine grained HMA which is used for pavement surfacing (Corrigan 2006; Kristjánsdóttir 2006). Romonta GmbH controls 80 percent of the global market in crude mined wax products (Hurley 2006). It is recommended that an addition rate of two to four percent by weight of the binder be used and that it can be blended in the binder at the mixing plant or at an asphalt terminal (U. S. Department of Transportation Federal Highway Administration). Further, compaction temperatures can be lowered by 36°F (20°C) as compared to those typically used and its melting temperature is approximately 210°F (Button et al. 2007; Damm et al. 2002; Hurley 2006).

## 2.3. Binder and Mixture Testing Methods Used throughout Research Work

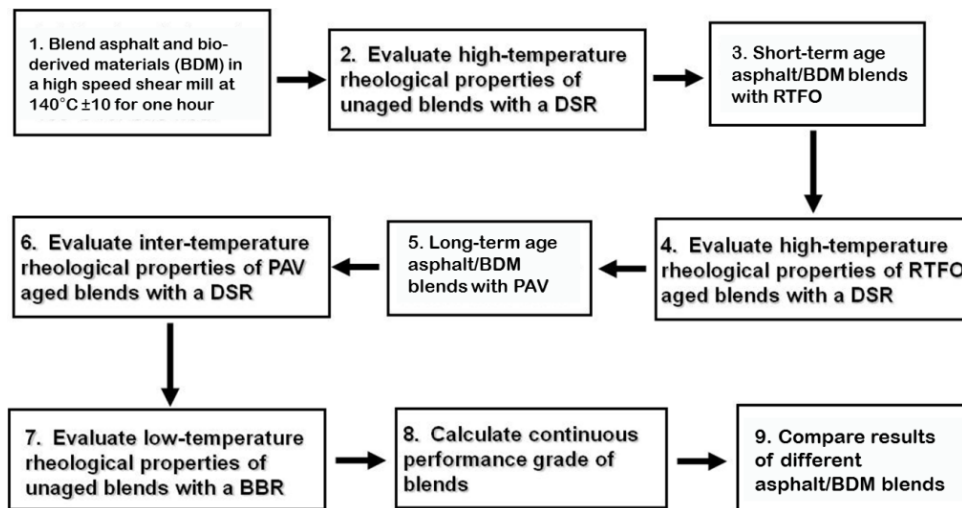
### 2.3.1. Binder rheology

To examine binder rheology Superpave criteria is used (Asphalt Institute 2003) to distinguish rheological differences between various binders, and binders modified with varying dosage rates of additives. Superpave criteria require the use of the Dynamic Shear Rheometer (DSR) (AASHTO T 315-10 2010), Rolling Thin Film Oven (RTFO) (AASHTO T 240-13 2013), Pressure Aging Vessel (PAV) (AASHTO R 28-12 2012) and the Bending Beam Rheometer (BBR) (AASHTO R 49-09 2009). To add additives to binders, a Silverson shear mill is used for blending. Temperatures at which blending should occur are dependent on the melting temperature of the additive and dependent on whether the binder is being used for warm mix asphalt or hot mix asphalt. Also binders can be evaluated for specific gravity (American Society for Testing and Materials (ASTM) 2009), rotational viscometer (AASHTO T 316-13 2013), and separation analysis (American Society for Testing and Materials (ASTM) 2014). The standards used in binder grading and the process at which the standards are used is shown in Table 2.1 and Figure 2.7 in steps 2 through 8 (AASHTO M 320-10 2010). Steps 1 through 9 of Figure 2.7 are used when additives are blended at various dosage rates with a control binder. Step 9 is used for the estimation of the optimum dosage rate of an additive

The work within this dissertation was done with the objective of comparing binders modified with new bio-derived additives to binders modified with commercially used chemical/organic additives and a hot asphalt binder control group. This was done by following the process shown in Figure 2.7 and the additional use of standards not

**Table 2.1. List of Standards Used in Binder Rheology Testing**

| Test Name                             | Aging                           | Standard Designation              | Title   | Specified for Grading |
|---------------------------------------|---------------------------------|-----------------------------------|---|-----------------------|
| Dynamic Shear Rheometer (DSR)         | Original, Short Term, Long Term | AASHTO T 315-10                   | Determining the Rheological Properties of Asphalt Binder Using a Dynamic Shear Rheometer (DSR)  | Yes                   |
| Rotational Viscometer (RV)            | Original                        | AASHTO T 316-13                   | Viscosity Determination of Asphalt Binder Using Rotational Viscometer   | Yes                   |
| Specific Gravity of Asphalt Binder    | Original                        | ASTM D70-09                       | Standard Test Method for Density of Semi-Solid Bituminous Materials (Pycnometer Method)   | No                    |
| Separation Tendency                   | Original                        | ASTM D7173 - 14                   | Standard Practice for Determining the Separation Tendency of Polymer from Polymer Modified Asphalt  | No                    |
| Rolling Thin Film Oven (RTFO)         | Short Term                      | AASHTO T 240-13                   | Effect of Heat and Air on a Moving Film of Asphalt Binder (Rolling Thin-Film Oven Test)   | Yes                   |
| Multiple Stress Creep Recovery (MSCR) | Short Term                      | AASHTO MP 19-10 & AASHTO TP 70-13 | Performance-Graded Asphalt Binder Using Multiple Stress Creep Recovery (MSCR) Test & Multiple Stress Creep Recovery (MSCR) Test of Asphalt Binder Using a Dynamic Shear Rheometer (DSR) | No                    |
| Pressure Aging Vessel (PAV)           | Long Term                       | AASHTO R 28-12                    | Accelerated Aging of Asphalt Binder Using a Pressurized Aging Vessel (PAV)  | Yes                   |
| Bending Beam Rheometer (BBR)          | Long Term                       | AASHTO R 49-09                    | Determination of Low-Temperature Performance Grade (PG) of Asphalt Binders  | Yes                   |

**Figure 2.7. AASHTO M320 Performance Grading of Blends (AASHTO M 320-10 2010)**



specified for use in binder grading as shown in Table 2.1. The main objective of this research was to identify viable bio-derived materials for use as warm mix asphalt additives. Important factors considered throughout this portion of work include various crude sources, polymer modified binders, and optimum dosage level for each of the bio-derived additives. Changes in binder properties are observed by testing binders with varying additive dosage levels at high, intermediate and low service temperatures and using the Superpave criteria.

The Rotational Viscometer (RV) is used to determine the viscosity of asphalt binders at temperatures used in mixing and compaction of asphalt concrete. For Superpave performance grade (PG) asphalt binder specification the test is always conducted at 275°F (135°C). The rotational viscometer test determines the pumpability as well as the mixing and compaction temperatures for each binder. Pumpability is a measure of how well an asphalt binder can be pumped between storage facilities and into a HMA manufacturing plant (Roberts et al. 1996). Some studies have shown that rotational viscometer test data will not always capture the full decrease in temperature that can be achieved by using WMA additives (Buss et al. 2011; Wasiuddin et al. 2007; Xiao et al. 2012). In a study done by (Rodríguez-Alloza et al. 2013), it was found that four organic additives reduced the viscosity of a binder modified with 15% rubber.

The dynamic shear rheometer (DSR) is used for characterizing the viscous and elastic behavior of asphalt binders between intermediate to high temperatures. DSR tests are conducted on unaged (original), RTFO aged, and PAV aged asphalt binder samples. Asphalt binders are viscoelastic. This means they act as both an elastic solid (recoverable deformation) and a viscous liquid (non-recoverable deformation) due to loading and

unloading. The DSR measures a specimen's complex shear modulus ( $G^*$ ) and phase angle ( $\delta$ ). The complex shear modulus ( $G^*$ ) is a sample's total resistance to deformation, and the phase angle ( $\delta$ ) is the lag between the applied shear stress and the resulting shear strain. Therefore, when the phase angle is closer to 90 degrees the material is more viscous, while when the phase angle is closer to 0 degrees the material is more elastic. The parameters  $G^*$  and  $\delta$  are used to predict whether the asphalt mix will experience rutting and/or fatigue cracking. For unaged (original) and short-term aged binder, rutting is the main concern; while for long-term aged binder, fatigue cracking is the main concern. In past research studies, WMA additives have been shown to not only reduce short-term aging effects on the rheological properties of the binder but to also retard the rate at which the stiffness grows over time as shown in DSR results (Banerjee et al. 2012).

The Rolling Thin-Film Oven (RTFO) provides a means to simulate the aging that binders experience during construction (short-term aging). Within this test, asphalt binder is exposed to air at a temperature of 163°C for 85 minutes. The RTFO also provides a means of measuring how much asphalt binder was lost due to oxidation during the test. The requirement to pass the RTFO mass loss test is achieved by having a mass loss of 1% or less. For long-term aging, the pressure aging vessel (PAV) test is used. This test simulates 7-10 years of in-service aging on the asphalt binder. The PAV test takes RTFO aged asphalt binder samples and places 50 grams of the short-term aged binder in stainless steel pans. Then the samples are aged for 20 hours in a heated vessel pressurized to 305 psi (2.10 MPa or 20.7 atmospheres). Afterwards, the PAV aged samples are placed in a vacuum degasser to rid the aged binder of air bubbles. To examine mix and

placement properties, the DSR would be used with RTFO aged binder. However, if in-service performance properties are wanted then the DSR and BBR tests would be used with PAV aged binder.

The Bending Beam Rheometer (BBR) test is used for measuring low temperature properties of long-term aged asphalt binder such as stiffness and relaxation. Stiffness and relaxation measurements give an indication of an asphalt binder's ability to resist low temperature cracking. The BBR is used to determine an asphalt binder's low temperature performance grade (PG) grade. The BBR test uses a small asphalt beam that is simply supported and immersed in a cold liquid bath. A load is applied to the center of the beam and the deflection measurements against time are obtained. Stiffness is calculated based on measured deflection and the standard beam dimensions used. The m-value is a measure of how the asphalt binder relaxes the load induced stresses when time is equal to 60 seconds.

Specific gravity testing is performed to verify mix design calculations because the specific gravity of asphalt binders changes with temperature. When buying asphalt binders from a supplier, the specific gravity given for that binder is a result of testing at 15.6° C (60° F). Typically, an asphalt binder has a specific gravity around 1.03. The average specific gravity value represents three pycnometer readings. Separation testing takes place on binders modified with polymers and additives. For this test, binder is poured in metal tubes which are placed in a 163°C oven for 24 hours. Afterwards the tubes of binder will be put in a freezer for 4 hours and then cut in thirds. For each tube, three DSR tests will be conducted on both the top and bottom thirds of the tubes using the

unaged (original) DSR testing procedure. This test is used to examine whether separation has occurred between the additive/polymer and the asphalt binder.

The Multiple Stress Creep Recovery (MSCR) test is the latest improvement to the Superpave Performance Graded (PG) Asphalt Binder specification for RTFO aged binder using the DSR (AASHTO MP 19-10 2010; AASHTO TP 70-13 2013). It provides a more accurate indication of rutting performance at high temperatures and is blind to polymer modification of an asphalt binder. The main benefits of this test are the elimination of running tests to measure elastic recovery, toughness and tenacity, and force ductility due to these tests being specifically designed to indicate whether or not an asphalt binder has been polymer modified. Using a DSR, creep and recovery are measured by applying a one-second creep load, after which the 1-second load is removed, and the sample is allowed to recover for 9 seconds. First a low stress of 0.1 kPa is applied for 10 creep/recovery cycles, and then the stress is increased to 3.2 kPa and repeated for an additional 10 cycles (Federal Highway Administration (FHWA) 2011). Polymer modified binders modified with warm mix asphalt additives tend to show increased rutting due to lower aging of the asphalt binder used with the MSCR test (Morea et al. 2012).

### **2.3.2. Moisture susceptibility and compaction**

It is not possible to prevent water from penetrating an asphalt pavement as cracks will let water in eventually. However, water infiltration can be avoided during the mixing process as long as the aggregates are adequately dried beforehand (Santucci 2002). Loss of strength and durability in asphalt mixtures caused by moisture is titled moisture damage (Little and Jones 2003). Stripping occurs when the environment, poor mix

materials, and traffic act together. Stripping is defined as the loss of the bond between aggregates and the asphalt binder. It begins at the bottom of the HMA layer and moves upward. When this process starts at the top of the HMA layer and moves downward it is known as raveling (Brown et al. 2001). For producing warm mix asphalt, the temperatures are lowered during both mixing and compaction. This could lead to inadequate drying of aggregates during the mixing process which would make warm mix asphalt more susceptible to moisture damage.

To evaluate mix compactibility between warm mix asphalt and hot mix asphalt, comparisons were made between the average number of gyrations needed to compact each groups' samples. HMA samples are mixed and compacted at 150°C, while WMA samples with bio-derived additives are mixed and compacted at 120°C. Some studies have shown that compaction in the superpave gyratory compactor (SGC) is usually independent of temperature. This is because the SGC is controlled through constant strain (Hurley 2006). More recent warm mix studies have found that there are very small differences between the compactibility of WMA and HMA at typical temperatures. This was shown by studying the measured air voids at a given compaction effort (Buss et al. 2014; Li et al. 2011). Since bio-derived WMA additives are new products, it is advantageous to collect and report data that shows no adverse impacts on mix compactability. Currently there is no standard method for measuring the compactibility/workability of an asphalt mix. This is a concern because there are limited ways to measure and evaluate the effect warm mix asphalt additives have on the workability/compactibility of a mixture in the laboratory.

To measure moisture susceptibility of hot and warm mix asphalt mixtures, moisture sensitivity tests such as the modified Lottman test (AASHTO T 283-07 2007) have been used in the past at Iowa State University and by the Iowa Department of Transportation (DOT). Currently, AASHTO T 283 has been phased out and replaced by the Hamburg Wheel-Track test (AASHTO T 324-11 2011). A brief overview of these testing methods will be discussed within this section. However, no results from the Hamburg Wheel-Track test are included in the present research work as this method was just adopted.

The original Lottman test was developed by Robert Lottman in 1978 at the University of Idaho (Lottman 1978). The laboratory procedure for fabricating samples entails the compacting of three sets of 100 mm diameter by 63.5 mm using a Marshall compactor. The three sets of specimens are tested dry or under accelerated moisture conditioning (Lottman et al. 1974). Each set was assigned different conditions before being tested: Group 1 - Control group, dry; Group 2 - vacuum saturated with water for 30-minutes; and Group 3 - vacuum saturation followed by freeze cycle at  $-18^{\circ}\text{C}$  for 15 hours and then subjected to a thaw at  $60^{\circ}\text{C}$  for 24 hours (Lottman et al. 1974). For testing the specimens, indirect tensile equipment is used to measure the tensile resilient modulus and tensile strength. Within this standard, the specimens are tested at  $13^{\circ}\text{C}$  or  $23^{\circ}\text{C}$  with a loading rate of 1.65 mm/min. The moisture damage is measured as a ratio of damage severity and is calculated by dividing the conditioned tensile strength results by the dry tensile strength results. This is the tensile strength ratio (TSR) (Lottman 1982a; Lottman et al. 1974). In NCHRP Report 246, it was recommended that the minimum allowable value be 0.70 for the TSR (Lottman 1982b).

The modified Lottman test (AASHTO T 283), “Resistance of Compacted Bituminous Mixture to Moisture Induced Damage,” was and still is the most commonly used test method for determining moisture susceptibility of HMA in the United States. It is similar to the original Lottman test, but there are a few slight differences. Instead of three groups (one control and two conditioned), there are now two groups (one control and moisture conditioned). The moisture conditioned samples now undergo vacuum saturation until a saturation level of 70% to 80% is reached. Now there is only one test temperature (25°C) and the loading rate is 50 mm/min (AASHTO T 283-07 2007). It is still recommended that minimum TSR value be 0.70, but most state DOTs have adopted a minimum TSR value of 0.80 (Roberts et al. 1996). Even though AASHTO T 283 used the Marshall mixture design, it was adopted by the Superpave system as the moisture test. Issues arose between the lab results gained and what was really happening in the field (Solaimanian et al. 2003; Stroup-Gardiner and Epps 1992). Several studies looked at different factors affecting TSR test results, such as compaction type, specimen diameter, degree of saturation, and freeze/thaw cycles. From these studies the researchers found that AASHTO T 283 does not evaluate moisture susceptibility correctly because the use of a ratio (TSR) does not measure moisture susceptibility properly as it hides information (Epps et al. 2000; Kanitpong and Bahia 2006).

With the adoption of AASHTO T 283 into Superpave and the use of the SGC instead of the Marshall compactor, the standard allowed for the use of either 150 or 100 mm samples, while the requirements remained the same. From research done in the past at Iowa State University, it was found that three freeze/thaw cycles are needed to condition the samples with 150 mm diameter produced using the SGC (Bausano et al.

2006; Kvasnak 2006). It was also found that if one freeze/thaw cycle is still used, then a TSR value of 0.87 and 0.85 should be used for SGC compacted samples with diameters 150 mm and 100 mm, respectively, to compare well in terms of probability against the TSR value of 0.80 for a 100 mm Marshall compacted sample. In essence, a TSR of 0.87 from a 150 mm SGC compacted sample would correspond to a TSR value of 0.80 from a 100 mm Marshall compacted sample (Bausano et al. 2006; Kvasnak 2006). From recent warm mix studies, it has been shown through the use of the modified Lottman test that addition of additives has improved moisture susceptibility of WMA (Sanchez-Alonso et al. 2011).

Currently AASHTO T 283 is no longer in use by the Iowa DOT, and the Hamburg test has replaced it as a measure of moisture susceptibility in asphalt mixtures. Across the United States wheel tracking tests are slowly being adopted by state agencies to replace AASHTO T 283. The Hamburg Wheel Tracking Device (HWTD) was originally manufactured in the 1970s by Esso, A. G. of Helmut-Wind Inc., Hamburg, Germany. It was initially intended to measure only rutting, but was found to be capable of testing for moisture susceptibility. It was introduced into the United States during the early 1990s by pavement engineers and officials as a technology transfer after a European asphalt study tour (European Asphalt Study Tour 1991; Yildirim and Kennedy 2001). The introduction of the HWTD initiated research to evaluate this equipment for characterization of moisture susceptibility in asphalt mixtures and prediction of field performance (Aschenbrener 1994; Aschenbrener and Far 1994; Aschenbrener 1995; Little and Choi 2007; Lu and Harvey 2006a; Lu and Harvey 2006b). The initial research found HWTD to be sensitive to aggregate quality, asphalt cement stiffness, short-term



aging duration, asphalt source or refining processes, antistripping treatments, and compaction temperatures (Aschenbrener 1994; Aschenbrener and Far 1994; Aschenbrener 1995). From recent studies of WMA with additives using the HWTD, it has been shown that resistance to permanent deformation (rutting) and stripping is decreased (Lugo et al. 2013; Mo et al. 2012).

### 2.3.3. $E^*_{\text{mix}}$ and $G^*_{\text{binder}}$ master curve construction

#### 2.3.3.1. Sigmoidal $E^*_{\text{mix}}$ master curves using measured data

The dynamic modulus test is a linear viscoelastic test used for asphalt mixtures where the complex dynamic modulus ( $E^*$ ) is determined by relating stress to strain at multiple temperatures, each under several repeated loading rates (frequencies).  $E^*$  is defined as the pavement stiffness and is a very important property because it is used to simulate a pavement's response under repeated traffic loading (Brown et al. 2009). The stiffness of an asphalt mix also depends on the temperature at which it is being loaded. When the stiffness is high under an applied stress, the asphalt mix will have lower strain. At high temperatures, high stiffness mixes are more resistant to permanent deformation, but at low temperatures, they are generally more prone to cracking (Brown et al. 2009).

The dynamic modulus test is defined as a uniaxial compression test with cyclic loading. In this test, a cyclic load is applied vertically in a sinusoidal wave form on a cylindrical sample. The complex modulus is the ratio of stress amplitude to strain in a sinusoidal wave form:

$$E^* = \frac{\sigma}{\varepsilon} = \frac{\sigma_0 \times e^{i\omega t}}{\varepsilon_0 \times e^{i(\omega t - \delta)}} = \frac{\sigma_0 \times \sin(\omega t)}{\varepsilon_0 \times \sin(\omega t - \delta)} \quad (2.1)$$

where

$E^*$  = complex modulus;

$\sigma_0$  = peak (maximum) stress;

$\varepsilon_0$  = peak (maximum) strain;

$\delta$  = phase angle (degrees);

$\omega$  = angular velocity;

$t$  = time (seconds);

$e$  = exponential; and

$i$  = imaginary component of the complex modulus (Garcia et al. 2007).

Ultimately the dynamic modulus is defined as the absolute value of the complex modulus:

$$|E^*| = \frac{\sigma_0}{\varepsilon_0} \quad (2.2)$$

where

$\sigma_0$  = maximum dynamic stress, and

$\varepsilon_0$  = peak recoverable axial strain (Garcia et al. 2007).

The complex modulus ( $E^*$ ) is made up of the storage modulus ( $E'$ ) and the loss modulus ( $E''$ ).  $E'$  deals with the asphalt concrete elastic behavior while  $E''$  deals with the viscous behavior of asphalt concrete (Kim et al. 2005), and

$$E^* = E' + iE'' \quad (2.3)$$

An asphalt mixture's dynamic modulus varies with temperature and loading frequency. Making comparisons between results from one temperature to another temperature is complicated. The development of dynamic modulus master curves provides a direct means of viewing dynamic modulus results and is much easier to interpret. A dynamic modulus master curve makes it easier to compare several sets of dynamic modulus results at various temperatures (Christensen and Anderson 1992). According to research conducted by Li and Williams (Li and Williams 2012), testing  $E^*$  values at three temperatures (4.4, 21.1, and 37.8°C) did not change the shape of master curves constructed by data from nine frequencies ranging from 25 Hz to 0.1 Hz as compared to curves based on data from 5 temperatures, each at six frequencies.

The dynamic modulus master curve is constructed using a reference temperature or frequency based on the time-temperature superposition principle. Asphalt mixtures exhibit higher dynamic modulus values at low temperatures and/or high loading frequencies. At a lower temperature, a dynamic modulus value could be equal to a dynamic modulus value gained through testing at a higher temperature but at a lower frequency. This means dynamic modulus values resulting from testing done at different temperatures and frequencies can be transposed to a single reference temperature or frequency. Dynamic modulus testing can be done easier at more frequencies and fewer temperatures than at fewer frequencies and more temperatures because of overall testing-time as it is more time consuming to change the test temperature. As a result, researchers usually test for dynamic modulus values at a few temperatures but at many different frequencies. It is much easier to transition from frequency to temperature than from temperature to frequency. A shift factor,  $a(T)$ , is used to equalize frequencies at different

temperatures. The following equation shows the mathematical expression of the shift factor,  $a(T)$ :

$$f_r = \frac{f}{a(T)} \rightarrow \log(f_r) = \log(f) - \log(a(T)) \quad (2.4)$$

$$\log(a(T)) = aT^2 + bT + c \quad (2.5)$$

where

$f_r$  = reduced frequency (loading frequency at the reference temperature);

$f$  = loading frequency;

$a(T)$  = shift factor; and

$a$ ,  $b$ , and  $c$  are coefficients for solving the shift factor  $a(T)$ .

The shift factor is equal to 1 at the reference temperature, and  $\log(a(T))$  is equal to 0. In the “2002 Guide for the Design of New and Rehabilitated Pavement Structures” the dynamic modulus master curve is fitted using the following sigmoidal function (Pellinen and Witzak 2002):

$$\log(|E^*|) = \delta + \frac{\alpha}{1 + e^{\beta + \gamma \log(t_r)}} \quad (2.6)$$

where

$|E^*|$  = dynamic modulus;

$t_r$  = reduced time at the reference temperature;

$\delta$  = minimum modulus value,  $\delta + \alpha$  = maximum modulus value; and  
 $\beta, \gamma$  = parameters describing the shape of the sigmoidal function.

The parameters that are used to create a master curve are back-calculated to match the estimated  $E^*$  values from the sigmoidal function to the  $E^*$  values resulting from lab testing with the following equation.

$$Error^2 = \sum_{i=1}^n [\log(PredictedE_i^*) - \log(MeasuredE_i^*)]^2 \quad (2.7)$$

From recent warm mix studies, it has been shown that use of additives has improved the dynamic modulus values of WMA in comparison to the performance shown by control HMA mixtures (You and Goh 2008; You and Goh 2009).

### 2.3.3.2. Predicted $G^*$ binder master curve methods from measured data

Within this dissertation two methods for constructing  $G^*b$  master curves were used. The first method (unmodified method) is a modified sigmoidal model developed by Marasteanu and Anderson (Marasteanu and Anderson 1999), while the second method is a variation of this model that was constructed by researchers at Michigan Technological University (Yao et al.). Method 2 (modified method) has further modifications that take into account the effect of phase angle. Method 1 is shown mathematically below in Equations 2.8 through 2.10 and method 2 is shown in Equations 2.11 through 2.13:

## Method 1

$$\log|G^*| = \delta + \frac{\alpha}{1 + e^{\beta + \gamma(\log t_r)}} \quad (2.8)$$

$$a(T) = \frac{t}{t_r} \quad (2.9)$$

$$\log a(T_i) = aT_i^2 + bT_i + c \quad (2.10)$$

## Method 2

$$\log|G^*| = \delta + \frac{\alpha}{1 + e^{\beta + \lambda \cos(\theta) + \gamma(\log t_r)}} \quad (2.11)$$

$$\log a(T_i) = \frac{aT_i^2 + bT_i + c}{\cos \varphi} \quad (2.12)$$

$$a(T) = \frac{t}{t_r} \quad (2.13)$$

where

$t_r$  = reduced time of loading at reference temperature (s);

$\theta$  = phase angle (°);

$\lambda$  = influence factor of phase angle;

$\delta, \alpha, \beta, \gamma$  = coefficients;

$a(T)$  = shift factor as a function of temperature;

$t$  = time of loading (s);

$T$  = temperature ( $^{\circ}\text{C}$ );

$a(T_i)$  = shift factor as a function of temperature  $T_i$ ;

$\varphi$  = shift angle; and

$a, b, c$  = coefficients for shift factor.

Both methods use the principle of time-temperature superposition to shift the measured data points from several temperatures, each with several frequencies, into one master curve at one temperature over a frequency range for the binder's complex shear modulus. Method 1 only deals with a horizontal shift in the data points, while method 2 has an added slope shift through the shift angle  $\varphi$ . The slope shift moves the data points both horizontally and vertically around the pivot point located at the reference temperature  $21^{\circ}\text{C}$  as shown in Figure 2.8. Below and above  $21^{\circ}\text{C}$ , method 2 has a smaller slope than method 1. When method 2 is below  $21^{\circ}\text{C}$ , the smaller slope means the

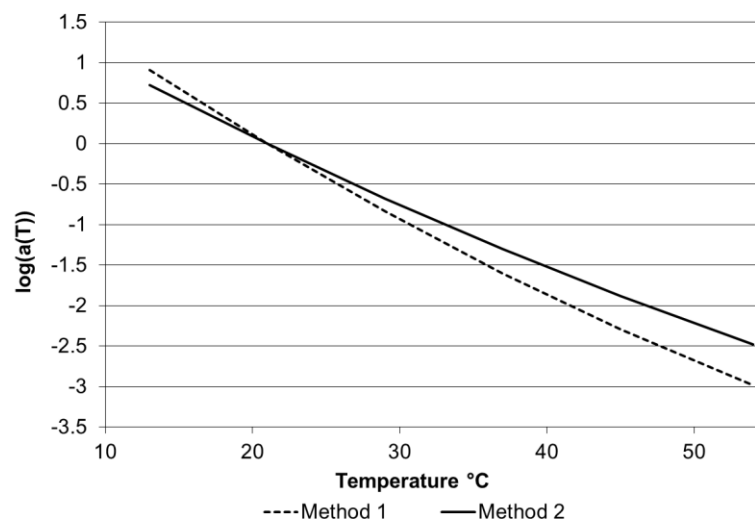


Figure 2.8. Log Shift Factors ( $\log(a(T))$ ) vs. Temperature for Method 1 and 2

shift factors are less, thereby method 2 shows the binder is more elastic below the reference temperature. When method 2 is above the reference temperature, the smaller slope shows that the shift factors are decreasing at a slower rate; this means the binder is more viscous. What this shows is that method 2 includes the impact of the phase angle. How the binder's viscoelastic properties respond to reduced frequency and reduced time determines the coefficients  $\delta$ ,  $\alpha$ ,  $\beta$ , and  $\gamma$  that are used to estimate a binder's complex shear modulus. In order to shift the data points and construct a master curve, the sum of log square error squared is minimized using Equation 2.14.

$$Error^2 = \sum_{i=1}^n [\log(G_i^*) - \log(Predicted G_i^*)]^2 \quad (2.14)$$

where

$G_i^*$  = measured asphalt binder complex shear modulus at  $i^{\text{th}}$  point; and

Predicted  $G_i^*$  = predicted asphalt binder complex shear modulus at  $i^{\text{th}}$  point.

These methods are used to construct the asphalt binder complex shear modulus as opposed to other models like the Christensen-Anderson-Marasteanu (CAM) model and the 1S2P1D model (name represents one spring, two parabolic creep elements and one dashpot), because the modified sigmoidal model has been shown to be more accurate in estimating the master curve compared to the measured data for unmodified unaged and aged binders (Christensen and Anderson 1992; Di Benedetto et al. 2004; Marasteanu and Anderson 1999; Md. Yusoff et al. 2013; Olard and Di Benedetto 2003; Yusoff et al.



2011). The above stated models have also been shown to be less accurate at estimating the asphalt binder master curve for polymer modified binders than methods 1 and 2 (Asgharzadeh et al. 2013; Hainin and Nim 2010).

#### **2.3.4. Semi-circular bend test at low temperatures**

In cold regions, the main distress observed is low temperature cracking in asphalt pavement. Under very low temperatures, the top asphalt layer shrinks; but it is constrained due to friction occurring at the interface area of the underlying layer. This produces thermal induced tensile stresses in the pavement which increase gradually as the temperature decreases until the asphalt concrete pavement cracks. Currently, specifications utilize a bending beam rheometer for low temperature characterization and do not take into account the response from the aggregate phase. The aggregate phase makes up 90-95 percent of the total weight of a typical asphalt concrete mixture. To address the impact of the aggregate phase on low temperature cracking in asphalt mixtures, a fracture mechanics-based approach is necessary. Among test methods available for measuring fracture at low temperature, the Semi-Circular Bend (SCB) test has received a considerable amount of attention because a notched SCB specimen can be easily prepared from standard laboratory compacted or field cored asphalt concrete samples (Chong and Kuruppu 1984; Krans et al. 1996; Marasteanu et al. 2004). Either mode I or mode II fracture can be studied using this testing method. The mode of fracture depends on the orientation of the initial notch. Within this research work, mode I fracture is examined. The SCB test is used to determine the fracture energy ( $G_f$ ), fracture

toughness (KIC), and stiffness (S) (Li et al. 2008; Li and Marasteanu 2004; Li and Marasteanu 2010; Lim et al. 1993; Marasteanu et al. 2012; Teshale 2012).

A vertical compressive load is applied at the top of each specimen. This produces a constant rate – crack mouth opening displacement (CMOD). The CMOD is measured using an Epsilon clip gauge located between two buttons glued at the bottom of each specimen as shown in Figure 2.9.

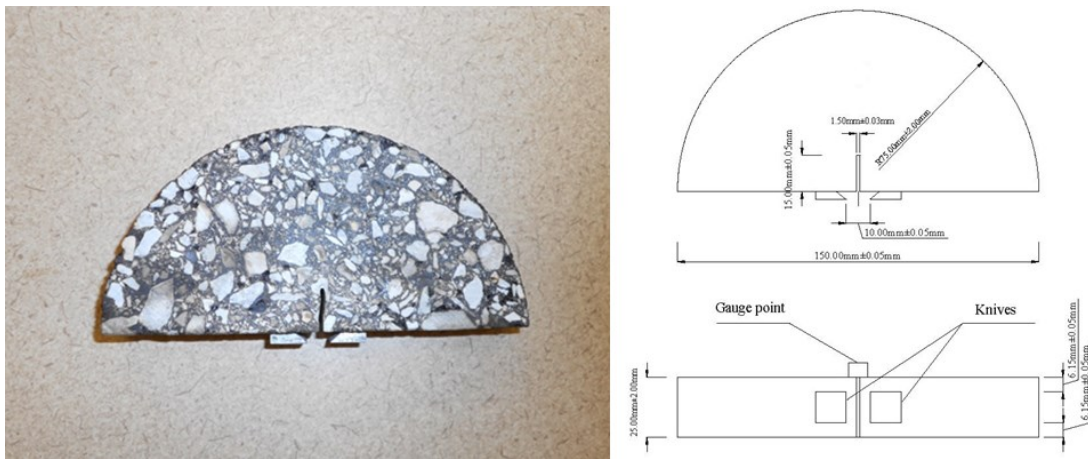


**Figure 2.9. Depiction of SCB Test Specimen with Knives Glued On, SCB Test Specimen Dimensions**

Fracture toughness is measured using the CMOD, while fracture energy is measured using load line displacement (LLD) – two vertically mounted Epsilon extensometers are attached to either side of the specimen with one button and to a specially made external frame with another button as shown in Figure 2.10. In this study, fracture energy was not computed using LLD measurements. The loading piston displacement recorded through its linear variable differential transformer (LVDT) was used instead (Marasteanu et al. 2012).



traffic loads and pavement performance. The main factors used in the analysis of pavement performance in AASHTOWare Pavement ME Design are traffic, climate/location, reliability, and pavement structure. AASHTOWare Pavement ME Design is the most recent version of the original program named the Mechanistic-Empirical Pavement Design Guide (MEPDG) developed by the National Cooperative Highway Research Program (NCHRP) in the early 2000s (National Cooperative Highway Research Program 2004).

AASHTOWare Pavement ME Design makes it possible for engineers to assign a “level of reliability” to a pavement design. A higher level of reliability will lead to a more conservative pavement design. Three levels of inputs can be used to produce a particular pavement design. Level 1 input values are the most detailed while Level 3 inputs are default values. Input level choice impacts the reliability of the performance generated for a certain pavement design as Level 3 inputs would produce more uncertainty in the results. The program also allows for the design of rehabilitated pavements. Using Level 1 inputs, an engineer can input detailed material information such as the mix dynamic modulus ( $E^*_{mix}$ ), binder complex shear modulus ( $G^*_{binder}$ ), and the phase angle ( $\delta$  - degrees). This ability allows an engineer to compare different mixtures and binders in terms of their impact on predicted pavement performance.

Past studies have shown that MEPDG is sensitive to the asphalt concrete  $E^*_{mix}$  values. This means reasonable predictions of pavement performance can be achieved using MEPDG (El-Basyouny and Witczak 2005). From recent warm mix studies, it has been shown that WMA has equal or slightly better pavement performance per results

from use of the MEPDG program (Buss et al. 2009; Buss and Williams 2012; Goh et al. 2007).

#### **2.4. Warm Mix Asphalt Emissions & Benefits**

Warm mix asphalt use can help to reduce asphalt plant emissions. Studies have been conducted throughout the world covering the reduction of asphalt plant emissions through the lowering of mixing and compaction temperatures to produce warm mix asphalt. For example, substantial reductions in emissions were recorded in a field trial done by MeadWestvaco in Ramara Township, Canada in 2005. Results from the field trial showed a 45% reduction in CO<sub>2</sub>, a 63.1% reduction in CO, a 41.2% reduction in SO<sub>2</sub> and a 58% reduction in NO<sub>x</sub>. The average stack gas temperature was reduced from 162°C when using hot mix asphalt to 121°C when using warm mix asphalt (Davidson 2005). Several other studies have shown similar results – that use of warm mix asphalt and the technologies used to produce WMA lead to significant reductions in asphalt plant emissions (D'Angelo 2008).

Benefits of lowering the temperature during mixing and compaction include a decrease in fuel consumption. Reductions in fuel usage from WMA have been shown to range from 11-35% (D'Angelo 2008). In a field trial done by MeadWestvaco in Ramara Township, Canada in 2005, fuel reductions of 55% were seen (Davidson 2005). Recently a study did a lifecycle cost analysis (LCA) for comparing hot mix asphalt to warm mix asphalt with an additive called synthetic zeolite (also known as Advera). Even with many factors taken into account like environmental impacts from energy consumption, air emissions, and extraction and processing of the materials used, it was found through the

total LCA that the impacts of WMA were almost equal to that of HMA when both used the same amount of recycled asphalt pavement (RAP) in their mix gradations.

Furthermore, this study found that the impact seen from lowering the manufacturing temperatures was overshadowed by the bigger impact due to addition of additives such as synthetic zeolites (Vidal et al. 2013).

## **2.5. Present Use of Warm Mix Asphalt in the United States**

In 2011, WMA made up about 20%-30% of all asphalt concrete produced in the United States, (about 69 million tons). This was a 67% increase from 2010, and a 309% increase since 2009. In 2011, both chemical and organic based additives made up about 20% of the market share in WMA use, while the other 80% was held by foaming technologies. Currently there are several concerns behind the use of foaming technologies (NCAT 2012). These concerns include the following: Will all binders foam? Is all foam equal? How long is the foam effective? Can foamed asphalt be replicated in the laboratory for mix design? These concerns are currently being investigated in part through NCHRP Project 9-53. In the foreseeable future, use of chemical and organic additives for WMA is likely to increase. Organic additives are only about 10% of the 20% market share held by chemical and organic additives. This is because organic additives, currently in the market, do not show as much benefit towards WMA performance as their competitors in the chemical additive group (NCAT 2012; TRB 2013).

In 2010, a survey was sent out by the National Center of Asphalt Technology (NCAT) to state departments of transportation (DOT), asphalt paving associations

(APAs), contractors, and WMA suppliers about the use of WMA in the United States. The results are shown in Figure 2.11. In 2011, another survey was conducted by the National Asphalt Pavement Association (NAPA) on warm mix asphalt usage. The results of the survey are shown in Figure 2.12. By looking at the differences between Figures 2.11 and 2.12, it can be seen that over the course of one year warm mix asphalt usage became fully implemented in several states and production and use doubled (Hansen and Copeland 2013; NCAT 2012).

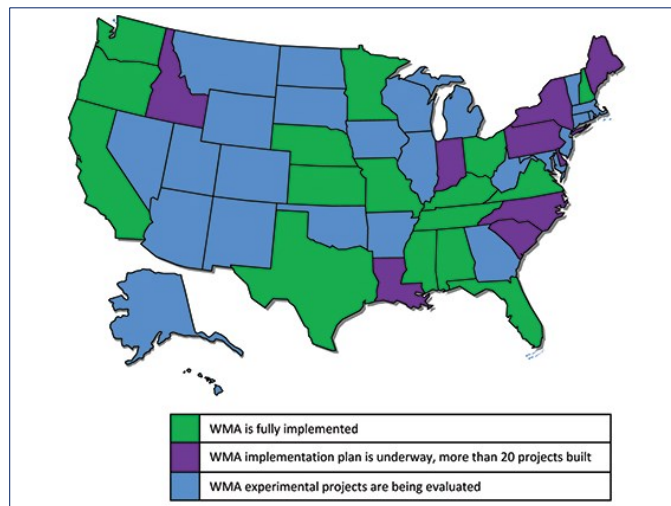


Figure 2.11. Status of WMA Implementation in 2010 (NCAT 2012)

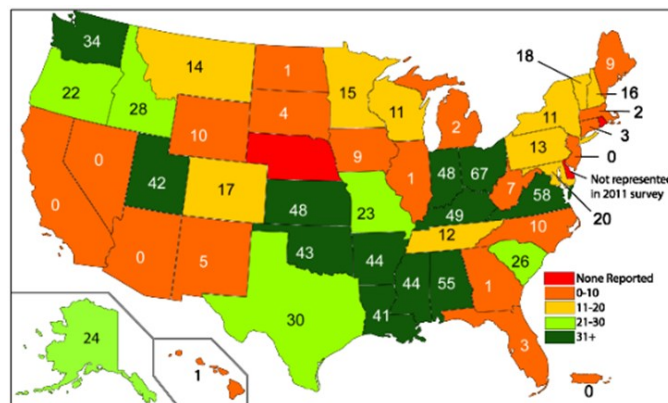


Figure 2.12. WMA Production as a Percentage of Total Asphalt Mix Production (Hansen and Copeland 2013)

## 2.6. Literature Review Summary

Use of warm mix asphalt in the United States has been steadily increasing since its introduction in 2002. From past and current studies in the field warm mix asphalt, with the use of additives to help achieve reductions in mixing and compaction temperature, as well as reductions in emissions and energy usage, performs just as well as hot mix asphalt. However, laboratory studies show that differences do exist between performance of warm mix asphalt and hot mix asphalt. The main research focus within this dissertation is to evaluate the impact of bio-derived materials for use as additives with warm mix asphalt in comparison to hot mix asphalt in terms of performance. The secondary focus of this dissertation is to evaluate how polymer modification impacts the performance of warm mix asphalt when bio-derived materials are used as additives. The third focus of this dissertation is to compare the performance of warm mix asphalt modified with commonly used chemical/organic additives to the performance shown by warm mix asphalt modified with additives from bio-derived materials. The literature review has demonstrated that there is a need to further evaluate warm mix asphalt when modified with bio-derived materials as there is not too much current and past research that covers this topic.

## 2.7. References

- AASHTO M 320-10. (2010). Performance-Graded Asphalt Binder Washington, D.C.: American Association of State Highway and Transportation Officials.
- AASHTO MP 19-10. (2010). Performance-Graded Asphalt Binder Using Multiple Stress Creep Recovery (MSCR) Test. Washington, DC.: American Association of State Highway and Transportation Officials.
- AASHTO R 28-12. (2012). Accelerated Aging of Asphalt Binder Using a Pressurized Aging Vessel (PAV). Washington, D.C.: American Association of State Highway and Transportation Officials.



- AASHTO R 49-09. (2009). Determination of Low-Temperature Performance Grade (PG) of Asphalt Binders Washington, DC.: American Association of State Highway and Transportation Officials.
- AASHTO T 240-13. (2013). Effect of Heat and Air on a Moving Film of Asphalt Binder (Rolling Thin-Film Oven Test) Washington, D.C.: American Association of State Highway and Transportation Officials.
- AASHTO T 283-07. (2007). Resistance of Compacted Bituminous Mixture to Moisture Induced Damage for Superpave *Standard Specifications for Transportation Materials and Methods and Sampling and Testing Part II: Tests*. Washington, D.C.: American Association of State Highway and Transportation Officials.
- AASHTO T 315-10. (2010). Determining the Rheological Properties of Asphalt Binder Using a Dynamic Shear Rheometer (DSR). Washington, D.C.: American Association of State Highway and Transportation Officials.
- AASHTO T 316-13. (2013). Viscosity Determination of Asphalt Binder Using Rotational Viscometer. Washington, D.C.: American Association of State Highway and Transportation Officials.
- AASHTO T 324-11. (2011). Hamburg Wheel-Track Testing of Compacted Hot Mix Asphalt (HMA). Washington, D.C.: American Association of State Highway and Transportation Officials.
- AASHTO TP 70-13. (2013). Multiple Stress Creep Recovery (MSCR) Test of Asphalt Binder Using a Dynamic Shear Rheometer (DSR). Washington, DC.: American Association of State Highway and Transportation Officials.
- American Society for Testing and Materials (ASTM). (2009). ASTM D70-09, Standard Test Method for Density of Semi-Solid Bituminous Materials (Pycnometer Method).
- American Society for Testing and Materials (ASTM). (2014). ASTM D7173-14, Standard Practice for Determining the Separation Tendency of Polymer from Polymer Modified Asphalt.
- Anderson et al. (2008). Engineering properties, emissions, and field performance of warm mix asphalt technologies *NCHRP 9-47, Interim Report*. Washington D.C.: National Cooperation Highway Research Program.
- Aschenbrener, T. (1994). Influence of Refining Processes and Crude Oil Sources Used in Colorado on Results from the Hamburg Wheel Tracking Device. Final Report No. CDOT-DTD-R-94-7. Colorado Department of Transportation, Denver, Colorado.
- Aschenbrener, T. (1995). Evaluation of Hamburg Wheel Tracking Device to Predict Moisture Damage in Hot-Mix Asphalt. *Transp. Res. Rec. 1492, TRB, National Research Council, Washington, D.C., 193-201*.
- Aschenbrener, T., & N. Far. (1994). Influence of Compaction Temperature and Anti-Stripping Treatment on the Results from the Hamburg Wheel Tracking Device. Report No. CDOT-DTD-R-94-9. Colorado Department of Transportation, Denver, Colorado.
- Asgharzadeh, S., Tabatabaee, N., Naderi, K., & Partl, M. (2013). Evaluation of rheological master curve models for bituminous binders. *Materials and Structures*, 1-14. doi: 10.1617/s11527-013-0191-5
- aspha-min GmbH. (2009). aspha-min GmbH Retrieved July 31st, 2014, from <http://www.aspha-min.com/>

- Asphalt Institute. (2003). Superpave Performance Graded Asphalt Binder Specification and Testing (SP-1). U.S.A.: Asphalt Institute.
- Astec Industries, I. (2008). Double Barrel Green System. *Hot-Mix Magazine*, Vol. 13, pp. 10–11.
- Astec Industries, I. (2014). Warm Mix Asphalt Systems Retrieved July 31st, 2014, from [http://www.astecinc.com/images/products/double\\_barrel/double\\_barrel\\_green\\_callouts\\_lg.jpg](http://www.astecinc.com/images/products/double_barrel/double_barrel_green_callouts_lg.jpg)
- Banerjee, A., de Fortier Smit, A., & Prozzi, J. A. (2012). The effect of long-term aging on the rheology of warm mix asphalt binders. *Fuel*, 97(0), 603-611. doi: <http://dx.doi.org/10.1016/j.fuel.2012.01.072>
- Bausano, J., Kvasnak, A., & Williams, R. (2006). *Transitioning Moisture Susceptibility Testing to Accommodate Superpave Gyrotory Compaction*. Paper presented at the Fifty-First Annual Conference of the Canadian Technical Asphalt Association (CTAA).
- Brown, E. R., Kandhal, P. S., Roberts, F. L., Kim, Y. R., Lee, D.-Y., Kennedy, T. W., . . . National Center for Asphalt Technology (U.S.). (2009). *Hot mix asphalt materials, mixture design, and construction* (3rd ed.). Lanham, Md.: NAPA Research and Education Foundation.
- Brown, E. R., Kandhal, P. S., & Zhang, J. (2001). Performance Testing for Hot Mix Asphalt *National Center for Asphalt Technology (NCAT)*. Auburn, Alabama: Report 2001-05.
- Buss, A., Kuang, Y., Williams, R. C., Bausano, J., Cascione, A., & Schram, S. A. (2014). *Influence of Warm Mix Asphalt Additive and Dosage Rate on Construction and Performance of Bituminous Pavements*. Paper presented at the Transportation Research Board 93rd Annual Meeting.
- Buss, A., Rashwan, M., Breakah, T. M., Williams, R. C., & Kvasnak, A. N. (2009). *Investigation of Warm-Mix Asphalt Performance Using the Mechanistic-Empirical Pavement Design Guide*. Paper presented at the 2009 Mid-Continent Transportation Research Symposium.
- Buss, A., & Williams, R. C. (2012). *Warm Mix Asphalt Performance Modeling Using the Mechanistic-Empirical Pavement Design Guide*. Paper presented at the 7th RILEM International Conference on Cracking in Pavements.
- Buss, A. F., Rashwan, M. H., & Williams, R. C. (2011). Investigation of warm-mix asphalt using Iowa aggregates *Iowa Highway Research Board Project Report TR-599*. Ames, IA.
- Button, J. W., Estakhri, C., & Wimsatt, A. (2007). A synthesis of warm mix asphalt *Rep. No. FHWA/TX-07/0-5597-1*. College Station, TX.: Texas Transportation Institute.
- Butz, T., Rahimian, I., & Hildebrand, G. (2001). Modification of road bitumens with the Fischer-Tropsch paraffin Sasobit (R). *Journal of Applied Asphalt Binder Technology*, 1(2).
- Chong, K. P., & Kuruppu, M. D. (1984). New specimen for fracture toughness determination for rock and other materials. *International Journal of Fracture*, 26(2), R59-R62. doi: 10.1007/bf01157555
- Christensen, D. W., & Anderson, D. A. (1992). Interpretation of dynamic mechanical test data for paving grade asphalt cements (with discussion). *Journal of the Association of Asphalt Paving Technologists*, 61.
- Corrigan. (2006). Warm mix asphalt technologies and research. *Federal Highway Administration Office of Pavement Technology*, 3(10), 26-28.

- Csanyi, L. H. (1959). *Foamed Asphalt. Technical Bulletin No. 240*. Washington, D.C.: American Road Builders Association.
- D'Angelo, J., et al. (2008). Warm-mix asphalt: European practice *Publication FHWA-PL-08-007*: FHWA, U.S. Dept. of Transportation, Washington, DC.
- Damm, K. W., Abraham, J., Butz, T., Hildebrand, G., & Riebesehl, G. (2002). Asphalt flow improvers as 'intelligent fillers' for hot asphalts-a new chapter in asphalt technology. *Journal of Applied Asphalt Binder Technology*, 2(1).
- Davidson, J. (2005). Evotherm® Trial–Ramara Township. *McAsphalt Industries Limited*.
- Di Benedetto, H., Olard, F., Sauzéat, C., & Delaporte, B. (2004). Linear viscoelastic behaviour of bituminous materials: From binders to mixes. *Road Materials and Pavement Design*, 5(sup1), 163-202. doi: 10.1080/14680629.2004.968992
- El-Basyouny, M. M., & Witczak, M. W. (2005). Verification of the Calibrated Fatigue Cracking Models for the 2002 Design Guide (With Discussion). *Journal of the Association of Asphalt Paving Technologists*, 74.
- Epps, J., Sebaaly, P., Penaranda, J., Maher, M., McCann, M., & Hand, A. (2000). NCHRP 444: Compatibility of a Test for Moisture Induced Damage with Superpave Volumetric Mix Design. Washington, D.C.: Transportation Research Board, National Highway Research Council.
- European Asphalt Study Tour. (1991). Report on the 1990 European Asphalt Study Tour. AASHTO, Washington, D.C.
- Federal Highway Administration. (FHWA). (2011). The multiple stress creep recovery (MSCR) procedure. *Tech Brief FHWA-HIF-11-038*. Retrieved from <http://www.fhwa.dot.gov/pavement/materials/pubs/hif11038/hif11038.pdf>
- Gandhi, T. (2008). Effects of warm asphalt additives on asphalt binder and mixture properties. Ph.D. dissertation, Clemson Univ., Clemson, SC.
- Garcia, G., Thompson, M. R., Illinois Center for Transportation., & Illinois. Department of Transportation. Bureau of Materials and Physical Research. (2007). HMA dynamic modulus predictive models a review *Civil engineering studies. Illinois Center for Transportation series no. 07-005* (pp. vii, 95 p.). Retrieved from <http://www.ict.uiuc.edu/Publications/report%20files/FHWA-ICT-07-005.pdf>
- <http://worldcat.org/oclc/247453828/viewonline>
- <http://ict.illinois.edu/Publications/report%20files/FHWA-ICT-07-005.pdf>
- Glare Group. Asphalt Retrieved August 3rd, 2014, from <http://www.glaregroup.com/index.php/product/asphalt/>
- Goh, S. W., You, Z., & Van Dam, T. J. (2007). *Laboratory evaluation and pavement design for warm mix asphalt*. Paper presented at the Proceedings of the 2007 Mid-Continent transportation research symposium.
- Hainin, M., & Nim, Y. (2010). Predictability of complex modulus using rheological models. *Asian Journal of Scientific Research*, 3(1), 18-30.

- Hansen, K. R., & Copeland, A. (2013). 2nd Annual Asphalt Pavement Industry Survey on Reclaimed Asphalt Pavement, Reclaimed Asphalt Shingles, and Warm-Mix Asphalt Usage: 2009–2011.
- Harrison, T., & Christodoulaki, L. (2000). Innovative processes in asphalt production and application: "Strengthening asphalt's position in helping to build a better world". Paper presented at the World of Asphalt Pavements, International Conference, 1st, 2000, Sydney, New South Wales, Australia.
- Hassan, M. (2009). *Life-cycle assessment of warm-mix asphalt: An environmental and economic perspective*. Paper presented at the Transportation Research Board 88th Annual Meeting.
- Hossain et al. (2011, June 9-11). *Effectiveness of Advera in Warm Mix Asphalt*. Paper presented at the ASCE GeoHunan 2011.
- Hurley, G. C., and Prowell, B. D. (2005a). Evaluation of Aspha-Min zeolite for use in warm mix asphalt *NCAT Rep. No. 05-04*. Auburn, AL.: National Center for Asphalt Technology.
- Hurley, G. C., and Prowell, B. D. (2005b). Evaluation of Sasobit for use in warm mix asphalt *NCAT Rep. No. 05-06*. Auburn, AL.: National Center for Asphalt Technology.
- Hurley, G. (2006). *Evaluation of new technologies for use in warm mix asphalt*. Masters Science, Auburn University, Auburn.
- Hurley, G. C., & Prowell, B. D. (2006). Evaluation of Evotherm for use in warm mix asphalt *Rep. No. 06-02* (Vol. 6). Auburn, AL.: National Center for Asphalt Technology.
- Jenkins, K., De Groot, J., van de Ven, M., & Molenaar, A. (1999). *Half-warm foamed bitumen treatment, a new process*. Paper presented at the 7th Conference on asphalt pavements for Southern Africa (CAPSA 99).
- Jones, W. (2004). Warm mix asphalt pavements: technology of the future? *Asphalt Institute, 19*(3).
- Kanitpong, K., & Bahia, H. (2006). Evaluation of HMA Moisture Damage in Wisconsin as it Relates to Pavement Performance. *Transportation Research Board CD-ROM, 85th Annual Meeting, January 22-26, 2006*.
- Kim, H., Lee, S., & Amirhanian, S. (2012). Influence of Warm Mix Additives on PMA Mixture Properties. *Journal of Transportation Engineering, 138*(8), 991-997. doi: 10.1061/(ASCE)TE.1943-5436.0000406
- Kim, M., Mohammad, L., & Elseifi, M. (2012). Characterization of Fracture Properties of Asphalt Mixtures as Measured by Semicircular Bend Test and Indirect Tension Test. *Transportation Research Record: Journal of the Transportation Research Board, 2296*(-1), 115-124. doi: 10.3141/2296-12
- Kim, Y. R., Momen, M., King, M., North Carolina. Department of Transportation. Research and Analysis Group., & North Carolina State University. Department of Civil Construction and Environmental Engineering. (2005). Typical dynamic moduli for North Carolina asphalt concrete mixtures (pp. 1 computer disc).
- Koenders, B., Stoker, D., Bowen, C., de Groot, P., Larsen, O., Hardy, D., & Wilms, K. (2000). *Innovative process in asphalt production and application to obtain lower operating temperatures*. Paper presented at the 2nd Euraspalt & Eurobitumen Congress, Barcelona, Spain.
- Koenders et al. (2002). *WAM-Foam, asphalt production at lower operating temperatures*. Paper presented at the Ninth International Conference on Asphalt Pavements, Copenhagen, Denmark.

- Krans, R., Tolman, F., & Van de Ven, M. (1996). *Semi-circular bending test: a practical crack growth test using asphalt concrete cores*. Paper presented at the RILEM PROCEEDINGS.
- Kristjánisdóttir, Ó. (2006). *Warm-mix asphalt for cold weather paving*. Master's thesis, Univ. of Washington, Seattle, WA.
- Kristjánisdóttir, Ó., Muench, S. T., Michael, L., & Burke, G. (2007). Assessing potential for warm-mix asphalt technology adoption. *Transp. Res. Rec.*, 2040, 91-99.
- Kvasnak, A. N. (2006). Development and evaluation of test procedures to identify moisture damage prone hot mix asphalt pavements. PhD Dissertation, Iowa State University.
- Larsen, O., Moen, Ø., Robertus, C., & Koenders, B. (2004). *WAM Foam asphalt production at lower operating temperatures as an environmental friendly alternative to HMA*. Paper presented at the 3rd Eurasphalt & Eurobitume Congress.
- Larsen, O. R., & Robertus, C. (2005). United States Patent No. US6846354 B2.
- Lee, D. (1980). *Treating Iowa's Marginal Aggregates and Soils by Foamix Process*. Ames, IA: Iowa State University.
- Li, B., Liu, J. X., & Su, X. L. (2011). Effects of Compaction Method and Temperature on Warm Mix Asphalt. *Advanced Materials Research*, 255, 3185-3189.
- Li, X., Braham, A. F., Marasteanu, M. O., Buttlar, W. G., & Williams, R. C. (2008). Effect of Factors Affecting Fracture Energy of Asphalt Concrete at Low Temperature. *Road Materials and Pavement Design*, 9(sup1), 397-416. doi: 10.1080/14680629.2008.9690176
- Li, X., & Marasteanu, M. (2004). Evaluation of the low temperature fracture resistance of asphalt mixtures using the semi circular bend test (with discussion). *Journal of the Association of Asphalt Paving Technologists*, 73.
- Li, X. J., & Marasteanu, M. O. (2010). Using Semi Circular Bending Test to Evaluate Low Temperature Fracture Resistance for Asphalt Concrete. *Experimental Mechanics*, 50(7), 867-876. doi: 10.1007/s11340-009-9303-0
- Li, X. J., & Williams, R. C. (2012). A Practical Dynamic Modulus Testing Protocol. *Journal of Testing and Evaluation*, 40(1), 100-106.
- Liddle, G., & Y. Choi. (2007). Case Study and Test Method Review on Moisture Damage. Austroads Project No. TT1135. Austroads Incorporated, Sydney, NSW, Australia.
- Lim, I., Johnston, I., & Choi, S. (1993). Stress intensity factors for semi-circular specimens under three-point bending. *Engineering Fracture Mechanics*, 44(3), 363-382.
- Little, D. N., & Jones, D. (2003). Chemical and mechanical processes of moisture damage in hot-mix asphalt pavements. Paper presented at the Transportation Research Board National Seminar, San Diego, CA, USA.
- Lottman, R. P. (1978). NCHRP 192: Predicting Moisture-Induced Damage to Asphaltic Concrete *Transportation Research Record, National Highway Research Council*. Washington, D.C.
- Lottman, R. P. (1982a). Laboratory test methods for predicting moisture-induced damage to asphalt concrete. *Transportation Research Record*(843), 88-95.

- Lottman, R. P. (1982b). NCHRP 246: Predicting Moisture-Induced Damage to Asphaltic Concrete - Field Evaluation *Transportation Research Record, National Highway Research Council*. Washington, D.C.
- Lottman, R. P., Chen, R., Kumar, K., & Wolf, L. (1974). A laboratory test system for prediction of asphalt concrete moisture damage. *Transportation Research Record*(515), 18-26.
- Lu, Q., & J. T. Harvey. (2006a). Evaluation of Hamburg Wheel Tracking Device Test with Laboratory and Field Performance Data. *Transp. Res. Rec. 1970, TRB, National Research Council, Washington, D.C., 25-44*.
- Lu, Q., & J. T. Harvey. (2006b). Long-Term Effectiveness of Antistripping Additives. *Transp. Res. Rec. 1970, TRB, National Research Council, Washington, D.C., 14-24*.
- Lugo, A. E. Á., Pimienta, A. L. A., & Estakhri, C. K. (2013). Laboratory evaluation of compactability and performance of warm mix asphalt. *Revista EIA*(19), 111-121.
- Marasteanu, M., & Anderson, D. (1999). *Improved model for bitumen rheological characterization*. Paper presented at the Eurobitume Workshop on Performance Related Properties for Bituminous Binders.
- Marasteanu, M., Buttlar, W., Bahia, B., and R. Christopher Williams. . (2012). *National Pooled Fund Study –Phase II: Final Report - Investigations of Low Temperature Cracking in Asphalt Pavements*. MN/RC 2012-23.
- Marasteanu, M. O., Li, X., Labuz, J. F., Petit, C., Al-Qadi, I., & Millien, A. (2004). *Low temperature fracture test for asphalt mixtures*. Paper presented at the Fifth International RILEM Conference on Reflective Cracking in Pavements.
- Md. Yusoff, N. I., Mounier, D., Marc-Stéphane, G., Rosli Hainin, M., Airey, G. D., & Di Benedetto, H. (2013). Modelling the rheological properties of bituminous binders using the 2S2P1D Model. *Construction and Building Materials*, 38(0), 395-406. doi: <http://dx.doi.org/10.1016/j.conbuildmat.2012.08.038>
- Middleton and Forfylow. (2009). Evaluation of warm-mix asphalt produced with the double barrel green process. *Transp. Res. Rec.*, 2126, 19-26.
- Mo, L., Li, X., Fang, X., Huurman, M., & Wu, S. (2012). Laboratory investigation of compaction characteristics and performance of warm mix asphalt containing chemical additives. *Construction and Building Materials*, 37(0), 239-247. doi: <http://dx.doi.org/10.1016/j.conbuildmat.2012.07.074>
- Morea, F., Marcozzi, R., & Castaño, G. (2012). Rheological properties of asphalt binders with chemical tensoactive additives used in Warm Mix Asphalts (WMAs). *Construction and Building Materials*, 29(0), 135-141. doi: <http://dx.doi.org/10.1016/j.conbuildmat.2011.10.010>
- National Cooperative Highway Research Program, (NCHRP). (2004). Guide for Mechanistic-Empirical Design of New and Rehabilitated Pavement Structures *NCHRP 1-37A*
- NCAT. (2012, Fall 2012). Market Analysis Identifies Strengths, Needs of WMA. *Asphalt Technology E-News* Volume 24, Number 2. Retrieved August 2, 2013, from <http://www.eng.auburn.edu/research/centers/ncat/info-pubs/newsletters/fall-2012/market-analysis-identifies-strengths-needs-of-wma.html>
- Newcomb, D. (2007). An introduction to warm-mix asphalt. Retrieved February, 16, 2009.

- Olard, F., & Di Benedetto, H. (2003). General "2S2P1D" Model and Relation Between the Linear Viscoelastic Behaviours of Bituminous Binders and Mixes. *Road Materials and Pavement Design*, 4(2), 185-224. doi: 10.1080/14680629.2003.9689946
- Pellinen, T., & Witczak, M. (2002). Stress dependent master curve construction for dynamic (complex) modulus (with discussion). *Journal of the Association of Asphalt Paving Technologists*, 71.
- Perkins, S. W. (2009). Synthesis of warm mix asphalt paving strategies for use in Montana highway construction *Rep. No. FHWA/MT-09-009/8117-38*. Helena, MT.: Western Transportation Institute.
- PQ Corporation. (2009). Advera® WMA Aluminosilicate Retrieved July 31st, 2014, from <http://www.adverawma.com/doc/WMArev200904.pdf>
- PQ Corporation. (2014). Advera® WMA Retrieved July 31st, 2014, from <http://www.adverawma.com/wma.html>
- Prowell, B. D., Hurley, G. C., & Crews, E. (2007). *Field performance of warm-mix asphalt at the NCAT test track*. Paper presented at the Transportation Research Board 86th Annual Meeting.
- Roberts, F., Kandhal, P., Brown, E., Lee, D., & Kennedy, T. (1996). Hot Mix Asphalt Materials, Mixture Design, and Construction, National Asphalt Pavement Association, NAPA Education Foundation, Lanham, Md.
- Roberts, F. L., Engelbrecht, J. C., & Kennedy, T. W. (1984). Evaluation of recycled mixtures using foamed asphalt
- Rodríguez-Alloza, A. M., Gallego, J., & Pérez, I. (2013). Study of the effect of four warm mix asphalt additives on bitumen modified with 15% crumb rubber. *Construction and Building Materials*, 43(0), 300-308. doi: <http://dx.doi.org/10.1016/j.conbuildmat.2013.02.025>
- Sanchez-Alonso, E., Vega-Zamanillo, A., Castro-Fresno, D., & DelRio-Prat, M. (2011). Evaluation of compactability and mechanical properties of bituminous mixes with warm additives. *Construction and Building Materials*, 25(5), 2304-2311. doi: <http://dx.doi.org/10.1016/j.conbuildmat.2010.11.024>
- Santucci, L. (2002). Moisture sensitivity of asphalt pavements. Technology Transfer Program, UC-Berkley's Institute of Transportation Studies.
- Solaimanian, M., Harvey, J., Tahmoressi, M., & Tandon, V. (2003). *Test methods to predict moisture sensitivity of hot-mix asphalt pavements*. Paper presented at the Transportation Research Board National Seminar. San Diego, California.
- Stroup-Gardiner, M., & Epps, J. (1992). Laboratory tests for assessing moisture damage of asphalt concrete mixtures. *Transportation Research Record*(1353), 15-23.
- Takamura, K. (2005). Binder Characterization for Latex Polymer-Modified Evotherm® Warm Mix. *Charlotte Technical Center, BASF Corporation, Charlotte, North Carolina*.
- Teshale, E. Z. (2012). Low-Temperature Fracture Behavior of Asphalt Concrete in Semi-Circular Bend Test. University of Minnesota.
- TRB. (2013). NCHRP 09-53 [Active]: Properties of Foamed Asphalt for Warm Mix Asphalt Applications Retrieved August 2, 2013, from <http://apps.trb.org/cmsfeed/TRBNetProjectDisplay.asp?ProjectID=3166>

- U. S. Department of Transportation Federal Highway Administration. Warm Mix Technologies and Research Retrieved August 3rd, 2014, from <http://www.fhwa.dot.gov/pavement/wma.html>,
- Vidal, R., Moliner, E., Martínez, G., & Rubio, M. C. (2013). Life cycle assessment of hot mix asphalt and zeolite-based warm mix asphalt with reclaimed asphalt pavement. *Resources, Conservation and Recycling*, 74(0), 101-114. doi: <http://dx.doi.org/10.1016/j.resconrec.2013.02.018>
- Wasiuddin, N. M., Selvamohan, S., Zaman, M. M., & Guegan, M. L. T. A. (2007). Comparative laboratory study of sasobit and aspha-min additives in warm-mix asphalt. *Transportation Research Record: Journal of the Transportation Research Board*, 1998(1), 82-88.
- Wielinski, J., Hand, A., & Rausch, D. M. (2009). Laboratory and field evaluations of foamed warm-mix asphalt projects. *Transportation Research Record: Journal of the Transportation Research Board*, 2126(1), 125-131.
- Xiao, F., Punith, V. S., & Amirkhanian, S. N. (2012). Effects of non-foaming WMA additives on asphalt binders at high performance temperatures. *Fuel*, 94(0), 144-155. doi: <http://dx.doi.org/10.1016/j.fuel.2011.09.017>
- Yao, H., You, Z., Li, L., Goh, S., & Dedene, C. Evaluation of the Master Curves for Complex Shear Modulus for Nano-Modified Asphalt Binders *CICTP 2012* (pp. 3399-3414).
- Yildirim, Y., & T. W. Kennedy. (2001). Correlation of Field Performance to Hamburg Wheel Tracking Device Results. Report No. FHWA/TX-04/0-4185-1, Texas Department of Transportation, Austin, Texas.
- Yin, H. (2009). Investigation of Rheological Behavior of Asphalt Binder Modified by the Advera Additive Retrieved from [http://www.utrc2.org/sites/default/files/pubs/rheological-asphalt-modified-advera-final\\_0.pdf](http://www.utrc2.org/sites/default/files/pubs/rheological-asphalt-modified-advera-final_0.pdf)
- You, Z., & Goh, S. W. (2008). Laboratory evaluation of warm mix asphalt: A preliminary study. *International Journal of Pavement Research and Technology*, 1(1), 34-40.
- You, Z., & Goh, S. W. (2009). Warm Mix Asphalt Using Sasobit in Cold Region *Cold Regions Engineering 2009* (pp. 288-298).
- Yusoff, N. I. M., Shaw, M. T., & Airey, G. D. (2011). Modelling the linear viscoelastic rheological properties of bituminous binders. *Construction and Building Materials*, 25(5), 2171-2189. doi: <http://dx.doi.org/10.1016/j.conbuildmat.2010.11.086>
- Zaman, M., O'Rear, E. A., Hossain, Z., & Chen, D.-H. (2011). Effectiveness of Advera in Warm Mix Asphalt *Emerging Technologies for Material, Design, Rehabilitation, and Inspection of Roadway Pavements* (pp. 9-16). Retrieved from <http://ascelibrary.org/doi/abs/10.1061/47629%28408%292> doi:doi:10.1061/47629(408)2
- Zhou, Z., Zhang, Y., Tierney, J. W., & Wender, I. (2004). Producing fuels from Fischer-Tropsch waxes. *Petroleum technology quarterly*, 9(1), 137-143.



## CHAPTER 3. INVESTIGATION OF ISOSORBIDE DISTILLATION BOTTOMS AS A BIO-BASED WARM-MIX ADDITIVE

Modified from a paper accepted by the *Journal of Materials in Civil Engineering*

Ashley Buss<sup>1,2</sup>, Joseph Podolsky<sup>1,2</sup>, R. Christopher Williams<sup>1</sup>, and Eric Cochran<sup>3</sup>

### 3.1. Abstract

Bio-refineries are increasing in numbers and size and include food, energy, and chemical based products. Depending upon size and targeted products, bio-refineries produce distillation bottoms with surfactant characteristics in sufficient quantities that can be used as a warm mix asphalt (WMA) technology. Isosorbide distillation bottoms (IDB) are derived as co-products of bio-based chemical production and show potential for reducing mixing and compaction temperatures as well as having low temperature performance grade (PG) benefits. The objective of this paper is to demonstrate the performance and potential of IDB as an asphalt additive through asphalt binder testing and mixture testing. Binder gradations were conducted for multiple binders at several dosage rates to verify compatibility with various petroleum crude sources and determine the optimum dosage level. Testing indicates promising results and shows an optimal dosage rate at approximately 0.5% by weight of binder. Mixture testing was performed to evaluate the impact of IDB on mix compactability and moisture susceptibility.

---

<sup>1</sup> Iowa State University, Department of Civil, Construction and Environmental Engineering, 394 Town Engineering Building, Ames, IA 50011.

<sup>2</sup> Co-researcher and co-author.

<sup>3</sup> Iowa State University, Department of Chemical & Biological Engineering, 1035 Sweeney, Ames, IA 50011.

Laboratory mixture and binder testing show favorable results for further implementation of IDB as an asphalt additive.

**KEYWORDS:** warm mix asphalt; bio-refineries; performance grade; moisture conditioning.

### 3.2. Introduction

Warm mix asphalt technologies have been shown to reduce mixing and compaction temperatures by up to 30°C during asphalt production using foaming agents, chemical, and wax additives (Capitão et al. 2012; D'Angelo et al. 2008; Oliveira et al. 2013; Romier et al. 2006). The decrease in production temperatures allows the asphalt industry the opportunity to reduce their carbon footprint, save money associated with increased plant temperatures and lessen fumes workers are exposed to during production and construction (Capitão et al. 2012; D'Angelo et al. 2008; Oliveira et al. 2013; Romier et al. 2006). These benefits can now be combined with the use of WMA technologies from bio-refineries to help make asphalt a more sustainable product for the environment, the contractor and the general public.

Isosorbide Distillation Bottoms (IDB) is a recently developed, bio-derived, chemical additive with surfactant properties. There are several other chemicals with surfactant properties that have been successfully used as a WMA technology, e.g. Evotherm® (Oliveira et al. 2012). This paper discusses the findings from a detailed testing plan which evaluated IDB for use in asphalt binder and asphalt mix. Complete binder grade evaluations were conducted for multiple binders at several dosage rates to verify compatibility with various petroleum crude sources and determine the optimum

dosage level. In addition, compaction and moisture sensitivity studies were done to determine how WMA with IDB would perform in the field as compared to HMA with no IDB (Aksoy et al. 2005; Kringos and Scarpas 2008; Mo et al. 2012; Sanchez-Alonso et al. 2011).

In addition to production cost savings, WMA has proven to be comparable with HMA performance in many in-service pavement sections. Laboratory studies have shown increased moisture susceptibility in WMA which is likely due to incomplete drying of aggregates (Hurley 2006). Overall, WMA has shown promise and continues to be implemented by owner agencies.

### 3.3. Experimental Materials and Methods

The primary objective of this study is to evaluate the use of IDB as a WMA additive. IDB is a residual derived from a broader sorbitol platform produced from biomass (corn). Biomass provides an alternative to some traditional crude oil-based products. The hydrogenation product of glucose from biomass is sorbitol. Sorbitol can be converted to isosorbide via sorbitan by performing a twofold dehydration reaction (Werpy et al. 2004). The changes in the molecular structure are shown in Figure 3.1.

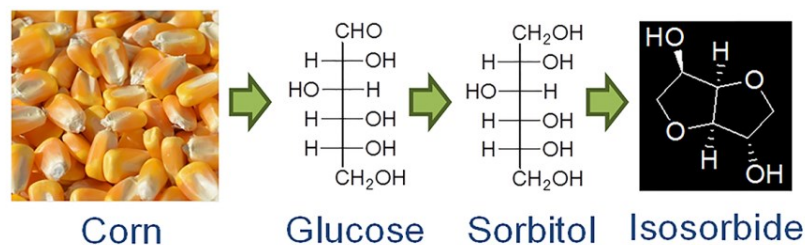


Figure 3.1. Molecular Changes from Corn to Isosorbide

Isosorbide has been included in the United States Department of Energy's top chemical building blocks derived from biomass (Werpy et al. 2004). Isosorbide provides a versatile chemical platform because of its high stability and two functional hydroxyl groups, which allow further chemical modification to take place (Werpy et al. 2004).

The IDB would act as a chemical additive to the asphalt. Since the additive is derived from corn, it is a renewable resource and helps to create a more sustainable asphalt product while decreasing production costs. The IDB stream is a thick viscous semi-liquid coproduct resulting from the production of isosorbide. The material is soluble in water as well as common polar organic solvents such as acetone, ethanol and chloroform. It solidifies near room temperature but is free flowing above 80°C.

Important factors considered throughout the testing include various crude sources, polymer modified binders, and optimum dosage level of IDB. Changes in binder properties are observed by testing binders at high, intermediate and low service temperatures using various IDB dosage levels: 0.5%, 1%, 2% and 5% by weight of binder. A key factor considered is the parent material-crude petroleum in order to determine differences between asphalts extracted from different locations. Two crude sources were used: Montana – similar to a Canadian crude, and a Texas crude. These crudes were selected based on the crudes most often used in the Midwestern United States. A polymer modified form of the Montana crude was also used in this study to examine the impact IDB would have on polymer modified binders and allow for a comparison between IDB impact on the original Montana and polymer modified Montana binders. The dosage level of IDB used in binder testing was 0%, 0.5%, 1%, 2% and 5% by weight of binder.

Supplementary mixture laboratory tests were performed to measure the influence IDB additives have on compaction and moisture susceptibility performance. The binders employed for the initial binder tests were used in the mixture tests with IDB dosage levels of 0%, 0.5% and 1% by weight of binder.

### **3.3.1. Asphalt binder experimental testing plan**

The binder experimental plan, based on Superpave criteria (Asphalt Institute 2003) will distinguish rheological differences that exist between various dosage rates of IDB by using the Dynamic Shear Rheometer (DSR) (AASHTO 2007a), Rolling Thin Film Oven (RTFO) (AASHTO 2007c), Pressure Aging Vessel (PAV) (AASHTO 2007b) and the Bending Beam Rheometer (BBR) (AASHTO 2007d). A Silverson shear mill was used for blending the IDB with the binders. Blending was performed at 140°C for one hour. The polymers were blended with the base asphalt by the binder supplier. The binders were also evaluated for specific gravity (ASTM Standard D70 2009), rotational viscometer (AASHTO 2007a) and separation analysis. The separation tests were performed on the binders containing 2% and 5% IDB. The binder was placed in metal tubes and placed in a 163°C oven for 24 hours. The tubes of binder were put in a freezer to cool quickly and the tubes were then cut in thirds. For each tube, three DSR tests were conducted for both the top and the bottom thirds. The rotational viscometer test determines the pumpability as well as the mixing and compaction temperatures for each binder; however, other studies have shown that rotational viscometer test data will not always capture the full decrease in temperature that can be achieved by using WMA additives (Buss 2011; Wasiuddin 2007).

The testing plan for each binder is shown in Table 3.1. Fifteen binders were graded for high and low temperature performance grades. Tests were run in triplicate to assure consistency in tests results and better comparisons between IDB dosage rates. A total of 270 binder tests results were used to evaluate optimum dosage rates, product impacts and possible advantages. This testing plan evaluates the impact IDB has on rheological properties at all pavement service temperatures.

**Table 3.1. Binder Testing Experimental Plan Repeated for Each Binder**

| Repeated for Texas, Montana and Montana Polymer Modified Asphalt |              |      |      |      |      |
|--|--------------|------|------|------|------|
| Percent IDB  | Control (0%) | 0.5% | 1.0% | 2.0% | 5.0% |
| Rotational Viscometer  | XXX*         | XXX  | XXX  | XXX  | XXX  |
| DSR  | XXX          | XXX  | XXX  | XXX  | XXX  |
| DSR RTFO   | XXX          | XXX  | XXX  | XXX  | XXX  |
| DSR PAV  | XXX          | XXX  | XXX  | XXX  | XXX  |
| BBR  | XXX          | XXX  | XXX  | XXX  | XXX  |
| Sp. Gravity  | XXX          | XXX  | XXX  | -    | -    |
| Separation Tests   | -*           | -    | -    | XXX  | XXX  |

\*Each "X" represents one test and each "-" designates no test for that category

### 3.3.2. Asphalt mixture experimental testing plan

Initial binder tests showed favorable results for IDB and established the need for a laboratory experimental plan to supplement the findings of the binder study. The objectives are to compare the compactability and moisture susceptibility performance of a known, well performing, HMA mix design (Aksoy et al. 2005; Kringos and Scarpas 2008; Mo et al. 2012; Sanchez-Alonso et al.2011). The mix design is an Iowa Department of Transportation (DOT) approved mix with an ESAL design of 10 million. All samples were mixed with an optimum binder content of 5.2%, using 0%, 0.5% and

1% IDB in each of the three binders. The HMA and WMA mixes were prepared in the laboratory and differed only by the IDB additive and the mixing and compaction temperatures. The IDB dosages of 0%, 0.5% and 1% were studied using the three binders employed in the binder analysis: Texas, Montana and polymer modified Montana. Compactability was evaluated by looking at compaction data for each of the samples and moisture susceptibility was evaluated by conducting indirect tensile (IDT) strength tests according to AASHTO T-283 (AASHTO 2007e; Aksoy et al. 2005; Kringos and Scarpas 2008; Mo et al. 2012; Sanchez-Alonso et al. 2011).

Six, 100 mm diameter samples for each dosage rate were compacted and three of the six were moisture conditioned. The testing plan, shown in Table 3.2, will generate test results and compaction data from 54 samples. All samples were compacted within  $7 \pm 0.5\%$  air voids. HMA control samples were mixed and compacted at  $150^{\circ}\text{C}$  and the WMA samples containing IDB were mixed and compacted at  $120^{\circ}\text{C}$ . The samples were cured in an oven at the respective temperatures for two hours. The mixes were compacted

**Table 3.2. Mixture Testing Experimental Plan**

| Binder           | Percent IDB | Not Moisture Conditioned | Moisture Conditioned |
|------------------|-------------|--------------------------|----------------------|
| Montana          | 0.0%        | XXX*                     | XXX                  |
| Crude            | 0.5%        | XXX                      | XXX                  |
| PG 64-22         | 1.0%        | XXX                      | XXX                  |
| Polymer Modified | 0.0%        | XXX                      | XXX                  |
| Montana          | 0.5%        | XXX                      | XXX                  |
| PG70-22          | 1.0%        | XXX                      | XXX                  |
| Texas            | 0.0%        | XXX                      | XXX                  |
| Crude PG         | 0.5%        | XXX                      | XXX                  |
| 67-22            | 1.0%        | XXX                      | XXX                  |

\* Each "X" represents one tested sample

to a specified height using a Superpave Gyratory Compactor. For each sample, a compaction curve was developed with number of gyrations versus height. Sample height readings from SGC were recorded every 5 gyrations along with the total number of gyrations needed to reach a sample height of 62.5mm. The samples were moisture conditioned and tested for their IDT strength following AASHTO T-283 (AASHTO 2007e). Pairs were chosen based upon air void content and the moisture conditioned samples within the pair was randomly selected. Moisture conditioning followed the standard practice of vacuum saturating samples between 70 and 80 percent saturation, freezing the samples at -18°C for a minimum of 16 hours, submerging samples in 60°C water for 24 hours and submerging samples in 25°C water for 2 hours.

### **3.4. Discussion of Binder and Mixture Test Results**

The binder testing incorporated the key factors of crude source, dosage level, and polymer modification using a wide variety of tests such as, specific gravity, RTFO mass loss, rotational viscometer, separation tests, as well as a complete binder performance grade study. Mixture testing evaluated the impact of IDB on compactability and moisture susceptibility performance. These test results weigh the potential of using IDB as a bio-based WMA additive.

#### **3.4.1. Binder test results**

First, separation tests showed that IDB will not separate after being mixed with an asphalt binder. This was done by testing binder from the top and bottom thirds of prepared tubes in a DSR. Six DSR tests were performed for each tube: three for the top, three for the bottom. The dosage rates used for this test were 2% and 5% because if



separation is occurring, it will be most evident for high dosage levels. Separation tests for each binder are shown in Figure 3.2, Figure 3.3 and Figure 3.4. Test results showed no consistent evidence of separation between the IDB and the binder, this is likely due to the surfactant nature of IDB which decreases the likelihood of separation occurring.

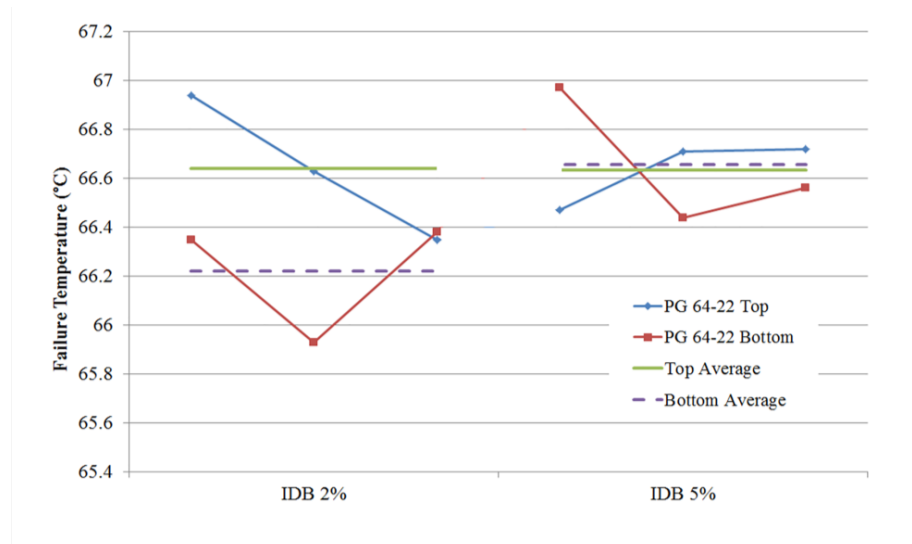


Figure 3.2. Separation Test Results for Montana Binder PG 64-22 for 2% and 5% IDB

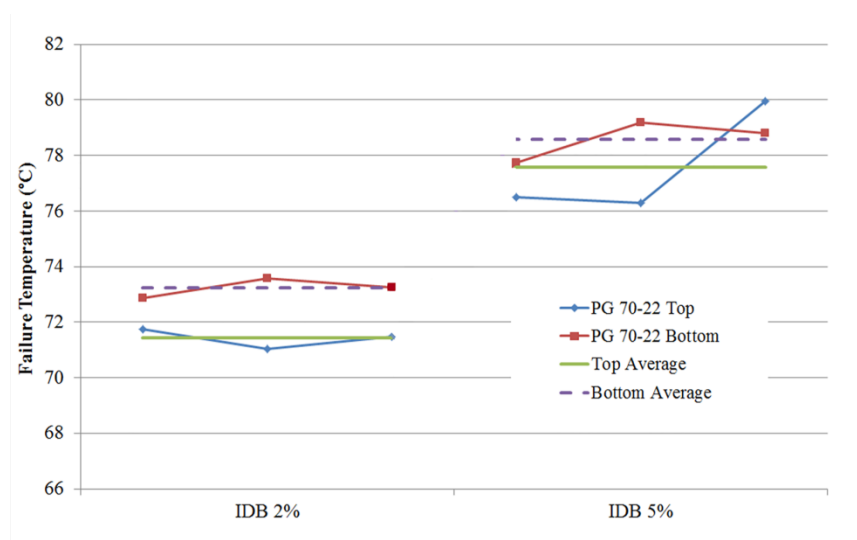
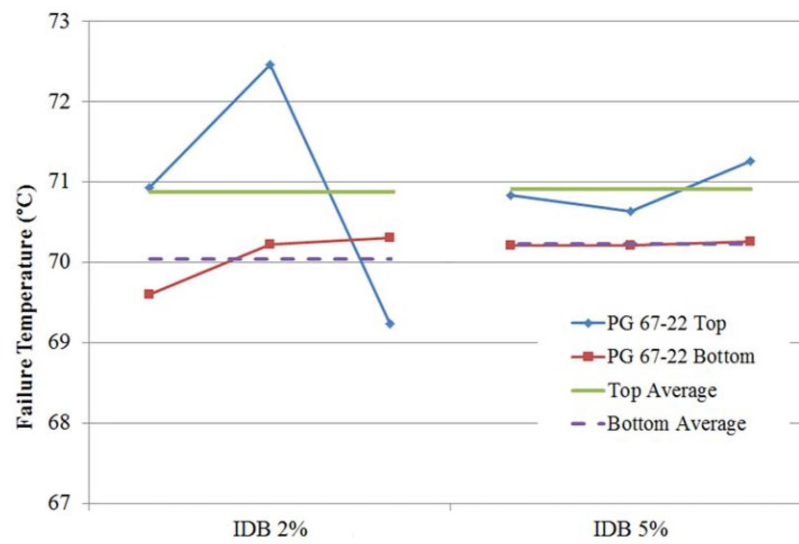


Figure 3.3. Separation Test Results for Polymer Modified Montana Binder PG 70-22 for 2% and 5% IDB



**Figure 3.4. Separation Test Results for Texas Binder PG 67-22 for 2% and 5% IDB**

#### 3.4.1.1. High and intermediate temperature binder test results

After separation tests showed IDB will remain homogeneous in a binder medium, high temperature binder properties were tested using a DSR to investigate the binder rheological properties with several binders at increasing IDB dosage levels. Test results for the Montana and Texas binders, in Table 3.3, show the average of three test results and indicate how binder properties change with varying dosage levels of IDB. Table 3.3 shows the IDB binders maintaining an adequate high temperature grade at all dosage levels. Binders with 0.5% and 1% IDB appear to have desirable material changes with the rutting factor slightly increasing for the RTFO aged material and a decreasing intermediate failure temperature which may indicate better fatigue performance.

The results for the Montana polymer modified binder, PG70-22, at the dosage level of 5% IDB show a relatively higher failure temperature for high temperature tests and a relatively lower failure temperature at intermediate temperature tests after PAV aging. This would be beneficial; however, the binders at this dosage level of IDB did not

pass the mass loss requirement of less than one percent, shown in Table 3.4. Overall, the dosage levels did not appear to have a significant impact on the measured parameters and failure temperatures.

**Table 3.3. DSR Results for Original, RTFO Aged and PAV Aged Binders**

| % IDB                           | Montana (MT) PG 64-22 |      |      |      |      | Poly. Mod. MT PG 70-22 |      |      |      |      | Texas PG 67-22 |      |      |      |      |      |
|---------------------------------|-----------------------|------|------|------|------|------------------------|------|------|------|------|----------------|------|------|------|------|------|
|                                 | 0                     | 0.5  | 1.0  | 2.0  | 5.0  | 0                      | 0.5  | 1.0  | 2.0  | 5.0  | 0              | 0.5  | 1.0  | 2.0  | 5.0  |      |
| Original<br>G*/sin( $\delta$ )  | 58°C                  | 3.3  | 3.3  | 3.2  | 3.4  | 2.9                    | --   | --   | --   | --   | --             | 4.2  | --   | --   | 4.1  | 4.3  |
|                                 | 64°C                  | 1.4  | 1.4  | 1.4  | 1.5  | 1.3                    | 2.9  | 2.6  | 3.0  | 2.6  | --             | 2.0  | 2.2  | 2.1  | 1.9  | 2.1  |
|                                 | 70°C                  | 0.7  | 0.7  | 0.7  | 0.7  | 0.6                    | 1.5  | 1.3  | 1.5  | 1.3  | 2.1            | 1.0  | 1.1  | 1.0  | 0.9  | 1.0  |
|                                 | 76                    | --   | --   | --   | --   | --                     | 0.8  | 0.7  | 0.8  | 0.6  | 1.1            | --   | 0.5  | 0.5  | --   | 0.5  |
|                                 | 82                    | --   | --   | --   | --   | --                     | --   | --   | --   | --   | 0.6            | --   | --   | --   | --   | --   |
|                                 | Failure Temp. (°C)    | 67.0 | 67.0 | 66.9 | 67.4 | 66.4                   | 73.7 | 72.3 | 73.7 | 72.0 | 77.2           | 69.5 | 70.8 | 70.1 | 69.5 | 70.4 |
| RTFO Aged<br>G*/sin( $\delta$ ) | 58                    | 8.2  | 10.1 | 9.4  | 7.4  | 7.5                    | --   | --   | --   | --   | --             | --   | --   | --   | 9.6  | 8.9  |
|                                 | 64                    | 3.4  | 4.3  | 4.2  | 3.2  | 3.3                    | 6.2  | 6.7  | 7.5  | 5.3  | --             | 5.0  | 5.0  | 5.1  | 4.5  | 4.2  |
|                                 | 70                    | 1.6  | 2.0  | 2.0  | 1.5  | 1.5                    | 3.1  | 3.3  | 3.8  | 2.7  | 4.2            | 2.4  | 2.4  | 2.4  | 2.2  | 2.0  |
|                                 | 76                    | --   | --   | --   | --   | --                     | 1.5  | 1.7  | 1.9  | 1.3  | 2.2            | 1.2  | 1.2  | 1.2  | --   | --   |
|                                 | 82                    | --   | --   | --   | --   | --                     | --   | --   | --   | --   | 1.2            | --   | --   | --   | --   | --   |
|                                 | Failure Temp. (°C)    | 67.4 | 69.0 | 69.2 | 66.9 | 67.2                   | 72.9 | 73.3 | 74.9 | 71.7 | 76.2           | 70.8 | 70.7 | 70.9 | 69.9 | 69.2 |
| PAV Aged<br>G*/sin( $\delta$ )  | 25                    | 3528 | 3388 | 3534 | 3534 | 3438                   | --   | --   | --   | --   | --             | 2889 | 2941 | 3105 | 2781 | 2686 |
|                                 | 22                    | 5193 | 4945 | 4992 | 5304 | 5202                   | 3026 | 2998 | 3210 | 2948 | 2801           | 4029 | 4102 | 4315 | 3917 | 3805 |
|                                 | 19                    | --   | --   | 6692 | --   | --                     | 4203 | 4122 | 4429 | 4139 | 3929           | 5560 | 5645 | 5912 | 5250 | 5333 |
|                                 | 16                    | --   | --   | --   | --   | --                     | 5761 | 5624 | 6027 | 5714 | 5454           | --   | --   | --   | --   | --   |
|                                 | Failure Temp. (°C)    | 22.3 | 21.9 | 19.0 | 22.5 | 22.3                   | 17.4 | 17.1 | 17.8 | 17.2 | 16.8           | 17.0 | 17.2 | 17.6 | 16.8 | 16.5 |

**Table 3.4. IDB Mass Loss**

| IDB Percentage | Average Mass Loss |                |          |
|----------------|-------------------|----------------|----------|
|                | MT PG 64-22       | PM-MT PG 70-22 | TX 67-22 |
| 0.00%          | 0.90%             | 1.00%          | 0.70%    |
| 0.50%          | 0.86%             | 0.56%          | 0.29%    |
| 1.00%          | 1.06%             | 0.99%          | 0.85%    |
| 2.00%          | 1.39%             | 1.10%          | 1.98%    |
| 5.00%          | 1.92%             | 1.80%          | 2.34%    |

The Texas binder, PG67-22, showed relatively small changes with IDB percentages. Average failure temperatures increased only slightly for 0.5% and 1% IDB. Overall, the data indicate that IDB is not going to adversely impact the high temperature grade for the binders tested. There is also no evidence of substantial changes in the asphalt aging properties due to the addition of IDB, even at a high dosage level of 5%; however, higher dosage levels are more likely to exceed the mass loss maximum criteria of 1%.

A study of mass loss with dosage level was performed and additional tests beyond the initial experimental plan were conducted. Variability in the test results were observed due to the control binders showing relatively high initial mass loss as well as mass loss with increasing levels of IDB. The average mass loss values, in Table 3.4, increase as the IDB dosage increases and for all binders, there is an initial drop in all the mass loss values between 0 and 0.5%. This reduction can be attributed to the binder blending process in which the blended binder was held at 140°C for one hour and blended with the IDB using a shear mill which caused the initial decrease in mass loss for 0.5%. For each subsequent dosage level, the mass loss increases. This trend is evident in all three binders at every dosage level. For future studies, thermo-gravimetric analysis (TGA) would be useful for a detailed understanding how IDB binders react to elevated temperatures and the associated mass loss sensitivity.

The specific gravity testing was performed to verify mix design calculations. From initial test results, 0.5% and 1% were chosen for mix design purposes so specific gravity was measured at only 0.5% and 1% IDB. The specific gravity showed only small

changes with the addition of IDB at these dosage levels and mix design volumetric calculations will not be impacted.

The rotational viscometer tests were performed at 20 rpm at temperatures ranging from 135°C up to 180°C. All binders met the pumpability requirement of 3 Pa\*s at 135°C. WMA additives typically do not appear to significantly reduce the mixing and compaction temperatures when looking solely at rotational viscometer results. The results show no clear trends when comparing binder viscosity to IDB dosages. The rate of change in viscosity with temperature remains the same regardless of IDB dosage indicating temperature susceptibility of the binder is not affected. The IDB appeared to have little impact on the overall viscosity of the binders and no trends for dosage level were delineated using this test.

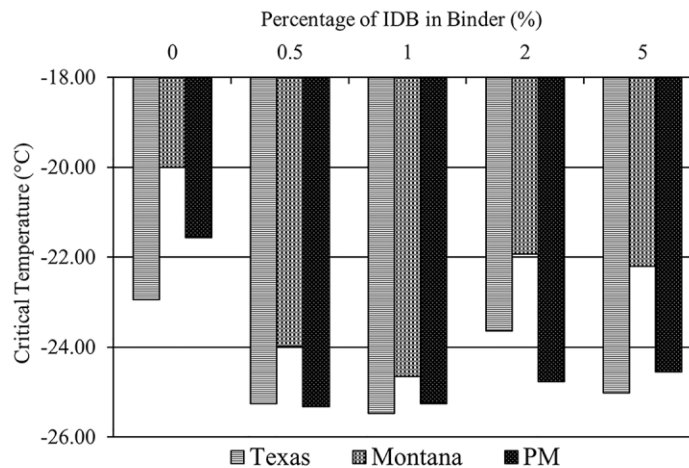
#### 3.4.1.2. Low temperature binder test results

Table 3.5 displays the results of the bending beam rheometer testing for -12°C and -18°C taken at 60 seconds of loading. The Superpave criteria was interpolated from the data between the temperatures of -12°C and -18°C using a linear relationship and 0°C was subtracted from the actual test temperature to find the critical temperature. In Table 3.5, trends can be observed by noting how test parameters change with increasing IDB. The largest change in data occurs between 0 and 0.5% IDB. Figure 3.5 shows the critical low temperature grade at the five dosage levels. IDB decreases the critical temperature at all dosage levels with 0.5% and 1% being the most favorable. The results indicate IDB may be useful in low temperature climates where pavements are susceptible to thermal

cracking. There are larger changes occurring in the low temperature data than what was seen for the intermediate and high temperature testing in the DSR.

**Table 3.5. Bending Beam Rheometer Test Results**

|                                      | Temp<br>(°C) | Parameter                   | Percent IDB   |               |               |               |               |
|--------------------------------------|--------------|-----------------------------|---------------|---------------|---------------|---------------|---------------|
|                                      |              |                             | 0%            | 0.50%         | 1.00%         | 2.00%         | 5.00%         |
| Texas PG 67-22                       |              | S(t)                        | 81.1          | 84.4          | 82.1          | 68            | 68.1          |
|                                      | -12          | m-value                     | 0.308         | 0.346         | 0.348         | 0.316         | 0.334         |
|                                      |              | S(t)                        | 139.3         | 219.7         | 215.7         | 126.3         | 137.7         |
|                                      | -18          | m-value                     | 0.251         | 0.261         | 0.265         | 0.257         | 0.266         |
|                                      |              | <b>Critical Temperature</b> | <b>-22.93</b> | <b>-25.26</b> | <b>-25.46</b> | <b>-23.64</b> | <b>-25.02</b> |
| Montana PG 64-22                     |              | S(t)                        | 156.3         | 186.7         | 132.3         | 147.3         | 149.3         |
|                                      | -12          | m-value                     | 0.285         | 0.333         | 0.341         | 0.3           | 0.302         |
|                                      |              | S(t)                        | 300           | 468.3         | 347           | 245.7         | 277.7         |
|                                      | -18          | m-value                     | 0.233         | 0.233         | 0.248         | 0.232         | 0.238         |
|                                      |              | <b>Critical Temperature</b> | <b>-20</b>    | <b>-23.97</b> | <b>-24.65</b> | <b>-21.93</b> | <b>-22.2</b>  |
| Polymer Modified<br>Montana PG 70-22 |              | S(t)                        | 74.1          | 85.9          | 86.6          | 76.8          | 68.8          |
|                                      | -12          | m-value                     | 0.296         | 0.345         | 0.345         | 0.331         | 0.329         |
|                                      |              | S(t)                        | 142.7         | 230           | 224           | 149.7         | 142           |
|                                      | -18          | m-value                     | 0.255         | 0.264         | 0.262         | 0.262         | 0.26          |
|                                      |              | <b>Critical Temperature</b> | <b>-21.57</b> | <b>-25.32</b> | <b>-25.25</b> | <b>-24.76</b> | <b>-24.55</b> |



**Figure 3.5. Bending Beam Rheometer Test Results**

### 3.4.2. Mixture data and analysis

#### 3.4.2.1. Compaction study

The compaction data, shown in Figure 3.6, displays the average number of gyrations needed to compact each sample group according to the binder used. HMA samples, containing no IDB, were mixed and compacted at 150°C, while WMA samples with 0.5% and 1% IDB were mixed and compacted at 120°C. The binders shown in Figure 3.6 are grouped by pattern. The 95% confidence intervals, indicated by error bars, show a relatively high variability in the number of gyrations needed to reach the sample height. By visual observation of the data, no statistical difference is apparent between the three groups of IDB dosage percentages.

An analysis of variance (ANOVA) will verify if any factors are statistically significant. From the ANOVA analysis, multiple comparison testing was conducted, shown in Table 3.6. Visual analysis of the averages in Figure 3.6 shows that dosage

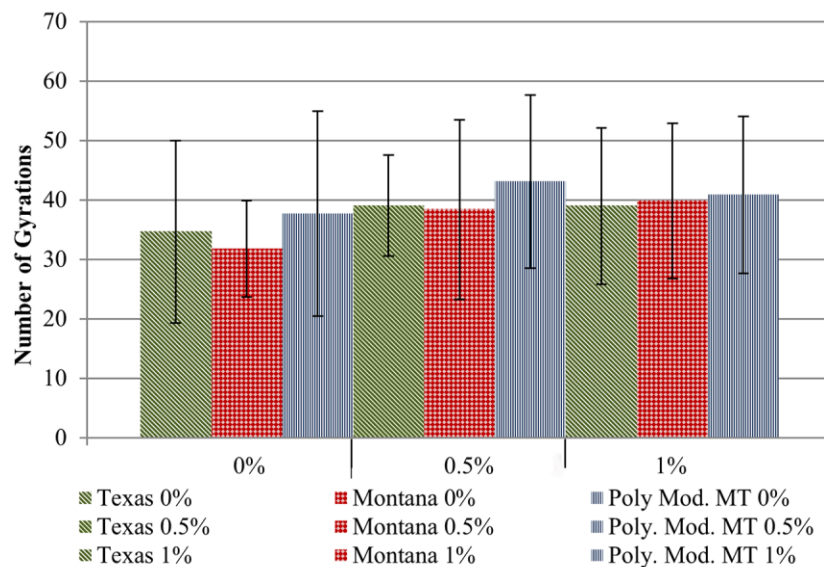


Figure 3.6. Average Number of Gyrations to 62.5mm with 95% Confidence Intervals

**Table 3.6. Tukey HSD Multiple Comparison for Compactability**

| Binder             |          | Level* |    | Least Square Mean |
|--------------------|----------|--------|----|-------------------|
| Montana            | PG 64-22 | 1.0    | A  | 39.89             |
|                    |          | 0.5    | AB | 38.44             |
|                    |          | 0.0    | B  | 31.77             |
| Poly. Mod. Montana | PG 70-22 | 0.5    | A  | 43.11             |
|                    |          | 1.0    | A  | 40.89             |
|                    |          | 0.0    | A  | 37.69             |
| Texas              | PG 67-22 | 0.5    | A  | 39.08             |
|                    |          | 1.0    | A  | 39.00             |
|                    |          | 0.0    | A  | 34.67             |

\*Levels not connected by same letter are significantly different

levels are noticeably different, but when Tukey HSD multiple comparison tests are used for the comparison, the high variability between the averages lead to a statistical conclusion that no comparison is different from all other dosage levels at the 95% confidence level. An important factor when making conclusions is that 0% IDB was compacted as an HMA mix at 150°C and that 0.5% and 1% IDB samples were compacted as WMA mixes at 120°C. It is important to keep this in mind when comparing the averages and to draw conclusions accordingly. In general, the 0%, compacted at 150°C had a lower average number of gyrations in each of the three cases. Previous studies have shown that compaction in the SGC is typically independent of temperature because of its constant strain behavior (Hurley 2006). Other warm mix studies have also shown relatively small differences between WMA and HMA compactability at typical temperatures that were used in this study by measuring air voids at a given compaction effort (Li et al. 2011); however, since IDB is a new product, it is advantageous to collect and report this data to show that the additive is not adversely impacting mix compactability. There is not an industry accepted method for measuring workability of an



asphalt mix. This is problematic because there are limited options for evaluating the effect WMA additives have on compactability in a laboratory setting.

#### 3.4.2.2. Indirect tensile strength study

The tensile strength ratio (TSR) is calculated by using the peak stress of the moisture conditioned sample divided by the peak stress of the non-moisture conditioned sample. Table 3.7 shows the average TSR, standard deviation ( $\sigma$ ) and coefficient of variation (COV) for each mix tested. The COV is mathematically, the standard deviation divided by the average. The TSR values, on average are lower with the addition of IDB but the lower TSR may also be due to the lower compaction temperature. Many State agencies set TSR minimum criteria at 80% and all samples tested for this study are above 80%. The averages show very little difference between 0.5% and 1% IDB for the Montana crude. The Texas crude shows no drop in TSR values between 0% and 0.5%, although we observe a significant decrease between 0.5% and 1% IDB. This evidence

**Table 3.7. Tensile Strength Ratios**

| Binder        | IDB  | Average | $\sigma$ | COV   |
|---------------|------|---------|----------|-------|
| MT<br>PG64-22 | 0%   | 94%     | 9%       | 10.0% |
|               | 0.5% | 87%     | 7%       | 8.0%  |
|               | 1.0% | 87%     | 7%       | 8.0%  |
| MT<br>PG70-22 | 0%   | 96%     | 11%      | 11.0% |
|               | 0.5% | 85%     | 9%       | 10.0% |
|               | 1.0% | 85%     | 10%      | 12.0% |
| TX<br>PG67-22 | 0%   | 94%     | 10%      | 10.0% |
|               | 0.5% | 94%     | 7%       | 8.0%  |
|               | 1.0% | 82%     | 9%       | 9.0%  |

strongly suggests that the optimal dosage level is 0.5% because greater percentages indicate no further benefits and may cause increased moisture susceptibility for other binders. TSR values indicate there may be some aspects of dosage level that cannot be evaluated by binder testing alone. Binder tests, namely mass loss in the RTFO oven, also support the conclusion of a 0.5% dosage level.

Table 3.8 displays the peak load averages, standard deviation ( $\sigma$ ) and the coefficient of variation (COV) for each IDB dosage level. When evaluating the TSR, peak load values should also be considered in the analysis because peak loads will be a better indicator of how IDB dosage levels may impact the strength of the sample. Units of force were used in the comparison because samples were the same height, keeping the area on which the force is applied constant. The Montana PG64-22 binder showed decreases in peak strength with increasing dosages of IDB. It is unclear if this is a consequence of IDB addition, lower compaction temperature, or a combination thereof.

**Table 3.8. Average IDT Strength Values**

|   | IDB   | Not Moisture Conditioned |          |        | Moisture Conditioned |          |        |
|---|-------|--------------------------|----------|--------|----------------------|----------|--------|
|   |       | Average (N)              | $\sigma$ | COV    | Average (N)          | $\sigma$ | COV    |
| <b>Montana<br/>PG 64-22</b>                           | 0%    | 9936                     | 586      | 5.90%  | 9303                 | 837      | 9.00%  |
|   | 0.50% | 9187                     | 822      | 8.90%  | 7908                 | 327      | 4.10%  |
|   | 1.00% | 9058                     | 969      | 10.70% | 7867                 | 629      | 8.00%  |
| <b>Polymer-<br/>Modified<br/>Montana<br/>PG 70-22</b> | 0%    | 8196                     | 434      | 5.30%  | 7911                 | 788      | 10.00% |
|   | 0.50% | 7855                     | 659      | 8.40%  | 6607                 | 269      | 4.10%  |
|   | 1.00% | 7836                     | 798      | 10.20% | 6622                 | 159      | 2.40%  |
| <b>Texas<br/>PG 67-22</b>                             | 0%    | 7425                     | 568      | 7.60%  | 6894                 | 389      | 5.60%  |
|   | 0.50% | 6708                     | 340      | 5.10%  | 6315                 | 285      | 4.50%  |
|   | 1.00% | 7247                     | 427      | 5.90%  | 5888                 | 276      | 4.70%  |

The 0.5% and 1.0% dosage rates show virtually the same values; thus, the higher dosage of 1.0% IDB did not cause further strength loss.

The Montana binder, a PG64-22, and the polymer modified binder, a PG70-22, display similar trends in strength and TSR values. Strength reductions were observed with both moisture conditioning and the addition of IDB. This may be due to the addition of IDB but could be due to the decrease in mixing and compaction temperatures. Peak load averages for 0.5% and 1.0% IDB dosages are similar. There appears to be no additional benefit to adding a higher dosage of IDB for moisture susceptibility benefits.

The trends for the Texas binder differed slightly from the trends observed with the Montana binders. Unconditioned samples with 1.0% IDB have a higher average strength than 0.5% IDB but the moisture conditioned samples with 1.0% IDB indicated a large decrease in strength. The COV values are generally lower for the Texas binder when compared to the Montana binders.

An ANOVA analysis for the IDT data was performed and used to determine statistical differences in conjunction with multiple comparison tests. Overall, the statistical analysis drew similar conclusions to the inferences drawn from observing test data averages. Moisture conditioning significantly dropped the average strength values. Typically, the samples with IDB additive had statistically lower strength values but did not drop TSR values below the minimum criteria of 80%. The lower values obtained in the IDB addition categories is also confounded with a lower production/compaction temperature. Additional evidence to support this is found by reviewing the binder test results which show minimal differences at high and intermediate temperature testing. Interactions of factors were analyzed but none were statistically significant for the

Montana binders. For the Texas binder, the only significant interaction effect indicates a higher decrease in peak strength due to moisture conditioning for the 1.0% IDB when compared with the 0.5%. The non-conditioned samples, 1.0% IDB samples had higher peak strength than the 0.5% IDB. Prior to field use, it is recommended to perform moisture sensitivity testing with the aggregates used in the field to further understand the effect, if any, that IDB may have on moisture sensitivity of the field mix design.

### 3.5. Conclusions

Isosorbide Distillation Bottoms have the potential to be used as a WMA additive. The testing plan included binder testing to fully evaluate the potential of this additive and to determine optimal dosage levels. Binder testing showed how IDB impacts rheological properties. The main objectives were to address feasibility as well as potential concerns and benefits of using IDB as a WMA additive.

The DSR test results verify that using IDB in asphalt binder has no negative impacts to binder rheology at high and intermediate temperature testing as well as at virgin, short- and long-term aging. Mass loss data showed high variability and increases with higher IDB dosage levels. From observing the mass loss averages, the safe optimum is around 0.5% to ensure that the mass loss criterion of 1% maximum is met. TGA may be useful in future research in order to fully understand the mass loss properties of IDB and best practices for blending methods. The binder specific gravity testing showed no noticeable differences with the addition of IDB. The bending beam rheometer tests showed IDB improving binder properties at low temperatures. The data showed an optimal additive rate at approximately 0.5%. Higher percentages do not achieve

additional low temperature reductions and may pose a problem for meeting mass loss criteria. The BBR test results documented that IDB decreased a binder's low temperature grade. This is beneficial for northern climates because of potential thermal cracking. This could be further investigated by performing low temperature cracking studies with the IDB as a binder additive.

Compaction data showed that IDB at 0.5% and 1.0% dosage levels was successfully used to compact WMA at 120°C with no statistical difference in compaction effort when compared with HMA compacted at 150°C. Conclusions cannot be based on compaction data alone because other studies have shown that temperature is independent of compaction effort when compacting samples in the Superpave gyratory compactor (Hurley 2006; Li et al. 2011). Moisture conditioning, as documented in other studies (Kvasnak 2009), is a primary concern with WMA implementation. The IDT strength test AASHTO T-283 (AASHTO 2007e), addresses this concern and showed that no samples fell below the TSR criteria of 80%. The peak strength for the 0.5% and 1% IDB were on average lower but this may be confounded with lower laboratory production temperatures. A moisture sensitivity study is recommended when IDB is used with other mix designs to understand the effects of IDB with other aggregate structures and to ensure moisture sensitivity issues do not occur with aggregates of different compositional chemistry.

A field trial produced with a similar binder would be beneficial for fully determining and implementing the use of IDB as a WMA additive. Plant operating temperatures are determined by multiple factors and would be left to the discretion of the contractor. Additional performance tests would be beneficial for evaluating IDB

additives. Additional binder testing should include solubility tests with binders containing IDB additives in order to measure the amount of impurities in the binder. The BBR test results showed IDB decreased the low temperature PG grade. The low temperature benefits indicate that there may be potential for IDB to be used to enhance the low temperature properties of binders as well as for WMA. Further development and implementation of this material is recommended based on the initial laboratory binder and mixture testing.

### 3.6. References

- AASHTO, American Association of State Highway and Transportation Officials (2007a). ""Standard Method of Test for Determining the Rheological Properties of Asphalt Binder Using a Dynamic Shear Rheometer (DSR)"." *AASHTO Designation T315, Standard Specifications for Transportation Materials and Methods for Sampling and Testing., 27th Ed* Washington, D.C.
- AASHTO, American Association of State Highway and Transportation Officials (2007b). ""Accelerated Aging of Asphalt Binder Using a Pressurized Aging Vessel (PAV)"." *AASHTO Designation R28, Standard Specifications for Transportation Materials and Methods of Sampling and Testing., 27th Ed* Washington, D.C.
- AASHTO, American Association of State Highway and Transportation Officials (2007c). ""Standard Method of Test for Effect of Heat and Air on a Moving Film of Asphalt Binder (Rolling Thin-Film Oven Test)"." *AASHTO Designation T240, Standard Specifications for Transportation Materials and Methods of Sampling and Testing., 27th Ed* Washington, D.C., 2007.
- AASHTO, American Association of State Highway and Transportation Officials (2007d). ""Determining the Flexural Creep Stiffness of Asphalt Binder Using the Bending Beam Rheometer (BBR)"." *AASHTO Designation T313, Standard Specifications for Transportation Materials and Methods of Sampling and Testing., 27th Ed* Washington, D.C.
- AASHTO, American Association of State Highway and Transportation Officials (2007e). ""Resistance of Compacted Hot Mix Asphalt (HMA) to Moisture Induced Damage"." *AASHTO Designation T283-07, Standard Specifications for Transportation Materials and Methods of Sampling and Testing., 27th Ed* Washington, D.C.
- Aksoy, A., Şamlioglu, K., Tayfur, S., and Özen, H. (2005). "Effects of various additives on the moisture damage sensitivity of asphalt mixtures." *Construction and Building Materials*, 19(1), 11-18.
- Asphalt Institute (2003). "*Superpave Performance Graded Asphalt Binder Specification and Testing (SP-1)*." U.S.A.: Asphalt Institute.

- ASTM Standard D70 (2009). "Standard Test Method for Density of Semi-Solid Bituminous Materials (Pycnometer Method)". *ASTM International*/West Conshohocken, PA, 2009, DOI: 10.1520/D0070-09E01, [www.astm.org](http://www.astm.org).
- Buss, A., Rashwan, M., Williams, R.C. (2011). "Investigation of Warm-mix Asphalt Using Iowa Aggregates." *Iowa Highway Research Board Project Report TR-599*. Ames, IA.
- Capitão, S. D., Picado-Santos, L. G., and Martinho, F. (2012). "Pavement engineering materials: Review on the use of warm-mix asphalt." *Construction and Building Materials*, 36(0), 1016-1024.
- D'Angelo, J., United States. Federal Highway Administration. Office of International Programs., United States. Federal Highway Administration. International Scanning Study Team., American Trade Initiatives Inc., American Association of State Highway and Transportation Officials., and National Cooperative Highway Research Program. (2008). *Warm mix asphalt : European practice*, Federal Highway Administration, Office of Policy, Office of International Programs, Washington, D.C.
- Hurley, G. (2006). "Evaluation of New Technologies for Use in WMA. Master's Thesis.", Auburn University, Auburn, AL.
- Kringos, N., and Scarpas, A. (2008). "Physical and mechanical moisture susceptibility of asphaltic mixtures." *International Journal of Solids and Structures*, 45(9), 2671-2685.
- Kvasnak, A., West, R., Moore, J., Nelson, J., Turner, P., & Tran, N. (2009). "Case Study of Warm-Mix Asphalt Moisture Susceptibility in Birmingham, Alabama." *Transportation Research Board 88th Annual Meeting Compendium of Papers*. Washington, D.C.: *Transportation Research Board of National Academies*.
- Li, B., Liu, J. X., and Su, X. L. (2011). "Effects of Compaction Method and Temperature on Warm Mix Asphalt." *Adv Mater Res-Switz*, 255-260, 3185-3189.
- Mo, L., Li, X., Fang, X., Huerman, M., and Wu, S. (2012). "Laboratory investigation of compaction characteristics and performance of warm mix asphalt containing chemical additives." *Construction and Building Materials*, 37(0), 239-247.
- Oliveira, J. R. M., Silva, H. M. R. D., Abreu, L. P. F., and Fernandes, S. R. M. (2013). "Use of a warm mix asphalt additive to reduce the production temperatures and to improve the performance of asphalt rubber mixtures." *Journal of Cleaner Production*, 41(0), 15-22.
- Oliveira, J. R. M., Silva, H. M. R. D., Abreu, L. P. F., and Gonzalez-Leon, J. A. (2012). "The role of a surfactant based additive on the production of recycled warm mix asphalts – Less is more." *Construction and Building Materials*, 35(0), 693-700.
- Romier, A., Audeon, M., David, J., Martineau, Y., and Olard, F. (2006). "Low-Energy Asphalt with Performance of Hot-Mix Asphalt." *Transportation Research Record: Journal of the Transportation Research Board*, 1962(-1), 101-112.
- Sanchez-Alonso, E., Vega-Zamanillo, A., Castro-Fresno, D., and DelRio-Prat, M. (2011). "Evaluation of compactability and mechanical properties of bituminous mixes with warm additives." *Construction and Building Materials*, 25(5), 2304-2311.
- Wasiuddin, M. M., Selvamohan, S., Zaman, M. M., Guegan, M. L (2007). "Comparative Laboratory Study of Sasobit and Aspha-min Additives in Warm-Mix Asphalt." *Transportation Research Record*:

*Journal of the Transportation Research Board, No.1990, Transportation Research Board of National Academies, Washington D.C., 82-88.*

Werpy, T. A., Holladay, J. E., and White, J. F. (2004). "Top Value Added Chemicals From Biomass: I. Results of Screening for Potential Candidates from Sugars and Synthesis Gas." Medium: ED; Size: PDFN.



## **CHAPTER 4. ESTIMATION AND ASSESSMENT OF HIGH TEMPERATURE MIX PERFORMANCE GRADE FOR SELECT BIO-BASED WMA ADDITIVES**

Modified from a paper published in *Construction and Building Materials*<sup>1</sup>

Joseph Herbert Podolsky<sup>2</sup> and R. Christopher Williams<sup>3</sup>

### **4.1. Abstract**

The Hirsch and Al-Khateeb models are commonly used to predict an asphalt mixture's dynamic modulus ( $E^*$ ) at intermediate temperatures. However,  $G_b^*$  and the mix volumetrics are needed to make these predictions. The main objectives of this paper are to demonstrate how mix testing and binder results can be used to estimate the high temperature performance grade (PG) of warm mix asphalts (WMA) with and without bio-based additives and to compare dynamic modulus performance between different asphalt binders and select bio-based additives. The results indicate that prediction of high temperature performance grade for an asphalt mixture cannot be done using the Hirsch model, but is possible using the Al-Khateeb model and that the additives and non-modified binder were not found to be statistically different from one another overall as well as within each binder type.

**Keywords:**  $E^*$ ;  $G_b^*$ ; WMA; Hirsch model; Al-Khateeb model; Bio-based additives.

<sup>1</sup> Reprinted with permission of *Construction and Building Materials* 69 (2014) 310-322.

<sup>2</sup> Primary Researcher; Primary and Corresponding Author; Iowa State University, Department of Civil, Construction, and Environmental Engineering, 174 Town Engineering, Ames, IA, United States.

<sup>3</sup> Iowa State University, Department of Civil, Construction, and Environmental Engineering, 490 Town Engineering, Ames, IA, United States.

## 4.2. Introduction

Warm mix asphalt technologies reduce binder viscosity as well as mixing and compaction temperatures by 20-55 °C during asphalt mix production and laydown. Reducing mixing temperatures provides the asphalt industry the ability to both lower their carbon footprint and save money due to reduced energy use in mixing plants. Due to the reduced binder viscosity, compaction temperatures in the field can be reduced which improves mix compactibility, extends the paving season, allows longer haul distances, and increases the potential for using more reclaimed asphalt pavement (RAP) in mixes. Reductions in both mixing and compacting temperatures also lessen the fumes workers are exposed to during the production and laydown process of an asphalt mix [1-12].

Isosorbide distillation bottoms (IDB) is a recently bio-derived co-product from corn that has surfactant properties. IDB is produced from the conversion of sorbitol to isosorbide by using sorbitan to perform a dehydration reaction twice. Sorbitol is produced by hydrogenating the glucose from the corn biomass [13]. In the past the cost for producing a bio-based WMA additive such as IDB would not have been viable due to the lower cost of petro-chemical based additives [13]. With the increasing number and growth of emerging markets around the globe as well as increasing demand for bio-based renewable products, a bio-based WMA additive such as IDB becomes viable from an economic and environmental perspective. However, a bio-based material must be also viable in terms of performance as compared to the material it is intended to replace [13]. A recently derived chemical additive from the forest products industry called forest product (FP) will also be used for binder modification in this study [14]. FP is a water-

free chemical additive that displays surfactant properties. When asphalt binder with FP is added to aggregates, the aggregate-binder interface friction is reduced due to the surfactant properties of FP. This reduction makes it possible to lower mixing and compaction temperatures [15, 16]. In the literature it is recommended that the FP optimum dosage level is 0.5% by weight of the total binder, and in recently completed binder studies it was found that the optimum dosage level for IDB addition is 0.5% by weight of the total binder. Therefore, 0.5% addition level was used in this study [5].

Currently there is a procedure for determining the performance grade of asphalt binders unmodified and modified with WMA additives. This procedure is done by following the steps in AASHTO R 29-08 in conjunction with ASTM D7173 and verifying the performance grade of the binder through the use of AASHTO M 320-10 [17-19]. However, there is no standard or clear method for determining the high temperature performance for an asphalt mixture let alone warm mix asphalt. The main objective of this paper is to illustrate how a warm mix asphalt mix's performance can be determined using both mix testing results (dynamic modulus test) with the Hirsch and Al-Khateeb models, and binder testing results (RTFO aged DSR results) [20, 21]. The secondary objective is to compare the mix performance grade of WMA with 0.5% IDB by weight of the total binder against the mix performance grade of WMA with 0.5% FP by weight of the total binder and see if IDB is a viable warm mix asphalt technology.

### 4.3. Experimental Materials

#### 4.3.1. Materials

This research used one crude source of binder from Montana, which is similar to a Canadian crude. The Montana crude was tested at its original grade of PG 64-22 (Binder I), and tested as a polymer modified binder (1.5% SBS), PG 70-22 (Binder II). The mix design that was used in the laboratory to construct dynamic modulus samples is an Iowa DOT approved mix with a 10 million ESAL design level. The aggregates, their gradation, and suppliers used for this mix design are shown in Table 4.1 and Figure 4.1. The gradation for each aggregate was verified and checked with the mix gradation in the job mix formula from the Iowa Department of Transportation (DOT). One adjustment needed to be made in the laboratory gradation was to increase the fines in the blended gradation. This was done through the addition of commercially produced hydrated lime as 100% of this material passes the No. 200 sieve. Before the blended gradation was matched to the job formula, each aggregate was sieved in their appropriate proportions to create less variability between batches. With this addition of the hydrated lime the blended gradation was matched to the job mix formula.

Two additives will be used in this study – IDB and FP – both at addition rates of 0.5% by weight of the binder. As stated earlier, IDB is a recently bio-derived co-product from corn that has surfactant properties. FP is a WMA chemical additive derived from tall oil (tree oil) [14]. The research literature recommends that the FP optimum dosage level is 0.5% by weight of the total binder, and in recently completed binder studies at Iowa State University it was found that the optimum dosage level for IDB addition is 0.5% by

weight of the total binder. Therefore, 0.5% addition level was used in this study to compare the two technologies [5].

**Table 4.1. Mix Design Gradation and Supplier Information**

| Supplier          |                | Ames Mine/<br>Martin Marietta | Ames Mine/<br>Martin<br>Marietta | Dell Rapids E.<br>Minnchaha<br>Co/Everist Inc. | Ames Mine/<br>Martin<br>Marietta | Ames Mine/<br>Martin<br>Marietta | Ames South/<br>Hallet<br>Materials Co. | Commercially<br>Produced |
|-------------------|----------------|-------------------------------|----------------------------------|--|----------------------------------|----------------------------------|--|--------------------------|
| Aggregate         |                | 1/2<br>CRUSHED<br>EC          | 3/4 CL CHIP<br>EC                | 1/2 X 4<br>QUARTZITE                           | 3/8 CL CHIP<br>LC                | MANF SAND<br>LC                  | SAND                                   | Hydrated Lime            |
| % Used            |                | 26%                           | 11%                              | 13%  | 8%                               | 24%                              | 17%                                    | 2%                       |
| U.S. Sieve,<br>mm | Mesh<br>Number | % Passing                     | % Passing                        | % Passing                                      | % Passing                        | % Passing                        | % Passing                              | % Passing                |
| 37.5              |                | 100                           | 100                              | 100  | 100                              | 100                              | 100                                    | 100                      |
| 25                | 1 in.          | 100                           | 100                              | 100  | 100                              | 100                              | 100                                    | 100                      |
| 19                | 3/4 in.        | 100                           | 98                               | 100  | 100                              | 100                              | 100                                    | 100                      |
| 12.5              | 1/2 in.        | 91                            | 58                               | 99   | 100                              | 100                              | 100                                    | 100                      |
| 9.5               | 3/8 in.        | 70                            | 32                               | 78   | 92                               | 100                              | 100                                    | 100                      |
| 4.75              | No.4           | 35                            | 5                                | 7.7  | 25                               | 98                               | 98                                     | 100                      |
| 2.36              | No.8           | 19                            | 1.5                              | 1.2  | 3.1                              | 68                               | 87                                     | 100                      |
| 1.18              | No.16          | 12                            | 1.4                              | 0.6  | 1.8                              | 36                               | 69                                     | 100                      |
| 0.6               | No.30          | 10                            | 1.3                              | 0.4  | 1.6                              | 16                               | 40                                     | 100                      |
| 0.3               | No.50          | 8.5                           | 1.2                              | 0.3  | 1.5                              | 6                                | 8                                      | 100                      |
| 0.15              | No.100         | 8.2                           | 1.1                              | 0.2  | 1.2                              | 2                                | 0.6                                    | 100                      |
| 0.075             | No.200         | 8                             | 0.9                              | 0.1  | 1                                | 1.2                              | 0.2                                    | 100                      |

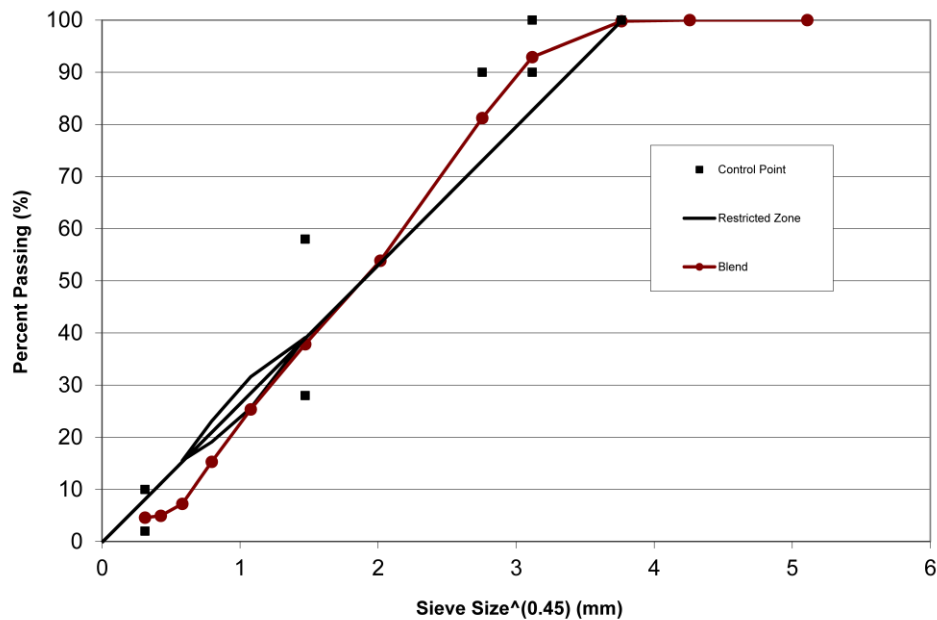


**Figure 4.1. Mix Design Gradation Chart (12.5mm NMA5)**

### 4.3.2. Mix design, sample preparation, and testing

#### 4.3.2.1. Dynamic shear rheometer binder sample experimental testing plan

Testing was done using a Dynamic Shear Rheometer (DSR) on multiple samples from each binder (Montana Crude – PG 64-22, and Polymer Modified Montana Crude – PG 70-22) that were not modified with any additives. The DSR was used to test the binders at multiple frequencies and at several temperatures [20]. Testing in a DSR at six temperatures (13 °C, 21 °C, 29 °C, 37 °C, 45 °C, and 54 °C) and ten frequencies (1 Hz, 1.59 Hz, 2.51 Hz, 3.98 Hz, 6.31 Hz, 10 Hz, 15.85 Hz, 25.12 Hz, 39.81 Hz, and 50 Hz), was done for creating a  $G_b^*$  master curve using binder samples from the original PG 64-22 and original PG 70-22 binders [20].

#### 4.3.2.2. Dynamic modulus asphalt mixture experimental testing plan

The dynamic modulus testing was performed on three groups of samples: no additive, 0.5% IDB, and 0.5% FP samples using two binder types; the Montana PG 64-22 binder, and the Polymer Modified Montana PG 70-22 binder. The dynamic modulus values and phase angles were calculated at several different frequency-temperature combinations for the mix combinations. The temperatures used in testing were 4 °C, 21 °C, and 37 °C while the test frequencies were 25 Hz, 20 Hz, 10 Hz, 5 Hz, 2 Hz, 1 Hz, 0.5 Hz, 0.2 Hz, and 0.1 Hz.

For dynamic modulus testing, 2600 g aggregate samples were proportioned and mixed with an optimum binder content of 5.2% to produce test samples. Dynamic modulus sample weights were estimated to be 2670 for achieving 7%±1% air voids. The WMA mixtures used for the dynamic modulus test in this paper differed by binder type

and additive choice, but were mixed and compacted at the same temperatures (mix temperature – 130°C, and compaction temperature – 120°C). Three replicate samples for each group were used in the development of this paper. Each sample tested was used with the Hirsch and the Al-Khateeb models to back-calculate individually to the  $G_b^*$  master curve. The three samples' back-calculated results for each group were averaged and are used to make comparisons in this paper.

#### 4.4. Experimental Methods

##### 4.4.1. Estimated $G^*$ binder master curve methods back-calculated from measured $E^*$ data

Two methods were used for back calculating the binder modulus master curves from predicted complex dynamic modulus master curves made using measured  $E^*$  data. The first method used was the Hirsch model, while the second method used was the Al-Khateeb model [22, 23]. The purpose of using the Hirsch model is to use binder modulus ( $G_b^*$ ) and volumetric composition (voids in mineral aggregate - VMA, and voids filled with asphalt - VFA) to estimate the modulus of asphalt concrete ( $E^*$ ). In this paper, VMA, VFA, and  $E^*$  are known and are used to estimate the binder modulus. The Al-Khateeb model is used to estimate the asphalt concrete dynamic modulus using only two inputs: asphalt binder dynamic shear modulus ( $G_b^*$ ), and voids in mineral aggregate (VMA). The Al-Khateeb model is a simpler form of the Hirsch model, but was constructed using more data than the former which enables it to estimate the asphalt dynamic modulus for a wider range of temperatures and frequencies.

#### 4.4.1.1. Sigmoidal $E^*$ master curves using measured data

The dynamic modulus test is a linear viscoelastic test used for asphalt mixtures where the complex dynamic modulus ( $E^*$ ) is determined by relating stress to strain at multiple temperatures each under several repeated loading rates (frequencies).  $E^*$  is defined as the pavement stiffness and is a very important property because it is used to simulate a pavement's response under repeated traffic loading [24]. The stiffness of an asphalt mix also depends on the temperature at which it is being loaded. When the stiffness is high under an applied stress, the asphalt mix will have lower strain. At high temperatures, high stiffness mixes are more resistant to permanent deformation, but high stiffness mixes at low temperatures are generally more prone to cracking [24].

The dynamic modulus test is defined as an uniaxial compression test with cyclic loading. In this test, a cyclic load is applied vertically in a sinusoidal wave form on a cylindrical sample. The complex modulus is the ratio of stress amplitude to strain in a sinusoidal wave form:

$$E^* = \frac{\sigma}{\varepsilon} = \frac{\sigma_0 \times e^{i\omega t}}{\varepsilon_0 \times e^{i(\omega t - \delta)}} = \frac{\sigma_0 \times \sin(\omega t)}{\varepsilon_0 \times \sin(\omega t - \delta)} \quad (4.1)$$

where

$E^*$  = complex modulus;

$\sigma_0$  = peak (maximum) stress;

$\varepsilon_0$  = peak (maximum) strain;

$\delta$  = phase angle (degrees);

$\omega$  = angular velocity;



t = time (seconds);

e = exponential; and

i = imaginary component of the complex modulus [25].

Ultimately the dynamic modulus is defined as the absolute value of the complex modulus:

$$|E^*| = \frac{\sigma_0}{\varepsilon_0} \quad (4.2)$$

where

$\sigma_0$  = maximum dynamic stress, and

$\varepsilon_0$  = peak recoverable axial strain [25].

The complex modulus ( $E^*$ ) is made up of the storage modulus ( $E'$ ), and the loss modulus ( $E''$ ).  $E'$  deals with the asphalt concrete elastic behavior while the  $E''$  deals with the viscous behavior of asphalt concrete [26], and

$$E^* = E' + iE'' \quad (4.3)$$

An asphalt mixture's dynamic modulus varies with temperature and loading frequency. Making comparisons between results from one temperature to another temperature complicated. The development of dynamic modulus master curves provides a direct means of viewing a much easier to interpret representation of dynamic modulus results. A dynamic modulus master curve makes it much easier to make a comparison

between several sets of dynamic modulus results at various temperatures [27]. According to research conducted by Li and Williams [28], testing  $E^*$  values at three temperatures (4.4, 21.1, and 37.8 °C) did not change the shape of master curves constructed by data from nine frequencies ranging from 25 Hz to 0.1 Hz when compared to using data from 5 temperatures each at six frequencies.

The dynamic modulus master curve is constructed using a reference temperature or frequency based on the time-temperature superposition principle. Asphalt mixtures exhibit higher dynamic modulus values at low temperatures and/or high loading frequencies. At a lower temperature, a dynamic modulus value could be equal to a dynamic modulus value gained through testing at a higher temperature but at a lower frequency. This means dynamic modulus values resulting from testing done at different temperatures and frequencies can be transposed to a single reference temperature or frequency. Dynamic modulus testing can be done more easily at several frequencies and fewer temperatures than at several temperatures and fewer frequencies because of overall testing-time as changing the test temperature is time consuming. As a result, researchers usually test for dynamic modulus values at few temperatures but at many different frequencies. To transition from frequency to temperature is much easier than from temperature to frequency. A shift factor,  $a(T)$ , is used to equalize frequencies at different temperatures. The following equation shows the mathematical expression of the shift factor,  $a(T)$ :

$$f_r = \frac{f}{a(T)} \rightarrow \log(f_r) = \log(f) - \log(a(T)) \quad (4.4)$$

$$\log(a(T)) = aT^2 + bT + c \quad (4.5)$$

where

$f_r$  = reduced frequency (loading frequency at the reference temperature);

$f$  = loading frequency;

$a(T)$  = shift factor; and

$a$ ,  $b$ , and  $c$  are coefficients for solving the shift factor  $a(T)$ .

The shift factor is equal to 1 at the reference temperature, and  $\log(a(T))$  is equal to 0. In the “2002 Guide for the Design of New and Rehabilitated Pavement Structures” the dynamic modulus master curve is fitted using the following sigmoidal function [29]:

$$\log(|E^*|) = \delta + \frac{\alpha}{1 + e^{\beta + \gamma \log(t_r)}} \quad (4.6)$$

where

$|E^*|$  = dynamic modulus;

$t_r$  = reduced time at the reference temperature;

$\delta$  = minimum modulus value;

$\delta + \alpha$  = maximum modulus value; and

$\beta$ ,  $\gamma$  = parameters describing the shape of the sigmoidal function.

These parameters that are used to create a master curve are back-calculated to match the estimated  $E^*$  values from the sigmoidal function to the  $E^*$  values resulting from lab testing with the following equation.

$$Error^2 = \sum_{i=1}^n [\log(Predicted E_i^*) - \log(Measured E_i^*)]^2 \quad (4.7)$$

This process was done for each sample from each of the binder type/additive groups. To obtain the dynamic modulus master curve for each sample at 1.59 Hz for temperatures ranging from 13 °C to 70 °C for PG 64-22 and to 13 °C to 76 °C for PG 70-22 and additive group the variable  $c$  has to be changed with the addition of  $\log(1.59 \text{ Hz})$  in Equation 4.5. The shift from 1 Hz to 1.59 Hz for frequency is chosen because the high temperature binder grade is determined at this frequency in accordance with AASHTO R29 and M320 Standards. This shifts the calculation of  $\log(a(T))$  for a chosen range of temperatures from a frequency of 1 Hz to 1.59 Hz.  $\log(a(T))$  is equal to  $\log(f_r)$ . Therefore to obtain the reduced time ( $t_r$ ), one can use the following equation:

$$t_r = \left(1 / \left(10^{\log(a(T))}\right)\right) \quad (4.8)$$

where  $\left(10^{\log(a(T))}\right) = \text{reduced frequency } (f_r)$ .

Using the shifted reduced time ( $t_r$ ) values with Equation 4.1, one can attain the  $E^*$  values for a range of temperature values at a frequency of 1.59 Hz.

#### 4.4.1.2. Hirsch model

The Hirsch model is a semi-empirical method that can be used for estimating the dynamic modulus of asphalt concrete. The Hirsch model is based on the law of mixtures and combines both parallel and series elements. At high temperatures, asphalt concrete

acts like the series component while at low temperatures, the asphalt concrete acts in parallel. For this model to be useful it needed to be modified several times to be both time and temperature dependent - Christensen et al. created an alternative version of the modified Hirsch model (Figure 4.2.) in 2003 where the subscripts p and s denote parallel and series components. In this version  $V_a$  is the aggregate volume limited to the contact volume,  $V_m$  - binder volume, and  $V_v$  - air void volume [23].

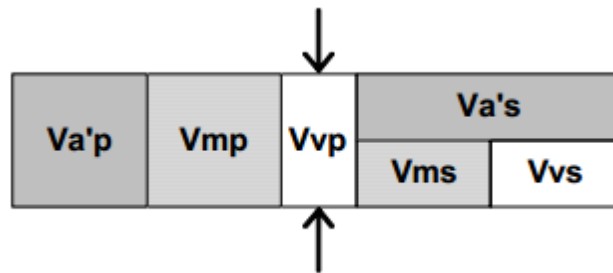


**Figure 4.2. Final Alternate Version of the Modified Hirsch Model**

The alternative version of the modified Hirsch model in Figure 4.2 is mathematically represented in the following equation:

$$E_c = P_c(V_a'E_a + V_mE_m) + (1 - P_c) \left[ \frac{V_a'}{E_a} + \frac{(V_m + V_v)^2}{V_mE_m} \right]^{-1} \quad (4.9)$$

where

$E_c$  = modulus of asphalt concrete;

$E_a$  = aggregate modulus;

$E_m$  = mastic modulus; and

$P_c$  = aggregate contact volume fraction.

The final aggregate contact volume fraction is calculated through Equation 4.10 whereas the final mixture dynamic modulus prediction model is shown in Equation 4.11:

$$P_c = \frac{\left(20 + \frac{VFA \times 3|G^*|_{binder}}{VMA}\right)^{0.58}}{650 + \left(\frac{VFA \times 3|G^*|_{binder}}{VMA}\right)^{0.58}} \quad (4.10)$$

$$\begin{aligned} |E^*|_{mix} = P_c & \left[ 4,200,000(1 - VMA/100) \right. \\ & \left. + 3|G^*|_{binder} \left( \frac{VFA \times VMA}{10,000} \right) \right] \\ & + (1 - P_c) \left[ \frac{1 - VMA/100}{4,200,000} + \frac{VMA}{3VFA|G^*|_{binder}} \right]^{-1} \end{aligned} \quad (4.11)$$

where

VMA = voids in mineral aggregate,

VFA = voids filled with asphalt binder,

$E_m = 3|G^*|_{binder}$ , and

$|E^*|_{mix}$  = predicted mixture dynamic modulus in psi.

To solve for  $E^*_{mix}$  using the Hirsch model, the  $G^*_{binder}$  needs to be known. Using the results already determined using the sigmoidal function from Section 4.4.1.1,  $E^*_{mix}$  values were estimated at a frequency of 1.59 Hz for temperatures ranging from 13 °C to 70 °C and 13 °C to 76 °C for the PG 64-22 and PG 70-22 binders, respectively. These results will be used as the actual  $E^*_{mix}$  results so back-calculation can be done to solve for

$E^*_{mix}$  using the Hirsch model. By solving the Hirsch model  $E^*_{mix}$  results, the  $G^*_{binder}$  results are also determined. This process was done by using the results obtained in Section 4.4.1.1 with Equations 4.10, 4.11 and 4.12. The optimum parameters were determined by minimizing the error represented in Equation 4.12. Due to the Hirsch model not having a version of Equations 4.10 and 4.11 in terms of pa, the conversion of the units had to be made from psi to pa after the  $G^*_{binder}$  results were already determined using Equations 4.10, 4.11 and 4.12.

$$Error^2 = \sum_{i=1}^n [\log(SigmoidE_i^*) - \log(PredictedHirschE_i^*)]^2 \quad (4.12)$$

#### 4.4.1.3. Al-Khateeb model

Al-Khateeb et al. studied the Hirsch model extensively in 2006 and came up with the following model to more accurately predict  $E^*_{mix}$  at high temperatures and reduced frequencies in Equation 4.13 (psi) and Equation 4.14 (Pa) [22].

$$|E^*|_m = 3 \left( \frac{100 - VMA}{100} \right) \left( \frac{\left( 90 + 10,000 \frac{|G^*|_b}{VMA} \right)^{0.66}}{1,100 + \left( 900 \frac{|G^*|_b}{VMA} \right)^{0.66}} \right) |G^*|_g \quad (4.13)$$

$$|E^*|_m = 3 \left( \frac{100 - VMA}{100} \right) \left( \frac{\left( 90 + 1.45 \frac{|G^*|_b}{VMA} \right)^{0.66}}{1,100 + \left( 0.13 \frac{|G^*|_b}{VMA} \right)^{0.66}} \right) |G^*|_g \quad (4.14)$$

where

$|G^*|_g$  = dynamic shear modulus of asphalt binder at the glassy state

(assumed to be 145,000 psi (999,050,000 Pa));

$|E^*|_m$  = dynamic modulus of asphalt concrete mixture (psi or Pa);

$|G^*|_b$  = asphalt binder complex shear modulus (psi or Pa); and

VMA = voids filled with mineral aggregates.

The Al-Khateeb model is also based on the law of mixtures for composite materials like the Hirsch model. However, the asphalt, aggregate and air phases are assumed to exist in parallel. Due to this assumption, this model is simpler than the Hirsch model and only needs two inputs ( $G^*_b$  and VMA) rather than three ( $G^*_b$ , VMA, and VFA) to estimate  $E^*_{mix}$ . The strengths the researchers observed through use of this model included improved prediction of  $|E^*|$  data at high temperatures and low frequencies for mixtures used in the FHWA accelerated loading facility (ALF) test strips. The main weaknesses of this model are its lack of verification and that the model was created using  $|E^*|$  values acquired at strain amplitudes higher than the recommended levels (200  $\mu\epsilon$  vs. a recommended 75–150  $\mu\epsilon$ ).

The  $G^*$  of the binder needs to be known to solve for  $E^*_{mix}$  using the Al-Khateeb model. Using the results already determined using the sigmoidal function from Section 4.4.1.1,  $E^*_{mix}$  values were estimated at a frequency of 1.59 Hz for temperatures ranging from 13 °C to 70 °C and 13 °C to 76 °C for the PG 64-22 and PG 70-22 binders, respectively. These results will be used as the actual  $E^*_{mix}$  results so back-calculation can be done to solve for  $E^*_{mix}$  using the Al-Khateeb model. By solving the Al-Khateeb



model  $E^*_{mix}$  results the  $G^*_{binder}$  results are also determined. This process was done by using the results gained through Section 4.4.1.1 with Equations 4.14 and 4.15. Equation 4.15 is used for optimizing the parameters by minimizing the error.

$$Error^2 = \sum_{i=1}^n [\log(SigmoidE_i^*) - \log(PredictedA1 - KhateebE_i^*)]^2 \quad (4.15)$$

#### 4.4.2. Predicted $G^*$ binder master curve methods from measured data

Two methods were used for constructing the  $G^*_b$  master curves. The first method (unmodified method) used a modified sigmoidal model developed by Marasteanu and Anderson [30], while the second method used a variation of this model that was constructed by researchers at Michigan Technological University [31]. Method 2 (modified method) has further modifications that take into account the effect of phase angle. Method 1 is shown mathematically below in Equations 4.16 through 4.18 and method 2 is shown in Equations 4.19 through 4.21:

$$\text{Method 1} \\ \log|G^*| = \delta + \frac{\alpha}{1 + e^{\beta + \gamma(\log t_r)}} \quad (4.16)$$

$$a(T) = \frac{t}{t_r} \quad (4.17)$$

$$\log a(T_i) = aT_i^2 + bT_i + c \quad (4.18)$$

$$\text{Method 2}$$

$$\log|G^*| = \delta + \frac{\alpha}{1 + e^{\beta + \lambda \cos(\theta) + \gamma(\log t_r)}} \quad (4.19)$$

$$\log a(T_i) = \frac{aT_i^2 + bT_i + c}{\cos \varphi} \quad (4.20)$$

$$a(T) = \frac{t}{t_r} \quad (4.21)$$

where

$t_r$  = reduced time of loading at reference temperature (s);

$\theta$  = phase angle (°);

$\lambda$  = influence factor of phase angle;

$\delta, \alpha, \beta, \gamma$  = Coefficients;

$a(T)$  = shift factor as a function of temperature;

$t$  = time of loading (s);

$T$  = temperature (°C);

$a(T_i)$  = shift factor as a function of temperature  $T_i$ ;

$\varphi$  = shift angle; and

$a, b, c$  = coefficients for shift factor.

Both methods use the principle of time-temperature superposition to shift the measured data points from several temperatures each with several frequencies into one master curve at one temperature over a frequency range for the binder's complex shear

modulus. Method 1 only deals with a horizontal shift in the data points, while method 2 has an added slope shift through the shift angle  $\phi$ . The slope shift moves the data points both horizontally and vertically around the pivot point located at the reference temperature 21 °C as shown in Figure 4.3. Below and above 21 °C method 2 has a smaller slope than method 1. When method 2 is below 21 °C the smaller slope makes the shift factors smaller, thereby the binder is more elastic for method 2 than for method 1 below the reference temperature, 21 °C. When method 2 is above the reference temperature, the smaller slope impacts the shift factors by decreasing them at a slower rate than that of method 1; this means that the binder is more viscous above the reference temperature using method 2 over that of method 1. What this is showing is that method 2 includes the impact of the phase angle; how the binder's viscoelastic properties impact reduced frequency and reduced time which determines the coefficients  $\delta$ ,  $\alpha$ ,  $\beta$ , and  $\gamma$  that estimate a binder's complex shear modulus. In order to shift the data points and construct a master curve, the sum of log square error squared is minimized using Equation 4.22.

$$Error^2 = \sum_{i=1}^n [\log(G_i^*) - \log(Predicted G_i^*)]^2 \quad (4.22)$$

where

$G_i^*$  = measured asphalt binder complex shear modulus at  $i^{\text{th}}$  point; and

Predicted  $G_i^*$  = predicted asphalt binder complex shear modulus at  $i^{\text{th}}$  point.

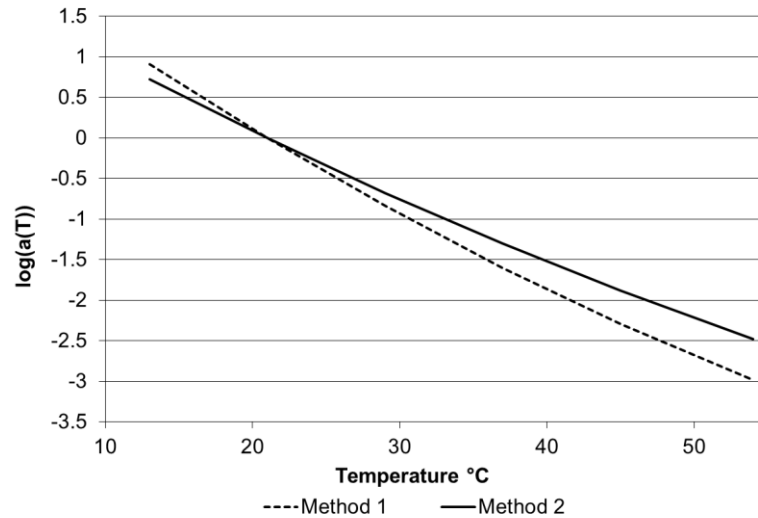


**Figure 4.3. Log Shift Factors ( $\log(a(T))$ ) vs. Temperature for Method 1 and 2**

These methods were used to construct the asphalt binder complex shear modulus over that of other models like the Christensen-Anderson-Marasteanu (CAM) model, and the 1S2P1D model (name represents one spring, two parabolic creep elements and one dashpot) because the modified sigmoidal model has been shown to be more accurate in estimating the master curve compared to the measured data for unmodified unaged and aged binders [27, 30, 32-35]. The above stated models have been shown to be not as accurate at estimating the asphalt binder master curve for polymer modified binders in literature as that of methods 1 and 2 so it was decided to use the same two methods as stated earlier [36, 37]. In this approach the two methods can be compared for use with the polymer modified binder used in this study (Polymer Modified Montana Crude – PG 70-22). For each of the two methods R-squared values were determined and compared for each binder type (PG 64-22 and PG 70-22).

## 4.5. Analysis of Results and Discussion

### 4.5.1. Comparison of $G^*$ sigmoidal models from binder data

For this analysis, both methods of determining  $G^*_{\text{binder}}$  master curves were used on multiple samples of each binder type. The master curves were constructed using Excel Solver, one of which is shown in Figure 4.4. In the construction of all the master curves, 21 °C was used as the reference temperature and 1 Hz was used as the reference frequency for shifting the measured data.

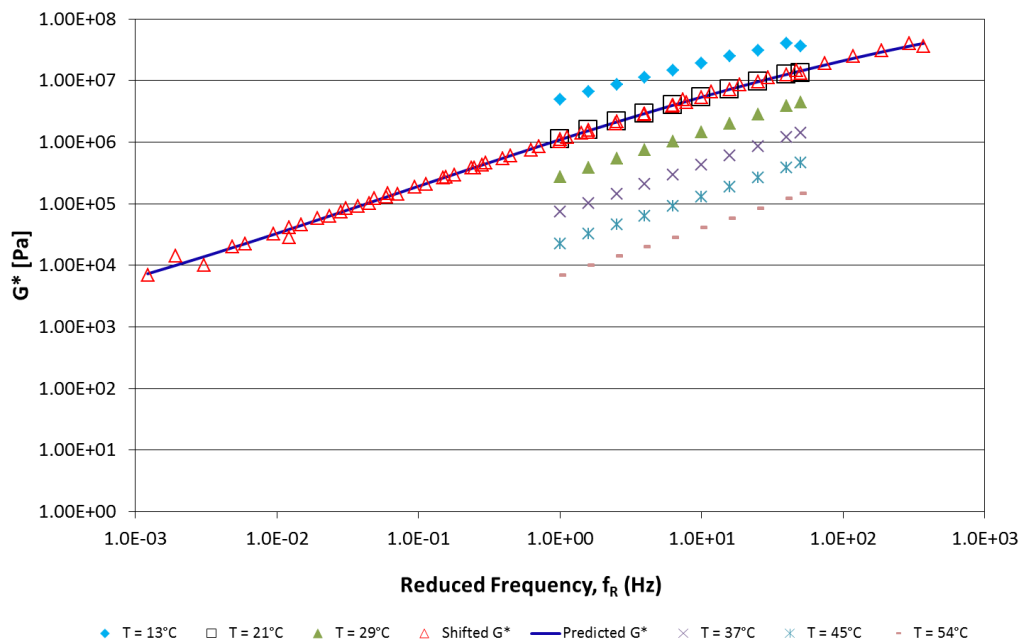


Figure 4.4. Binder  $G^*$  Master Curve for Sample 2 of PG 70-22 using Method 2

After constructing the sigmoidal master curves, the measured data was compared against the predicted data for each method and each sample. The results of these comparisons are shown in Table 4.2. According to the results both methods have about the same accuracy at predicting the binder  $G^*$  sigmoidal for the binder type PG 64-22 and binder type PG 70-22. This is the case even though the  $R^2$  values are higher for

method 1 than that of method 2 for the PG 64-22 binder. There is not a statistical difference between the two methods for the PG 64-22 binder. The situation for the PG 70-22 binder is different because both models do not appear to be different in terms of predicting the binder  $G^*$  master curves. The PG 70-22 binder is polymer modified, but utilized the PG 64-22 binder for polymer modification with 1.5% styrene-butadiene-styrene (SBS). The modified model would be expected to work better with modified binders, but in this case this does not appear to be true. Rather the modified model (method 2) performs the same as the unmodified model (method 1) in terms of  $R^2$  and  $R^2_{Adjusted}$  for the PG 70-22 binder. To choose which method will be used for comparing to the back-calculated  $G^*_{binder}$  results from the Hirsch model and Al-Khateeb models, the results of these two methods at 1.59 Hz need to be estimated for temperatures ranging from 58 to 70 °C and 58 to 76 °C for the PG 64-22 and PG 70-22 binders, respectively. These results can then be used to create charts of  $G^*/\sin\delta$  vs. Temperature (°C) to estimate the high temperature binder grade.

**Table 4.2. Results from Comparing Methods Used in Constructing Binder  $G^*$  Master Curves**

| Binder Type | Sample No. | Model Type | $R^2$    | $R^2_{Adjusted}$ | F        | Prob > F |
|-------------|------------|------------|----------|------------------|----------|----------|
| PG 64-22    | 1          | Unmodified | 0.99405  | 0.993947         | 9689.484 | <0.0001* |
|             | 2          | Unmodified | 0.992992 | 0.992871         | 8218.022 | <0.0001* |
|             | 1          | Modified   | 0.975152 | 0.974723         | 2276.182 | <0.0001* |
|             | 2          | Modified   | 0.974466 | 0.974026         | 2213.485 | <0.0001* |
| PG 70-22    | 1          | Unmodified | 0.997639 | 0.997598         | 24506.48 | <0.0001* |
|             | 2          | Unmodified | 0.990085 | 0.989914         | 5791.959 | <0.0001* |
|             | 1          | Modified   | 0.997863 | 0.997826         | 27085.3  | <0.0001* |
|             | 2          | Modified   | 0.989899 | 0.989725         | 5684.156 | <0.0001* |

To create the charts where the high temperature binder grade can be determined visually and mathematically, Equations 4.18 and 4.20 will be used for methods 1 and 2. However, the variable  $c$  has to be changed with the addition of  $\log(1.59 \text{ Hz})$ . The shift from 1 Hz to 1.59 Hz for frequency is chosen because the high temperature binder grade is determined at this frequency according to AASHTO R29 and M320 Standards. This shifts the calculation of  $\log(a(T))$  for a chosen range of temperatures from a frequency of 1 Hz to 1.59 Hz.  $\log(a(T))$  is equal to  $\log(f_r)$ . Therefore to obtain reduced time ( $t_r$ ) one can use the following equation:

$$t_r = \left(1 / \left(10^{\log(a(T))}\right)\right) \quad (4.23)$$

where  $\left(10^{\log(a(T))}\right) = \text{reduced frequency } (f_r)$ .

Using the shifted reduced time ( $t_r$ ) values with Equations 4.16 and 4.19 one can obtain the binder  $G^*$  values for a range of temperature values at 1.59 Hz frequency for both methods. To estimate the phase angles, a plot of measured angles (y variable) vs. reduced frequency ( $f_r$ ) was created for each sample tested after the master curve was constructed. From this plot a logarithmic trend line was created in the following form:

$$\text{Phase Angle } (^\circ) = a \times \ln\left(10^{\log(a(T))}\right) + b \quad (4.24)$$

Where variables  $a$  and  $b$  are determined through fitting the trend line to each individual set of data. The following two figures display the results gained through using Equations 4.16, 4.17, 4.18, 4.19, 4.20, 4.21, 4.23 and 4.24, with temperatures ranging

from 58 to 70 °C and 58 to 76 °C for the two different binders. Since the binders used are short-term-aged, the failure temperature or high temperature grade is determined when  $G^*/\sin\delta = 2.2$  kPa. From Figure 4.5 it is observed that the failing high temperature is 60.88 °C and 64.52 °C for methods 1 and 2, respectively, using the PG 64-22 binder. For the PG 70-22 binder in Figure 4.6 the failing high temperature is 71.01 °C, and 74.41 °C for methods 1 and 2. Method 2 for both binders provided the accurate grade and thus will be used for further analysis in Sections 4.5.2 and 4.5.3. Thus the modified model will be used for comparisons with the back-calculated binder  $G^*$  values for the PG 64-22 binder without any additive, with 0.5% IDB, and with 0.5% FP. Both methods 1 and 2 have failing high temperature grades above 70 °C, but for simplicity, the modified model (method 2) will also be used for further analysis in Sections 4.5.2 and 4.5.3 of this paper for the PG 70-22 binder without any additive, with 0.5% IDB, and with 0.5% FP.

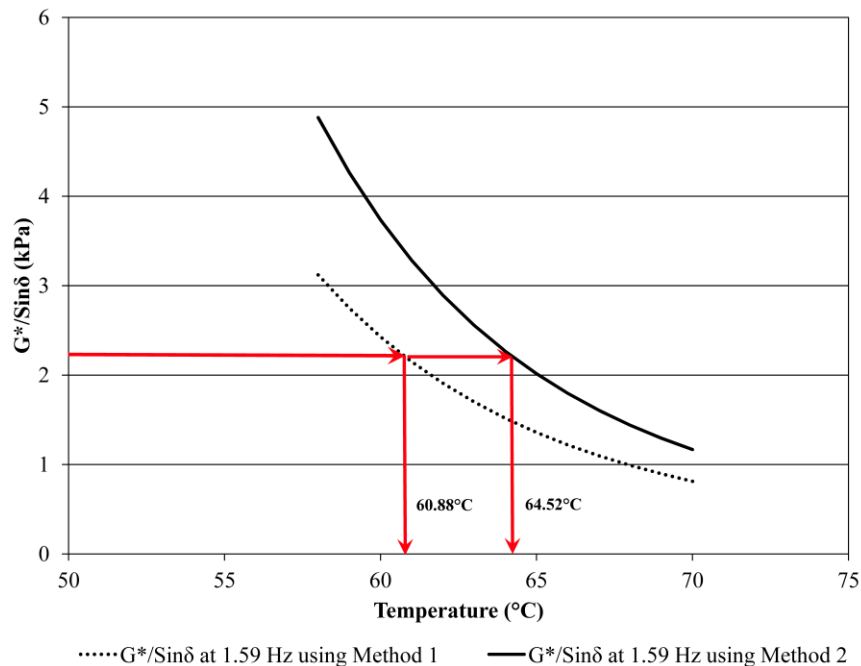
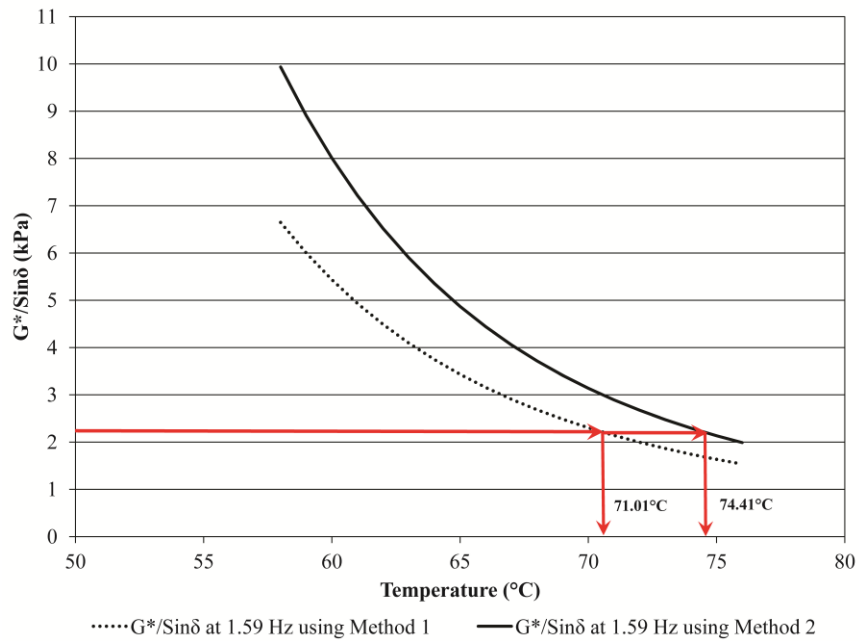
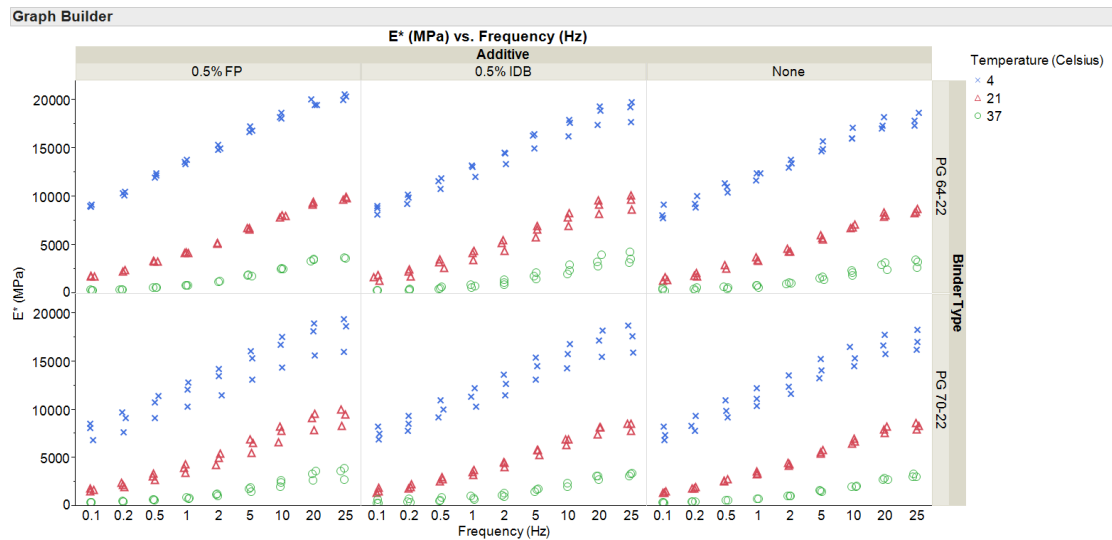


Figure 4.5. Short-Term-Aged High Temperature Grade of PG 64-22 using Method 1 and Method 2





**Figure 4.6. Short-Term-Aged High Temperature Grade of PG 70-22 using Method 1 and Method 2**



**Figure 4.7. Comparison of all Measured E\* Results across Additive and Binder Type**

#### 4.5.2. Statistical analysis of measured E\* results

The measured E\* results for each additive by binder type across temperature (°C) and frequency (Hz) are shown in Figure 4.7. From the trends shown in Figure 4.7 it is

observed that  $E^*$  values for all six groups of samples increase with an increase in frequency and a decrease in temperature at which each test is conducted.

To conduct a statistical analysis using the raw measured  $E^*$  results, the data needs to be examined to see if the central limit theorem is met. The spread of the raw measured unshifted  $E^*$  results for each group is shown in Figure 4.8. From Figure 4.8 it is shown that the central limit theorem is not met as the variance decreases with increasing temperature for each group. A variance stabilization transformation was done to the raw  $E^*$  values. First, a logarithmic transformation was done as shown in Figure 4.9, and then a square root transformation was done as shown in Figure 4.10. After examining both transformations of the raw measured  $E^*$  results, the square root transformation was selected for use in statistical analysis as the variance was more uniform with increasing temperature among the six groups.

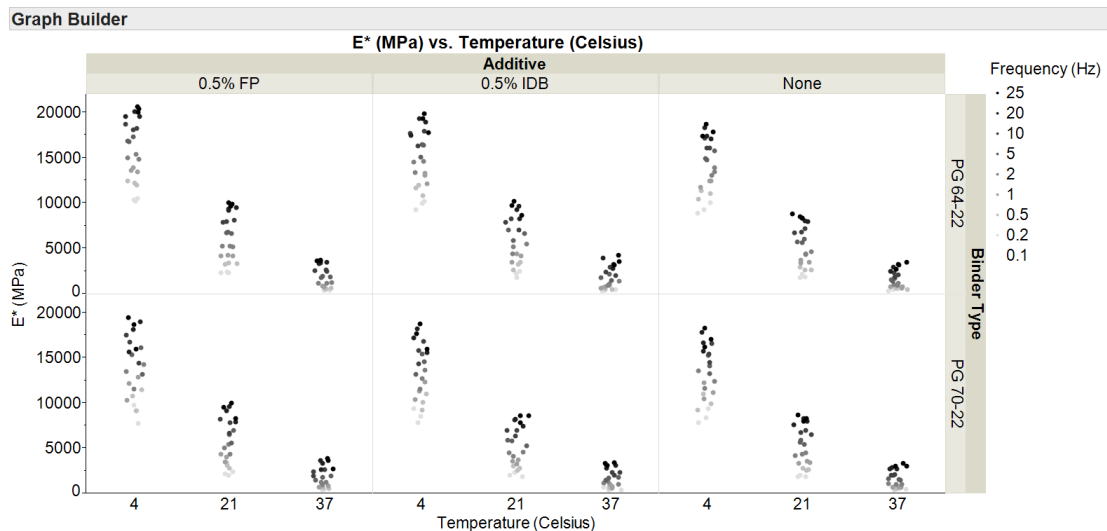


Figure 4.8. Distribution of  $E^*$  Results not Transformed

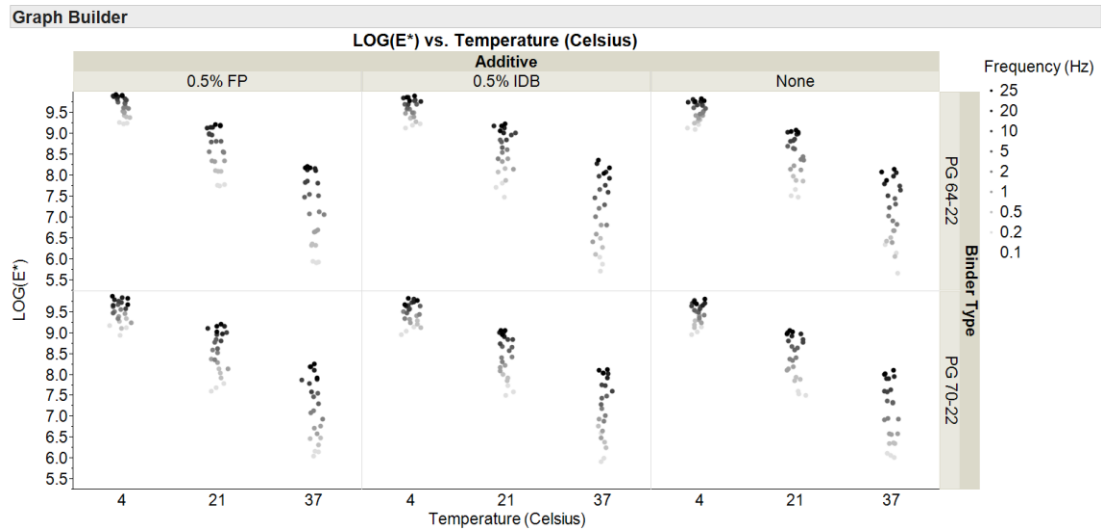


Figure 4.9. Distribution of E\* Results after Logarithmic Transformation

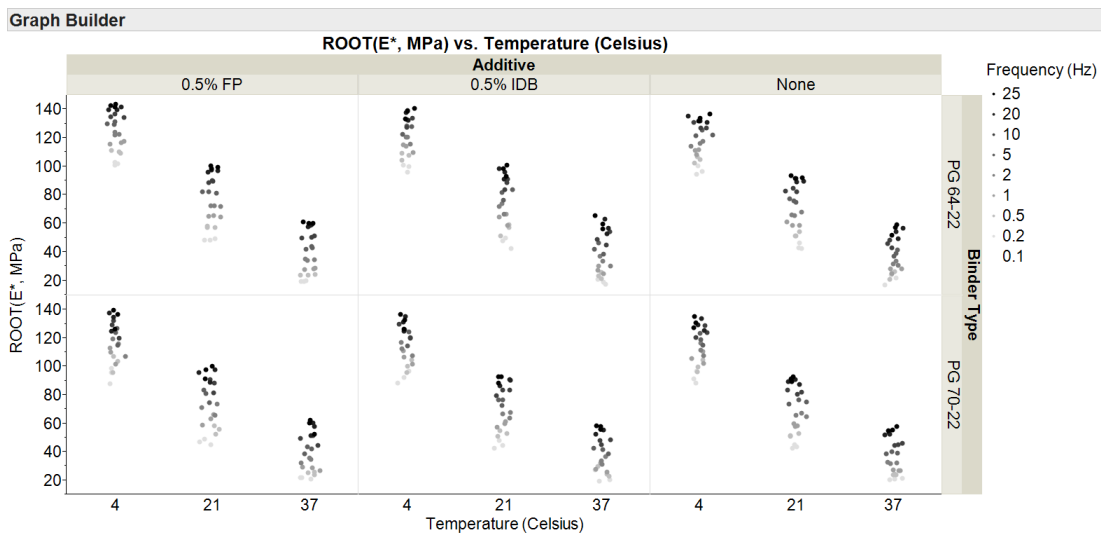


Figure 4.10. Distribution of E\* Results after Square Root Transformation

An analysis of variance (ANOVA) was conducted to examine which variability factors are significant in affecting the square root transformed E\* values. A split plot repeated measures design was used to conduct the ANOVA. The whole plot factors examined are Binder Type - A, and Additive - B, while the subplot factors examined are Temperature (°C) - C, and Frequency (Hz) – D. All the interactions between Binder Type - A, Additive - B, Temperature (°C) - C, and Frequency (Hz) – D are also studied. A

statistical program called JMP with the results shown in Table 4.3 below was used to evaluate the split plot repeated measure design for this ANOVA.

In Table 4.3, it is evident that both Temperature (°C) - C and Frequency (Hz) - D are statistically significant sources of variability by themselves as well as crossed. To be a statistical significant source of variability, the p-value must be less than or equal to 0.05. The only interactions that are not statistically significant sources of variability are

**Table 4.3. ANOVA of ROOT(E\*, MPa) Results Using Split Plot Repeated Measure Design**

| Source                   | DF  | Sum of Squares | Mean Squares | F-value  | P-value | Status          |
|--------------------------|-----|----------------|--------------|----------|---------|-----------------|
| A                        | 1   | 977.778        | 977.778      | 5.9962   | 0.0307  | Significant     |
| B                        | 2   | 1166.01        | 583.003      | 3.5753   | 0.0605  | Not-significant |
| A*B                      | 2   | 94.5256        | 47.2628      | 0.2898   | 0.7535  | Not-significant |
| C                        | 2   | 510357         | 255179       | 66604.3  | 0.0001  | Significant     |
| A*C                      | 2   | 754.558        | 377.279      | 98.4737  | 0.0001  | Significant     |
| B*C                      | 4   | 154.611        | 38.6529      | 10.0888  | 0.0001  | Significant     |
| A*B*C                    | 4   | 96.3243        | 24.0811      | 6.2854   | 0.0001  | Significant     |
| D                        | 8   | 124900         | 15612.5      | 4075.037 | 0.0001  | Significant     |
| A*D                      | 8   | 65.6097        | 8.20122      | 2.1406   | 0.0319  | Significant     |
| B*D                      | 16  | 105.543        | 6.59642      | 1.7217   | 0.0417  | Significant     |
| A*B*D                    | 16  | 44.7416        | 2.79635      | 0.7299   | 0.7630  | Not-significant |
| C*D                      | 16  | 3006.83        | 187.927      | 49.0509  | 0.0001  | Significant     |
| A*C*D                    | 16  | 53.7242        | 3.35776      | 0.8764   | 0.5971  | Not-significant |
| B*C*D                    | 32  | 27.9181        | 0.87244      | 0.2277   | 1.00    | Not-significant |
| A*B*C*D                  | 32  | 24.8722        | 0.77726      | 0.2029   | 1.00    | Not-significant |
| Sample No.[A,B] & Random | 12  | 1956.78        | 163.065      | 42.5618  | 0.0001  | Significant     |
| Error                    | 312 | 1195.35        | 3.83         |          |         |                 |
| Total                    | 485 |                |              |          |         |                 |

A = Binder Type, B = Additive, C = Temperature (°C), and D = Frequency (Hz)

B, A\*B, A\*B\*D, A\*C\*D, B\*C\*D, and A\*B\*C\*D, while the rest of the interactions are statistically significant sources of variability. It is important to point out that Additive (B), as well as Binder Type\*Additive (A\*B) are not statistically significant sources of variability, while Binder Type (A) is a statistically significant source of variability. This means that the additives were not found to be statistically significantly different from one another overall as well as within each binder type according to a 95% confidence level. The interaction plot for Binder Type\*Additive (A\*B) is shown in Figure 4.11.

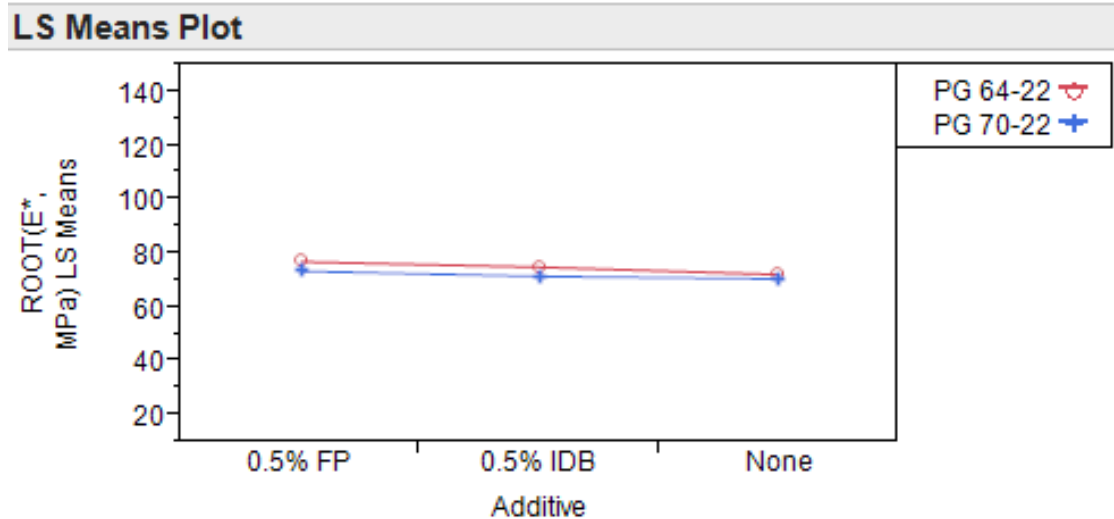


Figure 4.11. Interaction Plot for A\*B (Binder Type\*Additive)

From Table 4.3 it is also important to note that Additive\*Temperature (B\*C), Binder Type\*Temperature (A\*C), and Binder Type\*Additive\*Temperature (A\*B\*C) are statistically significant sources of variability, with the interaction plot for the last one shown below in Figure 4.12. These statistical findings mean that the additives are statistically significantly different from one temperature to another as well as statistically significantly different from one temperature to another within each binder type according to a 95% confidence level. Other interactions of interest are Binder Type\*Frequency

(A\*D), Additive\*Frequency (B\*D), Binder Type\*Additive\*Frequency (A\*B\*D), and Binder Type\*Temperature\*Frequency (A\*C\*D). The interactions A\*D, and B\*D are statistical significant sources of variability, while the other two interactions were found not to have statistical significant sources of variability. The interaction plot for A\*B\*D is shown in Figure 4.13. This interaction plot shows that the additives are not statistically significantly different from one another for each frequency within each binder type according to a 95% confidence level.

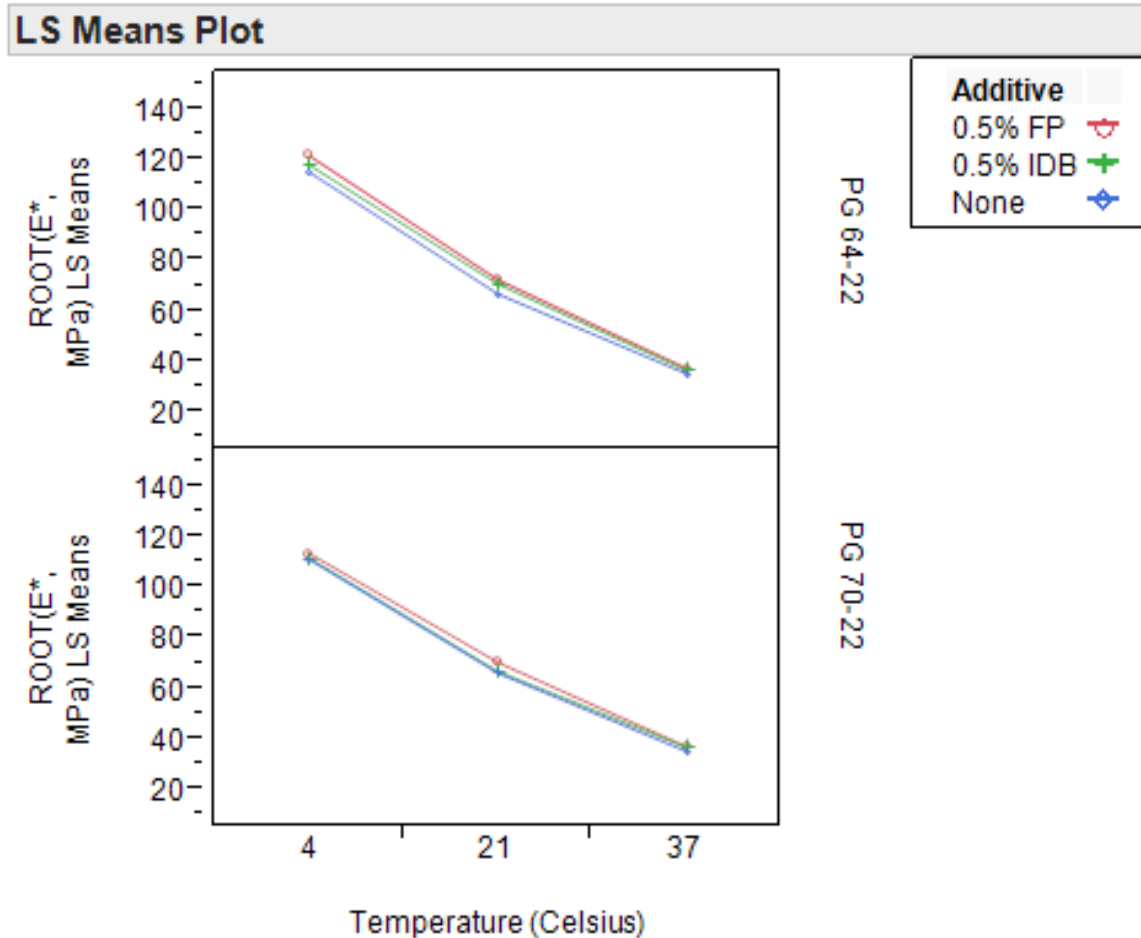


Figure 4.12. Interaction Plot for A\*B\*C (Binder Type\*Additive\*Temperature (°C))

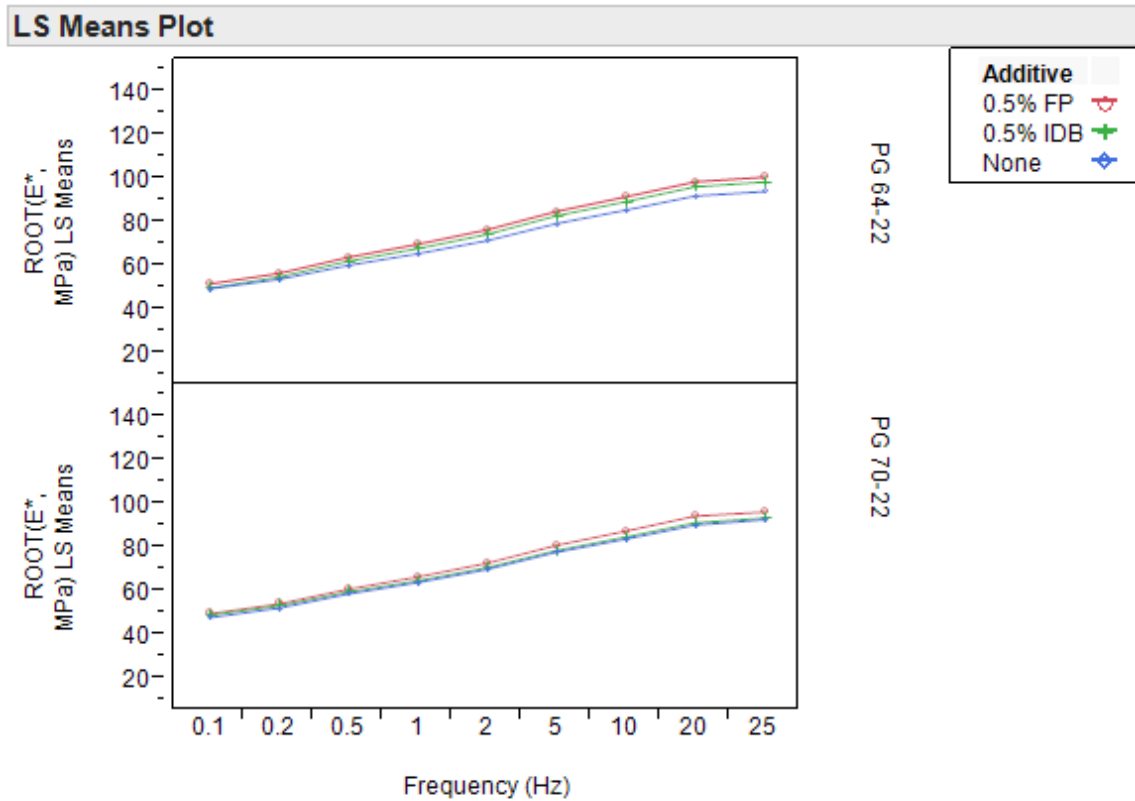


Figure 4.13. Interaction Plot for A\*B\*D (Binder Type\*Additive\*Frequency (Hz))

#### 4.5.3. Prediction of high temperature mix performance grade using Hirsch model

Using the Hirsch model as discussed in Section 4.4.1.2 of this paper, the  $G^*_{binder}$  results were estimated for each of the two additive and one control group in each binder type. These results were then compared to the  $G^*_{binder}$  results gained through using method 2 as discussed in Section 4.4.1. These comparisons are shown in the following figures.

From Figures 4.14 and 4.15 it is observed that the Hirsch model works in the case of back-calculating  $G^*_{binder}$  from the  $E^*_{mix}$  results. This occurs for the PG 64-22 binder groups with 0.5% IDB (Hirsch model stops working at 56 °C) and 0.5% FP (Hirsch model stops working at 55 °C), but not for the PG 64-22 binder group with no additive.

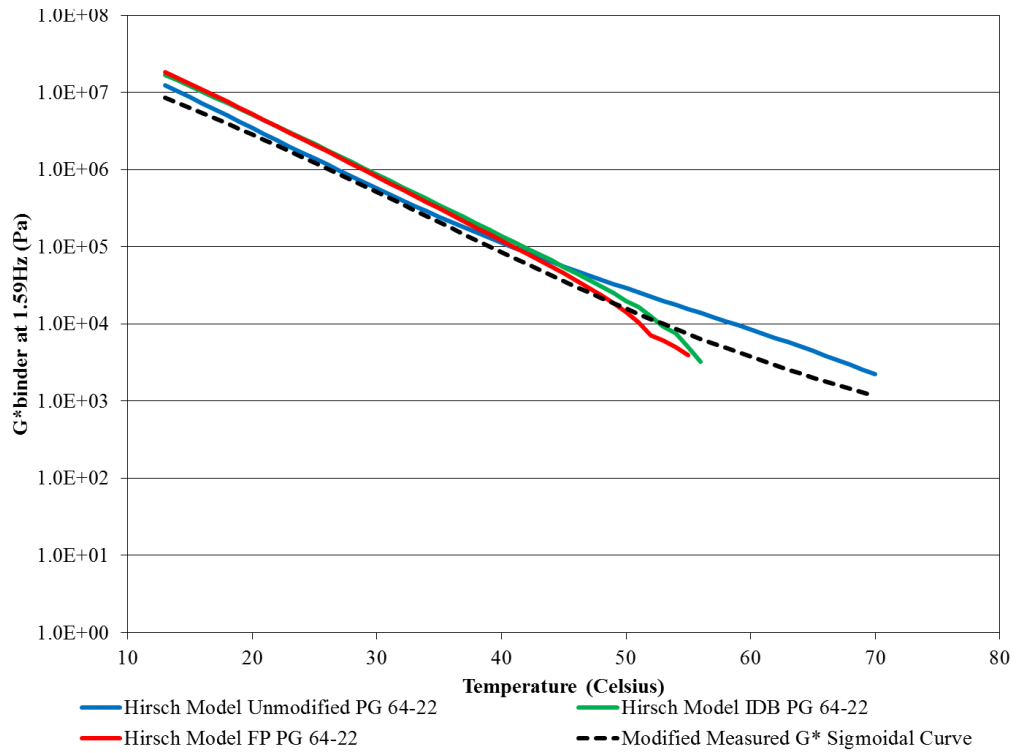


Figure 4.14. Back-Calculated Hirsch Binder  $G^*$  vs. Measured Binder  $G^*$  at 1.59 Hz for PG 64-22

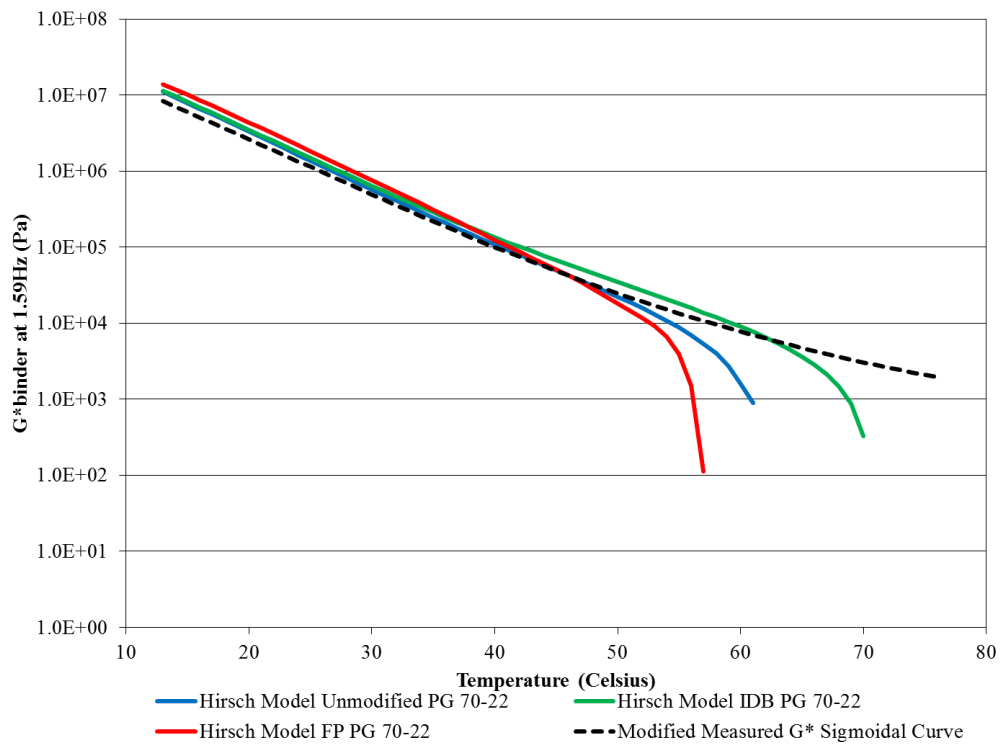


Figure 4.15. Back-Calculated Hirsch Binder  $G^*$  vs. Measured Binder  $G^*$  at 1.59 Hz for PG 70-22



For the PG 70-22 binder, the Hirsch model does not work for all three groups (PG 70-22 binder – no additive, PG 70-22 binder with 0.5% IDB, and the PG 70-22 binder with 0.5% FP). The stopping points are at 61 °C, 70 °C, and 57 °C for the three groups (PG 70-22 binder– no additive, PG 70-22 binder with 0.5% IDB, and the PG 70-22 binder with 0.5% FP). The Hirsch model has three input parameters –  $G^*_b$  (binder complex shear modulus), VMA (voids in mineral aggregate), and VFA (voids filled with asphalt). Since there is only one mix design/gradation used in this study, the input parameters VMA and VFA are not changing which means the back-calculated  $G^*_b$  values are entirely dependent on the predicted  $E^*_{mix}$  results gained through dynamic modulus testing.

Considering that comparisons for  $G^*/\sin\delta$  against temperature take place from 58 to 70 °C for the PG 64-22 binder and 58 to 76 °C for the PG 70-22 binder, the high temperature grade cannot be determined using the Hirsch model. This is due to the Hirsch model being constructed from a limited supply of data gained through limited testing criteria. This limits how low the model can go in estimating  $E^*_{mix}$  values e.g., there is a minimum limit on the  $E^*_{mix}$  values the Hirsch model can estimate. A minimum limit on  $E^*_{mix}$  values limits how low  $G^*_{binder}$  can be for certain volumetric parameters (VMA and VFA) [38]. Another source of weakness in the Hirsch model is seen when trying to back-calculate  $G^*_{binder}$  for the PG 70-22 binder without any additive as compared to the back-calculation of  $G^*_{binder}$  for the PG 64-22 binder without any additive. The Hirsch model does not work well in estimating  $E^*_{mix}$  nor in back-calculating  $G^*_{binder}$  for polymer-modified binders and mixtures. There is an equation that calculates the minimum  $E^*_{mix}$  at which the Hirsch model can no longer be used. The equation is shown below [38]:

$$|E^*|_{\min \text{ mix}} = \frac{20^{0.58}}{650} [4,199,999 - 42,000VMA] + 1 \quad (4.25)$$

Using the volumetrics for the mix design used for this study, a VMA of 16.54 would create a minimum  $E^*_{\text{mix}}$  of 30,648 psi (211,312 kPa) at 60 °C. Using equations from Section 4.4.1.2 the minimum  $G^*_{\text{binder}}$  value can be estimated through back-calculation. The minimum  $G^*_{\text{binder}}$  value would be 0.0001 psi (0.0007 kPa) at the same corresponding temperature of 60 °C and would not be reasonable.

#### 4.5.4. Prediction of high temperature mix performance grade using Al-Khateeb model

The  $G^*_{\text{binder}}$  results were estimated for each of the two additive and one control groups in each binder type using the Al-Khateeb model as discussed in Section 4.4.1.3 of this paper. These results were then compared to the  $G^*_{\text{binder}}$  results gained through using method 2 as discussed in Section 4.4.2. These comparisons are shown in the Figures 4.16 and 4.17.

From Figures 4.16 and 4.17 it is observed that the Al-Khateeb model works in back-calculating  $G^*_{\text{binder}}$  from  $E^*_{\text{mix}}$  results up to 70 °C for the PG 64-22 binder and up to 76 °C for the PG 70-22 binder. For the PG 64-22 binder groups with 0.5% IDB and 0.5% FP the back-calculated  $G^*_{\text{binder}}$  estimates are shown to be fairly close to the modified measured results that were gained from testing using the DSR results in conjunction with method 2. However, the  $G^*_{\text{binder}}$  estimates gained through back-calculation of the measured, unmodified PG 64-22 binder results begin to deviate from the modified measured results around 44 °C. This deviation appears to grow larger until the stop point

at 70 °C, but in reality is not growing substantially as the  $G^*_{binder}$  estimates are plotted in log scale.

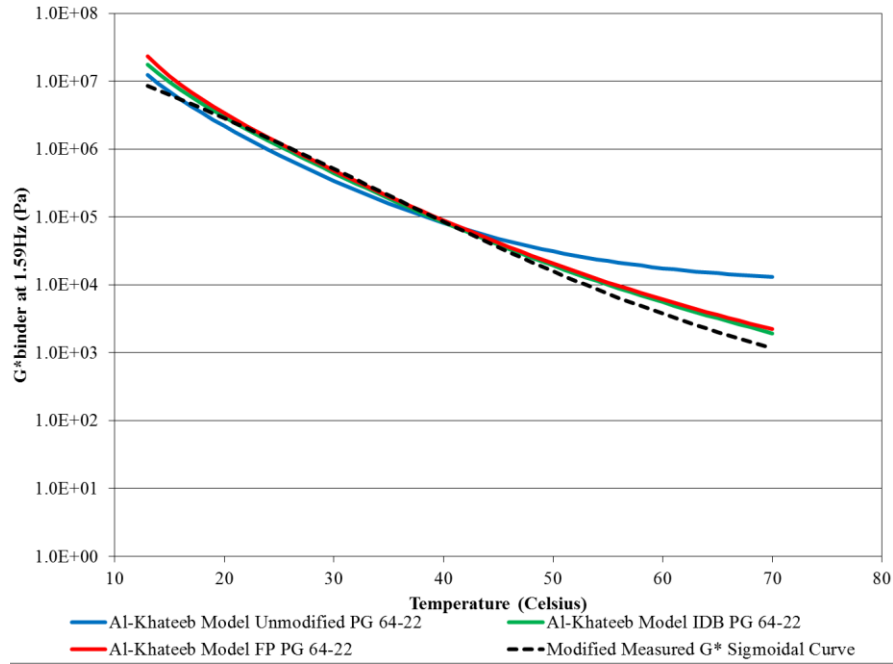


Figure 4.16. Back-Calculated Al-Khateeb Binder  $G^*$  vs. Measured Binder  $G^*$  at 1.59 Hz for PG 64-22

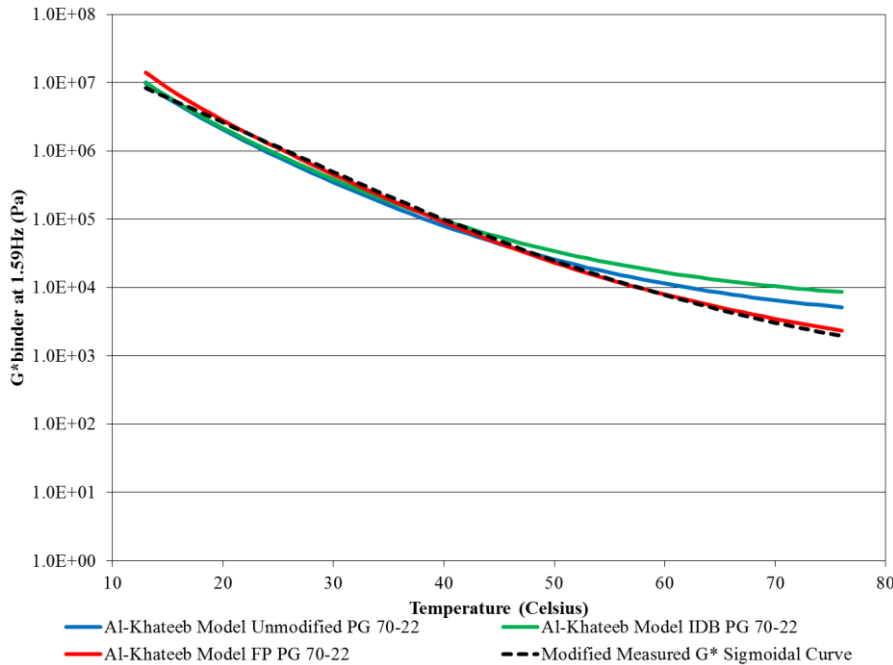


Figure 4.17. Back-Calculated Al-Khateeb Binder  $G^*$  vs. Measured Binder  $G^*$  at 1.59 Hz for PG 70-22

From Figure 4.17, the PG 70-22 binder group with 0.5% FP's back-calculated  $G^*_{\text{binder}}$  estimates are shown to be the most similar to the modified measured results. This is not the case for the PG 70-22 binder groups with 0.5% IDB and without any additives. The PG 70-22 binder with 0.5% IDB starts to deviate from the modified measured  $G^*_{\text{binder}}$  results at 45 °C and continues until the stop point at 76 °C. For the unmodified PG 70-22 binder the deviation starts at 51 °C and continues until the stop point at 76 °C. As stated earlier about Figure 4.17, even though the deviations appear to grow larger as the temperature increases, this is the opposite of what is really occurring due to the log scale assigned to the y-axis.

To further examine if the deviations between the estimated  $G^*_{\text{binder}}$  results and modified measured  $G^*_{\text{binder}}$  results are significant,  $G^*/\sin\delta$  results were estimated for the unmodified, 0.5% IDB modified, and 0.5% FP modified PG 64-22 and PG 70-22 binders and compared against the  $G^*/\sin\delta$  results gained from testing binder samples using the DSR. The  $G^*/\sin\delta$  estimated results for the PG 64-22 binder and the PG 70-22 are shown in Figures 4.18 and 4.19. These results can then be used to estimate the binder high temperature performance grade according to DSR criteria for RTFO aged binder.

The measured binder high temperature performance grade for an unmodified PG 64-22 binder is 64 due to the failure temperature being 64.5 °C as shown in Figure 4.18. For the PG 64-22 binder modified with 0.5% IDB the failure temperature is 68.5 °C, meaning its performance grade is estimated to be 64 as the next grade up is 70. To reach a high temperature grade of 70, the failure temperature has to be at least above 70 °C and below 76 °C. This is not the case with the PG 64-22 binder modified with 0.5% IDB,

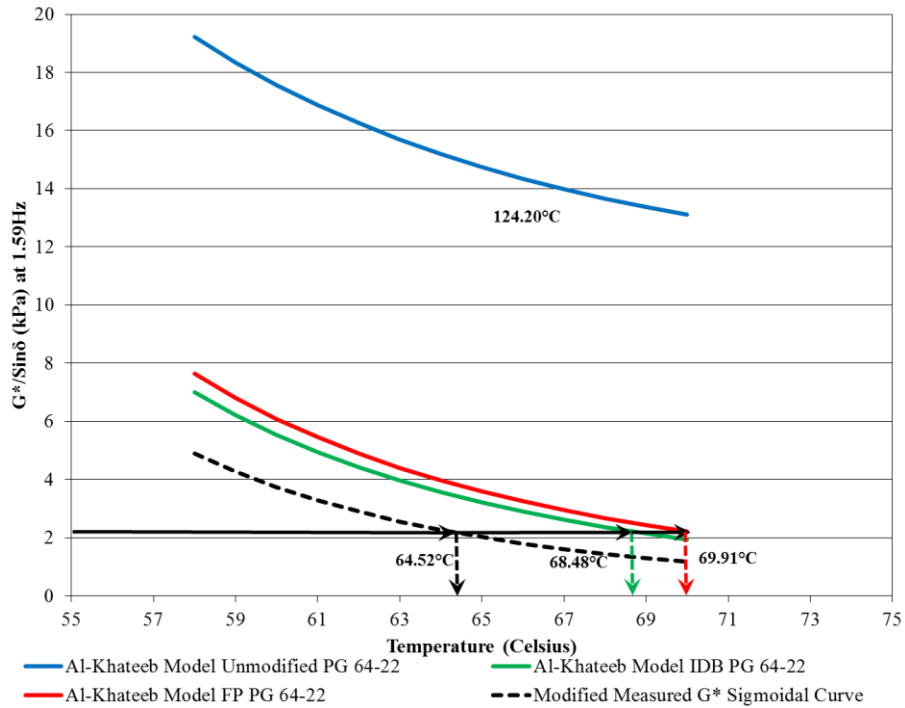


Figure 4.18. Predicted vs. High Temperature Grades for PG 64-22

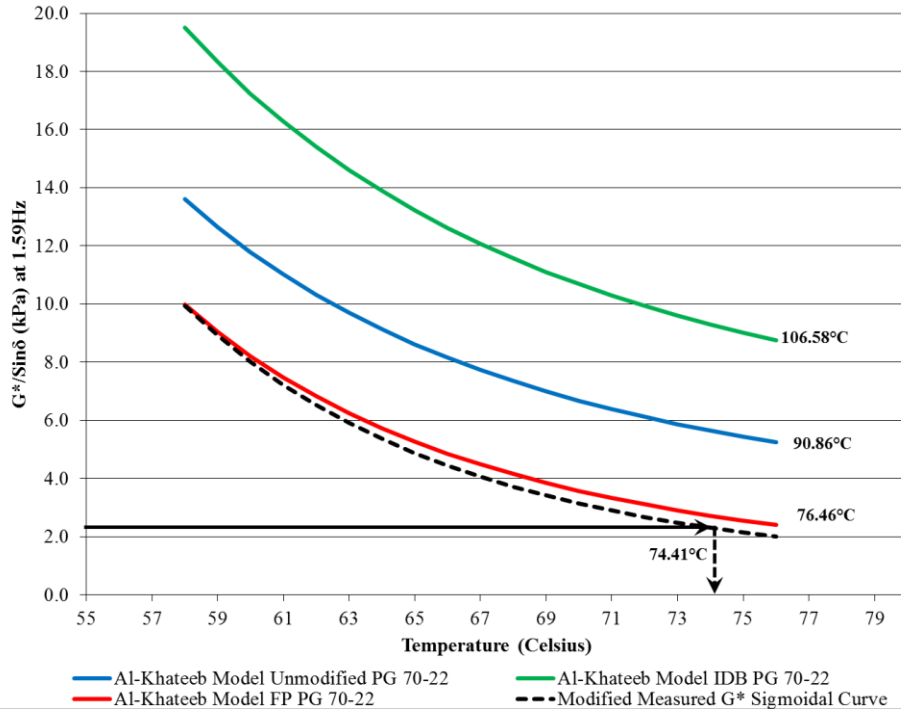


Figure 4.19. Predicted vs. High Temperature Grades for PG 70-22

therefore it is estimated to have a high temperature grade of 64. When the PG 64-22 binder is modified with 0.5% FP the failure temperature is 69.9 °C, which means that this modified binder also has an estimated high temperature grade of 64. From past binder studies, IDB and FP at a 0.5% addition by weight of the binder have been shown to have no impact in terms of either increasing or decreasing the high temperature binder performance grade. However, the estimated  $G^*/\sin\delta$  results for the unmodified PG 64-22 binder are significantly different from the results gained through testing and the estimates from the modified binders with 0.5% IDB and 0.5% FP. The estimated  $G^*/\sin\delta$  results for the unmodified PG 64-22 binder imply the estimated failure temperature is 124.2 °C. This is not realistic as this binder is a PG 64-22 and should have a failure temperature between 64 °C and 70 °C. From the estimates for the PG 64-22 binder it can be garnered that the Al-Khateeb model is fairly accurate at back-calculating from the measured  $E^*_{mix}$  results to  $G^*_{binder}$  estimates, when the  $E^*_{mix}$  measured results are more accurate at higher temperatures.

The measured binder high temperature performance grade for an unmodified PG 70-22 binder is 70 due to the failure temperature being 74.4 °C (higher than 70 °C, but lower than 76 °C) as shown in Figure 4.19. To reach a high temperature grade of 76 the failure temperature has to be at least above 76 °C and below 82 °C. The difference between the estimates and the measured  $G^*_{binder}$  results is pretty large for the PG 70-22 binder with no additive and the PG 70-22 binder with 0.5% IDB. For the PG 70-22 binder modified with 0.5% IDB the estimated failure temperature is 106.6 °C, while the estimated failure temperature for PG 70-22 without any additive is 90.9 °C. These

estimates were made using the  $E^*_{mix}$  measured results with the Al-Khateeb model to back-calculate to the  $G^*_{binder}$  estimates. These results cannot be used realistically to estimate the binder high temperature performance grade as they are much greater than the actual grade. The PG 70-22 binder modified with 0.5% FP had an estimated failure temperature of 76.5 °C, which implies its estimated high temperature performance grade is 76. In reality these three binders should be equal in terms of performance grade to the measured binder high temperature performance grade, but the Al-Khateeb model shows that the mixtures do not have the same binder high temperature performance grade.

The Al-Khateeb model has two input parameters –  $G^*_b$  (binder complex shear modulus), and the VMA (voids in mineral aggregate). Since there is only one mix design/gradation used in this study the input parameter VMA is unchanged which means the back-calculated  $G^*_b$  values are entirely dependent on the predicted  $E^*_{mix}$  results gained through dynamic modulus testing. Comparisons for  $G^*/\sin\delta$  against temperature can take place using the Al-Khateeb model from 58 to 70 °C for the PG 64-22 binder and 58 to 76 °C for the PG 70-22 binder. However, the binder high temperature performance grade cannot be estimated for all combinations. This is primarily due to the high variability, and low accuracy when testing dynamic modulus samples at high temperatures. Even though the differences between the dynamic modulus results at higher temperatures are smaller when compared to the differences at low temperatures, the differences are much larger at high temperatures as a proportion of the measured result. These large differences affect the COV values and make them greater at higher temperatures. This leads to high variability of measured data which is effecting the

binder high temperature performance grade estimate through back-calculation of  $E^*_{mix}$  measured results, and is not currently reasonable.

#### 4.6. Conclusions and Recommendations

Method 2 was found to be the better alternative over that of method 1 in the estimation of the binder high temperature performance grade for RTFO short-term aged binder using the DSR test results from the control binders to create the  $G^*_b$  master curves. Warm mix asphalt performance during the dynamic modulus test has shown that Isosorbide Distillation Bottoms can be used as a WMA additive and is highly comparable to WMA without an additive and WMA with FP in terms of performance. Comparisons of performance between the additives and binder types were made using a split plot repeated measure design for the statistical analysis. From the statistical analysis it was found that the additives were not found to be statistically significantly different from one another overall as well as within each binder type. Across the different temperatures the additives were found to be statistically significantly different from one another as well as statistically significantly different from another within each binder type. When looking at interactions with frequency the additives are not statistically significantly different from one another for each frequency within each binder type, as well as for each frequency within each temperature and binder type.

From the results gathered in this paper, estimation of the mixture high temperature performance grade through back-calculation to the binder shear complex modulus is possible, but the results are highly variable and are dependent on the methods used in back-calculation as well as the accuracy during dynamic modulus testing at high



temperatures. While the Al-Khateeb model worked for the required temperature range with somewhat high variability, the Hirsch model did not work beyond a certain temperature (around 54 °C). The Al-Khateeb model could be used for back-calculating to  $G^*_b$  up to 70 °C for the PG 64-22 binder and 76 °C for the PG 70-22 binder, while the Hirsch model could go no farther than back-calculating up to approximately 54 °C for both binders. High variability from the estimated binder high temperature performance grade was found to be due more from variability of the test results themselves at high temperatures as well as extrapolation of the data to higher temperatures using the same highly variable data gained from testing at high temperatures. For estimation of the mixture high temperature performance grade to work with less variability in the results, it is recommended that dynamic modulus testing not only take place at 4 °C, 21 °C, and 37 °C, but at 54 °C as well. It is also recommended that more samples be used in the determination of the performance grade for each group. Lastly, it is recommended that in the future other models also be explored other than the Hirsch and Al-Khateeb models.

Limitations of this paper were that the testing plan for this paper only included DSR testing for the control binders (PG 64-22 binder, and a PG 70-22 binder) for creating  $G^*_b$  master curves, while the mix testing plan included dynamic modulus tests for three samples from each of the six groups. In the future, it is recommended that the other binder groups also be put through DSR testing for use in creating  $G^*_b$  master curves. This would allow the estimation of the binder high temperature performance grade for RTFO short-term aged binder for each of the non-control groups.

## 4.7. References

- [1] Button JW, Estakhri C, Wimsatt A. A synthesis of warm mix asphalt. Rep No FHWA/TX-07/0-5597-1. College Station, TX.: Texas Transportation Institute; 2007.
- [2] D'Angelo J, et al. Warm-mix asphalt: European practice. Publication FHWA-PL-08-007: FHWA, U.S. Dept. of Transportation, Washington, DC.; 2008.
- [3] Gandhi T. Effects of warm asphalt additives on asphalt binder and mixture properties: Ph.D. dissertation, Clemson Univ., Clemson, SC.; 2008.
- [4] Hassan M. Life-cycle assessment of warm-mix asphalt: An environmental and economic perspective. Transportation Research Board 88th Annual Meeting: Washington, DC.; 2009.
- [5] Hurley GC, Prowell BD. Evaluation of Evotherm for use in warm mix asphalt. Rep No 06-02. Auburn, AL.: National Center for Asphalt Technology; 2006.
- [6] Jenkins K, De Groot J, van de Ven M, Molenaar A. Half-warm foamed bitumen treatment, a new process. 7th Conference on asphalt pavements for Southern Africa (CAPSA 99)1999.
- [7] Kristjánsdóttir Ó. Warm-mix asphalt for cold weather paving. Seattle, WA: Univ. of Washington; 2006.
- [8] Kristjánsdóttir Ó, Muench ST, Michael L, Burke G. Assessing potential for warm-mix asphalt technology adoption. Transp Res Rec. 2007;2040:91-9.
- [9] Larsen O, Moen Ø, Robertus C, Koenders B. WAM Foam asphalt production at lower operating temperatures as an environmental friendly alternative to HMA. 3rd Eurasphalt & Eurobitume Congress: Foundation Eurasphalt, Breukelen, Netherlands.; 2004.
- [10] Perkins SW. Synthesis of warm mix asphalt paving strategies for use in Montana highway construction. Rep No FHWA/MT-09-009/8117-38. Helena, MT.: Western Transportation Institute; 2009.
- [11] Prowell BD, Hurley GC, Crews E. Field performance of warm-mix asphalt at the NCAT test track. Transportation Research Board 86th Annual Meeting: Washington, DC.; 2007.
- [12] Kim H, Lee S, Amirkhanian S. Influence of Warm Mix Additives on PMA Mixture Properties. Journal of Transportation Engineering. 2012;138(8):991-7.
- [13] Werpy TA, Holladay JE, White JF. Top Value Added Chemicals From Biomass: I. Results of Screening for Potential Candidates from Sugars and Synthesis Gas. 2004. p. Medium: ED; Size: PDFN.
- [14] Buss AF. Investigation of warm-mix asphalt using Iowa aggregates: M. Thesis, Iowa State Univ., Ames, IA; 2010.
- [15] Kuang Y. Evaluation of Evotherm as a WMA technology compaction and anti-strip additive: M. Thesis, Iowa State Univ., Ames, IA; 2012.
- [16] Leng Z, Gamez A, Al-Qadi I. Mechanical Property Characterization of Warm-Mix Asphalt Prepared with Chemical Additives. Journal of Materials in Civil Engineering. 2013;0(ja):null.

- [17] American Association of State Highway and Transportation Officials, (AASHTO). Standard practice for grading or verifying the performance grade of an asphalt binder. R 29-08, Washington, DC; 2011.
- [18] American Association of State Highway and Transportation Officials, (AASHTO). Performance-Graded Asphalt Binder. M 320-10, Washington, DC; 2011.
- [19] ASTM. Standard Practice for Determining the Separation Tendency of Polymer from Polymer Modified Asphalt. D7173, West Conshohocken, PA: ASTM International; 2011.
- [20] American Association of State Highway and Transportation Officials, (AASHTO). Determining the Rheological Properties of Asphalt Binder Using a Dynamic Shear Rheometer (DSR). T 315-10, Washington, DC; 2011.
- [21] American Association of State Highway and Transportation Officials, (AASHTO). Determining Dynamic Modulus of Hot Mix Asphalt (HMA). T 342-11, Washington, DC; 2011.
- [22] Al-Khateeb G, Shenoy A, Gibson N, Harman T. A new simplistic model for dynamic modulus predictions of asphalt paving mixtures. Journal of the AAPT. 2006;75.
- [23] Christensen Jr D, Pellinen T, Bonaquist R. Hirsch model for estimating the modulus of asphalt concrete. Journal of the Association of Asphalt Paving Technologists. 2003;72.
- [24] Brown ER, Kandhal PS, Roberts FL, Kim YR, Lee D-Y, Kennedy TW, et al. Hot mix asphalt materials, mixture design, and construction. 3rd ed. Lanham, Md.: NAPA Research and Education Foundation; 2009.
- [25] Garcia G, Thompson MR, Illinois Center for Transportation., Illinois. Department of Transportation. Bureau of Materials and Physical Research. HMA dynamic modulus predictive models a review. Civil engineering studies Illinois Center for Transportation series no 07-005. Urbana, Ill.: Illinois Center for Transportation; 2007. p. vii, 95 p.
- [26] Kim YR, Momen M, King M, North Carolina. Department of Transportation. Research and Analysis Group., North Carolina State University. Department of Civil Construction and Environmental Engineering. Typical dynamic moduli for North Carolina asphalt concrete mixtures. Raleigh, NC: N.C. Dept. of Transportation Research & Analysis; 2005. p. 1 computer disc.
- [27] Christensen DW, Anderson DA. Interpretation of dynamic mechanical test data for paving grade asphalt cements (with discussion). Journal of the Association of Asphalt Paving Technologists. 1992;61.
- [28] Li XJ, Williams RC. A Practical Dynamic Modulus Testing Protocol. J Test Eval. 2012;40(1):100-6.
- [29] Pellinen T, Witzczak M. Stress dependent master curve construction for dynamic (complex) modulus (with discussion). Journal of the Association of Asphalt Paving Technologists. 2002;71.
- [30] Marasteanu M, Anderson D. Improved model for bitumen rheological characterization. Eurobitume Workshop on Performance Related Properties for Bituminous Binders: European Bitumen Association Brussels, Belgium; 1999.
- [31] Yao H, You Z, Li L, Goh S, Dedene C. Evaluation of the Master Curves for Complex Shear Modulus for Nano-Modified Asphalt Binders. CICTP 2012. p. 3399-414.

- [32] Olard F, Di Benedetto H. General “2S2P1D” Model and Relation Between the Linear Viscoelastic Behaviours of Bituminous Binders and Mixes. *Road Materials and Pavement Design*. 2003;4(2):185-224.
- [33] Di Benedetto H, Olard F, Sauzéat C, Delaporte B. Linear viscoelastic behaviour of bituminous materials: From binders to mixes. *Road Materials and Pavement Design*. 2004;5(sup1):163-202.
- [34] Yusoff NIM, Shaw MT, Airey GD. Modelling the linear viscoelastic rheological properties of bituminous binders. *Construction and Building Materials*. 2011;25(5):2171-89.
- [35] Md. Yusoff NI, Mounier D, Marc-Stéphane G, Rosli Hainin M, Airey GD, Di Benedetto H. Modelling the rheological properties of bituminous binders using the 2S2P1D Model. *Construction and Building Materials*. 2013;38(0):395-406.
- [36] Asgharzadeh S, Tabatabaee N, Naderi K, Partl M. Evaluation of rheological master curve models for bituminous binders. *Mater Struct*. 2013:1-14.
- [37] Hainin M, Nim Y. Predictability of complex modulus using rheological models. *Asian Journal of Scientific Research*. 2010;3(1):18-30.
- [38] Xiao S. Investigation of performance parameters for hot-mix asphalt: Doctoral Dissertation, Purdue Univ., West Lafayette, IN; 2006.

## CHAPTER 5. INVESTIGATION OF WARM MIX ASPHALT PERFORMANCE WITH AND WITHOUT SELECT BIO-DERIVED/CHEMICAL ADDITIVES IN IOWA USING AASHTOWARE PAVEMENT ME DESIGN

Modified from a paper to be submitted to *Construction and Building Materials*

Joseph H. Podolsky<sup>1</sup>, Ashley Buss<sup>2</sup>, R. Christopher Williams<sup>3</sup>, and Eric Cochran<sup>4</sup>

### 5.1. Abstract

An industry wide emphasis on sustainable asphalt practices has given rise to increasing use of warm mix asphalt technologies. WMA reduces both binder viscosity and mixing and compaction temperatures by 20-55°C during the asphalt mix production and laydown process. This research investigates several bio-derived WMA additives that act as chemical modifiers with surfactant properties. Two established additives derived from the forest products industry are studied as well as a WMA additive in development that is derived from corn. The objective of this research is to use the new AASHTOWare Pavement ME Design to compare the established forest product WMA additives with the new WMA corn derived additive that is in development. The results of this research work will expand the WMA knowledge base by also comparing the sensitivity of

---

<sup>1</sup> Primary Researcher; Primary and Corresponding Author; Graduate Research Assistant, Department of Civil, Construction and Environmental Engineering, Iowa State University, 174 Town Engineering Building, Ames, IA 50011, USA.

<sup>2</sup> Contributing Researcher and Author; Postdoctoral Researcher, Department of Civil, Construction and Environmental Engineering, Iowa State University, 174 Town Engineering Building, Ames, IA 50011, USA.

<sup>3</sup> Professor, Department of Civil, Construction and Environmental Engineering, Iowa State University, 482 Town Engineering Building, Ames, IA 50011, USA.

<sup>4</sup> Associate Professor, Department of Chemical and Biological Engineering, Iowa State University, 1035 Sweeney, Ames, IA 50011, USA.

AASHTOWare to pavement design parameters such as traffic loading, climate and pavement design conditions as well as variable  $E^*$  reliability values. The WMA material responses are measured for binder testing and mixture testing. The WMA test results are used to forecast pavement performance in the AASHTOWare Pavement ME Design program to understand how the material parameters will influence overall pavement performance. All binder testing with the additives was conducted using a Performance Grade (PG) 64-22 binder and the same binder was polymer modified with an SBS polymer to attain a PG 70-22 binder. Dynamic modulus testing on a State DOT approved 10 million ESAL mix design was performed to compare stiffness at a wide range of temperatures and frequencies. The results from the binder and mixture testing were used as input values to the AASHTOWare Pavement ME Design; however, the predicted pavement performance using these test results were evaluated for sensitivity to different traffic loading, climate and pavement design conditions as well as variable  $E^*$  reliability. Results indicate that the pavement design/traffic has a large impact on the pavement performance compared with the two climates and reliability levels that were included. The corn-derived WMA additive was similar to the other established WMA additives showing similar pavement performance predicted by the AASHTOWare Pavement ME Design. The pavement performance in the control group did not show large differences compared to WMA additives showing that the pavement performance models forecast equal performance between the WMA additives studied and the HMA control group.

**KEYWORDS:** warm mix asphalt, AASHTOWare Pavement ME Design, bio-derived, pavement performance,  $E^*$  reliability.

## 5.2. Introduction

The notion or idea of warm mix asphalt (WMA) came about when the European Union (EU) started creating more sustainable technologies after the ratification of the Kyoto Protocol in the mid-1990s. Several companies in Europe researched different ways of implementing the Kyoto Protocol and lower emissions by reducing production temperatures in asphalt mix plants. This brought about the creation of WMA. WMA was first introduced in the United States by the National Asphalt Pavement Association (NAPA) in 2002. In 2003, a joint meeting was held between NAPA, the Federal Highway Administration (FHWA), and the National Center for Asphalt Technology to explore further opportunities with WMA use in the United States. The next year, the “World of Asphalt Show and Conference” had a live demonstration of WMA being constructed. In 2007, the Federal Highway Administration’s International Technology Scanning Program organized a team of U.S. experts to visit four European countries and evaluate whether WMA use in the United States was feasible. The team of experts recommended WMA as an alternative to HMA for use in the United States after the visit (D'Angelo 2008; Newcomb 2007).

During asphalt mix and laydown WMA enables reductions in viscosity and reductions in mixing and compaction temperatures by as much as 20°C-55°C. By lowering the temperatures at which asphalt mix is mixed and compacted money is saved due to lower fuel use, which also lowers the carbon footprint as an effect. By reducing binder viscosity, lower compaction temperatures can be used in the field; which in turn improves mix compactibility, and extends the time paving can be done by allowing for longer haul distances. Reductions in viscosity allow for increased use of reclaimed

asphalt pavement (RAP) in a mix. An added benefit from lower mixing and compacting temperatures is that there is less fumes produced that workers will be exposed to (Button et al. 2007; D'Angelo 2008; Gandhi 2008; Hassan 2009; Hurley and Prowell 2006; Jenkins et al. 1999; Kim et al. 2012; Kristjánsdóttir 2006; Kristjánsdóttir et al. 2007; Larsen et al. 2004; Perkins 2009; Prowell et al. 2007).

WMA technologies are generally split between four groups; foaming – water based, foaming – water bearing additive, chemical additive, and organic/bio-derived additive. The first of the two foaming technologies (water based) is physical in terms of the production process due to introduction of water to create the foaming effect. There are two main methods for foaming (water based) asphalt at lower temperatures; the WAM-foam method, and the Astec Double Barrel Green method (Anderson et al. 2008; Koenders et al. 2002; Middleton and Forfylyow 2009). The second foaming technology (water bearing additive) creates the foaming effect in asphalt through the release of water from additives during the mixing process. The two most commonly used water bearing additive technologies are Advera and Aspha-min (Anderson et al. 2008; Hossain et al. 2011; Hurley and Prowell 2005a). Both chemical and organic/bio-derived additives when blended to asphalt binder reduce the binder viscosity. Commonly used chemical and organic/bio-based additives in WMA are Evotherm® 3G, Sasobit®, and Asphaltan B (Button et al. 2007; Corrigan 2006; Hurley and Prowell 2005b; Hurley and Prowell 2006).

Isosorbide distillation bottoms (IDB) is a bio-derived co-product from corn with properties similar to other WMA chemical modifiers and has surfactant properties. IDB is produced as part of the conversion of sorbitol to isosorbide. Sorbitol is produced by



hydrogenating the glucose from the corn biomass (Werpy et al. 2004). IDB will be studied as a WMA bio-derived additive in this study. Recently derived chemical/bio-based additives from the forest products industry called forest product 1 and 2 (FP 1 and FP 2) will also be used for binder modification in this study. FP 1 and 2 are water-free chemical/bio-based additives that display surfactant properties. When asphalt binder modified with FP 1 or FP 2 is added to aggregates the aggregate-binder interface friction is reduced due to the surfactant properties of both FP 1 and 2. A reduction in the interface friction between the aggregates and binder make it possible to lower the mixing and compaction temperatures (Buss et al. 2014; Leng et al. 2013). In the literature it is recommended that chemical/bio-derived additives from the forest products industry are added at an optimum dosage level of 0.5% by weight of the total binder, and in a recently completed binder study it was found that the optimum dosage level for IDB addition is 0.5% by weight of the total binder. Therefore, 0.5% addition level was used in this study (Hurley and Prowell 2006).

American Association of State Highway and Transportation Officials (AASHTO), AASHTOWare Pavement ME Design is a mechanistic empirical pavement design software program that allows an engineer to estimate pavement performance using both engineering mechanics in combination with historical data from the field. The program uses mechanistic models to predict pavement responses due to traffic loads and pavement performance and is estimated using historical calibrated data from the field. The main factors used in the analysis of pavement performance in AASHTOWare Pavement ME Design are traffic, climate/location, reliability, and pavement structure. AASHTOWare Pavement ME Design is the most recent version of the original program named the

Mechanistic-Empirical Pavement Design Guide (MEPDG) developed by the National Cooperative Highway Research Program (NCHRP) in the early 2000s (National Cooperative Highway Research Program 2004).

### **5.2.1. Objectives**

The main objective of this paper is to demonstrate the use of the AASHTOWare Pavement ME Design program to compare the simulated performance of WMA pavement sections constructed with and without various bio-based/chemical additives in Iowa (Buss and Williams 2012; Hajj et al. 2013). In AASHTOWare Pavement ME Design, dynamic modulus results and rolling thin film oven (RTFO) aged dynamic shear rheometer (DSR) results were used as Level 1 inputs. The distresses examined in AASHTOWare Pavement ME Design are Smoothness, Alligator Cracking, and Rutting (AC only, and Total Rutting). The main objective will be achieved by focusing on four areas of interest. First, the impact upon pavement performance from additive addition within each binder type will be examined through changes from the  $E^*$  results. Second, impacts on pavement performance from different climatic conditions, traffic loading, and pavement designs due to variation between  $E^*$  results of the various groups will be studied. Third, the impact on pavement performance from Level 1 RTFO aged DSR results will be examined. Finally, it will be shown how reliability of measured  $E^*$  (Level 1 inputs) results impact pavement performance.

### 5.3. Laboratory Testing Program

#### 5.3.1. Material description

Within this study one crude source of binder from Montana was used, which is similar to a Canadian crude source. The Montana crude was used at its original grade of PG 64-22 (Binder I), and also used as a polymer modified binder (1.5% SBS polymer modification), PG 70-22 (Binder II). An Iowa DOT approved surface mix with a 10 million ESAL design level (Mix No. 1BD11-33) was used to construct dynamic modulus samples in the laboratory. The aggregate types, gradation, and suppliers used for this mix design are shown in Table 5.1. The gradation for each aggregate was verified with the mix gradation in the job mix formula from the Iowa DOT. The laboratory mix gradation was adjusted to increase the fines in the blended gradation. This was done through the addition of commercially produced hydrated lime as 100% of this material passes the No. 200 sieve and simulates the change in gradation due to aggregate breakdown during plant production. Before the blended gradation was matched to the job formula, each

**Table 5.1. Mix Design Gradation and Supplier Information**

| Supplier          | Ames Mine/<br>Martin Marietta | Ames Mine/<br>Martin<br>Marietta | Dell Rapids E.<br>Minchaha<br>Co/Everist Inc. | Ames Mine/<br>Martin<br>Marietta | Ames Mine/<br>Martin<br>Marietta | Ames South/<br>Hallet<br>Materials Co. | Commercially<br>Produced | Blend<br>Gradation |
|-------------------|-------------------------------|----------------------------------|---|----------------------------------|----------------------------------|--|--------------------------|--------------------|
| Aggregate         | 1/2<br>CRUSHED<br>EC          | 3/4 CL CHIP<br>EC                | 1/2 X 4<br>QUARTZITE                          | 3/8 CL CHIP<br>LC                | MANF SAND<br>LC                  | SAND                                   | Hydrated Lime            |                    |
| % Used            | 26%                           | 11%                              | 13%   | 8%                               | 24%                              | 17%                                    | 2%                       |                    |
| U.S. Sieve,<br>mm | Mesh<br>Number                | % Passing                        | % Passing                                     | % Passing                        | % Passing                        | % Passing                              | % Passing                | % Passing          |
| 37.5              |                               | 100                              | 100   | 100                              | 100                              | 100                                    | 100                      | 100.0%             |
| 25                | 1 in.                         | 100                              | 100   | 100                              | 100                              | 100                                    | 100                      | 100.0%             |
| 19                | 3/4 in.                       | 100                              | 98  | 100                              | 100                              | 100                                    | 100                      | 99.8%              |
| 12.5              | 1/2 in.                       | 91                               | 58  | 99                               | 100                              | 100                                    | 100                      | 92.9%              |
| 9.5               | 3/8 in.                       | 70                               | 32  | 78                               | 92                               | 100                                    | 100                      | 81.2%              |
| 4.75              | No.4                          | 35                               | 5   | 7.7                              | 25                               | 98                                     | 98                       | 53.9%              |
| 2.36              | No.8                          | 19                               | 1.5   | 1.2                              | 3.1                              | 68                                     | 87                       | 37.8%              |
| 1.18              | No.16                         | 12                               | 1.4   | 0.6                              | 1.8                              | 36                                     | 69                       | 25.3%              |
| 0.6               | No.30                         | 10                               | 1.3   | 0.4                              | 1.6                              | 16                                     | 40                       | 15.3%              |
| 0.3               | No.50                         | 8.5                              | 1.2   | 0.3                              | 1.5                              | 6                                      | 8                        | 7.2%               |
| 0.15              | No.100                        | 8.2                              | 1.1   | 0.2                              | 1.2                              | 2                                      | 0.6                      | 4.9%               |
| 0.075             | No.200                        | 8                                | 0.9   | 0.1                              | 1                                | 1.2                                    | 0.2                      | 4.6%               |

aggregate was sieved in their appropriate proportions to create less variability between batches. With this addition of the hydrated lime the blended gradation was matched to the job mix formula.

Three additives were used in this study – IDB, FP 1 and FP 2 – all at addition rates of 0.5% by weight of the binder. As stated earlier, IDB is a recently bio-derived co-product from corn that has surfactant properties. FP 1 and 2 are WMA chemical additives derived from tall oil (tree oil). The research literature recommends that the optimum dosage level for both FP 1 and FP 2 is 0.5% by weight of the total binder, and in recently completed binder studies at Iowa State University it was found that the optimum dosage level for IDB addition is 0.5% by weight of the total binder. Therefore, 0.5% addition level was used in this study to compare the three technologies (Hurley and Prowell 2006). A Silverson shear mill was used for blending the binders with the WMA additives – IDB, FP 1 and FP 2 at  $140^{\circ}\text{C}\pm 10^{\circ}\text{C}$  for one hour with a blending speed of 3000 rpm. The polymers were blended by the binder supplier in the case of the polymer modified PG 70-22 binder.

### **5.3.2. Dynamic modulus test**

The dynamic modulus test was performed on four groups of samples: no additive, 0.5% IDB, 0.5% FP 1 and 0.5% FP 2 samples using two binder types; the Montana PG 64-22 binder, and the Polymer Modified Montana PG 70-22 binder. The dynamic modulus values and phase angles were calculated at several different frequency-temperature combinations for the mix combinations. The temperatures used in testing

were 4°C, 21°C, and 37°C while the test frequencies were 25Hz, 20Hz, 10Hz, 5Hz, 2Hz, 1Hz, 0.5Hz, 0.2Hz, and 0.1Hz.

An asphalt mixture's dynamic modulus varies with both temperature and loading frequency. This makes comparisons between results from one temperature to another temperature quite complicated. The development of dynamic modulus master curves provides a direct means of viewing a representation of dynamic modulus results that is much easier to interpret. With a dynamic modulus master curve it is much easier to make a comparison between several sets of dynamic modulus results at various temperatures (Christensen and Anderson 1992). According to research conducted by Li and Williams (Li and Williams 2012), testing  $E^*$  values at three temperatures (4.4, 21.1, and 37.8°C) did not change the shape of master curves constructed by data from nine frequencies ranging from 25 Hz to 0.1 Hz when compared to using data from 5 temperatures each at six frequencies.

For dynamic modulus testing 2600g aggregate samples were proportioned and mixed with an optimum binder content of 5.2% to produce dynamic modulus test samples. Dynamic modulus samples were compacted to  $7\% \pm 1\%$  air voids with dimensions of 100mm diameter and 150mm height. The WMA mixtures used for the dynamic modulus test in this paper differed by binder type and additive choice, but were mixed and compacted at the same temperatures (mix temperature – 130°C, and compaction temperature – 120°C). Five replicate samples for each group were tested for the development of this paper.

### 5.3.3. Dynamic shear rheometer test

High temperature binder testing was done using a Dynamic Shear Rheometer (DSR) on three samples for each of the four groups: no additive, 0.5% IDB, 0.5% FP 1 and 0.5% FP 2 using two binder types (Montana Crude – PG 64-22, and Polymer Modified Montana Crude – PG 70-22). A DSR was used to test the binders after they were RTFO aged (short-term aged) at one frequency (1.59 Hz – 10 rad/sec) and at three temperatures (58°C, 64°C, and 70°C for the PG 64-22 binder, and 64°C, 70°C, and 76°C for the PG 70-22 binder) (American Association of State Highway and Transportation Officials 2011b).

## 5.4. AASHTOWare Pavement ME Design SETUP

The following sections describe how results from the dynamic modulus test and DSR were used in setting up each of the files to be run in AASHTOWare Pavement ME Design. Each section will also describe how the data was used, and which inputs were used as Level 1 and which were used with default values.

### 5.4.1. Normalcy of measured E\* results using @RISK

Within this study five samples were tested for each group (2 binder and 4 additives for 8 groups in total) at nine frequencies and at three temperatures in the dynamic modulus test. Instead of using each individual sample's results for an individual file to run in AASHTOWare Pavement ME Design, it was decided that the measured results be normalized to save on time needed for running each file in the program. Values at 50% and the 95% percentile were determined and used from each normal distribution of results from each individual frequency at each temperature. These individual values

were compiled together to create the 50% and 95% percentile measured dynamic modulus results for each group (binder type/additive choice). A program called @RISK was used as an application in Microsoft Excel to normalize the measured  $E^*_{mix}$  results at each frequency within each temperature. The process used in obtaining the normalized values is shown below in Figure 5.1. This example shows the results for temperature 4°C, at frequency 25 Hz for the group – PG 64-22 binder with no additive.

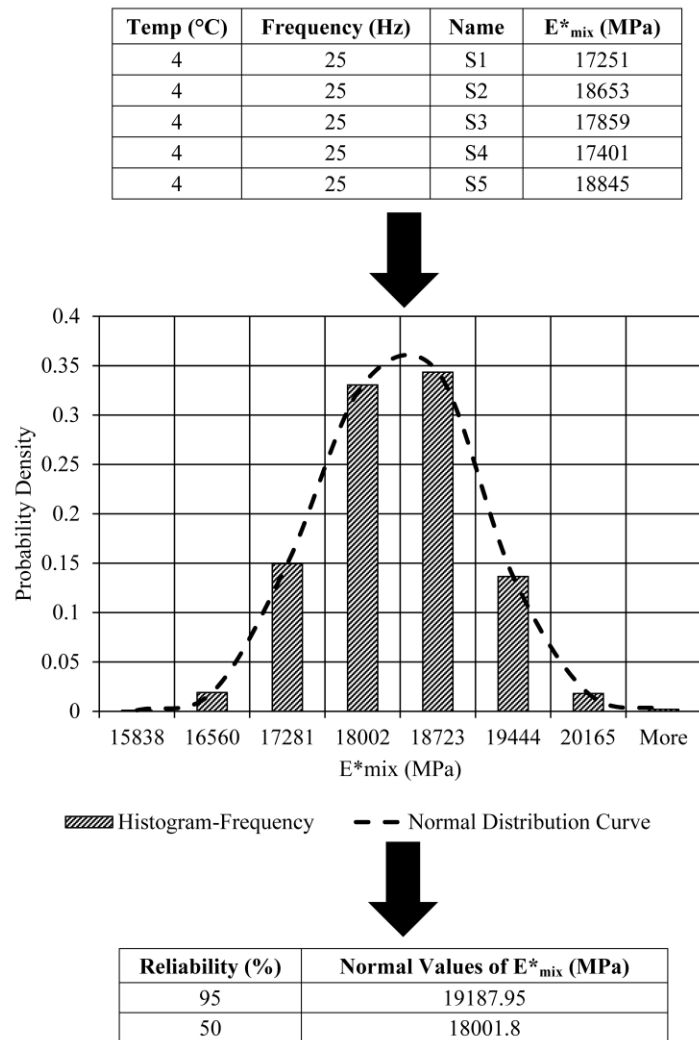


Figure 5.1. Visual Description of Process in @RISK

The graphical distribution in Figure 5.1 is a visual description of what @RISK does in terms of plotting the values in a normal distribution. @RISK also outputs the values along the normal distribution curve at 5% intervals (0, 5, 10, 15, 20, 25, 30, 35, 40, 45, 50, 55, 60, 65, 70, 75, 80, 85, 90, 95, and 100%) in a table. The values selected from this table for further use were the values at the 50% and 95% percentiles. After using @RISK for all nine frequencies within each of the three temperatures, the 50% and 95% normalized values were determined as shown in Table 5.2 for the PG 64-22 binder with no additive. This process was done using the results gained from testing five samples for each of the eight groups: no additive, 0.5% IDB, 0.5% FP 1 and 0.5% FP 2 samples using two binder types; the Montana PG 64-22 binder, and the Polymer Modified Montana PG 70-22 binder to create the 95% and 50% reliability dynamic modulus results. These results were then used as Level 1 input in AASHTOWare Pavement ME Design.

For AASHTOWare Pavement ME Design, there must be  $E^*_{mix}$  values at five temperatures and at six frequencies to represent the complete master curve. The frequencies chosen were 0.1, 1, 5, 10, 20, and 25 Hz. The five temperatures chosen are

**Table 5.2. Compiled Output for PG 64-22 with No Additive Using @RISK**

| 95% Reliability |      |       |       |       |       |       |       |       |       |
|-----------------|------|-------|-------|-------|-------|-------|-------|-------|-------|
| Frequency (Hz)  |      |       |       |       |       |       |       |       |       |
| Temp °C         | 0.1  | 0.2   | 0.5   | 1     | 2     | 5     | 10    | 20    | 25    |
| 4               | 9382 | 10274 | 11755 | 12995 | 14324 | 16130 | 17524 | 18749 | 19188 |
| 21              | 1772 | 2281  | 3165  | 4005  | 4949  | 6548  | 7465  | 8681  | 9058  |
| 37              | 528  | 617   | 794   | 1010  | 1431  | 2187  | 2970  | 3988  | 4277  |
| 50% Reliability |      |       |       |       |       |       |       |       |       |
| Frequency (Hz)  |      |       |       |       |       |       |       |       |       |
| Temp °C         | 0.1  | 0.2   | 0.5   | 1     | 2     | 5     | 10    | 20    | 25    |
| 4               | 8383 | 9409  | 10932 | 12154 | 13414 | 15098 | 16389 | 17586 | 18002 |
| 21              | 1446 | 1896  | 2696  | 3483  | 4404  | 5747  | 6884  | 8124  | 8523  |
| 37              | 331  | 422   | 589   | 770   | 1107  | 1683  | 2290  | 3116  | 3386  |

\* Note that units of  $E^*_{mix}$  are in MPa



-10, 4, 21, 37, and 54°C. The values at temperatures 4, 21, and 37°C are already known, but the values at -10 and 54°C are not. To obtain the values at the six chosen frequencies for temperatures -10 and 54°C, first the master curve must be determined using the test results from the temperatures 4, 21, and 37°C at the nine frequencies. Once the parameters to create the master curve are determined, back calculation can take place using Microsoft Excel Solver to determine an estimate of what the measured results should be at -10 and 54°C at each of the nine frequencies. Once these values are known, the 50% and 95% reliability data sets can be completely compiled for use in AASHTOWare Pavement ME Design. An example of data used for 50% and 95% reliability is shown in Table 5.3

**Table 5.3. Example of Data used for  $E^*_{mix}$  in AASHTOWare Pavement ME Design**

| 95% Reliability |       |       |       |       |       |       |
|-----------------|-------|-------|-------|-------|-------|-------|
| Frequency (Hz)  |       |       |       |       |       |       |
| Temp °C         | 0.1   | 1     | 5     | 10    | 20    | 25    |
| -10             | 18580 | 20479 | 21488 | 21842 | 22152 | 22243 |
| 4               | 9382  | 12995 | 16130 | 17524 | 18749 | 19188 |
| 21              | 1772  | 4005  | 6548  | 7465  | 8681  | 9058  |
| 37              | 528   | 1010  | 2187  | 2970  | 3988  | 4277  |
| 54              | 273   | 574   | 1065  | 1404  | 1848  | 2017  |
| 50% Reliability |       |       |       |       |       |       |
| Frequency (Hz)  |       |       |       |       |       |       |
| Temp °C         | 0.1   | 1     | 5     | 10    | 20    | 25    |
| -10             | 17462 | 19459 | 20565 | 20958 | 21302 | 21403 |
| 4               | 8383  | 12154 | 15098 | 16389 | 17586 | 18002 |
| 21              | 1446  | 3483  | 5747  | 6884  | 8124  | 8523  |
| 37              | 331   | 770   | 1683  | 2290  | 3116  | 3386  |
| 54              | 144   | 329   | 648   | 877   | 1188  | 1309  |

\*Note that units of  $E^*_{mix}$  are in MPa

#### 5.4.2. RTFO aged DSR data as Level 1 inputs

Three RTFO aged samples for each of the four groups: no additive, 0.5% IDB, 0.5% FP 1 and 0.5% FP 2 using two binder types (Montana Crude – PG 64-22, and Polymer Modified Montana Crude – PG 70-22) were tested in a DSR at one frequency (1.59 Hz – 10 rad/sec) and at three temperatures (58°C, 64°C, and 70°C for the PG 64-22 binder, and 64°C, 70°C, and 76°C for the PG 70-22 binder) (American Association of State Highway and Transportation Officials 2011). The RTFO aged DSR results were unchanged between the 95% and 50% reliability  $E^*_{mix}$  results used in AASHTOWare Pavement ME Design for each of the four groups: no additive, 0.5% IDB, 0.5% FP 1 and 0.5% FP 2 using two binder types (Montana Crude – PG 64-22, and Polymer Modified Montana Crude – PG 70-22). An example of the RTFO aged DSR results used in AASHTOWare Pavement ME Design is shown in Table 5.4.

**Table 5.4. Example of RTFO Aged DSR Results Used in AASHTOWare**

| Montana 64-22  |         |           |
|----------------|---------|-----------|
| Temperature °C | G* (Pa) | Delta (°) |
| 58             | 8134.5  | 80.9      |
| 64             | 3404.8  | 83.3      |
| 70             | 1547.5  | 85.3      |

\* Note that results are average of three samples tested

#### 5.4.3. Pavement structure, traffic level, and climatic locations

For this study three pavement structures were created with each being used with a specific traffic level. The pavement structures and their assigned traffic levels are shown in Figure 5.2. The only difference between the pavement structures is the thickness of the WMA layer. Thicknesses of 6 in., 10 in., and 12 in. were assigned traffic levels of low, medium, and high volume. Differences between the traffic levels are from the average

annual daily truck traffic (AADTT). The values of initial two-way AADTT for low, medium, and high volume traffic are 500, 1500, and 4000 as shown in Table 5.5. For the base layer and subgrade Level 3 inputs were used in AAHSTOWare Pavement ME Design. Excluding changing AADTT with WMA layer thickness, the rest of the traffic information used in AASHTOWare was setup with the default values as summarized in Table 5.5.

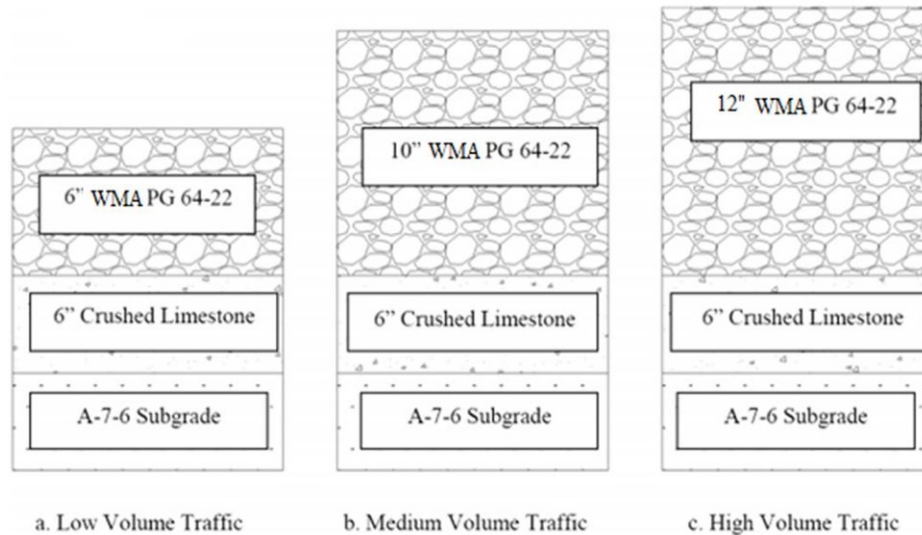


**Figure 5.2. Pavement: Structure Designs for Various Traffic Levels**

**Table 5.5. General Traffic Information**

| Traffic Parameter                   | Traffic Level |        |      |
|-------------------------------------|---------------|--------|------|
|                                     | Low           | Medium | High |
| Initial two-way AADTT               | 500           | 1500   | 4000 |
| Number of lanes in design direction | 2             | 2      | 2    |
| Trucks in design direction (%)      | 50            | 50     | 50   |
| Trucks in design lane (%)           | 95            | 95     | 95   |
| Operational Speed (kmh)             | 97            | 97     | 97   |
| Growth factor (%)                   | 3             | 3      | 3    |

Two climatic locations were used in this study, one being located in northern Iowa, and the other being located in southern Iowa. The northern location was chosen to be Mason City, IA, while the southern location was chosen to be Ottumwa, IA. Only two climatic locations were chosen to understand the impact in pavement performance due to limited changes in temperature and moisture profiles. The climatic file locations used are shown in Figure 5.3.

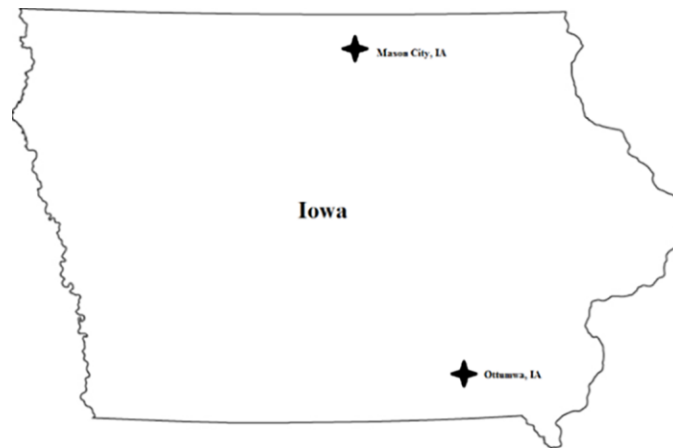


Figure 5.3. Locations of Climatic Files Used in AASHTOWare

## 5.5. Discussion of Results and Analysis

The first two sections go through the statistical analysis of the dynamic modulus results, and DSR results used for creating each of the files run in the AASHTOWare Pavement ME Design program. The third section gives comparison charts of each distress examined using the controlling variables in each file.

### 5.5.1. Dynamic modulus test results

The measured  $E^*$  results for each additive by binder type across temperature ( $^{\circ}\text{C}$ ) and frequency (Hz) are shown in Figure 5.4. From the trends in Figure 5.4 it is observed

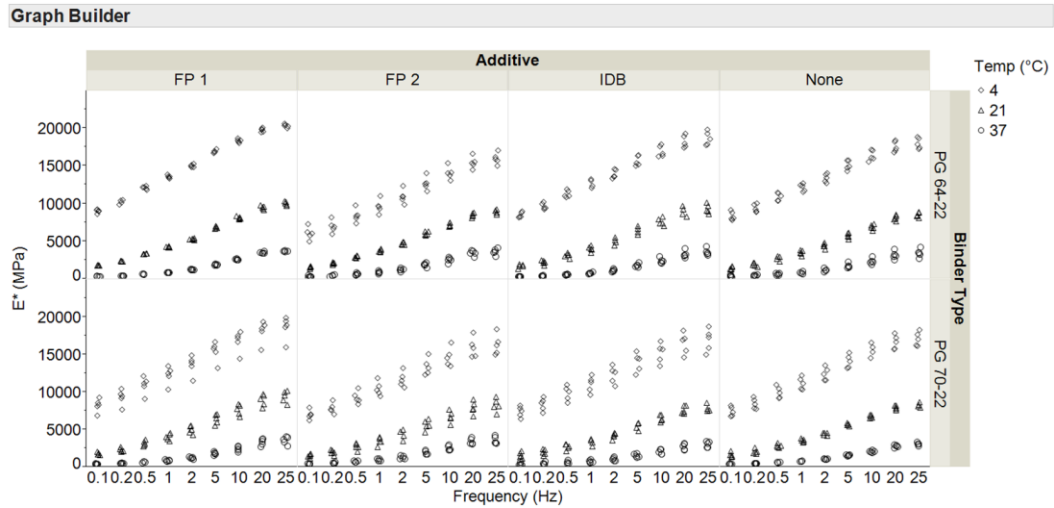


Figure 5.4. Comparison of all Measured  $E^*$  Results across Additive and Binder Type

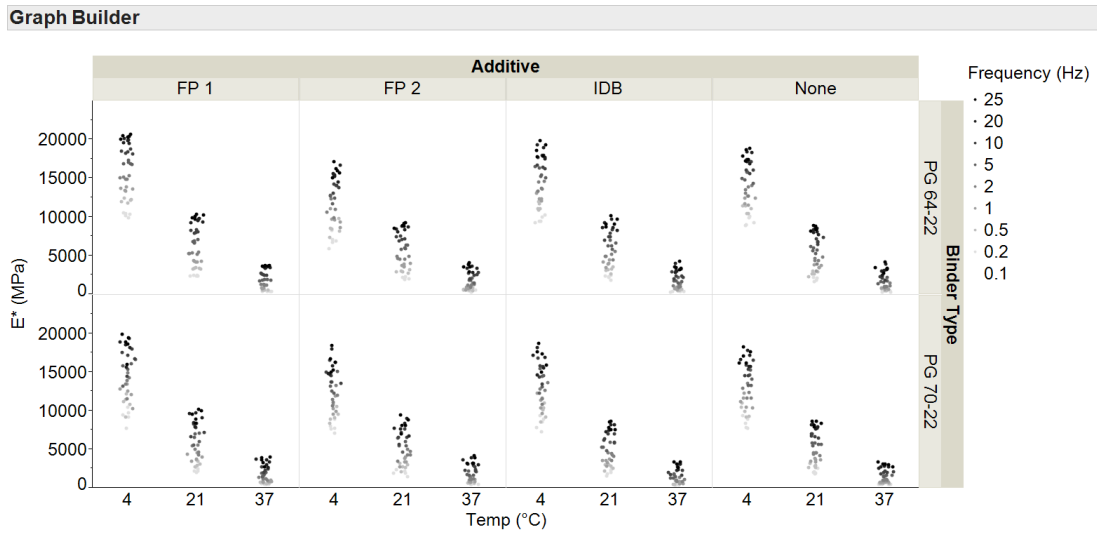


Figure 5.5. Distribution of  $E^*$  Results not Transformed

that  $E^*$  values for all eight groups of samples increase with an increase in frequency and a decrease in temperature at which each test is conducted.

To conduct a statistical analysis using the raw measured  $E^*$  results, the data needs to be examined to see if the central limit theorem is met. The spread of the raw measured unshifted  $E^*$  results for each group is shown in Figure 5.5. From Figure 5.5 it is shown that the central limit theorem is not met as the variance decreases with increasing temperature for each group and thus exhibits heteroscedasticity. A variance stabilization

transformation was done to the raw  $E^*$  values. A logarithmic transformation was done as shown in Figure 5.6 and a square root transformation was done as shown in Figure 5.7 for comparison. After examining both transformations of the raw measured  $E^*$  results, the square root transformation was selected for use in statistical analysis as the variance was more uniform with increasing temperature among the eight groups.

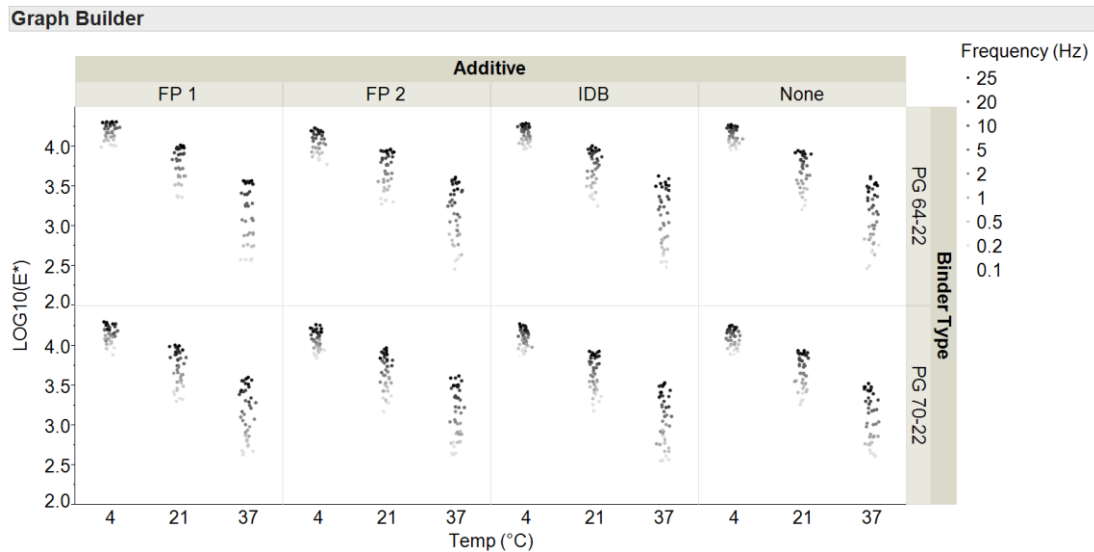


Figure 5.6. Distribution of  $E^*$  Results after Logarithmic Transformation

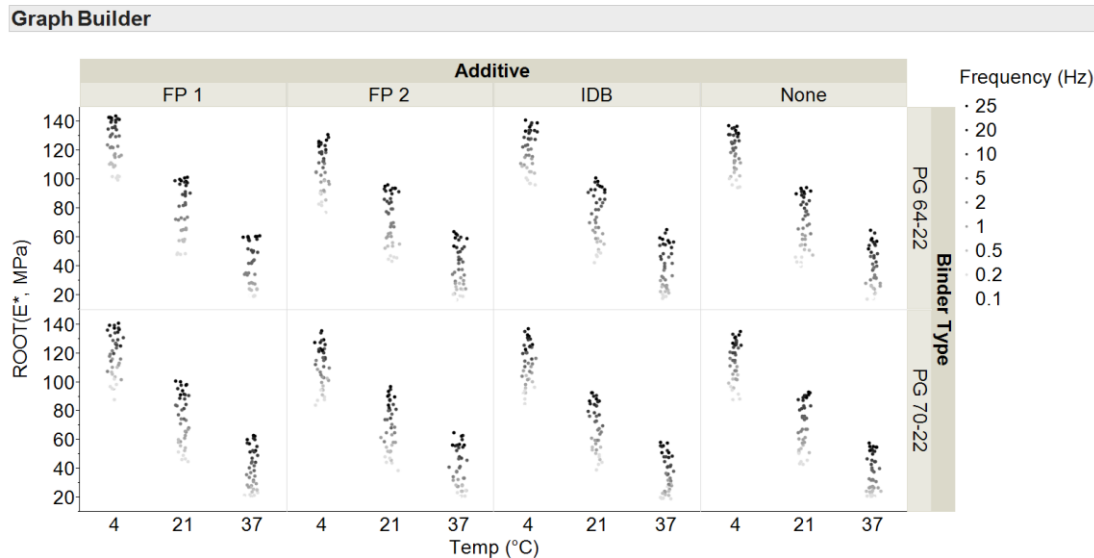


Figure 5.7. Distribution of  $E^*$  Results after Square Root Transformation

An analysis of variance (ANOVA) was conducted to examine which variability factors are significant in affecting the square root transformed  $E^*$  values. A split plot repeated measures design was used to conduct the ANOVA. The whole plot factors examined are Binder Type - A, and Additive - B, while the sub plot factors examined are Temperature ( $^{\circ}\text{C}$ ) - C, and Frequency (Hz) – D. All the interactions between Binder Type - A, Additive - B, Temperature ( $^{\circ}\text{C}$ ) - C, and Frequency (Hz) – D are also studied. A statistical program called JMP with the results shown in Table 5.6 below was used to evaluate the split plot repeated measure design for this ANOVA.

**Table 5.6. ANOVA of ROOT( $E^*$ , MPa) Using Split Plot Repeated Measure Design**

| Source  | SS       | MS Number | DF Number | F Ratio   | Prob > F |
|---|----------|-----------|-----------|-----------|----------|
| Binder Type - A   | 1.04E+03 | 1.04E+03  | 1         | 6.45      | 0.0161   |
| Additive - B  | 4.73E+03 | 1.58E+03  | 3         | 9.76      | 0.0001   |
| Binder Type*Additive  | 8.98E+02 | 2.99E+02  | 3         | 1.85      | 0.1572   |
| Temp ( $^{\circ}\text{C}$ ) - C                                 | 1.06E+06 | 5.28E+05  | 2         | 119317.98 | <.0001   |
| Binder Type*Temp ( $^{\circ}\text{C}$ )                         | 4.27E+02 | 2.13E+02  | 2         | 48.17     | <.0001   |
| Additive*Temp ( $^{\circ}\text{C}$ )                            | 4.57E+03 | 7.62E+02  | 6         | 171.97    | <.0001   |
| Binder Type*Additive*Temp ( $^{\circ}\text{C}$ )                | 9.97E+02 | 1.66E+02  | 6         | 37.50     | <.0001   |
| Frequency (Hz) - D  | 2.78E+05 | 3.47E+04  | 8         | 7842.51   | <.0001   |
| Binder Type*Frequency (Hz)                                      | 3.26E+02 | 4.08E+01  | 8         | 9.21      | <.0001   |
| Additive*Frequency (Hz)   | 2.56E+02 | 1.07E+01  | 24        | 2.41      | 0.0002   |
| Binder Type*Additive*Frequency (Hz)                             | 2.87E+01 | 1.20E+00  | 24        | 0.27      | 0.9998   |
| Temp ( $^{\circ}\text{C}$ )*Frequency (Hz)                      | 5.49E+03 | 3.43E+02  | 16        | 77.47     | <.0001   |
| Binder Type*Temp ( $^{\circ}\text{C}$ )*Frequency (Hz)          | 8.47E+01 | 5.29E+00  | 16        | 1.20      | 0.2655   |
| Additive*Temp ( $^{\circ}\text{C}$ )*Frequency (Hz)             | 6.29E+01 | 1.31E+00  | 48        | 0.30      | 1.00     |
| Binder Type*Additive*Temp ( $^{\circ}\text{C}$ )*Frequency (Hz) | 8.39E+01 | 1.75E+00  | 48        | 0.39      | 1.00     |
| Specimen No.[Binder Type, Additive]&Random                      | 5.17E+03 | 1.61E+02  | 32        | 36.44     | <.0001   |

In Table 5.6, it is evident that both Temperature ( $^{\circ}\text{C}$ ) - C and Frequency (Hz) - D are statistically significant sources of variability by themselves as well as crossed. To be a statistical significant source of variability, the p-value must be less than or equal to 0.05. The only interactions that are not statistically significant sources of variability are A\*B, A\*B\*D, A\*C\*D, B\*C\*D, and A\*B\*C\*D, while the rest of the interactions are statistically significant sources of variability. It is important to point out that Binder

Type\*Additive (A\*B) is not a statistically significant source of variability, while both Binder Type (A) and Additive (B) are statistically significant sources of variability. This means that the additives were found to be statistically significantly different from one another overall but not within each binder type according to a 95% confidence level. The plot for Additive (B) is shown in Figure 5.8.

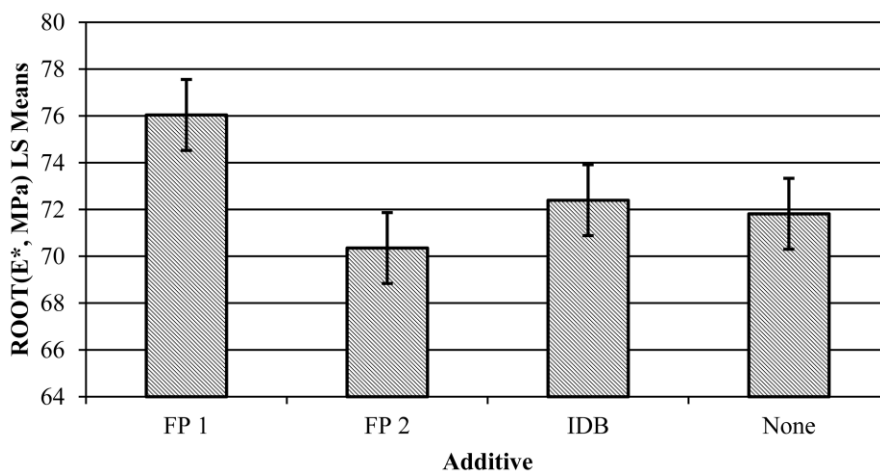


**Figure 5.8. Plot for B (Additive) using Least Squares (LS) Means**

Just by looking at the plot in Figure 5.8, it is hard to discern whether or not the additives are statistically significantly different from one another. This prompted the use of a Tukey Honestly Significant Differences (HSD) comparison to see which of the additives are statistically significantly different from one another as the p-value from the ANOVA in Table 5.6 is equal to 0.0001. The Tukey HSD comparison is shown in Table 5.7. The comparison of additives shows that FP 1 is statistically significantly different from that of FP 2, IDB and the control group according to a 95% confidence level.



**Table 5.7. Tukey Honestly Significant Differences Comparison for Additive (B)**

**LSMeans Differences Tukey HSD**

$\alpha = 0.050$   $Q = 2.70936$

| Level  | Least Sq Mean |
|--------|---------------|
| FP 1 A | 76.038093     |
| IDB B  | 72.397518     |
| None B | 71.817601     |
| FP 2 B | 70.354079     |

Levels not connected by same letter are significantly different.

Below in Figure 5.9 the measured  $E^*$  results for 50% and 95% reliability levels shifted using each groups reduced frequency results is shown. From Figure 5.9 it is shown that as temperature gets lower and as the frequency increases, the difference between the results at 50% and 95% reliability grows substantially larger. At high temperature and low frequency, the differences between the 50% and 95% reliability level results are not significant. Since the differences at high temperature are slight between the reliability levels, results like rutting should be fairly similar between the two levels for each additive/binder type group within each climatic location, and traffic level.

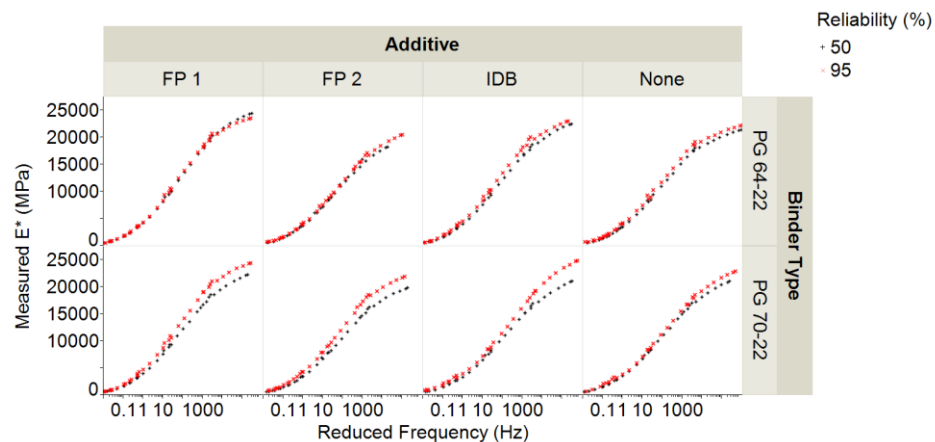


**Figure 5.9. 50% and 95% Reliability Measured  $E^*$  Results Shifted with Reduced Frequency**

### 5.5.2. RTFO aged DSR test results

The average  $G^*$  results for each additive by binder type across temperature is shown in Figure 5.10, while the average phase angle results for each additive by binder type across temperature is shown in Figure 5.11. From the trends shown in Figures 5.10 and 5.11 it is observed that the  $G^*$  and phase angle values decrease and increase with increasing temperature for each of the additives within each binder type. However, it is not clear from these trends whether the additives within each binder type are statistically significantly different from one another in terms of their  $G^*$  and phase angle values. Thus a statistical analysis is needed to see the differences more clearly.

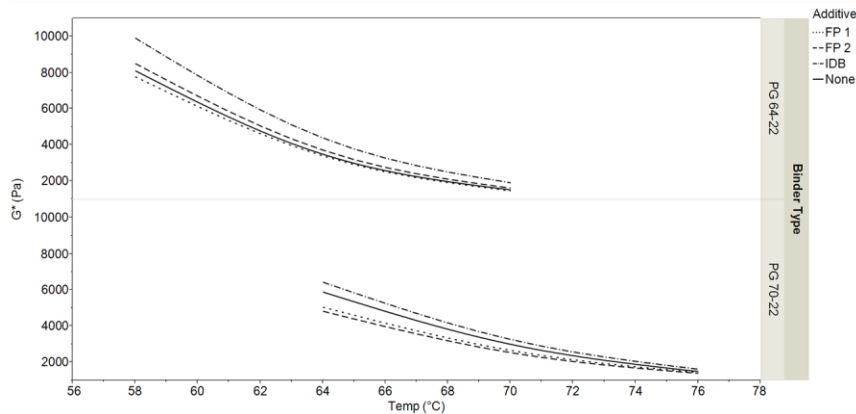


Figure 5.10. Comparison of Average  $G^*$  Results Used in AASHTOWare

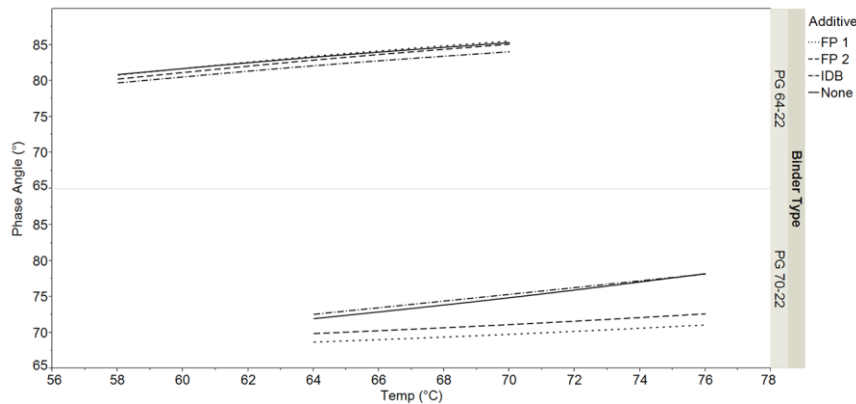


Figure 5.11. Comparison of Average Phase Angle Results Used in AASHTOWare

An ANOVA using a split plot repeated measure design was used to investigate if there are differences between the binders modified with each additive for the PG 64-22 and the PG 70-22 binders. An ANOVA was done separately for each binder type within JMP. The results of the statistical analysis are shown in Table 5.8 for both, binders PG 64-22 and PG 70-22,  $G^*$  and phase angle results. From Table 5.8 it can be seen that the source additive is statistically significant for both binders and for both  $G^*$  and phase angle results as the p-values are all less than 0.05, which is passing a 95% confidence level.

**Table 5.8. ANOVA of  $G^*$  and Phase Angle Using Split Plot Repeated Measure Design**

| G* (Pa) - PG 64-22         |          |           |           |          |          |
|----------------------------|----------|-----------|-----------|----------|----------|
| Source                     | SS       | MS Number | DF Number | F Ratio  | Prob > F |
| Additive                   | 7.54E+06 | 2.51E+06  | 3         | 61.48    | <.0001   |
| Temp (°C)                  | 3.07E+08 | 1.54E+08  | 2         | 13763.56 | <.0001   |
| Additive*Temp (°C)         | 2.58E+06 | 4.31E+05  | 6         | 38.62    | <.0001   |
| Spec No.[Additive]&Random  | 3.27E+05 | 4.09E+04  | 8         | 3.67     | 0.0129   |
| G* (Pa) - PG 70-22         |          |           |           |          |          |
| Source                     | SS       | MS Number | DF Number | F Ratio  | Prob > F |
| Additive                   | 4.10E+06 | 1.37E+06  | 3         | 5.37     | 0.0255   |
| Temp (°C)                  | 1.03E+08 | 5.16E+07  | 2         | 1428.81  | <.0001   |
| Additive*Temp (°C)         | 1.97E+06 | 3.28E+05  | 6         | 9.10     | 0.0002   |
| Spec No.[Additive]&Random  | 2.04E+06 | 2.55E+05  | 8         | 7.06     | 0.0005   |
| Phase Angle (°) - PG 64-22 |          |           |           |          |          |
| Source                     | SS       | MS Number | DF Number | F Ratio  | Prob > F |
| Additive                   | 9.47E+00 | 3.16E+00  | 3         | 118.81   | <.0001   |
| Temp (°C)                  | 1.27E+02 | 6.33E+01  | 2         | 8753.00  | <.0001   |
| Additive*Temp (°C)         | 2.71E-01 | 4.51E-02  | 6         | 6.24     | 0.0016   |
| Spec No.[Additive]&Random  | 2.12E-01 | 2.66E-02  | 8         | 3.67     | 0.0129   |
| Phase Angle (°) - PG 70-22 |          |           |           |          |          |
| Source                     | SS       | MS Number | DF Number | F Ratio  | Prob > F |
| Additive                   | 2.05E+02 | 6.83E+01  | 3         | 458.78   | <.0001   |
| Temp (°C)                  | 1.09E+02 | 5.45E+01  | 2         | 421.29   | <.0001   |
| Additive*Temp (°C)         | 1.76E+01 | 2.93E+00  | 6         | 22.68    | <.0001   |
| Spec No.[Additive]&Random  | 1.19E+00 | 1.49E-01  | 8         | 1.15     | 0.3837   |

The use of Tukey HSD comparison was done to see which of the additives are statistically significantly different from one another as the p-values from the ANOVA in Table 5.8 are all less than 0.05 for the binder PG 64-22 for both the G\* and phase angle results. The Tukey HSD comparison for G\* and phase angle results based on the source Additive are shown in Tables 5.9 and 5.10. The comparison of additives for G\* results in Table 5.9 shows that IDB is statistically significantly different from that of None (control group), FP 1, and FP 2 according to a 95% confidence level. Within Table 5.9 it is also seen that FP 1 is statistically significantly different from FP 2, while None (control group) is found to be not statistically significantly different from FP 1 and FP 2 for G\* results. In Table 5.10 IDB follows the same trend as that shown for IDB in Table 5.9.

**Table 5.9. Tukey Honestly Significant Differences Comparison of G\* (Pa) for Additive (B) within PG 64-22**

**LSMeans Differences Tukey HSD**

$\alpha = 0.050$   $Q = 3.20234$

| Level    | Least Sq Mean |
|----------|---------------|
| IDB A    | 5393.6111     |
| FP 2 B   | 4601.8889     |
| None B C | 4362.2778     |
| FP 1 C   | 4202.2222     |

Levels not connected by same letter are significantly different.

**Table 5.10. Tukey Honestly Significant Differences Comparison of Phase Angle (\*) for Additive (B) within PG 64-22**

**LSMeans Differences Tukey HSD**

$\alpha = 0.050$   $Q = 3.20234$

| Level  | Least Sq Mean |
|--------|---------------|
| FP 1 A | 83.269603     |
| None A | 83.174783     |
| FP 2 B | 82.758166     |
| IDB C  | 81.969861     |

Levels not connected by same letter are significantly different.

However, FP 2 is now statistically significantly different from the other three source Additive groups, while FP 1 and None (control group) are not statistically different from one another.

The use of Tukey HSD comparison was also done to see which of the additives are statistically significantly different from one another as the p-values from the ANOVA in Table 5.8 are all less than 0.05 for the binder PG 70-22 for both the G\* and phase angle results. The Tukey HSD comparison for G\* and phase angle results based on the source Additive are shown in Tables 5.11 and 5.12. The comparison of additives for G\* results in Table 5.11 show that IDB is statistically significantly different from that of FP 2 according to a 95% confidence level. Within Table 5.11 it is also seen that IDB is not

**Table 5.11. Tukey Honestly Significant Differences Comparison of G\* (Pa) for Additive (B) within PG 70-22**

**LSMeans Differences Tukey HSD**

$\alpha = 0.050$   $Q = 3.20234$

| Level    | Least Sq Mean |
|----------|---------------|
| IDB A    | 3775.2500     |
| None A B | 3461.5000     |
| FP 1 A B | 3054.1111     |
| FP 2 B   | 2920.8889     |

Levels not connected by same letter are significantly different.

**Table 5.12. Tukey Honestly Significant Differences Comparison of Phase Angle (°) for Additive (B) within PG 70-22**

**LSMeans Differences Tukey HSD**

$\alpha = 0.050$   $Q = 3.20234$

| Level  | Least Sq Mean |
|--------|---------------|
| IDB A  | 75.375882     |
| None A | 75.031907     |
| FP 2 B | 71.219930     |
| FP 1 C | 69.853616     |

Levels not connected by same letter are significantly different.

statistically significantly different from none (control group), and FP 1, while FP 2 is found to be not statistically significantly different from FP 1 and None (control group) for the  $G^*$  results. In Table 5.12, IDB is statistically significantly different from that of FP 1, and FP 2 according to a 95% confidence level. FP 1 is statistically significantly different from the other three source Additive groups. This is the same case for FP 2.

Complex shear modulus results indicate that IDB has the highest resistance to permanent deformation compared to the other additives, but the binder PG 70-22 shows that all of the additives excluding the control group (None) are statistically significantly different from one another. The phase angle results designate differences between each of the additive, but the rankings are not the same for the different binders. The phase angle, or time lag in material response is greatest for FP 1 for the PG 64-22 binder and lowest for IDB. The order for IDB and FP 1 is switched for the PG 70-22 binder. This suggests that there is an interaction between the polymer SBS and additive choice.

### **5.5.3. Performance evaluation using AASHTOWare Pavement ME Design**

The impact of additive choice on the performance of warm mix asphalt in Iowa using AASHTOWare Pavement ME Design was a primary objective of this research. The main performance parameters examined were asphalt concrete (AC) bottom up cracking (%), AC rutting (in.), total pavement system rutting (in.), and smoothness/International Roughness Index (IRI) in in/mile. To run these models successfully, four inputs will be controlled:  $E^*$  data based on reliability, RTFO aged DSR results, traffic level, and climatic location. These inputs are controlled through the selection of each binder type/additive group (8 groups total).

As there is only one run for each combination of variables, comparison figures will be used to see the differences between each of the additive choices within each binder type. Also comparisons can be made between the different binder types for each additive choice. The results determined through the AASHTOWare Pavement ME Design program are shown in Figures 5.12 through 5.15 (AC bottom up cracking, AC rutting, total rutting, and smoothness). The results are categorized by the examined variables. Within each category are two bars, one signifying 50% reliability  $E^*$  results used in AASHTOWare, while the other bar signifies 95% reliability  $E^*$  results used in AASHTOWare. The differences between the two reliability levels can be observed by noting the differences between the bars within each category.

#### 5.5.3.1. Asphalt concrete (AC) bottom up cracking

The AC bottom up cracking results appears to follow the same trend within each traffic level. The results for AC bottom up cracking are lower using 95% reliability  $E^*_{mix}$  results, and are slightly higher using 50% reliability  $E^*_{mix}$  results within each traffic level. Across the traffic levels, the low volume design appears to produce the highest resulting AC bottom up cracking, preceded by the high volume, and then the medium volume design. This makes sense as the pavement structure for low volume had an AC thickness of 6 inches, while the high and medium volume traffic levels had AC thicknesses of 12 inches and 10 inches, respectively.

For the two climatic locations, the southern location (Ottumwa, IA) produces higher AC bottom up cracking results across all the categories than the northern location (Mason City, IA). This difference although slight is most likely due to the annual rainfall,

and seasonal temperatures being slightly higher, and perhaps warmer temperatures lasting a little longer in Ottumwa, IA over that in Mason City, IA. The increase in moisture due to increased rainfall with increased temperatures over a longer period of time would make the pavement systems more susceptible to AC bottom up cracking. Within the binder type PG 64-22 using the 50% reliability E\* results, the additive FP 2 produces the highest AC bottom up cracking, while FP 1 produces the least amount of AC bottom up cracking. IDB has the second highest and None has the third highest results in AC bottom up cracking for 50% reliability E\* results. For the 95% reliability PG 64-22 E\* results, IDB and None have the lowest AC bottom cracking, with FP 2 the highest, and FP 1 the second highest. Within the binder type PG 70-22 using the 50% reliability E\* results, IDB produces the highest AC bottom up cracking, while FP 1 produces the least amount of AC bottom up cracking. FP 2 has the second highest and None has the third highest results in AC bottom up cracking for 50% reliability E\* results. For the 95% reliability PG 64-22 E\* results, FP 1 has the lowest AC bottom up cracking, with None the highest, IDB the second highest, and FP 2 the third highest AC bottom up cracking results.

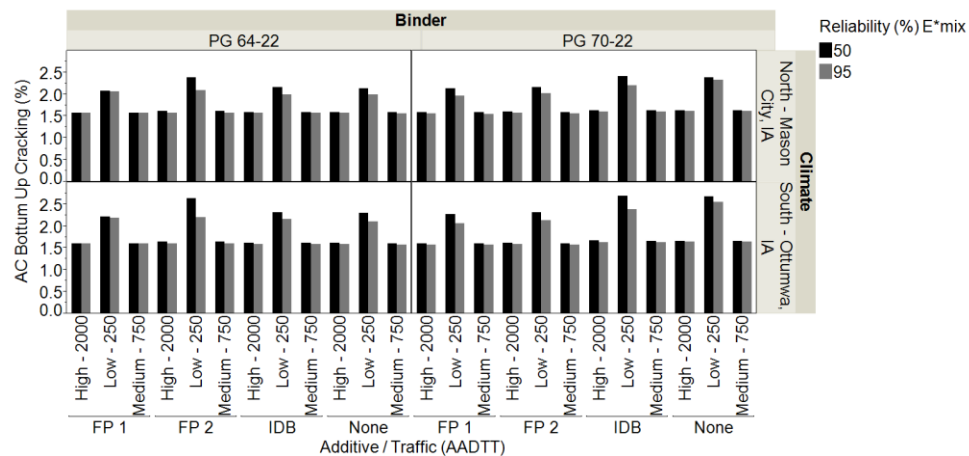


Figure 5.12. Comparison of AC Bottom Up Cracking Results



### 5.5.3.2. Rutting

The AC rutting results appears to follow the same trend within each traffic level. The results for AC rutting are lower using 95% reliability  $E^*_{mix}$  results, and are slightly higher using 50% reliability  $E^*_{mix}$  results within each traffic level. Across the traffic levels, the high volume design appears to produce the highest resulting AC rutting, preceded by medium, and then low volume design. This is primarily due to the high volume design having a higher AADTT than the other two traffic levels. For the two climatic locations, the southern location (Ottumwa, IA) produces higher AC rutting results across all the categories than the northern location (Mason City, IA). This difference although slight is most likely due to the difference between seasonal temperatures of the two locations with Ottumwa, IA having slightly higher temperatures all year round than the location Mason City, IA. This increase in temperature makes the mix softer under the repeated loading trucks making it more susceptible to rutting.

Within the binder type PG 64-22 using the 50% reliability  $E^*$  results, the additive FP 2 produces the highest AC rutting, while FP 1 produces the least amount of AC rutting. IDB has the second highest and None has the third highest results in AC rutting for 50% reliability  $E^*$  results. For 95% reliability PG 64-22  $E^*$  results, None has the lowest AC rutting and FP 1 has the highest AC rutting, with FP 2 the second highest, and IDB the third highest. Using the 50% reliability PG 70-22  $E^*$  results, IDB produces the highest AC rutting, while FP 1 and FP 2 produce the least amount of AC rutting. None has the second highest results in AC rutting for 50% reliability  $E^*$  results. For 95% reliability PG 70-22  $E^*$  results, FP 1 has the lowest AC rutting, with None the highest, IDB the second highest, and FP 2 the third highest AC rutting results.

Total pavement system rutting follows the same trends as that of AC rutting results. The only difference is that the total amount of rutting for each category has almost doubled from the results for AC rutting. This means that subgrade rutting is almost equal to that AC rutting occurring in each pavement system.

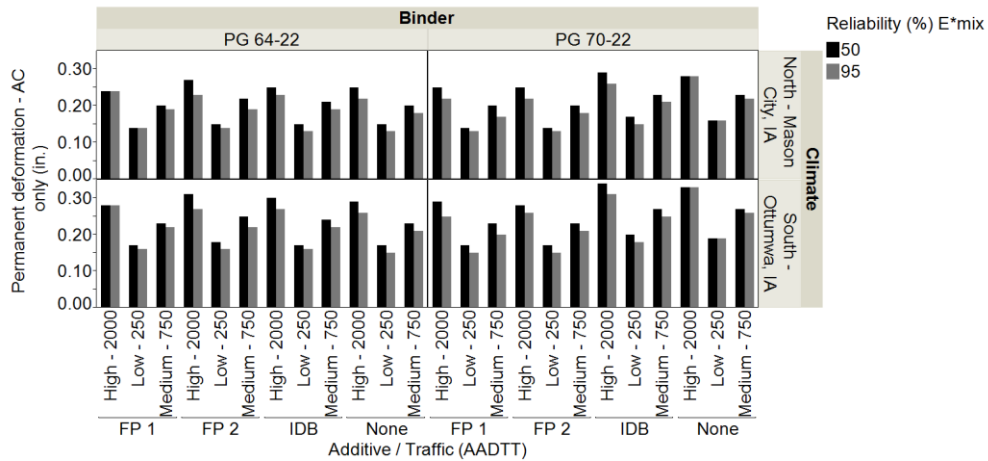


Figure 5.13. Comparison of Asphalt Concrete Rutting Results

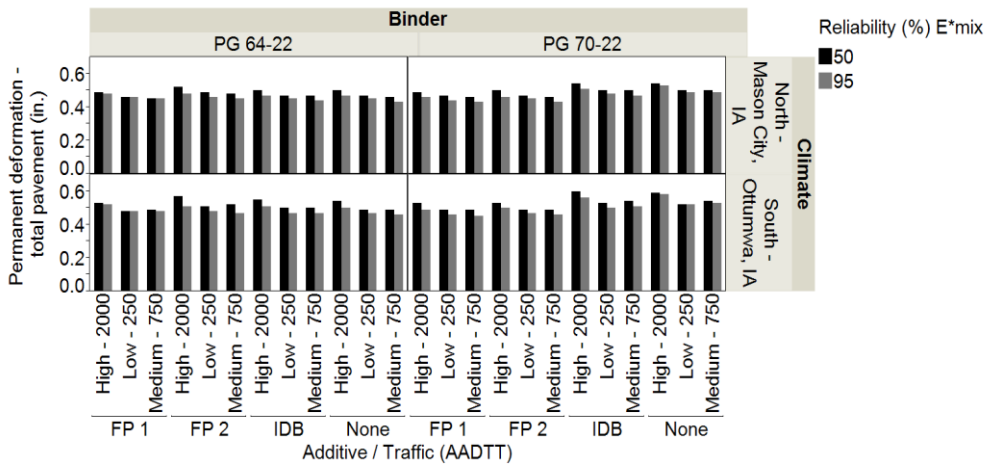


Figure 5.14. Comparison of Total Pavement System Rutting Results

### 5.5.3.3. Smoothness

The smoothness/International Roughness Index (IRI) results appear to follow the same trend within each traffic level. The results for IRI are lower using 95% reliability

$E^*_{mix}$  results, and are slightly higher using 50% reliability  $E^*_{mix}$  results within each traffic level. Across the traffic levels, the low volume design appears to produce the highest resulting IRI, preceded by high volume, and then medium volume design. For the two climatic locations, the southern location (Ottumwa, IA) produces lower IRI results across all the categories than the northern location (Mason City, IA). This is most likely due to seasonal temperatures being slightly higher, and perhaps warmer temperatures lasting a little longer in Ottumwa, IA over that in Mason City, IA. An asphalt pavement in Ottumwa, IA experiences a lower amount of freeze thaw damage than an asphalt pavement system in Mason City, IA. The more freeze thaw cycles a pavement goes through the rougher the surface will be generally. In terms of additive IRI performance, it can be observed that FP 1 produces the lowest IRI, while None (the control group) produces the highest IRI. The full trend for IRI is as follows: FP 1 < FP 2 < IDB < None. For the two binder types, the PG 64-22 produces on average higher IRI than the PG 70-22 binder.

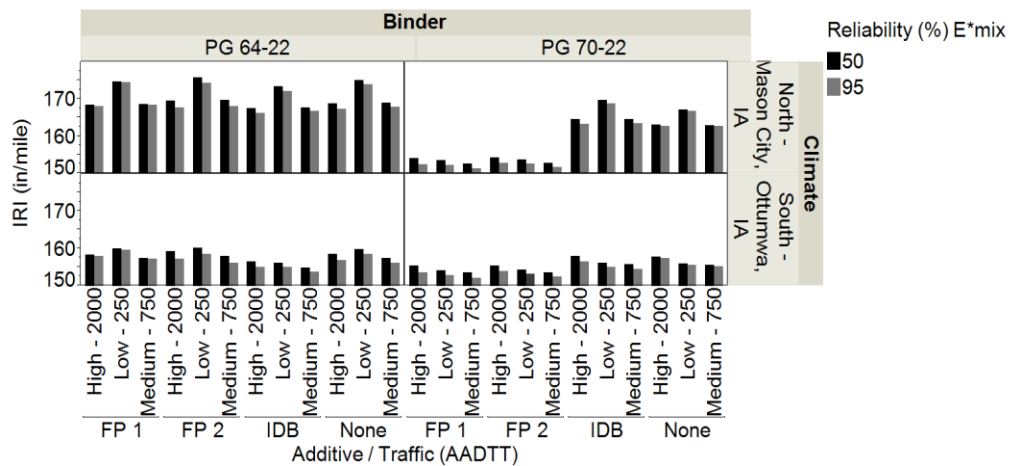


Figure 5.15. Comparison of Smoothness/International Roughness Index (IRI) Results

## 5.6. Conclusions

The dynamic modulus test has shown that Isosorbide Distillation Bottoms (IDB) can be used as a viable WMA additive in terms of performance when compared to the control group as well as the additives FP 1 and FP 2. Comparisons of performance between the additives and binder types were made using a split plot repeated measure design for the statistical analysis using root square transformed measured  $E^*_{mix}$  results from the dynamic modulus test. From the statistical analysis it was found that the additives were found to be statistically significantly different from one another overall, but were not found to be statistically significantly different from one another when crossed with binder type. It was found that FP 1 is statistically significantly different than FP 2, IDB and None (the control group). The additives when crossed with temperature were found to be statistically significantly different from one another as well as statistically significantly different from one another within each binder type. When looking at interactions with frequency, the additives are statistically significantly different from one another. However, when additives are crossed with frequency and binder type they are not statistically significantly different from one another. This also occurs when the additive is crossed with frequency, binder type, and temperature. Transforming the measured  $E^*$  results based on normalcy to the 50% and 95% percentile locations of the distribution curve was done to create a 50% reliability and 95% reliability set of  $E^*$  values for use in AASHTOWare Pavement ME Design as Level 1 inputs. The 50% and 95% reliability sets of  $E^*$  results within each binder type and for each additive are similar at high temperatures and low frequencies, but are different from one another at low temperatures and high frequencies.

Comparisons of RTFO aged DSR binder results within each binder type were made using a split plot repeated measure design for the statistical analysis. From the statistical analysis of PG 64-22, it was found that the additives were found to be statistically significantly different from one another for both  $G^*$  and phase angle. For the  $G^*$  results FP 2 and None (the control group) were not found to be statistically significantly different from one another, and for the phase angle results FP 1 and None (the control group) were not found to be statistically different from one another. In the statistical analysis of PG 70-22, it was found that the additives were found to be statistically significantly different from one another for both  $G^*$  and phase angle. For the  $G^*$  results IDB and FP 2 were found to be statistically significantly different from one another, and for the phase angle results IDB and None (the control group) were not found to be statistically different from one another. From the results shown in Tables 5.9 and 5.11 it can be stated that IDB has the highest resistance to permanent deformation when compared to the other additives and control group. When looking at Tables 5.10 and 5.12, there is definitive interaction between binder type and additive choice. This is shown by examining IDB and FP 1s' least square mean (LS mean) phase angle results for each binder type. For the PG 64-22 binder IDB has the lowest LS mean phase angle result, while FP 1 has the highest resulting LS mean phase angle. This is switched when the PG 64-22 is polymer modified as shown in Table 5.12. Now IDB shows the highest LS mean phase, while FP 1 has the lowest LS mean phase angle result.

From use of the AASHTOWare Pavement ME Design program, the predicted pavement performance was evaluated for sensitivity to different traffic loading, climate and pavement design conditions as well as variable  $E^*$  reliability. From the resulting

sensitivity study the pavement design/traffic level used for each run has a large impact on the pavement performance compared with the two climates and reliability levels that were included. The corn-derived WMA additive was similar to the other established WMA additives showing similar pavement performance predicted by the AASHTOWare Pavement ME Design. The pavement performance in the control group did not show large differences compared to WMA additives showing that the pavement performance models forecast equal performance between the WMA additives studied and the HMA control group. Limitations of this paper were that the  $E^*_{mix}$  results for each group of samples were converted into two sets (50% and 95% reliability data sets) under the assumption that normalcy was met. This limitation makes it impossible to do statistical analysis for the sensitivity study using the AASHTOWare Pavement ME Design program results. If each dynamic modulus sample within each of the additive/binder type groups was used individually in the program there would be five results for each category that could be examined. Assuming normalcy was done to alleviate on the amount of time as there would have been several hundred runs without this assumption. For future research, it is recommended that each individual sample's  $E^*_{mix}$  results be used for setup of the files to be run so a statistical analysis can be performed.

### 5.7. Acknowledgements

The authors would like to thank Bill Haman from the Iowa Energy Center (IEC) for funding this research work and thank Chris Brakke and the Iowa Department of Transportation for their assistance in using the AASHTOWare Pavement ME Design program in this research work.

## 5.8. References

- American Association of State Highway and Transportation Officials, (AASHTO). (2011). Determining the Rheological Properties of Asphalt Binder Using a Dynamic Shear Rheometer (DSR): T 315-10, Washington, DC.
- Anderson, R., Baumgardner, G., May, R., & Reinke, G. (2008). Engineering properties, emissions, and field performance of warm mix asphalt technologies *NCHRP 9-47, Interim Report*. Washington D.C.: National Cooperation Highway Research Program.
- Buss, A., Kuang, Y., Williams, R. C., Bausano, J., Cascione, A., & Schram, S. A. (2014). *Influence of Warm Mix Asphalt Additive and Dosage Rate on Construction and Performance of Bituminous Pavements*. Paper presented at the Transportation Research Board 93rd Annual Meeting.
- Buss, A., & Williams, R. C. (2012). Warm Mix Asphalt Performance Modeling Using the Mechanistic-Empirical Pavement Design Guide. In A. Scarpas, N. Kringos, I. Al-Qadi & L. A. (Eds.), *7th RILEM International Conference on Cracking in Pavements* (Vol. 4, pp. 1323-1332): Springer Netherlands.
- Button, J. W., Estakhri, C., & Wimsatt, A. (2007). A synthesis of warm mix asphalt *Rep. No. FHWA/TX-07/0-5597-1*. College Station, TX.: Texas Transportation Institute.
- Christensen, D. W., & Anderson, D. A. (1992). Interpretation of dynamic mechanical test data for paving grade asphalt cements (with discussion). *Journal of the Association of Asphalt Paving Technologists*, 61.
- Corrigan, M. (2006). Warm mix asphalt technologies and research. *Federal Highway Administration Office of Pavement Technology*, 3(10), 26-28.
- D'Angelo, J., et al. (2008). Warm-mix asphalt: European practice *Publication FHWA-PL-08-007*: FHWA, U.S. Dept. of Transportation, Washington, DC.
- Gandhi, T. (2008). *Effects of warm asphalt additives on asphalt binder and mixture properties*. Ph.D. dissertation, Clemson Univ., Clemson, SC.
- Hajj, E., Sebaaly, P., Sathanathan, T., & Shivakolunthar, S. (2013). Impact of Antistrip Additives on Pavement Performance Using Mechanistic-Empirical Pavement Design Guide. *Journal of Materials in Civil Engineering*, 25(3), 308-317. doi:10.1061/(ASCE)MT.1943-5533.0000582
- Hassan, M. (2009). *Life-cycle assessment of warm-mix asphalt: An environmental and economic perspective*. Paper presented at the Transportation Research Board 88th Annual Meeting.
- Hossain, Z., Zaman, M., O'Rear, E., & Chen, D. (2011, June 9-11). *Effectiveness of Advera in Warm Mix Asphalt*. Paper presented at the ASCE GeoHunan 2011.
- Hurley, G. C., & Prowell, B. D. (2005a). Evaluation of Aspha-Min zeolite for use in warm mix asphalt *NCAT Rep. No. 05-04*. Auburn, AL.: National Center for Asphalt Technology.
- Hurley, G. C., & Prowell, B. D. (2005b). Evaluation of Sasobit for use in warm mix asphalt *NCAT Rep. No. 05-06*. Auburn, AL.: National Center for Asphalt Technology.
- Hurley, G. C., & Prowell, B. D. (2006). Evaluation of Evotherm for use in warm mix asphalt *Rep. No. 06-02* (Vol. 6). Auburn, AL.: National Center for Asphalt Technology.

- Jenkins, K., De Groot, J., van de Ven, M., & Molenaar, A. (1999). *Half-warm foamed bitumen treatment, a new process*. Paper presented at the 7th Conference on asphalt pavements for Southern Africa (CAPSA 99).
- Kim, H., Lee, S., & Amirkhanian, S. (2012). Influence of Warm Mix Additives on PMA Mixture Properties. *Journal of Transportation Engineering*, 138(8), 991-997.  
doi:10.1061/(ASCE)TE.1943-5436.0000406
- Koenders, B., Stoker, D., Robertus, C., Larsen, O., & Johansen, J. (2002). *WAM-Foam, asphalt production at lower operating temperatures*. Paper presented at the Ninth International Conference on Asphalt Pavements, Copenhagen, Denmark.
- Kristjánsdóttir, Ó. (2006). *Warm-mix asphalt for cold weather paving*. Master's thesis, Univ. of Washington, Seattle, WA.
- Kristjánsdóttir, Ó., Muench, S. T., Michael, L., & Burke, G. (2007). Assessing potential for warm-mix asphalt technology adoption. *Transp. Res. Rec.*, 2040, 91-99.
- Larsen, O., Moen, Ø., Robertus, C., & Koenders, B. (2004). *WAM Foam asphalt production at lower operating temperatures as an environmental friendly alternative to HMA*. Paper presented at the 3rd Eurasphalt & Eurobitume Congress.
- Leng, Z., Gamez, A., & Al-Qadi, I. (2013). Mechanical Property Characterization of Warm-Mix Asphalt Prepared with Chemical Additives. *Journal of Materials in Civil Engineering*, 0(ja), null.  
doi:10.1061/(ASCE)MT.1943-5533.0000810
- Li, X. J., & Williams, R. C. (2012). A Practical Dynamic Modulus Testing Protocol. *Journal of Testing and Evaluation*, 40(1), 100-106.
- Middleton, B., & Forfylyow, R. W. (2009). Evaluation of warm-mix asphalt produced with the double barrel green process. *Transp. Res. Rec.*, 2126, 19-26.
- National Cooperative Highway Research Program, (NCHRP). (2004). Guide for Mechanistic-Empirical Design of New and Rehabilitated Pavement Structures *NCHRP 1-37A*
- Newcomb, D. (2007). An introduction to warm-mix asphalt. Retrieved August, 2, 2013.
- Perkins, S. W. (2009). Synthesis of warm mix asphalt paving strategies for use in Montana highway construction *Rep. No. FHWA/MT-09-009/8117-38*. Helena, MT.: Western Transportation Institute.
- Prowell, B. D., Hurley, G. C., & Crews, E. (2007). *Field performance of warm-mix asphalt at the NCAT test track*. Paper presented at the Transportation Research Board 86th Annual Meeting.
- Werpy, T. A., Holladay, J. E., & White, J. F. (2004). Top Value Added Chemicals From Biomass: I. Results of Screening for Potential Candidates from Sugars and Synthesis Gas (pp. Medium: ED; Size: PDFN).



## **CHAPTER 6. COMPARATIVE PERFORMANCE OF BIO-DERIVED/CHEMICAL ADDITIVES IN WARM MIX ASPHALT AT LOW TEMPERATURE**

Modified from a paper accepted by *Materials and Structures*

Joseph H. Podolsky<sup>1</sup>, Ashley Buss<sup>2</sup>, R. Christopher Williams<sup>3</sup>, and Eric Cochran<sup>4</sup>

### **6.1. Abstract**

A corn based bio-derived warm mix asphalt (WMA) additive is in the development stages and has been shown to successfully reduce the mixing and compaction temperatures by 30°C. The WMA additive, isosorbide distillation bottoms (IDB), is a co-product from the conversion of sorbitol to isosorbide where sorbitol is derived by hydrogenating glucose from corn biomass. A detailed investigation of binder properties at variable IDB dosages showed improvement in low temperature binder grades when tested in the BBR at a 0.5% dosage rate by weight of binder. This research investigates low temperature improvement in two types of binders by comparing IDB-modified binder with binder modified using two commercially available/bio-derived WMA additives from the forest products industry. Multiple stress creep recovery and BBR binder tests indicated that the degree of improvement in binder properties may be

---

<sup>1</sup> Primary Researcher and Author; Graduate Research Assistant, Department of Civil, Construction and Environmental Engineering – CCEE, Iowa State University, 174 Town Engineering Building, Ames, IA 50011, USA.

<sup>2</sup> Contributing Researcher and Author; Postdoctoral Researcher, Department of Civil, Construction and Environmental Engineering – CCEE, Iowa State University, 174 Town Engineering Building, Ames, IA 50011, USA.

<sup>3</sup> Professor, Department of Civil, Construction and Environmental Engineering – CCEE, Iowa State University, 490 Town Engineering Building, Ames, IA 50011, USA.

<sup>4</sup> Associate Professor, Department of Chemical and Biological Engineering – CBE, Iowa State University, 1035 Sweeney, Ames, IA 50011, USA.

binder dependent but improvement was observed for all WMA additives. Low temperature mix performance was evaluated in the semi-circular bending (SCB) test. SCB tests showed additive types were a statistically significant factor in the fracture toughness properties but not for stiffness and fracture energy. IDB was successfully used at reduced mixing and compaction temperatures and does not negatively impact low temperature fracture properties of warm mix asphalt. Improvement of binder properties was observed for all WMA additives studied but the degree of improvement for IDB was found to be binder dependent.

**Keywords:** bio-derived additive; warm mix asphalt; low temperature; bending beam rheometer (BBR); semi-circular bending (SCB) test.

## 6.2. Introduction

Warm mix asphalt (WMA) technologies are best known for reducing binder viscosity, mixing and compaction temperatures. Temperatures are reduced by as much as 20°C-55°C during the production and laydown of asphalt mixtures. By using WMA, production cost savings can be realized due to reduced fuel use and the thus carbon footprint can be lowered. There are many impacts from a reduction in binder viscosity. A reduction allows the use of lower compaction temperatures in the field. This in turn improves mix compactibility. It also enables a contractor to extend the paving season in colder climates, and allows for longer haul distances. Another added benefit is that WMA use can allow for increased use of reclaimed asphalt pavement (RAP) in a mix.

Concerning the health of workers in the field and plant, reducing mixing and compaction temperatures of asphalt mix exposes workers to less fumes (Button et al. 2007; D'Angelo

2008; Gandhi 2008; Hassan 2009; Hurley and Prowell 2006; Jenkins et al. 1999; Kim et al. 2012; Kristjánsdóttir 2006; Kristjánsdóttir et al. 2007; Larsen et al. 2004; Perkins 2009; Prowell et al. 2007).

WMA technologies are categorized into four groups; foaming – water based, foaming – water bearing additive, chemical additive, and organic/bio-derived additives. Isosorbide Distillation Bottoms (IDB) is a recently bio-derived co-product with surfactant properties. IDB is produced during the conversion of sorbitol to isosorbide. Sorbitol is produced by hydrogenating glucose from corn biomass (Werpy et al. 2004). In previous studies IDB has shown great potential in improving the low temperature performance grade (PG) benefits at an optimum dosage rate of 0.5% by weight of the binder. Due to this observation, it is hypothesized that there will be improvement in low temperature performance (reduction in low temperature cracking) of WMA when modified with IDB. However, the aggregate phase makes up 90-95 percent of the total weight of a typical asphalt concrete mixture. To assess this potential benefit for low temperature cracking in asphalt mixtures, a fracture mechanics-based approach is needed for use in this research work.

Among test methods available for measuring fracture at low temperature, the Semi-Circular Bend (SCB) test has received a considerable amount of attention because a notched SCB specimen can be easily prepared from standard laboratory compacted or field cored asphalt concrete samples (Chong and Kuruppu 1984; Krans et al. 1996; Marasteanu et al. 2004). Either mode I or mode II fracture can be studied using this testing method. The mode of fracture depends on the orientation of the initial notch. Within this research work, mode I fracture is examined. This test is used to determine the

fracture energy ( $G_f$ ), fracture toughness ( $K_{IC}$ ), and stiffness ( $S$ ) (Li et al. 2008; Li and Marasteanu 2004; Li and Marasteanu 2010; Lim et al. 1993; Marasteanu 2012; Teshale 2012). Within this study the effects of IDB addition to asphalt mix performance at low temperatures were examined for binders (Montana-PG 64-22, and Polymer Modified Montana-PG 70-22, a Montana-PG 64-22 polymer modified with 1.5% SBS). To determine if IDB was a viable WMA additive in terms of mix performance at low temperatures, three groups were used for comparison: no additive (control group) and two commercially available WMA additives derived from the forest products industry; FP 1 additive, and FP 2 additive.

FP 1 and 2 are water-free chemical/bio-derived additives that display surfactant properties. When asphalt binder is modified with FP 1 or FP 2 and is added to aggregates, a reduction in the aggregate-binder interface friction is produced. This is due to the surfactant properties of both FP 1 and 2. This interface friction reduction between the aggregates and the binder allow for lower mixing and compaction temperatures to be used (Buss et al. 2014; Leng et al. 2013). Recently in the literature it has been recommended that chemical/bio-derived additives from the forest products industry be added at an optimum dosage level of 0.5% by weight of the total binder (Hurley and Prowell 2006). In a recently completed binder study it was found that the optimum dosage level for IDB is 0.5% by weight of the total binder. Thus, 0.5% addition level was used in this research work (Hurley and Prowell 2006). The test used to examine mix performance at low temperatures was the semi-circular bend (SCB) test on aged material, while binder performance at low and high temperatures used the bending beam rheometer

(BBR) test with pressure aging vessel (PAV) aged material, and the multiple stress creep recovery (MSCR) with rolling thin film oven (RTFO) aged material.

### **6.3. Objectives**

The objectives of the research reported addresses both binder and mix performance. The objective for binder performance is to examine how binder modified with 0.5% IDB compares to a control binder, and the control modified with commercially available bio-based/chemical additives in the current market (namely 0.5% FP 1 and 0.5% FP 2). For mix performance there are two primary research questions: Does binder modified with 0.5% IDB improve low temperature performance of WMA as compared to a control binder's performance in WMA at low temperature? How does binder modified with 0.5% IDB compare in terms of WMA performance as compared to commercially available bio-derived/chemical additives in the current market (0.5% FP 1 and 0.5% FP 2) at low temperatures?

### **6.4. Materials & Methods**

#### **6.4.1. Material description**

In this research work one crude source of binder from Montana was used, which is similar to a Canadian crude source. The Montana crude that was used is a PG 64-22 binder. A second binder was used in this study as well – a polymer modified form of the PG 64-22 binder with 1.5% styrene-butadiene-styrene (SBS) to achieve a PG 70-22 binder. A surface mix with a 10 million ESAL design level approved for use from the Iowa Department of Transportation (DOT) was used to construct laboratory dynamic modulus samples. The blended aggregate gradation used for this mix design is shown in

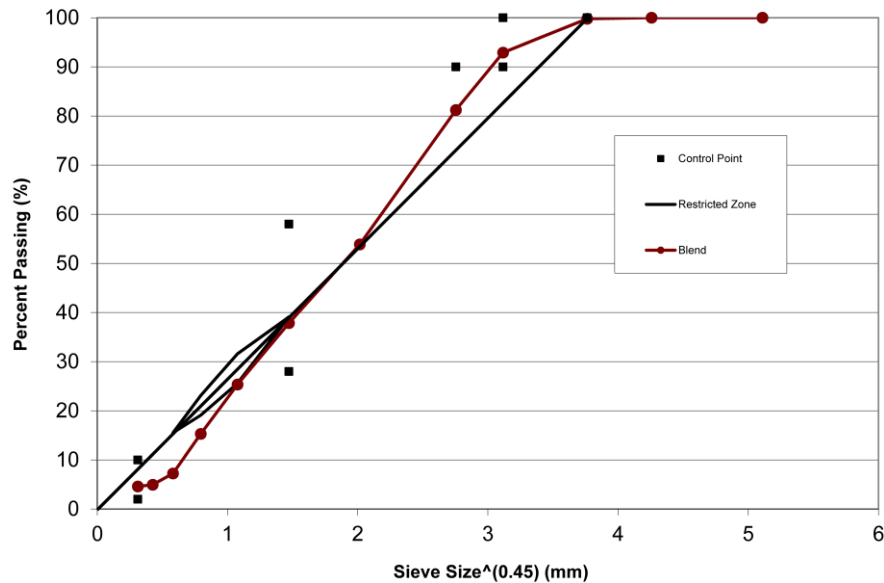


Figure 6.1. Mix Design Gradation Chart (12.5mm NMAS)

Figure 6.1. Each source aggregate's gradation was verified with the job mix formula from the Iowa DOT.

Three additives were used in this research work – IDB, FP 1 and FP 2 – all at addition rates of 0.5% by weight of the binder. For blending the binders with the WMA additives; IDB, FP 1 and FP 2, a Silverson shear mill was used with a blending speed of 3000 rpm at  $140^{\circ}\text{C} \pm 10^{\circ}\text{C}$  for one hour. The SBS polymer was blended with the PG 64-22 binder by the binder supplier to create the polymer modified PG 70-22 binder.

#### 6.4.2. Binder testing methods

High temperature binder testing was done using a dynamic shear rheometer (DSR) on one sample for each of the four groups: no additive, 0.5% IDB, 0.5% FP 1 and 0.5% FP 2 using two binder types, a Montana Crude – PG 64-22 and Polymer Modified Montana Crude – PG 70-22. The DSR using the multiple stress creep recovery (MSCR) method was done on RTFO aged (short-term aged) samples at one temperature ( $64^{\circ}\text{C}$ ,

and 70°C) for the PG 64-22 binder, and the PG 70-22 binder using AASHTO specifications AASHTO MP 19-10 and AASHTO TP 70-13 (AASHTO 2010; AASHTO 2013). Low temperature binder testing was done using a bending beam rheometer (BBR). The BBR enables a researcher to estimate the critical failure low temperature of the binder using AASHTO R 49-09. Testing was conducted at two temperatures, -12°C and -18°C with each group being tested in triplicate (AASHTO 2009).

#### **6.4.3. Mixture testing methods**

The semi-circular bend (SCB) test was performed on four groups of samples: no additive, 0.5% IDB, 0.5% FP 1 and 0.5% FP 2 samples using two binder types, the Montana PG 64-22 binder and the Polymer Modified Montana PG 70-22 binder. The fracture energy, fracture toughness, and stiffness were calculated at three different temperatures for the mix combinations. The test temperatures were -24°C, -12°C, and 0°C. Two bulk specific gravity ( $G_{mb}$ ) samples for each group were mixed at 130°C and compacted at 120°C to a height of 115 mm for a set mass to achieve  $7\% \pm 0.5\%$  air voids according to AASHTO T 312 and air voids were measured according to AASHTO T 166 (AASHTO 2011; AASHTO 2012). Each  $G_{mb}$  sample was cut into 6 SCB samples with approximate dimensions of thickness  $25 \pm 2$ mm, and  $150 \pm 9$ mm in diameter and notch length of  $15 \pm 0.5$  mm with width being no wider than 1.5 mm. If the dimension limits are not met then the specimen was discarded, and if the air voids were not  $7\% \pm 0.5\%$  then that specimen was also discarded. Before testing began, each sample underwent a preconditioning for two hours at their respective test temperature in the environmental

chamber. At least three samples were tested at each temperature for each of the eight groups to take into account failed test samples, human error, and outliers.

## 6.5. Results & Discussion

### 6.5.1. Binder results & discussion

#### 6.5.1.1. Multiple stress creep recovery (MSCR) results

Only 1 sample was tested for each group using the MSCR test. The results are shown in Table 6.1. From the table of results it is shown that all the groups for the PG 64-22 binder are rated for Standard Grade traffic (<10 million ESALs), while the results for the PG 70-22 binder groups indicate they are rated for High Grade traffic (10 to 30 million ESALs). However, two of the additives for the binder PG 70-22 could potentially be rated for Standard Grade traffic as some of the requirements are not achieved as written out in the specification. The first one, PG 70-22 binder modified with 0.5% IDB has a  $J_{nr\text{diff}}$  of 80.5% which is above the maximum allowable value of 75%. The second one, PG 70-22 binder modified with 0.5% FP 2 has a  $J_{nr3.2}$  value of 1.95 which is just under the allowable value of 2 that is stated in the specification. If the  $J_{nr3.2}$  was above 2 then the grade of traffic for FP 2 would be downgraded to Standard Grade from High Grade. Due to the  $J_{nr3.2}$  value being very close to 2, the traffic level could potentially be downgraded to Standard Grade from High Grade.

From Table 6.1 it is not clear how the groups compare in terms of performance in the MSCR test so Figure 6.2 was created to show how the additives and binder type impact percent recovery. Looking at Figure 6.2 it can be discerned that none of the additive groups helps improve percent recovery when they are used to modify the PG 64-



**Table 6.1. MSCR Results**

| Sample Identification | Original PG Grade | Test Temperature (°C) | R <sub>0.1</sub> | R <sub>3.2</sub> | R <sub>diff</sub> | J <sub>nr 0.1</sub> | J <sub>nr 3.2</sub> | J <sub>nr diff</sub> | MSCR Binder Grade |
|-----------------------|-------------------|-----------------------|------------------|------------------|-------------------|---------------------|---------------------|----------------------|-------------------|
| None                  | 64-22             | 64                    | 7.05             | 1.70             | 75.9              | 2.31                | 2.60                | 12.6                 | S                 |
| IDB                   | 64-22             | 64                    | 7.23             | 1.44             | 80.0              | 2.49                | 2.86                | 15.1                 | S                 |
| FP 1                  | 64-22             | 64                    | 5.36             | 2.00             | 62.6              | 2.12                | 2.35                | 10.9                 | S                 |
| FP 2                  | 64-22             | 64                    | 5.81             | 1.47             | 74.7              | 2.57                | 2.88                | 11.9                 | S                 |
| Sample Identification | Original PG Grade | Test Temperature (°C) | R <sub>0.1</sub> | R <sub>3.2</sub> | R <sub>diff</sub> | J <sub>nr 0.1</sub> | J <sub>nr 3.2</sub> | J <sub>nr diff</sub> | MSCR Binder Grade |
| None                  | 70-22             | 70                    | 65.36            | 44.65            | 31.7              | 0.88                | 1.53                | 74.8                 | H                 |
| IDB                   | 70-22             | 70                    | 69.53            | 49.30            | 29.1              | 0.76                | 1.37                | 80.5                 | H*                |
| FP 1                  | 70-22             | 70                    | 55.79            | 37.27            | 33.2              | 0.95                | 1.48                | 56.5                 | H                 |
| FP 2                  | 70-22             | 70                    | 48.36            | 29.08            | 39.9              | 1.32                | 1.95                | 47.5                 | H*                |

\* Note that only 1 sample has been run in the MSCR test so values are just estimates.

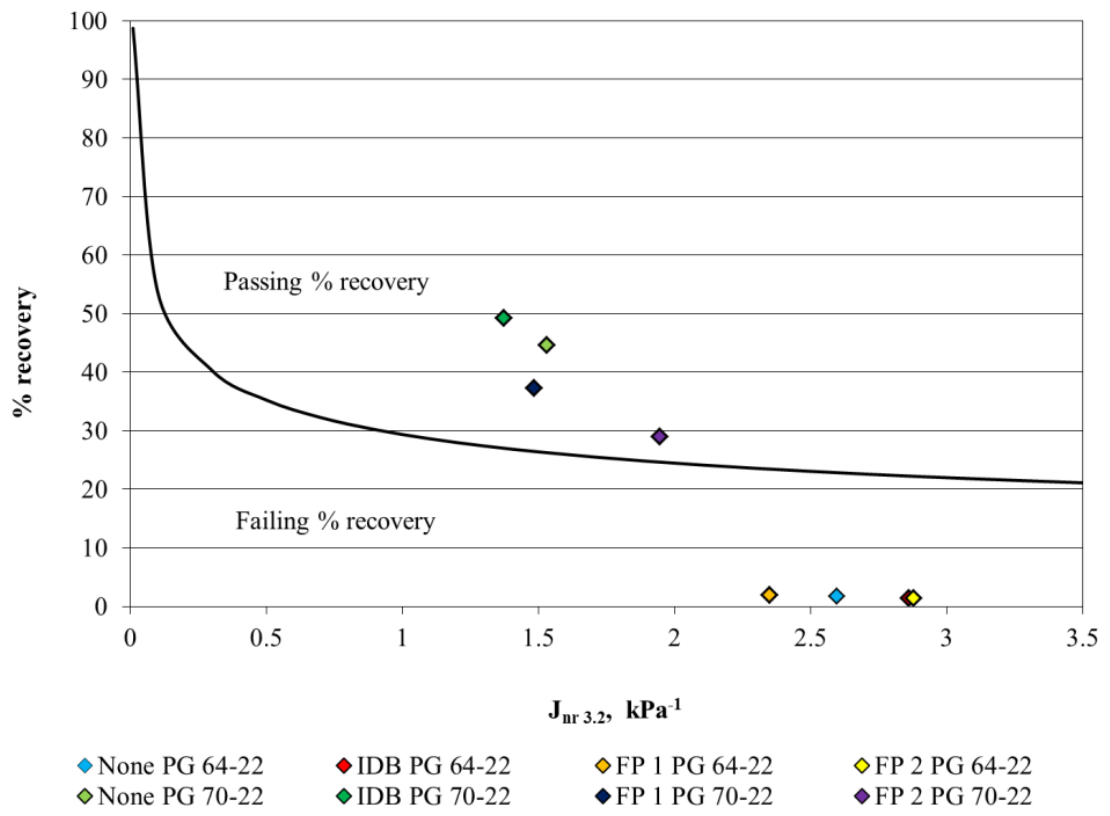


**Figure 6.2. Recovery vs. J<sub>nr 3.2</sub> for MSCR Results**

22 binder. However, the maximum allowable value of J<sub>nr 3.2</sub> for Standard Grade traffic is 4. Using this value it can be discerned that FP 1 shows the best performance as compared to the control group (None), while IDB and FP 2 show lower performance as compared to

the control group (None). For the PG 70-22 binder it can be observed that none of the additive groups fail in % recovery. As compared to the control group (None), IDB shows the largest improvement in recovery while FP 1 shows the second biggest improvement in recovery. FP 2 has lower % recovery than the control group (None). From these results it can be concluded that there is an interaction between the polymer SBS and the additive IDB as IDB showed the least performance when added to the PG 64-22 binder, but showed the best performance when added to the PG 70-22 binder.

#### 6.5.1.2. Bending beam rheometer (BBR) results

Tables 6.2 and 6.3 display the results of the bending beam rheometer testing for -12°C and -18°C taken at 60 seconds of loading. The Superpave criteria requires a creep stiffness,  $S(t)$ , value of less than or equal to 300 MPa at 60 seconds. The m-value, rate of change in the creep stiffness, is required to be greater than or equal to 0.300 at 60 seconds. Test temperatures are performed at 10°C above the critical temperature using the concept of time-temperature superposition. The Superpave criteria was both extrapolated and interpolated from the data between the temperatures of -12°C and -18°C using a linear relationship and 10°C was subtracted from the actual test temperature to find the critical temperature. In Tables 6.2 and 6.3, trends can be observed by noting how test parameters change with increasing dosage rates from 0 to 0.5% for each of the three bio-derived/chemical additives.

From Tables 6.2 and 6.3, all three bio-derived/chemical additives at dosage rates of 0.50% maintained the low temperature performance grade for long-term aged PG 64-22 binder and long-term aged PG 70-22 binder. All the additives improved performance

Table 6.2. Average BBR Results for PG 64-22

| PG 64-22                  | Temp (°C) | Parameter | Percent IDB (%)  |               | Trends |
|---------------------------|-----------|-----------|------------------|---------------|--------|
|                           |           |           | 0                | 0.5           |        |
|                           | -12       | S(t)      | 144.7            | 125.5         |        |
| m-value                   |           | 0.332     | 0.346            |               |        |
| -18                       | S(t)      | 246.7     | 226.7            |               |        |
|                           | m-value   | 0.272     | 0.290            |               |        |
| Critical Temperature (°C) |           |           | <b>-25.20</b>    | <b>-26.90</b> |        |
| PG 64-22                  | Temp (°C) | Parameter | Percent FP 1 (%) |               | Trends |
|                           |           |           | 0                | 0.5           |        |
|                           | -12       | S(t)      | 144.7            | 154.7         |        |
| m-value                   |           | 0.332     | 0.337            |               |        |
| -18                       | S(t)      | 246.7     | 312.7            |               |        |
|                           | m-value   | 0.272     | 0.288            |               |        |
| Critical Temperature (°C) |           |           | <b>-25.20</b>    | <b>-26.50</b> |        |
| PG 64-22                  | Temp (°C) | Parameter | Percent FP 2 (%) |               | Trends |
|                           |           |           | 0                | 0.5           |        |
|                           | -12       | S(t)      | 144.7            | 149.0         |        |
| m-value                   |           | 0.332     | 0.340            |               |        |
| -18                       | S(t)      | 246.7     | 271.7            |               |        |
|                           | m-value   | 0.272     | 0.288            |               |        |
| Critical Temperature (°C) |           |           | <b>-25.20</b>    | <b>-26.58</b> |        |

Table 6.3. Average BBR Results for PG 70-22

| PG 70-22                  | Temp (°C) | m-value | Percent IDB (%)  |               | Trends |
|---------------------------|-----------|---------|------------------|---------------|--------|
|                           |           |         | 0                | 0.5           |        |
|                           | -12       | S(t)    | 117.0            | 129.3         |        |
| m-value                   |           | 0.341   | 0.344            |               |        |
| -18                       | S(t)      | 236.0   | 228.3            |               |        |
|                           | m-value   | 0.267   | 0.280            |               |        |
| Critical Temperature (°C) |           |         | <b>-25.31</b>    | <b>-26.12</b> |        |
| PG 70-22                  | Temp (°C) | m-value | Percent FP 1 (%) |               | Trends |
|                           |           |         | 0                | 0.5           |        |
|                           | -12       | S(t)    | 117              | 118.3         |        |
| m-value                   |           | 0.341   | 0.369            |               |        |
| -18                       | S(t)      | 236.0   | 232.7            |               |        |
|                           | m-value   | 0.267   | 0.314            |               |        |
| Critical Temperature (°C) |           |         | <b>-25.31</b>    | <b>-29.52</b> |        |
| PG 70-22                  | Temp (°C) | m-value | Percent FP 2 (%) |               | Trends |
|                           |           |         | 0                | 0.5           |        |
|                           | -12       | S(t)    | 117              | 124.3         |        |
| m-value                   |           | 0.341   | 0.346            |               |        |
| -18                       | S(t)      | 236.0   | 257.3            |               |        |
|                           | m-value   | 0.267   | 0.297            |               |        |
| Critical Temperature (°C) |           |         | <b>-25.31</b>    | <b>-27.63</b> |        |

as compared to the performance of the original binders (control groups, PG 64-22 binder, and PG 70-22 binder) in terms of critical failure low temperature. For the PG 64-22 binder, IDB improved the critical failure low temperature the most as compared to the performance shown by FP 1 and FP 2 against the performance of the control group. For the PG 70-22 binder, the best improvement in critical failure low temperature was shown by the additive FP 1 with FP 2 second, and IDB third. The improvement shown by FP 1 was so large that the low temperature grade changed from  $-22^{\circ}\text{C}$  to  $-28^{\circ}\text{C}$  as the critical failure low temperature decreased by  $4.21^{\circ}\text{C}$  from  $-25.31^{\circ}\text{C}$  to  $-29.52^{\circ}\text{C}$ . FP 2 was close to shifting the low temperature binder grade, but did not improve the critical failure low temperature enough to effect the change from  $-22^{\circ}\text{C}$  to  $-28^{\circ}\text{C}$ .

## 6.5.2. Mix test results & discussion

### 6.5.2.1. Low temperature semi-circular bend (SCB) test results

The average fracture energy, fracture toughness, and stiffness values with their corresponding error bars (1 standard deviation in each direction) for the test temperatures  $0^{\circ}\text{C}$ ,  $-12^{\circ}\text{C}$ , and  $-24^{\circ}\text{C}$  are shown in Figures 6.3 through 6.5. Due to the large number of groups and test temperatures it is hard to tell if there are significant differences between test temperatures  $-12^{\circ}\text{C}$  and  $-24^{\circ}\text{C}$  results within each additive/binder type group and between other groups at the same temperature. Therefore, statistical analysis was done according to a 95% confidence level to examine if there were statistically significant differences between the four additive groups for each binder type within each test temperature.

The trends shown in Figure 6.3 for the fracture energy results are that as temperature increases, the fracture energy increases. The error bars are based on 1

standard deviation in each direction and illustrate the variability with changing temperature, binder type, and additive choice. For fracture toughness in Figure 6.4, when temperature increases from -24°C to -12°C the fracture toughness increases. The results are intuitive because the fracture energy increases with increasing temperature which

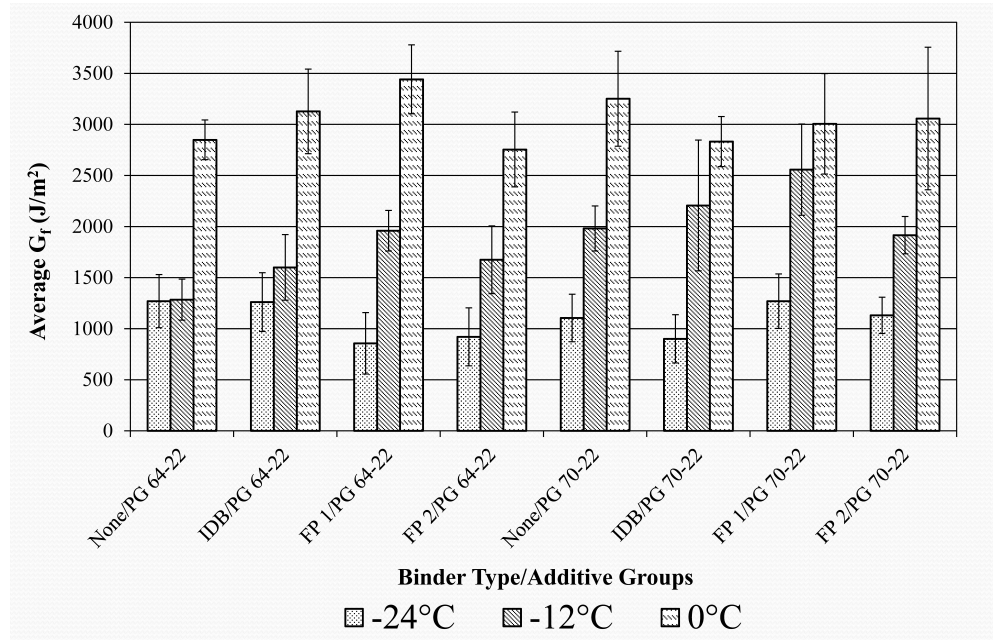


Figure 6.3. Fracture Energy Results

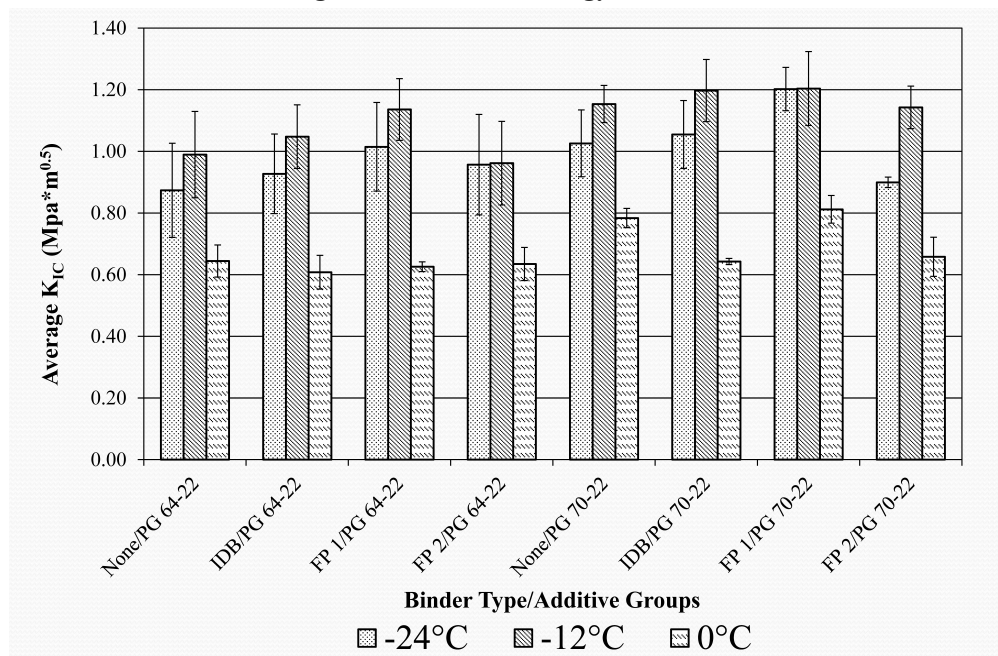


Figure 6.4. Fracture Energy Results

would lead to higher fracture toughness results at higher temperatures. However, the difference between  $-12^{\circ}\text{C}$  and  $0^{\circ}\text{C}$  is that as temperature increases the fracture toughness decreases. This does not follow the trend that as fracture energy increases so should fracture toughness. This could be happening due to the WMA transitioning from a more elastic state to a more viscoelastic state between  $-12^{\circ}\text{C}$  and  $0^{\circ}\text{C}$ . Between these two temperatures the samples are becoming softer and therefore cannot hold as high of a load, which would lead to lower fracture toughness.

In Figure 6.5, the stiffness results are that as temperature increases, the stiffness decreases. However, the PG 70-22 binder when modified with 0.5% FP 2 does not show this trend between  $-24^{\circ}\text{C}$  and  $-12^{\circ}\text{C}$ . This is most likely due to an experimental error as the trends in Figures 6.3 and 6.4 for PG 70-22 binder when modified with 0.5% FP 2 appear to be normal between  $-24^{\circ}\text{C}$  and  $-12^{\circ}\text{C}$ . The error bars based on 1 standard deviation in each direction are fairly variable with changing temperature, binder type, and

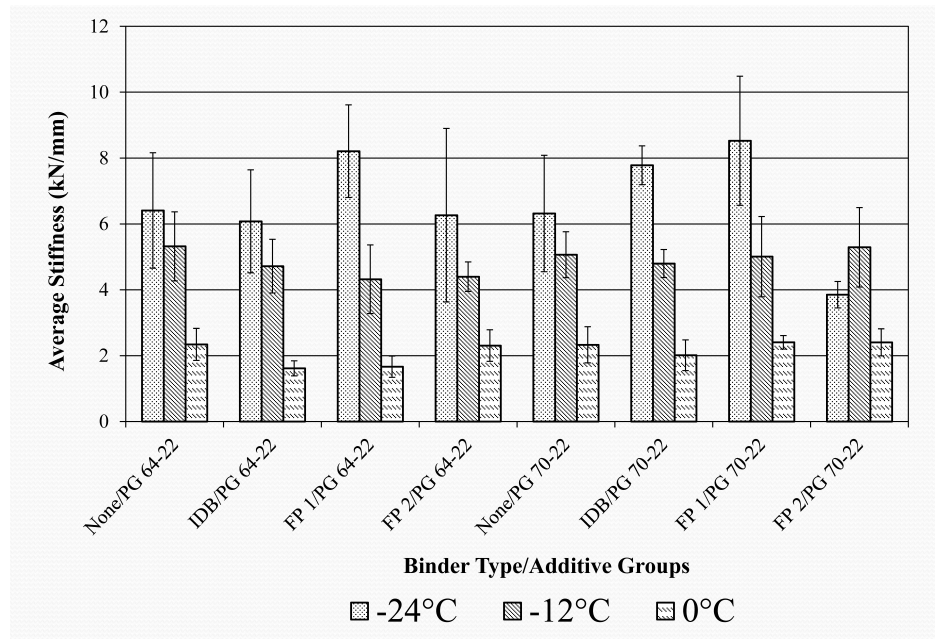


Figure 6.5. Stiffness Results

additive choice. This makes it hard to discern whether there is really a difference between the stiffness results of  $-24^{\circ}\text{C}$  and  $-12^{\circ}\text{C}$  for PG 70-22 binder when modified with 0.5% FP 2.

#### 6.5.2.2. Statistical analysis of SCB test results

An analysis of variance (ANOVA) was conducted to examine which variability factors are significant in affecting the fracture energy, fracture toughness, and stiffness values. A randomized complete block design was used to conduct the ANOVA. The block factors examined are Additive - A, and Binder Type - B, while at least three samples for each group were randomly assigned to one of the three temperatures; Temperature ( $^{\circ}\text{C}$ ) – C. All the interactions between Additive - A, Binder Type - B, and Temperature ( $^{\circ}\text{C}$ ) - C, are also studied. A statistical program called JMP was used to evaluate the results. The results are shown in Tables 6.4 through 6.6. For this statistical analysis air voids was not used as a factor because the air voids of the SCB samples used in testing were  $7\% \pm 0.5\%$  and the samples from each group were randomly assigned a temperature to test that sample at.

In Table 6.4, it is evident that Temp ( $^{\circ}\text{C}$ ) – C is a statistically significant source of variability by itself, but not when crossed with other variables for the fracture energy results. To be a statistical significant source of variability, the p-value must be less than or equal to 0.05. All the interactions are not statistically significant sources of variability as shown in Table 6.4 for fracture energy. It is important to point out that Additive (A) is not a statistically significant source of variability, while Binder Type (B) is a statistically significant source of variability. This means that the additives were not found to be

statistically significantly different from one another overall according to a 95% confidence level.

The fracture toughness in Table 6.5 shows Additive – A, Binder Type – B, and Temp (°C) – C are statistically significant sources of variability when by themselves, but not the interaction between variables. Additive (A) and Binder Type (B) are statistically significant source of variability separately, but when crossed (Binder Type\*Additive), their interaction is not statistically significant. This means that there were statistical differences identified for the additives and the binders but the interaction of additives and binders do not influence the fracture toughness results.

In Table 6.6, it is evident that Temp (°C) – C is the only factor that is a statistically significant source of variability, while Additive – A and Binder Type – B are

**Table 6.4. ANOVA Results for Fracture Energy**

| Source                         | SS       | MS Number | DF Number | F Ratio | Prob > F      |
|--------------------------------|----------|-----------|-----------|---------|---------------|
| Additive - A                   | 1.52E+06 | 5.06E+05  | 3         | 2.63    | <b>0.0602</b> |
| Binder Type - B                | 9.87E+05 | 9.87E+05  | 1         | 5.13    | 0.0278*       |
| Binder Type*Additive           | 4.16E+05 | 1.39E+05  | 3         | 0.72    | <b>0.5445</b> |
| Temp (°C) - C                  | 5.05E+07 | 2.53E+07  | 2         | 131.20  | <.0001*       |
| Temp (°C)*Additive             | 1.19E+06 | 1.99E+05  | 6         | 1.03    | <b>0.4151</b> |
| Temp (°C)*Binder Type          | 9.10E+05 | 4.55E+05  | 2         | 2.36    | <b>0.1043</b> |
| Temp (°C)*Binder Type*Additive | 8.10E+05 | 1.35E+05  | 6         | 0.70    | <b>0.6497</b> |

**Table 6.5. ANOVA Results for Fracture Toughness**

| Source                         | SS       | MS Number | DF Number | F Ratio | Prob > F      |
|--------------------------------|----------|-----------|-----------|---------|---------------|
| Additive - A                   | 1.41E-01 | 4.70E-02  | 3         | 4.92    | 0.0045*       |
| Binder Type - B                | 2.27E-01 | 2.27E-01  | 1         | 23.71   | <.0001*       |
| Binder Type*Additive           | 2.90E-02 | 9.67E-03  | 3         | 1.01    | <b>0.3954</b> |
| Temp (°C) - C                  | 2.52E+00 | 1.26E+00  | 2         | 131.61  | <.0001*       |
| Temp (°C)*Additive             | 6.71E-02 | 1.12E-02  | 6         | 1.17    | <b>0.3376</b> |
| Temp (°C)*Binder Type          | 9.22E-03 | 4.61E-03  | 2         | 0.48    | <b>0.6202</b> |
| Temp (°C)*Binder Type*Additive | 6.10E-02 | 1.02E-02  | 6         | 1.06    | <b>0.3973</b> |



**Table 6.6. ANOVA Results for Stiffness**

| Source                         | SS       | MS Number | DF Number | F Ratio | Prob > F      |
|--------------------------------|----------|-----------|-----------|---------|---------------|
| Additive - A                   | 7.51E+00 | 2.50E+00  | 3         | 2.06    | <b>0.1165</b> |
| Binder Type - B                | 4.32E-01 | 4.32E-01  | 1         | 0.36    | <b>0.5535</b> |
| Binder Type*Additive           | 4.21E+00 | 1.40E+00  | 3         | 1.16    | <b>0.3349</b> |
| Temp (°C) - C                  | 2.61E+02 | 1.30E+02  | 2         | 107.39  | <.0001*       |
| Temp (°C)*Additive             | 2.96E+01 | 4.93E+00  | 6         | 4.07    | 0.0021*       |
| Temp (°C)*Binder Type          | 7.35E-01 | 3.68E-01  | 2         | 0.30    | <b>0.7398</b> |
| Temp (°C)*Binder Type*Additive | 1.10E+01 | 1.84E+00  | 6         | 1.51    | <b>0.1927</b> |

not according to the stiffness results. The interactions are not statistically significant sources of variability except the temperature/additive interaction which indicates that the different test temperatures may influence the additive's impact on low temperature stiffness as shown in Table 6.6. The additives, and binder types were not found to be statistically significantly different from one another overall according to a 95% confidence level.

From Tables 6.4 through 6.6 it can be discerned that the best parameter for statistical analysis is fracture toughness, with fracture energy and stiffness following. The fracture toughness is a function of the sample's peak strength and results show that the variables Additive – A, Binder Type – B, and Temp (°C) – C are statistically significant sources of variability by themselves. However, this matter needs to be examined more closely especially when looking at the differences between the additives. To do this, least square means plots and student's t test tables are shown in Figure 6.6 for fracture energy, fracture toughness, and stiffness according to additive choice.

For fracture energy, even though Additive (A) is shown to not be a statistically significant source of variability, in Figure 6.6 it is shown that some of the additives are statistically significantly different from one another according to a 95% confidence

interval. FP 1 is shown to be statistically different from FP 2 and None (the control group), while IDB is not statistically different from all the additives including None (the control group) for fracture energy. For fracture toughness, Additive (A) is shown to be a statistically significant source of variability. In Figure 6.6, the second of the least square means plots and student's t tests shows FP 1 is shown to be statistically different from FP 2, IDB, and None (the control group). IDB, FP 2 and None (the control group) were not statistically significantly different from each other for fracture toughness. For fracture

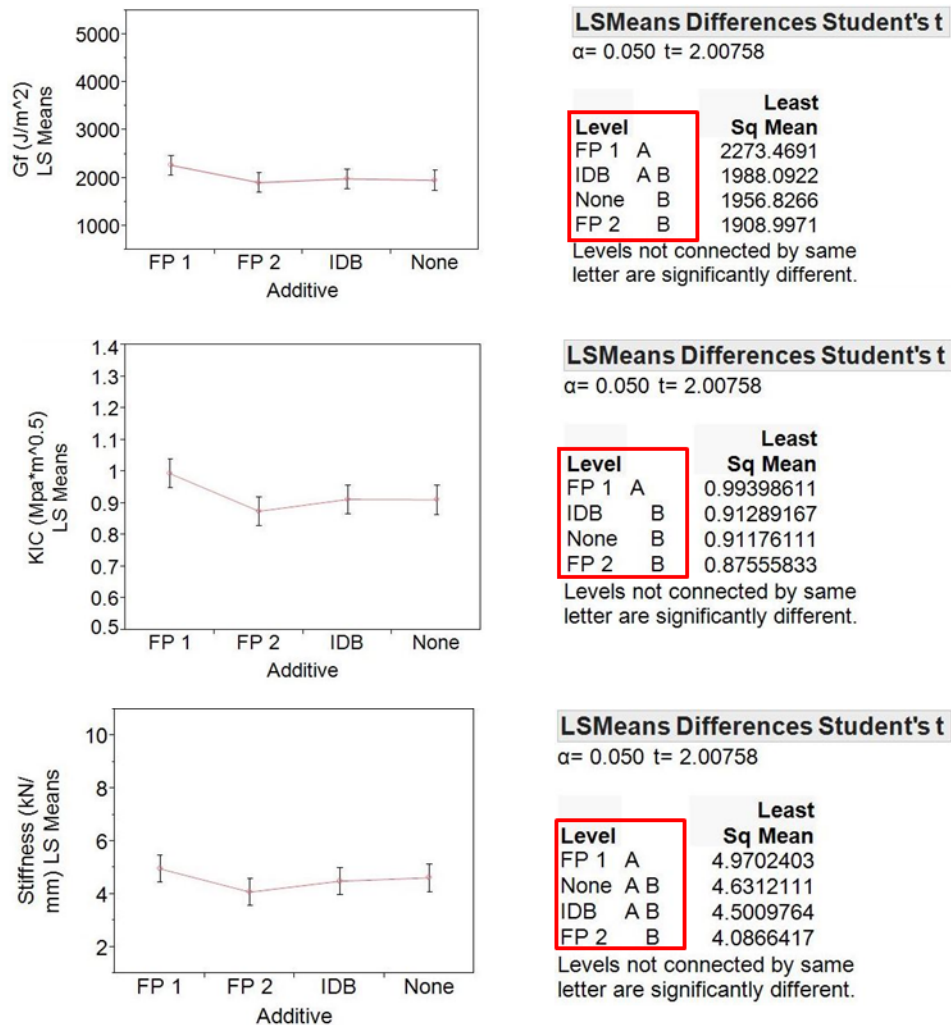


Figure 6.6. Least Square Means Plots and Student's t test for Additive Choice, 1<sup>st</sup> Fracture Energy, 2<sup>nd</sup> Fracture Toughness, and 3<sup>rd</sup> Stiffness from Top to Bottom

toughness, Additive (A) is not a statistically significant source of variability. In Figure 6.6, from all the least square means plots and student's t tests it is shown that FP 1 and FP 2 additives are statistically different from one another according to a 95% confidence interval. The other additives, FP 1, IDB and None (the control group), were not statistically different from each other for stiffness, while FP 2, IDB and None (the control group) were also not found to be statistically different from each other.

## 6.6. Conclusions

Warm mix asphalt performance during the semi-circular bend (SCB) test has shown that Isosorbide Distillation Bottoms (IDB) can be used as a WMA additive and is highly comparable to control hot mix asphalt (HMA) and WMA with FP 1 and FP 2 in terms of performance. From the results obtained, all the additives for the binder PG 64-22 are estimated to meet the Standard Grade of traffic, while all the additives for the binder PG 70-22 are estimated to meet the High Grade of traffic. Comparisons of RTFO aged DSR binder MSCR results within each binder type were made. From the comparisons made it is observed that there could be a possible interaction between polymer modification of the binder and IDB addition. For the PG 64-22 binder it was observed that IDB had the second highest  $J_{nr3.2}$  value and the lowest % recovery value, while the PG 70-22 binder modified with IDB had the highest % recovery value and lowest  $J_{nr3.2}$  value. From these results it can be concluded that there is an estimated interaction between the polymer SBS and the additive IDB as IDB showed the least performance when added to the PG 64-22 binder, but showed the best performance when added to the

PG 70-22 binder. The IDB is helping improve the bond between the polymer SBS and the PG 64-22 binder.

The BBR results on average show that all additives regardless of binder type (PG 64-22, or PG 70-22) show improvement in the critical failure low temperature as compared to each of the binder control groups. However, improvement is not significant enough to change the binder grade for most additives, except for the PG 70-22 binder modified with 0.5% FP 1. FP 1 improves the low temperature binder grade from  $-22^{\circ}\text{C}$  to  $-28^{\circ}\text{C}$  for the PG 70-22 binder. Overall the BBR results indicate that all the additives may be useful in low temperature climates where pavements are susceptible to thermal cracking.

From an overall statistical analysis the additives are shown to be statistically significantly different from one another for fracture toughness, but not for stiffness and fracture energy results. However, the low p-value for additive suggests a possible difference between additives for fracture energy. FP 1 is statistically significantly different from the control and FP 2 groups in terms of fracture energy, while IDB is not statistically significantly different from FP 1, FP 2, and the control group in terms of fracture energy. For fracture toughness, FP 1 is significantly different from the other additive choices, while the rest were not found to be statistically different from one another. FP 1 is statistically significantly different from FP 2 for stiffness. The statistical analysis shows there is little impact on the low temperature properties from addition of IDB as compared to the control group. IDB does not negatively impact low temperature properties of the warm mix asphalt when it comes to fracture performance.

Limitations of this paper were that the testing plan for this paper only included DSR RTFO aged binder MSCR testing for one sample from each of the eight groups, and that no statistical analysis was done using the BBR results with a 95% confidence interval. Due to only one sample being used for the MSCR test, it is impossible to statistically say with certainty that there is an interaction between the polymer SBS and the bio-derived additive IDB. In the future, it is recommended that each group be tested in triplicate for the MSCR test.

### **6.7. Future Research**

Future research will be done using several bio-derived materials that demonstrate performance equal to or better than the additives used in this research work. This future research will involve a full binder investigation to determine the optimum dosage rate of each additive and achieve the best asphalt binder performance at low, intermediate, and high temperatures. The second phase of this research will utilize mixture performance tests such as dynamic modulus, Hamburg wheel tracking device, semi-circular bend and disk compact tension testing.

### **6.8. Acknowledgements**

The authors would like to thank Bill Haman from the Iowa Energy Center (IEC) for funding this research work.

### **6.9. References**

AASHTO (2009) Determination of Low-Temperature Performance Grade (PG) of Asphalt Binders  
American Association of State Highway and Transportation Officials, Washington, DC

- AASHTO (2010) Performance-Graded Asphalt Binder Using Multiple Stress Creep Recovery (MSCR) Test. American Association of State Highway and Transportation Officials, Washington, DC
- AASHTO (2011) Bulk Specific Gravity of Compacted Hot Mix Asphalt (HMA) Using Saturated Surface-Dry Specimens American Association of State Highway and Transportation Officials, Washington, DC
- AASHTO (2012) Preparing and Determining the Density of Hot Mix Asphalt (HMA) Specimens by Means of the Superpave Gyrotory Compactor American Association of State Highway and Transportation Officials, Washington, DC
- AASHTO (2013) Multiple Stress Creep Recovery (MSCR) Test of Asphalt Binder Using a Dynamic Shear Rheometer (DSR). American Association of State Highway and Transportation Officials, Washington, DC
- Buss A, Kuang Y, Williams RC, Bausano J, Cascione A, Schram SA Influence of Warm Mix Asphalt Additive and Dosage Rate on Construction and Performance of Bituminous Pavements. In: Transportation Research Board 93rd Annual Meeting, 2014.
- Button JW, Estakhri C, Wimsatt A (2007) A synthesis of warm mix asphalt. Texas Transportation Institute, College Station, TX.
- Chong KP, Kuruppu MD (1984) New specimen for fracture toughness determination for rock and other materials Int J Fract 26:R59-R62 doi:10.1007/bf01157555
- D'Angelo J, et al. (2008) Warm-mix asphalt: European practice. FHWA, U.S. Dept. of Transportation, Washington, DC.,
- Gandhi T (2008) Effects of warm asphalt additives on asphalt binder and mixture properties. Ph.D. dissertation, Clemson Univ., Clemson, SC.
- Hassan M (2009) Life-cycle assessment of warm-mix asphalt: An environmental and economic perspective. In: Transportation Research Board 88th Annual Meeting, 2009. Washington, DC.,
- Hurley GC, Prowell BD (2006) Evaluation of Evotherm for use in warm mix asphalt vol 6. National Center for Asphalt Technology, Auburn, AL.
- Jenkins K, De Groot J, van de Ven M, Molenaar A (1999) Half-warm foamed bitumen treatment, a new process. In: 7th Conference on asphalt pavements for Southern Africa (CAPSA 99), 1999.
- Kim H, Lee S, Amirghanian S (2012) Influence of Warm Mix Additives on PMA Mixture Properties Journal of Transportation Engineering 138:991-997 doi:10.1061/(ASCE)TE.1943-5436.0000406
- Krans R, Tolman F, Van de Ven M Semi-circular bending test: a practical crack growth test using asphalt concrete cores. In: RILEM Proceedings, 1996. Chapman & Hall, pp 123-132
- Kristjánssdóttir Ó (2006) Warm-mix asphalt for cold weather paving. Univ. of Washington
- Kristjánssdóttir Ó, Muench ST, Michael L, Burke G (2007) Assessing potential for warm-mix asphalt technology adoption Transp Res Rec 2040:91-99
- Larsen O, Moen Ø, Robertus C, Koenders B (2004) WAM Foam asphalt production at lower operating temperatures as an environmental friendly alternative to HMA. In: 3rd Eurasphalt & Eurobitume Congress, 2004. Foundation Eurasphalt, Breukelen, Netherlands.,

- Leng Z, Gamez A, Al-Qadi I (2013) Mechanical Property Characterization of Warm-Mix Asphalt Prepared with Chemical Additives Journal of Materials in Civil Engineering 0:null  
doi:10.1061/(ASCE)MT.1943-5533.0000810
- Li X, Braham AF, Marasteanu MO, Buttlar WG, Williams RC (2008) Effect of Factors Affecting Fracture Energy of Asphalt Concrete at Low Temperature Road Materials and Pavement Design 9:397-416  
doi:10.1080/14680629.2008.9690176
- Li X, Marasteanu M (2004) Evaluation of the low temperature fracture resistance of asphalt mixtures using the semi circular bend test (with discussion) Journal of the Association of Asphalt Paving Technologists 73
- Li XJ, Marasteanu MO (2010) Using Semi Circular Bending Test to Evaluate Low Temperature Fracture Resistance for Asphalt Concrete Exp Mech 50:867-876 doi:10.1007/s11340-009-9303-0
- Lim I, Johnston I, Choi S (1993) Stress intensity factors for semi-circular specimens under three-point bending Engineering Fracture Mechanics 44:363-382
- Marasteanu M, Buttlar, W., Bahia, B., and R. Christopher Williams. (2012) National Pooled Fund Study – Phase II: Final Report - Investigations of Low Temperature Cracking in Asphalt Pavements. MN/RC 2012-23,
- Marasteanu MO, Li X, Labuz JF, Petit C, Al-Qadi I, Millien A Low temperature fracture test for asphalt mixtures. In: Fifth International RILEM Conference on Reflective Cracking in Pavements, 2004. RILEM Publications SARL, pp 249-256
- Perkins SW (2009) Synthesis of warm mix asphalt paving strategies for use in Montana highway construction. Western Transportation Institute, Helena, MT.
- Prowell BD, Hurley GC, Crews E (2007) Field performance of warm-mix asphalt at the NCAT test track. In: Transportation Research Board 86th Annual Meeting, 2007. Washington, DC.,
- Teshale EZ (2012) Low-Temperature Fracture Behavior of Asphalt Concrete in Semi-Circular Bend Test. University of Minnesota
- Werpy TA, Holladay JE, White JF (2004) Top Value Added Chemicals From Biomass: I. Results of Screening for Potential Candidates from Sugars and Synthesis Gas.

## **CHAPTER 7. CORRELATION BETWEEN LOW TEMPERATURE WARM MIX ASPHALT BINDER AND MIX TEST RESULTS – AN INVESTIGATIVE ANALYSIS**

Modified from a paper submitted to *The 8<sup>th</sup> International RILEM SIB Symposium*

Joseph H. Podolsky<sup>1</sup>, Mohamed Rashwan<sup>2</sup>, and R. Christopher Williams<sup>3</sup>

### **7.1. Abstract**

The main distress observed in asphalt pavements located in cold regions is low temperature cracking. Currently low temperature characterization for binders is possible, but there is no standard way of taking into account the response from the aggregate phase of the mixtures. To address this, the semi-circular bend (SCB) test will be used with warm mix asphalt to look at the fracture property stiffness. This property will be used to make correlations with stiffness values obtained from testing warm mix asphalt binder tested in a bending beam rheometer (BBR). Within this investigative analysis, results were examined using two binders – a Performance Grade (PG) 64-22 binder and the same binder polymer modified with 3% Styrene-Butadiene-Styrene (SBS) to attain a PG 70-22 binder. Two additives were used to produce warm mix asphalt mixtures and binders for binders from two different sources. A statistical analysis was done at  $-12^{\circ}\text{C}$  for both the BBR and SCB results to verify whether there were any statistical differences between the

---

<sup>1</sup> Primary Researcher; Primary and Corresponding Author; Doctoral Candidate, Iowa State University, Department of Civil, Construction, and Environmental Engineering, 174 Town Engineering Building, Ames, IA 50011, USA.

<sup>2</sup> Contributing Researcher and Author; Adjunct Assistant Professor, American University in Cairo, Department of Construction and Architectural Engineering, AUC Avenue, P.O. Box 74, New Cairo, 11835 Egypt.

<sup>3</sup> Professor, Iowa State University, Department of Civil, Construction, and Environmental Engineering, 482 Town Engineering Building, Ames, IA 50011, USA.



binder types (unmodified to polymer modified) and additives (control, Fisher-Tropsch (FT), and Forest Product (FP)). Air voids were also examined for the SCB results. It was found that air voids, and binder type crossed with air voids were statistically significant variables for the SCB results. Due to the lack of statistical significance among the other factors it was possible to create a correlation between the SCB stiffness results and BBR results by air void content and air void content statistically crossed with the binder type.

**Keywords** Low temperature, Warm mix asphalt, Stiffness.

## 7.2. Introduction

Low temperature cracking along with rutting and fatigue cracking has been regarded as one of the major modes of asphalt cement concrete distresses. It is frequently encountered in cold climate regions (Li and Marasteanu 2010). Under very low temperatures, the top asphalt layer contracts, but is constrained due to friction occurring between the interface area of the underlying layer (Teshale 2012). This generates thermal induced tensile stresses in the pavement which increase gradually as the temperature decreases until the asphalt concrete pavement cracks under tension. Currently, specifications mainly rely on the bending beam rheometer (BBR) test for characterizing and selecting asphalt binders that possess good low temperature cracking properties and do not take into account the behavior of the aggregate phase (Teshale 2012). Most design approaches that assess the fracture behavior of asphalt concrete rely on empirical relationships using conventional engineering parameters such as modulus and tensile strength (Wagnoner et al. 2005).

With the aggregate phase constituting approximately 90-95 percent of the total weight of a typical asphalt concrete mixture, predictions reliant on empirical formulations, using tests such as the indirect tension (IDT) test, are not satisfactory for accurately characterizing the low temperature cracking behavior of the asphalt concrete (Li and Marasteanu 2010). To address the impact of the aggregate phase on low temperature cracking in asphalt mixtures and to gain better understanding of the mechanisms that initiate and propagate cracks, fracture mechanics-based approaches are regarded essential in developing fracture tests that can improve performance-based pavement design methodologies (Wagnoner et al. 2005). Fracture mechanics techniques have been applied in analyzing asphalt concrete since the 1970s and several fracture tests were used to assess asphalt concrete such as the single-edge notched beam SE(B) test, the disk-shaped compact tension (DCT) test, the notched direct tension test and the semi-circular bend (SCB) test (Wagnoner et al. 2005).

The SCB test has been employed by other researchers lately in the asphalt industry in studying low-temperature cracking behavior due to the ease of sample preparation from the gyratory compacted cylinders or field cored samples (Chong and Kuruppu 1984; Krans et al. 1996; Li and Marasteanu 2010; Marasteanu et al. 2004). This test method is simplistic in both preparation of samples and testing and can be used to study both mode I and II fracture based on the orientation of the initial notch; this paper examines mode I fracture. The SCB test is used to determine fracture energy ( $G_f$ ), fracture toughness ( $K_{IC}$ ), and stiffness ( $S$ ) (Li and Marasteanu 2010; Teshale 2012). Li and Marasteanu studied the impact of different combinations of factors such as binder type and binder modifiers, aggregate type, air voids, loading rate and initial notch length

on the fracture resistant of asphalt concrete. It was found that fracture resistance is affected significantly by aggregate type and the air voids content. Moreover, it was reported that the binder grade and modifier type have significant impact on the cracking resistance while the effect of the loading rate and the initial notch length was more evident at higher test temperatures (Li and Marasteanu 2010).

Aurangzeb et al. studied the effect of incorporating reclaimed asphalt pavement on the susceptibility of eight asphalt mixtures to low-temperature cracking (Aurangzeb et al. 2012). The SCB test results showed that the thermal cracking potential of asphalt concrete increased because of the addition of the RAP due to increased mixture stiffness. The authors suggested double-bumping, or increasing the high temperature grade by 6°C and decreasing the low temperature grade by 6°C (Aurangzeb et al. 2012). Teshale et al. investigated the feasibility of determining the creep compliance of asphalt concrete from SCB test so that both viscoelastic and fracture behavior of asphalt at low temperatures can be captured. This was performed by developing expressions relating displacement measurements acquired from the SCB test to a creep function. The authors reported good agreement between the creep function obtained from the SCB test and the corresponding functions acquired from the Three-Point Bending Beam and the Indirect Tensile (IDT) creep tests (Zegeye Teshale et al. 2013). Previous research conducted by Huang and others have shown that the SCB test was also utilized to understand the fatigue cracking behavior of asphalt mixtures (Biligiri et al. 2012; Huang et al. 2013; Shu et al. 2005).

Warm mix asphalt (WMA) technologies reduce binder viscosity as well as mixing and compaction temperatures by 20-55°C during asphalt mixture production and placement. Reducing the mixing temperature enables the asphalt industry to reduce their

carbon footprint and reduce costs due to lower energy consumption in mixing plants. Moreover, lowering the compaction temperatures in the field through reducing binder viscosity improves mix compactibility, extends the paving season, allows longer haul distances and allows the use of higher contents of reclaimed asphalt pavements in asphalt mixtures. Furthermore, reduction in the mixing and compaction temperatures lowers the fumes workers can be exposed to during the production and laydown process of an asphalt mixture (Buss et al. 2011; Button et al. 2007; D'Angelo et al. 2008; Gandhi 2008; Gandhi et al. 2010; Hurley and Prowell 2006; Jamshidi et al. 2013; Kim et al. 2012; Mogawer et al. 2011; Rashwan and Ronald 2012).

In this work, the fracture resistance and low temperature properties of six different warm mix asphalt and binder combinations were evaluated using the SCB and BBR tests. Three mixtures and binders were modified using SBS polymer while the other three mixtures and binders were not modified. Each subgroup comprised one control mix with no warm mix additive (a PG 64-22 binder), a warm mix prepared using a surfactant material derived from the forest products industry and another WMA prepared using long chained hydrocarbon based upon the Fisher-Tropsch process. The main objective of this paper is to examine whether a relationship exists between the stiffness values of both the SCB and BBR test. In addition, whether a correlation can be made to analyze how much of an impact the aggregate phase and binder have on the mix stiffness values.

### 7.3. Experimental Materials and Methods

#### 7.3.1. Materials

This work used a Canadian crude source of binder. This binder was tested at its basic grade PG 64-22 as control binder (Control- C) and as a SBS polymer modified binder with PG 70-22 at a dosage of 1.5 % (Polymer Modified Control-PMC). These two versions of the binder were used to incorporate two WMA additives to investigate the effect of WMA additives: FP and FT on the low temperature cracking performance of asphalt binders and mixtures. FP is a chemical additive derived from tall oil that exhibits surfactants properties. It is added at a dosage of 0.5% by total weight of the binder according to previous research (Gandhi et al. 2010). Moreover, FT is a long chained hydrocarbon wax derived from the Fischer-Tropsch process that is typically added at a dosage rate of 1.5% by total weight of the binder.

The mix design used in this study to prepare the SCB specimens is a mixture approved by the Iowa DOT with a design level of 10 million ESALS. The gradation and the source of aggregates used in this work are shown in Table 7.1 below. The gradation of each aggregate portion was verified and checked with Iowa DOT job mix formula.

Six mixtures were prepared in this study divided into two main subgroups: control group (C) and polymer modified group (PMC) with each subgroup comprising three mixtures. In the first subgroup, the base PG 64-22 binder was used while the SBS polymer modified version of the binder with a PG of 70-22 was utilized in the second subgroup. Within each subgroup, two mixtures incorporated two WMA additives investigated in this study, FP and FT, while the third mixture in each subgroup did not include any WMA additives.

**Table 7.1. Mix Design Gradation and Source Information**

| Source     |           | Martin Marietta (Ames) | Martin Marietta (Ames) | Manatts (Ames) | Hallet (Ames) | Martin Marietta (Ames) | Martin Marietta (Ames) | Trial Blend |
|------------|-----------|------------------------|------------------------|----------------|---------------|------------------------|------------------------|-------------|
| Aggregate  |           | 12.5 mm Limestone      | 9.5 mm Limestone       | Quartize       | Natural Sand  | Manuf. Sand            | Agg Lime               |             |
|            |           | 29%                    | 16%                    | 15%            | 13%           | 15%                    | 12%                    | 100%        |
| U.S. Sieve | Sieve, mm | % Passing              | % Passing              | % Passing      | % Passing     | % Passing              | % Passing              | % Passing   |
| 3/4"       | 19        | 100.0                  | 100.0                  | 100.0          | 100.0         | 100.0                  | 100.0                  | 100.0       |
| 1/2"       | 12.5      | 79.7                   | 100.0                  | 99.6           | 100.0         | 100.0                  | 100.0                  | 94.1        |
| 3/8"       | 9.5       | 65.8                   | 90.1                   | 84.3           | 100.0         | 100.0                  | 100.0                  | 86.1        |
| #4         | 4.75      | 37.2                   | 20.5                   | 14.8           | 96.8          | 95.2                   | 99                     | 55.1        |
| #8         | 2.36      | 18.1                   | 2.1                    | 2.9            | 64.2          | 65.5                   | 97                     | 35.8        |
| #16        | 1.18      | 12.5                   | 0.7                    | 2.0            | 33.7          | 36.3                   | 75                     | 22.9        |
| #30        | 0.60      | 9.5                    | 0.4                    | 1.7            | 11.4          | 17.4                   | 53                     | 13.6        |
| #50        | 0.30      | 7.5                    | 0.3                    | 1.4            | 0.9           | 6.5                    | 38                     | 8.1         |
| #100       | 0.15      | 6.2                    | 0.3                    | 1.1            | 0.1           | 1.9                    | 29                     | 5.8         |
| #200       | 0.075     | 5.2                    | 0.3                    | 0.8            | 0.0           | 0.8                    | 22.3                   | 4.5         |

### 7.3.2. Sample preparation and testing procedure

#### 7.3.2.1. Binder testing

Three replicates were prepared for each of the six binders studied in this work.

The six binders investigated were: control non-modified binder C, FP-C incorporating the FP WMA additive, FT-C that contains the FT WMA wax additive in addition to their polymer modified counterparts, PMC, FP-PMC and FT-PMC. Testing on these binders was done using a Bending Beam Rheometer (BBR) at  $-6^{\circ}\text{C}$ ,  $-12^{\circ}\text{C}$  and  $-18^{\circ}\text{C}$  taken at 60 seconds of loading. In order for a binder to be deemed acceptable, the binder grading criteria requires that the creep stiffness,  $S(t)$ , be less than or equal to 300 MPa at 60 seconds and the m-value, rate of change in the creep stiffness, is required to be greater than or equal to 0.300 at 60 seconds when tested at the effective binder grade which is  $10^{\circ}\text{C}$  above the critical temperature.

#### 7.3.2.2. Asphalt mixture testing

Seventy two specimens were prepared to investigate the fracture performance of the six asphalt mixtures by studying the effect of binder modification, WMA additives'

incorporation and air void content on the stiffness parameter (S) generated from the SCB test. Moreover, this paper will look into the relationship between the stiffness values generated from the BBR and SCB tests. Two levels of air voids were chosen to study the effect of air voids on the fracture behavior of asphalt mixtures, 4 % and 7 %. The former percentage represents the design value while the later percentage represents the typical as-constructed values of percent air voids common in pavement construction practice (Li and Marasteanu 2010).

For each of the six mixtures, cylindrical specimens with 150 mm in diameter and 115 mm in height were compacted in the laboratory. The actual air content for the specimens of all mixtures were checked and verified to be in the range of  $1\% \pm$  target air voids content. The cylindrical specimens were cut symmetrically from the middle section into three slices each with a thickness of  $25\text{mm} \pm 2\text{mm}$ . Each SCB slice cut from the cylindrical samples was cut symmetrically into two identical semicircular bend samples. A notch 15 mm in length and a maximum width of 1.5mm is cut using a laboratory saw with diamond disc and water cooling applied. Three replicates of each mixture were tested at a given test temperature.

A UTS servo-hydraulic testing arrangement was used to perform the tests inside an environmental chamber that can control temperature in the range between  $-40$  and  $85^{\circ}\text{C}$ . Specimens were conditioned in the temperature controlled environmental chamber for 2 hours. After conditioning, the sample was placed in the test setup similar to that described in the test method proposed in NCHRP 09-46 report where the sample is supported by two fixed rollers with a span of 120 mm. The crack mouth opening displacement (CMOD) was recorded by a clip gauge attached to the bottom of the

specimen. The test is initiated by applying a contact load until a maximum value of 0.3 kN to make sure that there is uniform contact between the specimen and the loading plate before the application of the actual load. Throughout the test, a constant CMOD rate of 0.0005 mm/s was used and the load and the load line displacement were recorded through the actuator head electronically. The test stops when either the load drops to 0.5 kN in the post-peak region or when the CMOD clip gauge range limit is reached whichever occurs first.

The stiffness parameter (S) is calculated from the data acquired from the SCB test. The stiffness is calculated as the slope of the linear ascending portion of the load-load line displacement (P-u) curve in kN/mm.

## 7.4. Discussion of Results and Analysis

The first two sections go through the analysis of the bending beam rheometer results, and semi-circular bend test stiffness results used individually for examining whether a relationship exists between stiffness results of both the SCB and the BBR test. The final section provides comparison charts of SCB stiffness against BBR stiffness as determined for each air void content as well as air void content and polymer modification.

### 7.4.1. Analysis of BBR results

Table 7.2 displays the results of the bending beam rheometer testing at  $-6^{\circ}\text{C}$ ,  $-12^{\circ}\text{C}$  and  $-18^{\circ}\text{C}$  taken at 60 seconds of loading. Binder grading criteria interpolated from the data between the temperatures of  $-6^{\circ}\text{C}$  and  $-12^{\circ}\text{C}$  for groups PMC and FT – PMC, while interpolation took place between  $-12^{\circ}\text{C}$  and  $-18^{\circ}\text{C}$  for groups C, FT – C, FP



– C, and FP – PMC. This was done using a linear relationship between the test temperatures and reducing the determined temperature by 10°C to arrive at the continuous low temperature binder grade.

From Table 7.2, the control group (C) and warm mix additive modified control groups maintained and improved the low temperature performance grade for long-term aged binder. The warm mix additive group FP – C improved the low temperature performance grade from –22°C to –28°C. For the polymer modified control group (PMC) and group FT – PMC, the low temperature performance grade for long-term aged binder was not maintained and the low temperature performance grade went from –22°C to –16°C. The forest product modified polymer modified control binder (FP – PMC) maintained the low temperature performance at –22°C for the long-term aged binder. For the control group binders, FP improved the critical failure low temperature the most as compared to the performance shown by FT against the performance of the control group. For the polymer modified control group binders, the best performance in critical failure low temperature was shown by the additive FP with the control and FT groups underperforming in low temperature performance. The improvement shown by FP for the control binder was so large that the low temperature grade changed from –22°C to

**Table 7.2. Summary of BBR Results**

| Group Name                     | Temperatures (°C) |        |         |        |         |        | Critical Failure Low Temperature (°C) |
|--------------------------------|-------------------|--------|---------|--------|---------|--------|---------------------------------------|
|                                | -6                |        | -12     |        | -18     |        |                                       |
|                                | m-value           | S(t)   | m-value | S(t)   | m-value | S(t)   |                                       |
| Control - C                    | N/A               | N/A    | 0.33    | 127.17 | 0.26    | 327.00 | -24.5                                 |
| FT - C                         | N/A               | N/A    | 0.32    | 169.33 | 0.25    | 327.00 | -23.8                                 |
| FP - C                         | N/A               | N/A    | 0.36    | 137.00 | 0.31    | 308.50 | -29.1                                 |
| Polymer Modified Control - PMC | 0.37              | 93.83  | 0.30    | 159.00 | N/A     | N/A    | -21.8                                 |
| FT - PMC                       | 0.33              | 105.80 | 0.28    | 209.00 | N/A     | N/A    | -19.9                                 |
| FP - PMC                       | N/A               | N/A    | 0.31    | 176.33 | 0.25    | 297.67 | -23.0                                 |

–28°C as the critical failure low temperature decreased by 4.6°C from –24.5°C to –29.1°C.

An analysis of variance (ANOVA) was conducted to examine which variability factors are significant in affecting the BBR stiffness values. A randomized complete block design was used to conduct the ANOVA. The block factors examined are Binder Type - A, and Additive - B, where three samples were tested for each group. All the interactions between Binder Type - A, and Additive - B are also studied. A statistical program called JMP was used to evaluate the results. The results are shown in Table 7.3. To be a statistical significant source of variability, the p-value must be less than or equal to 0.05. It is important to point out that Binder Type – A, and Additive – B are not statistically significant source of variability. This means that the additives and binder types were not found to be statistically significantly different from one another overall according to a 95% confidence level. Due in part to these results it is possible to use BBR stiffness values to correlate to SCB stiffness.

**Table 7.3. ANOVA Results for BBR Stiffness at –12°C**

| Source          | DF | Sum of Squares | Mean Squares | F-value | P-value | Status          |
|-----------------|----|----------------|--------------|---------|---------|-----------------|
| Binder Type - A | 1  | 6142.014       | 6142.014     | 3.504   | 0.0858  | Not-significant |
| Additive - B    | 2  | 6728.861       | 3364.431     | 1.919   | 0.1891  | Not-significant |
| A*B             | 2  | 58.861         | 29.431       | 0.017   | 0.9834  | Not-significant |

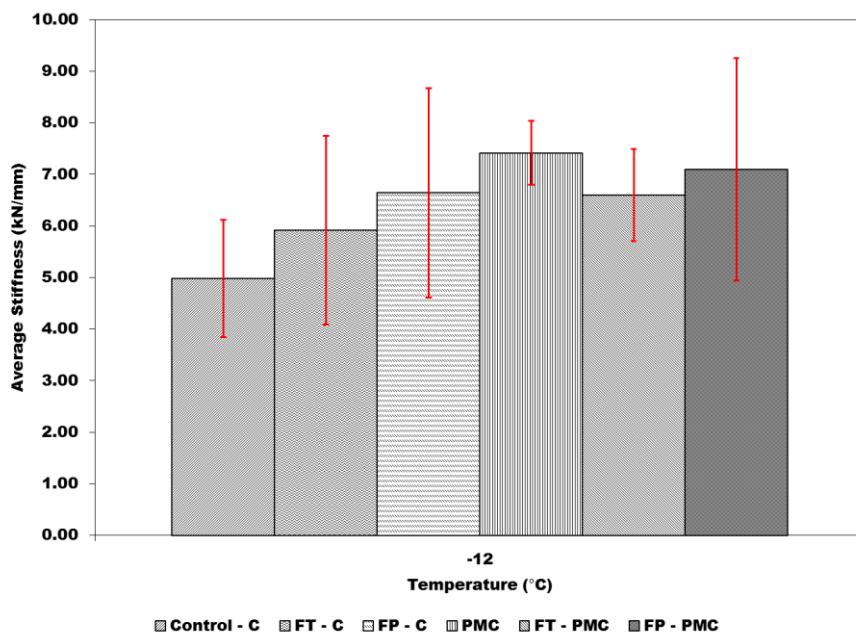
#### **7.4.2. Analysis of SCB results**

The average stiffness values with their corresponding error bars (1 standard deviation above and below the mean values) for test temperature –12°C for mixtures with 4% and 7% air voids are shown in Figures 7.1 and 7.2, while a summary of the results is

shown in Tables 7.4 and 7.5. Due to the large number of groups and samples tested, it is difficult to see if there are significant differences between the groups according to additive/binder type overall and also between the groups according to additive/binder type within each air void content. Therefore, a statistical analysis was done according to a 95% confidence level to examine if there were statistically significant differences between the groups according to additive/binder type overall and air void content.

**Table 7.4. SCB Stiffness Results at 4% Air Voids**

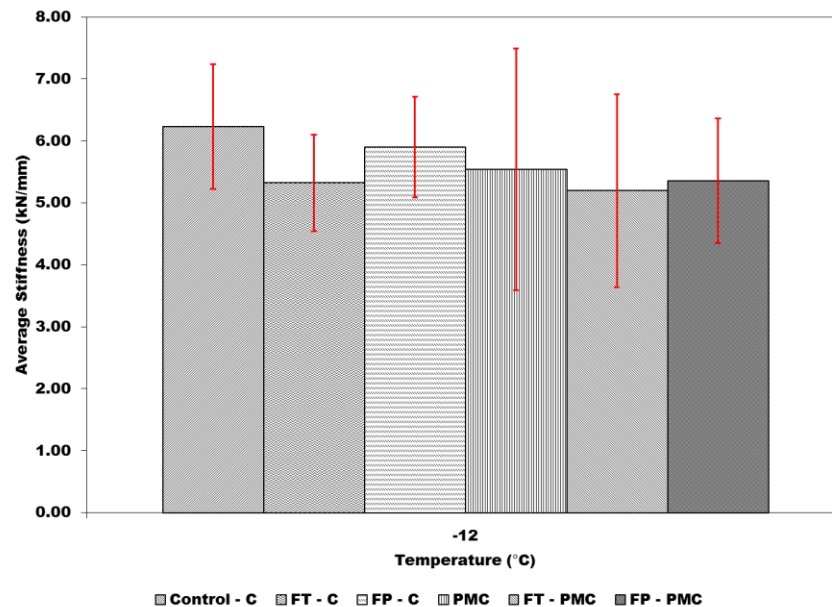
| Binder Type | Additive | Temperature (°C) | Average Stiffness (kN/mm) | Stdev (kN/mm) | COV (%) |
|-------------|----------|------------------|---------------------------|---------------|---------|
| PG 64-22    | Control  | -12              | 4.98                      | 1.14          | 22.9    |
|             |          | -18              | 5.03                      | 1.02          | 20.3    |
|             | FT       | -12              | 5.92                      | 1.83          | 31.0    |
|             |          | -18              | 8.58                      | 2.26          | 26.4    |
|             | FP       | -12              | 6.64                      | 2.03          | 30.6    |
|             |          | -18              | 6.74                      | 3.20          | 47.4    |
| PG 70-22    | Control  | -6               | 4.44                      | 0.78          | 17.6    |
|             |          | -12              | 7.41                      | 0.62          | 8.3     |
|             | FT       | -6               | 4.63                      | 1.12          | 24.1    |
|             |          | -12              | 6.60                      | 0.89          | 13.5    |
|             | FP       | -12              | 7.09                      | 2.16          | 30.4    |
|             |          | -18              | 6.62                      | 1.46          | 22.0    |



**Figure 7.1. Average SCB Stiffness Results at 4% Air Voids**

**Table 7.5. SCB Stiffness Results at 7% Air Voids**

| Binder Type | Additive | Temperature (°C) | Average Stiffness (kN/mm) | Stdev (kN/mm) | COV (%) |
|-------------|----------|------------------|---------------------------|---------------|---------|
| PG 64-22    | Control  | -12              | 6.23                      | 1.01          | 16.1    |
|             |          | -18              | 4.75                      | 0.74          | 15.5    |
|             | FT       | -12              | 5.32                      | 0.78          | 14.6    |
|             |          | -18              | 3.84                      | 1.00          | 26.1    |
|             | FP       | -12              | 5.90                      | 0.82          | 13.8    |
|             |          | -18              | 6.67                      | 1.10          | 16.4    |
| PG 70-22    | Control  | -6               | 3.45                      | 0.41          | 11.9    |
|             |          | -12              | 5.54                      | 1.95          | 35.2    |
|             | FT       | -6               | 5.79                      | 0.95          | 16.4    |
|             |          | -12              | 5.20                      | 1.56          | 30.0    |
|             | FP       | -12              | 5.36                      | 1.01          | 18.8    |
|             |          | -18              | 4.96                      | 0.38          | 7.6     |

**Figure 7.2. Average SCB Stiffness Results at 7% Air Voids**

An analysis of variance (ANOVA) was conducted to examine which variability factors are significant in affecting the stiffness values. A randomized complete block design was used to conduct the ANOVA. The block factors examined are Binder Type - A, Additive - B, and Air Voids (%) – C, where at least three samples were tested for each group. All the interactions between Binder Type - A, Additive - B, and Air Voids (%) - C, are also studied. JMP was used to evaluate the results which are shown in Table 7.6.

In Table 7.6, it is evident that Air Voids (%) – C is a statistically significant source of variability by itself, but not when crossed with Additive – B, nor crossed with both Binder Type – A and Additive – B. To be a statistical significant source of variability, the p-value must be less than or equal to 0.05. It is important to point out that Binder Type – A, and Additive – B are not statistically significant source of variability. This means that the additives and binder types were not statistically significantly different from one another overall according to a 95% confidence level. Due in part to the results summarized in Table 7.5, it is possible to make comparisons between BBR stiffness and SCB stiffness according to air void content, and air void content crossed with binder type. These comparisons will be shown in the next section.

**Table 7.6. ANOVA Results for SCB Stiffness at -12°C**

| Source            | DF | Sum of Squares | Mean Squares | F-value | P-value | Status          |
|-------------------|----|----------------|--------------|---------|---------|-----------------|
| Binder Type - A   | 1  | 1.940          | 1.940        | 0.900   | 0.3477  | Not-significant |
| Additive - B      | 2  | 3.300          | 1.650        | 0.765   | 0.4709  | Not-significant |
| A*B               | 2  | 2.087          | 1.044        | 0.484   | 0.6194  | Not-significant |
| Air Voids (%) - C | 1  | 15.102         | 15.102       | 7.001   | 0.0110* | Significant     |
| A*C               | 1  | 9.823          | 9.823        | 4.554   | 0.0380* | Significant     |
| B*C               | 2  | 0.505          | 0.252        | 0.117   | 0.8899  | Not-significant |
| A*B*C             | 2  | 3.914          | 1.957        | 0.907   | 0.4104  | Not-significant |

#### 7.4.3. BBR stiffness vs. SCB stiffness

From previous statistical analyses done in sections 7.4.1 and 7.4.2 it was shown that binder type, additive choice and the interaction between binder type and additive choice are not significant sources of variability among both the BBR and SCB test results. Air void content and the interaction between air void content and binder type were found to be significant sources of variability from the SCB test results as seen in

Table 7.6. Overall comparisons were made between the average BBR results and average SCB results according to air void content and air void content crossed with binder type. These comparisons are shown in Figures 7.3 and 7.4.

For Figure 7.3, 7% air voids has a  $R^2$  value equal to 0.8475, and a  $R^2_{\text{adjusted}}$  equal to 0.8094, while 4% air voids had a  $R^2$  and  $R^2_{\text{adjusted}}$  equal to 0.1884 and  $-0.0145$ . It is not clear just by examining air void content why the  $R^2$  and  $R^2_{\text{adjusted}}$  are so different for 4% air voids as compared to 7% air voids as the comparison between BBR stiffness and SCB stiffness for 7% air voids shows there is some correlation/relationship occurring from the binder to binder/aggregate composite phase. To look more closely at this relationship the comparison between SCB stiffness and BBR stiffness was made using the interaction between air void content and binder type as shown in Figure 7.4.

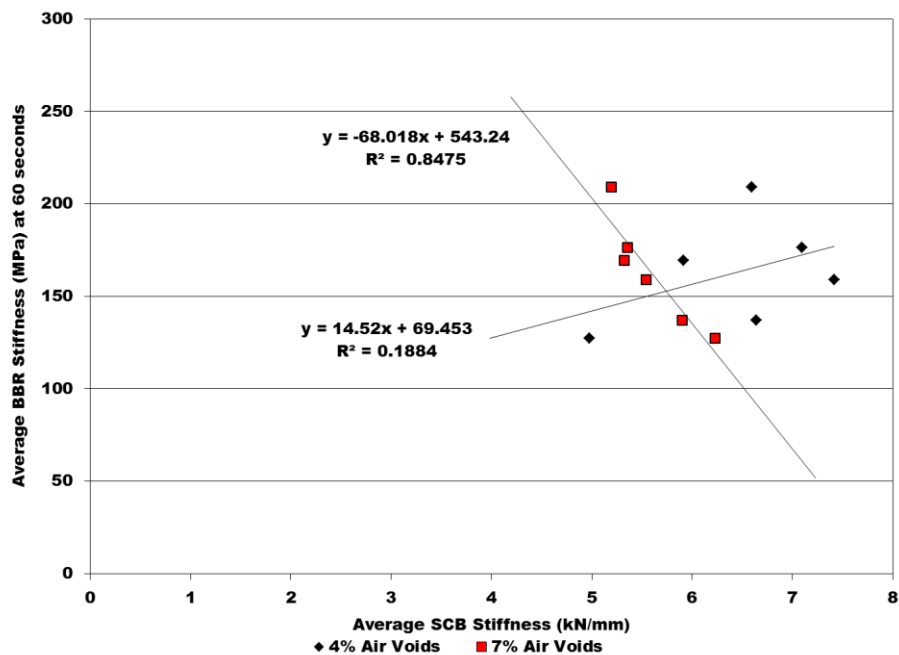


Figure 7.3. Average BBR Stiffness Compared to Average SCB Stiffness at Low Temperature PG+10

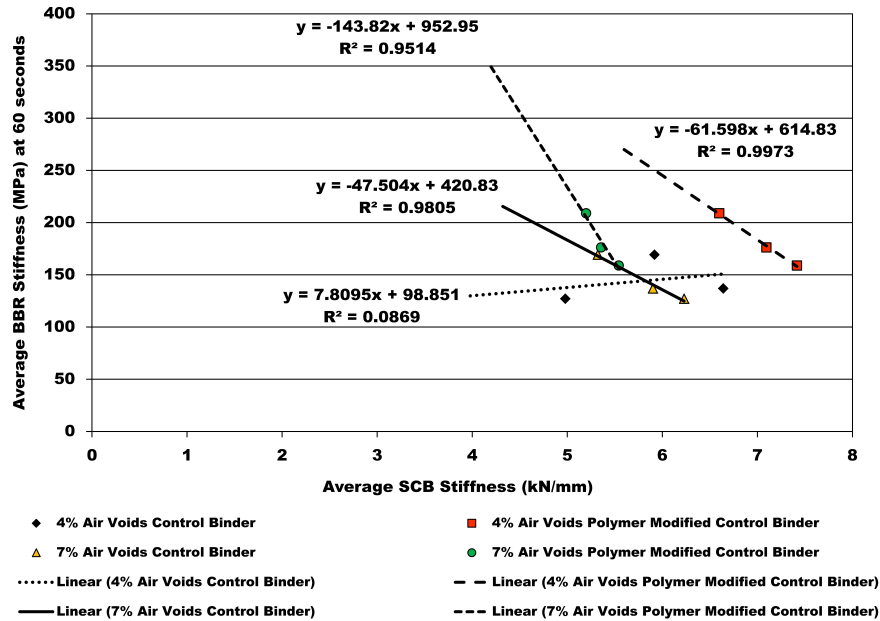


Figure 7.4. Average BBR Stiffness Compared to Average SCB Stiffness by Binder Type at Low Temperature PG+10

When air void content is crossed with binder type the  $R^2$  and  $R^2_{adjusted}$  values are much higher for all the groups except for the group 4% air voids crossed with the original control binder. For 7% air voids crossed with the original binder and crossed with the polymer modified original binder the  $R^2$  and  $R^2_{adjusted}$  values are equal to 0.9805, 0.9514, 0.9611 and 0.9028. The polymer modified original binder crossed with 4% air voids had  $R^2$  and  $R^2_{adjusted}$  values of 0.9973, and 0.9945. However, the original binder crossed with 4% air voids had  $R^2$  and  $R^2_{adjusted}$  values of 0.0869, and  $-0.8261$ . This means a linear relationship cannot be made for the original binder crossed with 4% air voids. Previously it was thought a relationship could not be made for all 4% air void results, but this was not the case. Excluding the case for the 4% air voids crossed with the original binder, the other relationships from Figure 7.4 show that with decreasing BBR creep stiffness, SCB

stiffness increases. This was only done with the results from test temperature  $-12^{\circ}\text{C}$  as there were not enough tests done at  $-6^{\circ}\text{C}$  and  $-18^{\circ}\text{C}$  using both the BBR and SCB tests.

## 7.5. Conclusions & Recommendations

Performance of warm mix asphalt and binder performance from the semi-circular bend (SCB) test and bending beam rheometer (BBR) tests has shown that a correlation/relationship is possible to make between warm mix asphalt and warm asphalt binder test results. This was due to the fact that additive selection and binder type were not found to be statistically significant variables in the analysis of the BBR and SCB test results. However air voids and the interaction between air voids and binder type were found to be significant sources of variation within the SCB test results. Comparisons were made using air voids and the interaction between air voids and binder type. From examining the comparison using only air void contents it was found there was linear relationship for samples made with 7% air voids, but not those with 4% air voids. By taking it one step further and examining the comparison made using the interaction of air voids and binder type it was found that there are clear relationships for the original binder, and polymer modified binder groups with 7% air voids, and that there is a clear relationship for the 4% air void group crossed with polymer modification. This was not the case for the interaction between 4% air voids and the original binder. Overall it was found that as BBR stiffness decreases the SCB stiffness increases at  $-12^{\circ}\text{C}$ .

Since there were not enough tests done at  $-6^{\circ}\text{C}$  and  $-18^{\circ}\text{C}$  using the BBR and SCB test comparisons were not possible to make at these temperatures. It is thought that with additional testing at these two test temperatures, comparisons discussed within this



paper can be done, but also a comparison across temperatures could be done as well. With a comparison across several temperatures a much better understanding of the relationship between BBR creep stiffness at 60 seconds and SCB stiffness could be made. This would also enable a much better statistical analysis as temperature could be examined as an important variable besides binder type, additive choice, and air void content.

## 7.6. Future Research

In the future, further testing will be done at  $-6^{\circ}\text{C}$  and  $-18^{\circ}\text{C}$  using the BBR and SCB tests. This future research will enable a better comparison to be made within each temperature as well as across all the temperatures to examine the relationship between binder and binder/aggregate stiffness. Secondly a multiple regression model can be made to delve into more details to examine the relationship and look at correlations.

## 7.7. References

- Aurangzeb Q, Al-Qadi I, Pine W, Trepanier J, Abuawad I (2012) Thermal Cracking Potential in Asphalt Mixtures with High RAP Contents. In: Scarpas A, Kringos N, Al-Qadi I, A L (eds) 7th RILEM International Conference on Cracking in Pavements, vol 4. RILEM Bookseries. Springer Netherlands, pp 1271-1280. doi:10.1007/978-94-007-4566-7\_121
- Biligiri K, P, Said S, Hakim H (2012) Asphalt Mixtures' Crack Propagation Assessment using Semi-Circular Bending Tests. International Journal of Pavement Research and Technology Vol. 5, Issue 4:209-217
- Buss AF, Rashwan MH, Williams RC (2011) Investigation of warm-mix asphalt using Iowa aggregates. Iowa Highway Research Board Project Report TR-599. Ames, IA.
- Button JW, Estakhri C, Wimsatt A (2007) A synthesis of warm mix asphalt. Rep. No. FHWA/TX-07/0-5597-1. Texas Transportation Institute, Texas A & M University System.
- Chong KP, Kuruppu MD (1984) New specimen for fracture toughness determination for rock and other materials Int J Fract 26:R59-R62 doi:10.1007/bf01157555
- D'Angelo JA et al. (2008) Warm-mix asphalt: European practice. FHWA-PL-08-007: FHWA, U.S. Dept. of Transportation, Washington, DC.

- Gandhi T (2008) Effects of warm asphalt additives on asphalt binder and mixture properties. Doctoral dissertation. Clemson University, Clemson, SC.
- Gandhi T, Rogers W, Amirkhanian S (2010) Laboratory evaluation of warm mix asphalt ageing characteristics International Journal of Pavement Engineering 11:133-142
- Huang B, Shu X, Zuo G (2013) Using notched semi circular bending fatigue test to characterize fracture resistance of asphalt mixtures Engineering Fracture Mechanics 109:78-88  
doi:<http://dx.doi.org/10.1016/j.engfracmech.2013.07.003>
- Hurley GC, Prowell BD (2006) Evaluation of potential processes for use in warm mix asphalt Journal of the Association of Asphalt Paving Technologists 75:41-90
- Jamshidi A, Hamzah Mo, You Z (2013) Performance of Warm Mix Asphalt containing Sasobit®: State-of-the-art Construction and Building Materials 38:530-553  
doi:<http://dx.doi.org/10.1016/j.conbuildmat.2012.08.015>
- Kim H, Lee S, Amirkhanian S (2012) Influence of Warm Mix Additives on PMA Mixture Properties Journal of Transportation Engineering 138(8):991-997 doi:10.1061/(ASCE)TE.1943-5436.0000406
- Krans R, Tolman F, Van de Ven M Semi-circular bending test: a practical crack growth test using asphalt concrete cores. In: RILEM Proceedings, 1996. Chapman & Hall, pp 123-132
- Li XJ, Marasteanu MO (2010) Using Semi Circular Bending Test to Evaluate Low Temperature Fracture Resistance for Asphalt Concrete Experimental Mechanics 50(7):867-876 doi:10.1007/s11340-009-9303-0
- Marasteanu MO, Li X, Labuz JF, Petit C, Al-Qadi I, Millien A Low temperature fracture test for asphalt mixtures. In: Fifth International RILEM Conference on Reflective Cracking in Pavements, 2004. RILEM Publications SARL, pp 249-256
- Mogawer WS, Austerman AJ, Kassem E, Masad E (2011) Moisture damage characteristics of warm mix asphalt mixtures Journal of the Association of Asphalt Paving Technologists 80:491-526
- Rashwan M, Williams RC An Evaluation of Warm Mix Asphalt Additives and Reclaimed Asphalt Pavement on Performance Properties of Asphalt Mixtures. In: Transportation Research Board 91st Annual Meeting, No. 12-4469, 2012.
- Shu X, Huang B, Tang Y (2005) Comparison of Semi-Circular Bending and Indirect Tensile Strength Tests for HMA Mixtures. In: Advances in Pavement Engineering. pp 1-12. doi:10.1061/40776(155)14
- Teshale EZ (2012) Low-Temperature Fracture Behavior of Asphalt Concrete in Semi-Circular Bend Test. Doctoral dissertation, University of Minnesota
- Wagnoner MP, Buttlar WG, Paulino GH (2005) Disk-shaped compact tension test for asphalt concrete fracture Experimental Mechanics 45:270-277 doi:10.1007/bf02427951
- Zegeye Teshale E, Stolarski HK, Marasteanu MO (2013) Determination of Creep Compliance of Asphalt Concrete from Notched Semi-Circular Bend (SCB) Test Experimental Mechanics 53:919-928 doi:10.1007/s11340-012-9688-z

## **CHAPTER 8. CONCLUSIONS AND RECOMMENDATIONS FOR FUTURE WORK**

### **8.1. Summary**

This thesis reports research work that investigates whether newly produced bio-derived materials such as isosorbide distillation bottoms (IDB) are viable alternatives to present commercially used warm mix asphalt additives through both the study of binder rheology and mix performance. This document is organized into five articles that summarize the main results of this doctoral work. Each article includes conclusions and recommendations that are drawn from the work reported therein. This last section, presents conclusions and recommendations found by relating results of the work done within the five articles and indicates areas where future research is needed.

### **8.2. Conclusions**

The optimum dosage rate for IDB addition (0.5% by weight of the total binder) in asphalt binder was determined through the research work shown in the first article (Chapter 3). This optimum dosage rate of 0.5% IDB by weight of the total binder was then used for the warm mix asphalt production in the studies reported in articles two, three and four (Chapters 4, 5 and 6). The results from Chapter 3 also indicated that warm mix asphalt modified with IDB at dosage levels of 0.5% and 1.0% by weight of the total binder produced at 120°C had no statistical differences in terms of compaction when compared to hot mix asphalt (HMA) compacted at 150°C. Furthermore, it was shown that warm mix asphalt modified with IDB at dosage levels of 0.5% and 1.0% by weight of the total binder met the TSR criteria of 80%, but the peak strength values were lower than

that of the control HMA. Article two (Chapter 4) examined whether it was possible to use mix dynamic modulus results for use in estimating the high temperature performance grade of the binder. From this article, it was discovered that methods used for constructing the binder shear complex modulus master curve were more accurate and displayed truer viscoelastic behavior when the phase angle was used to induce a slope shift in combination with the time temperature superposition principle. In terms of using prediction models to back calculate to the binder shear modulus values, it was found that the Al-Khateeb model worked at temperatures above 54°C while the Hirsch model did not. However, it was found that high variability at higher temperatures was most likely due to the higher variability of the measured results gained from testing at higher temperatures as well as extrapolation of said results.

Within article three (Chapter 5) results obtained from mix testing and binder testing using the dynamic modulus test and RTFO aged DSR test were used as level one inputs in a mechanic empirical pavement design program called AASHTOWare Pavement ME Design. For this research work, the binder and mix results were first examined statistically. From the mix results, it was found that overall the additives are statistically different from one another. The same results were found when examining the RTFO aged binder results. From use of the AASHTOWare Pavement ME Design program, the predicted pavement performance was evaluated for sensitivity to different traffic loading, climate and pavement design conditions as well as variable  $E^*$  reliability. From the resulting sensitivity study, the pavement design/traffic level used for each run had a large impact on the pavement performance compared with the two climates and reliability levels that were included. The corn-derived WMA additive was similar to the

other established WMA additives in terms of pavement performance predicted by the AASHTOWare Pavement ME Design. The pavement performance in the control group did not show large differences compared to WMA additives showing that the pavement performance models forecast equal performance between the WMA additives studied and the HMA control group.

Articles four and five (Chapters 6 and 7) cover low temperature fracture properties (SCB) as well as low temperature binder properties (BBR); in addition, Chapter 6 covers samples tested using the MSCR method. From Chapter 6, it was shown that Isosorbide Distillation Bottoms (IDB) can be used as a WMA additive and is highly comparable to control hot mix asphalt (HMA) and WMA with FP 1 and FP 2 in terms of performance obtained from the semi-circular bend (SCB) test at low temperatures. Comparisons of RTFO aged DSR binder MSCR results within each binder type were made. From these comparisons, it was observed that there could be a possible interaction between polymer modification of the binder and IDB addition. For the PG 64-22 binder, it was observed that IDB had the second highest  $J_{nr3.2}$  value and the lowest % recovery value, while the PG 70-22 binder modified with IDB had the highest % recovery value and lowest  $J_{nr3.2}$  value. From these results, it can be inferred that there is an interaction between the polymer SBS and the additive IDB, as IDB showed the least performance when added to the PG 64-22 binder, but showed the best performance when added to the PG 70-22 binder. This leads to the conclusion that IDB is helping improve the bond between the polymer SBS and the PG 64-22 binder.

The BBR results from Chapter 6 on average showed that all the additives regardless of binder type (PG 64-22 or PG 70-22) showed improvement in the critical

failure low temperature as compared to each of the binder control groups. Overall, the BBR results indicate that all the additives may be useful in low temperature climates where pavements are susceptible to thermal cracking. From an overall statistical analysis of the SCB results at low temperatures, the additives were shown to be statistically significantly different from one another for fracture toughness, but not for stiffness and fracture energy results. The statistical analysis showed there was little impact on the low temperature properties from addition of IDB as compared to the control group. IDB did not negatively impact low temperature properties of the warm mix asphalt in terms of fracture performance.

The last article (Chapter 7) showed through performance of warm mix asphalt and binder performance from the semi-circular bend (SCB) test and bending beam rheometer (BBR) tests that a correlation/relationship is possible to make between warm mix asphalt and warm asphalt binder test results. This was due to the fact that additive selection and binder type were not found to be statistically significant variables in the analysis of the BBR and SCB test results. However, air voids and the interaction between air voids and binder type were found to be significant sources of variation within the SCB test results. Comparisons were made using air voids and the interaction between air voids and binder type. From examining the comparison using only air void contents, it was found there was a linear relationship for samples made with 7% air voids, but not those with 4% air voids. Upon further examination of the comparison made using the interaction of air voids and binder type, it was found that there are clear relationships for the original binder, and polymer modified binder groups with 7% air voids, and that there is a clear relationship for the 4% air void group crossed with polymer modification. This was not

the case for the interaction between 4% air voids and the original binder. Overall it was found that as BBR stiffness decreases, the SCB stiffness increases at  $-12^{\circ}\text{C}$ .

### **8.3. Recommendations for Future Work**

Several topics were covered fairly thoroughly in this research work, but improvements could be made to the general knowledge gained from this work. This deals with the use of IDB as a future warm mix asphalt additive. Currently, IDB will no longer be produced from the production of isosorbide due to cost and marketing issues. However, new streams of products based off isosorbide are currently being tested in various binders to estimate the optimum dosage rate, with further testing being planned for mixture performance.

Concerning the work covered in Chapter 3, it was important that the estimated dosage rate was determined to be 0.5% by weight of the total binder. This gave crucial starting information for future research of related materials to IDB in binder investigations. The mix study done in Chapter 3 covering compaction and moisture susceptibility brings more questions than answers. To address these issues, it is suggested that a compaction study be undertaken to look at differences between compaction energy/shear energy by keeping the mix temperature constant at  $135^{\circ}\text{C}$  while changing the compaction temperature to have three groupings. (For example, compact one group at  $135^{\circ}\text{C}$ , one at  $120^{\circ}\text{C}$ , and one at  $105^{\circ}\text{C}$ ; each using three different binder types.) This future work would give better understanding of whether there are differences between additives in WMA as compared to HMA.

For moisture susceptibility, it would be beneficial to run tests with mixtures using different binders, old and new bio-derived additives as well as commercially available WMA additives. To study moisture susceptibility effectively, it is advised that in the future the Hamburg Wheel Track test be used so rutting can also be examined as well moisture susceptibility. In binder testing, potential for rutting can be examined by running the multiple stress creep recovery (MSCR) procedure using RTFO aged binder in a DSR. This was done in Chapter 6; but it was done to see if there were any differences between additives when interacted with the two binder types. An interaction was found, but additional testing is needed to see if this is a true interaction or not. In the future, MSCR results could be compared to Hamburg Wheel Track test results to see the impact of aggregates, binder, and additive choice on rut resistance.

Chapter 4 explores whether mix dynamic results can be used to estimate the high temperature performance grade of asphalt binder. From this work, it was shown that it is possible using certain models to back-calculate to the binder shear complex modulus values through use of the dynamic modulus values. However, the results are more variable as the temperature increases due to data extrapolation and high variability among dynamic modulus test results at higher temperatures. The prediction models that work were found to be more accurate than the test results themselves due to high variability at higher temperatures. For this to be addressed, the dynamic modulus testing method needs to be examined and investigated to see if there are ways to modify the test and test setup to make results more accurate at higher testing temperatures.

The work done in Chapter 5 has brought to attention the need to study the effects of moisture conditioning on pavement performance as well as to collect field samples for



comparing against laboratory made specimens. Another crucial benefit of Chapter 5 is to see if new or currently produced WMA additives perform differently.

To address future research needs in examining low temperature fracture properties (Chapters 6 and 7), different testing methods such as the disk compact tension (DCT) test need to be evaluated for use in the laboratory for comparisons to be made to results obtained from the semi-circular bend (SCB) test. This should be done to see if the test method has an impact or if the impact is the same regardless of the test method used for each of the bio-derived/chemical WMA additives studied.

Additionally, through the research done in Chapter 7, questions were raised as to how much of an impact does the asphalt binder really have in the mix tests at low temperatures. The following idea was suggested to address this concern -- to fabricate DCT and SCB sample molds for creating either 100% asphalt binder samples or mastic samples to investigate as close as possible the true fracture properties of asphalt binder at low temperature. This would enable future researchers to gain a much better idea on how much of an impact aggregates have in the asphalt mix performance at low temperatures in terms of fracture properties.

Finally, it should be stated that bio-derived materials from isosorbide for use as warm mix asphalt additives is in its infancy. There are many challenges to be addressed, particularly running field trials of WMA against that of control HMA sections. Hopefully, this research work will open many new areas of research for those interested in bio-derived materials for use in asphalt material applications.